

ABSTRACT

Title of Dissertation: PROXIMATE AND ULTIMATE INSIGHTS IN
THE EVOLUTION OF COLOR VISION IN
TROPICAL FRESHWATER FISH

Daniel Escobar Camacho, Doctor of
Philosophy, 2019

Dissertation directed by: Professor Karen L. Carleton
Department of Biology

Evolutionary biology aims to understand diversity and the different mechanisms shaping this organismal variation. Furthermore, several animals vary greatly in coloration patterns and the adaptive mechanisms they have to optimally perceive visual signals in their light environment. The visual system of fish, due to their extensive variation in spectral sensitivities and their numerous adaptations to the underwater light environment, offers a unique opportunity to disentangle this phenotypic diversity.

Throughout this dissertation, I analyze the visual systems of two major groups of Neotropical teleosts: cichlids and characins. Through transcriptome, genome and physiological experiments, I characterized the extant opsin gene complements of their visual system, which is a product of highly dynamic opsin gene evolution, and their color vision, which is based on the expression

of at least three spectrally different visual pigments. The diversity of visual pigments found in these fish is the product of several spectral tuning mechanisms, which they use to fine-tune their spectral sensitivities to specific wavelengths. Our results follow the sensitivity hypothesis because the visual sensitivities of cichlids and characins match the available light in Neotropical ecosystems.

Furthermore, through behavioral assays complemented with visual modeling, I show that African cichlids possess true color vision, the capacity of discriminating color regardless of brightness. This is followed by behavioral experiments analyzing the limits of their chromatic discrimination and discussing the adaptive significance of color vision and its relevance in the visual ecology of Lake Malawi.

This dissertation enhances our understanding of color vision in freshwater fish using molecular and behavioral methods. This work encompasses experiments analyzing the genetic complement of visual pigments, builds knowledge in the evolution of these molecules and their relationship with aquatic environments, and analyzes the color dimensionality of visual systems through behavioral trials. Overall, this dissertation demonstrates the evolution of fish color vision with several methodologies highlighting the importance of an integrative and comparative approach in vision research.

PROXIMATE AND ULTIMATE INSIGHTS IN THE EVOLUTION OF COLOR
VISION IN TROPICAL FRESHWATER FISH

by

Daniel Escobar Camacho

Dissertation submitted to the Faculty of the Graduate School of the
University of Maryland, College Park, in partial fulfillment
of the requirements for the degree of
Doctor of Philosophy
2019

Advisory Committee:

Professor Karen Carleton, Chair

Professor Thomas Kocher

Professor Gerald Wilkinson

Assistant Professor Heidi Fisher

Associate Professor Jens Herberholz

© Copyright by
Daniel Escobar Camacho
2019

Preface

This dissertation is based on chapters where the student, Daniel Escobar Camacho was the primary contributor in all aspects of this thesis research. This dissertation was also completed with the assistance of several co-authors, which justifies their inclusion in publications. Following are the references for the mentioned chapters:

Chapter 1: Introduction

Chapter 2: The Opsin Genes of Amazonian Cichlids

Previously published under: Daniel Escobar-Camacho, Erica Ramos, Cesar Martins and Karen L Carleton. The Opsin Genes of Amazonian Cichlids. *Molecular Ecology*; 2017, 25, 1343-1356.

Chapter 3: Variable vision in variable environments: the visual system of an invasive cichlid (*Cichla monoculus*, Agassiz, 1831) in Lake Gatun, Panama.

Previously published under: Daniel Escobar-Camacho, Michele E.R. Pierotti, Victoria Ferenc, Diana M.T. Sharpe, Erica Ramos, Cesar Martins and Karen L Carleton. *Journal of Experimental Biology*, 2019, jeb188300.

Chapter 4: Visual pigment evolution in Characiformes: insights of dynamic evolution of teleost whole genome duplication surviving opsins and spectral tuning.

In preparation under: Daniel Escobar-Camacho, Karen L. Carleton, Devika Narain, Michele E.R. Pierotti.

Chapter 5: Behavioral color vision in a cichlid fish: *Metriaclima benetos*

Previously published under: Daniel Escobar-Camacho, Justin Marshall and Karen L. Carleton. Behavioral color vision in a cichlid fish: *Metriaclima benetos*. *Journal of Experimental Biology* 2017, jeb.160473.

Chapter 6: Behavioral color thresholds in a cichlid fish: *Metriaclima benetos*

In Review under: Daniel Escobar-Camacho, Michael A. Taylor, Karen L. Cheney, Naomi, F. Green, Justin N. Marshall, Karen L. Carleton. Behavioral color thresholds in a cichlid fish: *Metriaclima benetos*. *Journal of Experimental Biology*. 2019

Chapter 7: Synthesis

Dedication

I would like to dedicate this work to all the people that somehow contributed to the realization of this project. From friends and family that have always supported me along the way, to colleagues and strangers that I have met during my PhD. Thank you all for your advice, enthusiasm, support, friendship, love and most importantly, for putting up with me.

Acknowledgements

I would like to thank everybody who made this dissertation work possible. Most importantly, I would like to thank my mentor Karen Carleton. I have been privileged to work with her and learn from such a remarkable scientist. Karen supported and guided me through my graduate studies. She gave me freedom to pursue my scientific questions while providing invaluable feedback and encouragement. Karen is a tireless and thoughtful mentor who made my PhD experience amazing. I honestly couldn't have asked for anyone better.

I wish to thank my committee members Drs. Gerald Wilkinson, Heidi Fisher, and Jens Herberholz for their time and feedback through this entire process. Special thanks go to Tom Kocher for all of his thoughtful insight into my research. In addition, I would like to acknowledge Dr. Michele Pierotti, who contributed to my research development.

I am grateful to past and present members of the cichlid labs who were always eager to discuss my research ideas and who took care of my fish: Pratima Nandamuri, Miranda Yourick, Ben Sandkam, Matt Conte, Betsy Clark, Will Gammerdinger, and Brian Dalton. I would like to thank Michaela Taylor for her invaluable assistance in our behavioral experiments.

In addition, many people from all over have also contributed their time and expertise to my research. Many thanks to collaborators in Brazil: Cesar

Martins and Erica Ramos; Australia: Karen Cheney, Naomi Green, and Justin Marshall; and Panama: Diana Sharpe. I would also like to thank all of the people who assisted me in my field seasons in Panama, including the staff at STRI and the field assistants who worked with me in 2016 and 2017.

I am also grateful for the unconditional love and support from my family and friends back home. I would like to offer a special thanks to all of the BEES community for making my years at the University of Maryland truly enjoyable: Natalia Umaña, Jessica “Jessenia” Goodheart, Gabriel Arellano, Vanessa Rubio, Grace DiRenzo, Grace Capshaw, Danielle Adams, Jake Weissman, Julie Mallon, Elske Tielens, and Nicki Barbour. Thank you for keeping up with my wicked sense of humor; we had so much fun.

The acknowledgements for the individuals and organizations that supported my research can be found at the end of each chapter.

Table of Contents

Preface	ii
Dedication.....	iv
Acknowledgements	v
Table of Contents	vii
List of Tables	xi
List of Figures	xii
Chapter 1: Introduction	1
1.1 Introduction	1
1.2 Color vision	2
1.2.1 Color in nature	2
1.2.2. Detecting light and colors	3
1.3 Visual systems in fish.....	4
1.4 Goals of research.....	9
Chapter 2: The opsin genes of Amazonian cichlids	11
2.1 Abstract.....	11
2.2 Background.....	12
2.3 Materials and Methods.....	15
2.3.1 Genome analysis.....	16
2.3.2 RNA analysis	16
2.3.3 Opsin sequencing by PCR	17
2.3.4 Phylogenetic trees	17
2.3.5 Gene expression	18
2.3.6 Spectral sensitivities	18
2.3.7 Pseudogenes divergence times	19
2.4 Results	20
2.4.1 Opsin genomic sequences	20
2.4.2 Opsin RNA seq.....	22
2.4.3 Phylogenetic trees	23
2.4.4 Gene expression	26
2.4.5 Spectral tuning	28
2.4.6 Pseudogene divergence time	30
2.5 Discussion.....	31
2.5.1. Opsin gene complement	31
2.5.2 Opsin gene expression.....	33
2.5.3 Opsin sequence variation	36
2.5.4 Ecological adaptation	38
2.6 Acknowledgements.....	41
Chapter 3: Variable vision in variable environments: the visual system of an invasive cichlid (<i>Cichla monoculus</i> , Agassiz, 1831) in Lake Gatun, Panama	42
3.1 Abstract.....	43
3.2 Introduction	44
3.3 Materials and Methods.....	47

3.3.1 Study site and sample collection	47
3.3.2 Experimental set up.....	48
3.3.3 Spectral measurements	48
3.3.4 Microspectrophotometry (MSP).....	51
3.3.4 RNA seq and opsin gene expression analysis	53
3.3.5 Opsin sequence analysis	54
3.4 Results	56
3.4.1 Light environment in Lake Gatun	56
3.4.2 Ocular media	57
3.4.3 Visual sensitivities of <i>Cichla monoculus</i>	58
3.4.4 Opsin gene characterization and sequence analysis	60
3.4.5 Gene expression	63
3.5 Discussion.....	66
3.5.1. Visual system adaptation	66
3.5.2 Spectral measurements	66
3.5.3 Microspectrophotometry	69
3.5.4 Transcriptome analysis	70
3.6 Acknowledgments	76
Chapter 4: Visual pigment evolution in Characiformes: insight of dynamic evolution of teleost whole-genome duplication surviving opsins and spectral tuning.....	78
4.1 Abstract.....	79
4.2 Introduction	80
4.3 Materials and methods.....	83
4.3.1 Animals.....	83
4.3.2 RNA seq	83
4.3.3 Opsin phylogenetics and molecular analysis	84
4.3.4 Ancestral state reconstruction	85
4.3.5 Opsin gene expression.....	87
4.3.6 Microspectrophotometry	87
4.3.7 DNA extraction, sequencing and phylogenetic analysis.....	89
4.4 Results	90
4.4.1 Opsin gene sequences.....	90
4.4.2 Opsin gene expression.....	98
4.4.3 Microspectrophotometry (MSP).....	99
4.4.4 Genomic sequencing.....	100
4.5 Discussion.....	103
4.5.1 Dynamic opsin evolution in Characiformes	103
4.5.2 Opsin neofunctionalization: evolution of spectral tuning and opsin gene expression	105
4.5.3 Opsins and characins phylogenetics	109
4.6 Conclusions	110
4.7 Acknowledgements	111
Chapter 5: Behavioral color vision in a cichlid fish: <i>Metriaclima benetos</i> ...	113
5.1 Abstract.....	114
5.2 Introduction	115

5.3 Materials and methods.....	118
5.3.1 Data measurements	118
5.3.2 Behavioral approach	119
5.3.3 Fish training.....	120
5.3.4 Fish care.....	121
5.3.5 Experiment 1: Binary choice.....	121
5.3.6 Experiment 2: multiple-choice gray	122
5.3.7 Experiment 3: multiple-choice color	122
5.3.7 Data analysis.....	123
5.3.8 Differential interference contrast (DIC) images of <i>M. benetos</i> cone photoreceptors	123
5.3.9 Visual modeling	124
5.4 Results	129
5.4.1 Stimuli, illumination, and visual system properties	129
5.4.2 Experiment 1: binary choice	129
5.4.3 Experiment 2 & 3: multiple-choice.....	130
5.4.4 Quantum catches	131
5.4.5 Chromatic distances	132
5.5 Discussion.....	137
5.5.1 Cichlid behavior	137
5.5.2 Color opponency and opsin coexpression	138
5.5.3 Color discrimination and the Weber fraction	143
5.5.4 Color vision and its relationship with cichlid ecology and evolution	147
5.6 Conclusions	149
5.7 Acknowledgements.....	150
Chapter 6: Behavioral color thresholds in a cichlid fish: <i>Metriaclima benetos</i>	151
6.1 Abstract.....	152
6.2 Introduction	153
6.3 Methods	157
6.3.1 Behavioral approach and fish training	157
6.3.2 Visual modeling	159
6.4.2 Calibration of colored stimuli and quantum catch.....	162
6.4.3 Experiment 1: Color threshold between blue and purple	164
6.4.4 Experiment 2: Multiple choice with brightness variation.....	165
6.4.5 Experiment 3: Color threshold with different background illumination	166
6.4.6 Experiment 4: Cichlid visual modeling in Lake Malawi.....	167
6.4.7 Data analysis.....	168
6.5 Results	169
6.5.1 Experiment 1: Color threshold between blue and purple	169
6.5.2 Experiment 2: Multiple choice with brightness variation.....	170
6.5.3 Experiment 3: Color threshold with different background illumination	170
6.5.4 Experiment 4: Cichlid visual modeling in Lake Malawi.....	174

6.6 Discussion.....	174
6.6.1 Color thresholds and receptor noise	174
6.6.2 Color discrimination under different background illumination	176
6.6.3 Individual performance variation	178
6.6.4 Visual ecology in Malawi	180
6.6.5 Future directions.....	182
6.7 Conclusions	183
6.8 Acknowledgements.....	184
Chapter 7: Synthesis	185
7.1 Introduction	185
7.2 Opsin gene evolution in Neotropical cichlids	185
7.3 Opsin Expression in Neotropical cichlids	187
7.4 Visual pigment evolution in Neotropical Characiformes.....	192
7.5 Fish visual pigment diversity and future directions	193
7.6 Cichlid behavioral color vision.....	195
7.7 Cichlid visual palettes and future directions.....	196
Appendix A: Supplementary material Chapter 2	200
Appendix B: Supplementary material Chapter 3	200
Appendix C: Supplementary material Chapter 4	201
Appendix D: Supplementary material Chapter 5	217
Appendix E: Supplementary material Chapter 6	218
Glossary.....	225
Bibliography	227

List of Tables

Table 2.1: Opsin gene classes across species	22
Table 2.2: Summary of South American cichlids variation	30
Table 2.3: Distances between sequences ($dACi$, $dBCi$), for nonsynonymous and synonymous sites ($l = ns$ or s , as substitutions per site), rates of non-synonymous and synonymous substitutions (a_i , in substitutions per site per year), and time since pseudogenization (Tn given in My). Ψ denotes pseudogenes	31
Table 3.1: Range of cone and rod visual pigment peak sensitivities (λ_{max}) measured in <i>C. monocolus</i> with micro-spectrophotometry. Vitamin A_1 proportion was estimated from the reference 100% A_1 nomograms and the corresponding 100% A_2 nomograms obtained from Whitmore & Bowmaker's (1989) equation (see main text)	59
Table 3.2: Amino acid substitutions between <i>C. monocolus</i> vs <i>O. niloticus</i>	62
Table 3.3: Amino acid substitution variation between Neotropical cichlids (<i>A. ocellatus</i> , <i>S. discus</i> , <i>P. scalare</i> and <i>C. frenata</i>)	62
Table 4.1: Range of cone and rod visual pigment peak sensitivities (λ_{max})	101
Table 4.2: Cone and rod λ_{max} based on pure chromophore type	101

List of Figures

Figure 1.1: Visual scene of a fish.....	6
Figure 1.2: Spectral tuning mechanisms and adaptations	7
Figure 2.1: Opsin maximum-likelihood phylogenetic tree of Cichlids	24
Figure 2.2: RH2A gene conversion scenario	26
Figure 2.3: Relative cone opsin expression profiles of <i>P. scalare</i> , <i>S. discus</i> and <i>A. ocellatus</i>	27
Figure 2.4: Amino acid substitution variation for each opsin class of the three species.....	29
Figure 2.5: Schematic representation of visual system adaptation in a phylogenetic context.....	40
Figure 3.1: Map showing the light sampling localities around BCI.....	50
Figure 3.2: Underwater light environment variation around Barro Colorado Island in Lake Gatun, Panama Canal	56
Figure 3.3: Ocular media transmission measurements in <i>C. monocolus</i> .	58
Figure 3.4: Rod spectral sensitivity variation	60
Figure 3.5: Opsin and Cyp27c1 expression	64
Figure 4.1: LWS-opsin tree of Characiformes	92
Figure 4.2: RH1-RH2-opsin tree of Characiformes	93
Figure 4.3: Opsin gene complement in Characiformes	94
Figure 4.4: Number of sites with amino-acid substitution variation for each opsin class of 15 Characiformes species	95
Figure 4.5: Ancestral state reconstruction of spectral tuning in LWS-opsin-genes	97
Figure 4.6: Opsin expression in Characiformes	99
Figure 4.7: Microspectrophotometry of Characiformes.....	102
Figure 5.1: Reflectance spectra, side-dwelling irradiance, lens transmission and cone sensitivities	130
Figure 5.2: Proportion of times the stimuli was chosen correctly in the first binary choice experiment	135
Figure 5.3: Proportion of times the stimuli were chosen correctly for multiple-choice experiments.....	136
Figure 5.4: Normalized quantum catch of colors in Experiments 1, 2 & 3	142
Figure 5.5: Chromatic distances, ΔS (JNDs), of colors in experiments 1 and 2	146
Figure 5.6: Chromatic distances, ΔS (JNDs), of colors in experiment 3	147
Figure 6.1: Spectral parameters for color thresholds experiments	162

Figure 6.2: Quantum catch of colors from thresholds experiments	165
Figure 6.3: Color discrimination in the three experiments	172
Figure 6.4: Variation of ΔS of cichlid-blue vs. backgrounds and other cichlid-colors	173
Figure 6.5: Variation under different light illumination of ΔS between colors vs. background and correct choice frequency	180
Figure 7.1: Opsin gene expression of Neotropical and African cichlids in a phylogenetic context	189
Figure 7.2: Spectral absorbance (λ_{max}) of visual pigments across Neotropical and African cichlids	191
Figure 7.3: Range of the main spectral sensitivities (λ_{max}) of an Amazonian cichlid, the peacock-bass (<i>Cichla monoculus</i>), relative to the downwelling irradiance of incoming light at sub-surface (below 1 m) in Amazonian Rivers	192
Figure 7.4: Spectral absorbance (λ_{max}) of visual pigments across Neotropical Otophysans	195
Figure 7.5: Normalized quantum catch of colors from Lake Malawi (Chapter 6) for each visual palette	197
Figure 7.6: Chromatic distances (ΔS) are given of the blue-hue of <i>M. benetos</i> vs. Lake Malawi colors	199

Chapter 1: Introduction

1.1 Introduction

Animal communication is based on the use of signals where the emitter conveys information to the receiver. This inevitably leads to the evolution of efficient signal production and reception [1]. Within visual communication there is great diversity in animal color patterns and evolutionary biology aims to understand the selective mechanisms shaping such diversity. Coloration patterns are essential for animal communication where color signals are mediated through color vision. Consequently, visual systems need to optimally discriminate color in order to accurately receive and process color signals. Since vision research has characterized a number of visual systems that view different color signals in different environments, this makes color vision a suitable model for understanding evolution.

Furthermore, animal color vision can also be examined in the context of visual ecology. Color vision relies on the absorption of photons by spectrally different visual-pigments, however, more photons can be absorbed at some wavelengths than at others [2]. This is because there is great heterogeneity in light environments that inevitably creates variation in the best visual system to absorb photons at specific wavelengths. Animals often match their spectral sensitivities to the available wavelengths in their habitats and this correlation has been termed the 'sensitivity hypothesis' [2]. Although the spectral match to the light

environment has been observed in animals with a single type of visual pigment, many animals with spectrally different visual pigments (color vision) often follow the same pattern.

Overall, color vision is part of animal communication, with several interacting factors such as color patterns, the environment, as well as the signalers and receivers. Thus, color vision research provides the unique opportunity to better understand how evolution influences color signals and the environmental adaptations of visual systems.

1.2 Color vision

1.2.1 Color in nature

The capacity of an organism to obtain information from the environment is essential for its survival and among sensory channels photodetection is one of the most complex and studied senses. As a result of the evolution of sensing light, animals have evolved sensitivity to spectral wavelengths (colors) and hence the ability to discriminate colors (color vision). Consequently, as animal coloration patterns arise, color sensitive animals exploit this capacity in order to survive. Color vision is involved in numerous behaviors mediated by animal coloration: inter- and conspecific interactions, finding mates, predators and prey detection, and foraging, among others. Therefore, color vision and animal coloration are strongly interconnected and research is divided between four major topics:

production, perception, function and application. In this dissertation, we will focus primarily on the perception of color.

The scope of disciplines involved in tackling color vision research are quite broad as its study encompasses the approach from several fields like optical physics, genetics, physiology, psychology, functional morphology, behavioral ecology and evolution [3]. Thus, due to the interdisciplinary nature of this research, scientists studying color vision have to develop an integrative approach. Certainly, color vision is an expanding research field where the way scientists tackle questions has become broader by analyzing evolutionary patterns through proximate and ultimate causation. This dissertation analyzes chromatic perception in fish and thus, their capacity to discriminate color in nature.

1.2.2. Detecting light and colors

Vision starts as light reflected from color patterns, background illumination (where color patterns are not of interest) and veiling light [4] are collected by the eye. Light is refracted by the cornea and lens, the ocular media, and ultimately reaches the retina. In the retina, light is detected by rod and cone photoreceptors. Night vision (scotopic) is mediated by rods, whereas bright diurnal vision (photopic), including color vision, is mediated by cones [5]. Photoreceptors are packed with visual pigments which are composed of an apoprotein, the opsin, which is covalently bound to a light sensitive chromophore,

11-cis-retinal [6,7]. Typically there are multiple cone types containing different visual pigments that absorb light maximally in different parts of the wavelength spectrum. As photons excite the chromophore, it photoisomerizes from 11-cis to all-trans retinal inducing a conformational change in the opsin protein that initiates the phototransduction cascade and ultimately generates a neural signal. This photoreceptor signal interacts with other major classes of retinal neurons: bipolar, horizontal, amacrine and ganglion cells. The axons of the latter are the output of the retina as they form the optic nerve and transmit the information to the visual centers of the brain [8].

Having color vision implies two basic requirements: (1) an animal has to possess photoreceptors with different spectral sensitivities, and (2) it must have a mechanism to compare the signals of these photoreceptors types [9]. Therefore, color vision is the product of neural comparison of photoreceptor signals [10]. The comparison of these signals are said to be “opponent interactions” where color opponency is the basis for color vision.

1.3 Visual systems in fish

Fish are ideal for the study of color vision evolution for two main reasons. First, they inhabit a diverse range of habitats. Because of the physicochemical properties of water, this medium has a profound effect on light transmission. Water absorbs and scatters much of the incoming light, which has a dramatic effect on the intensity, spectral composition, angular distribution and degree of

polarized light with increasing depth [11]. Therefore, as underwater visual perception is mediated by the propagation of light, color vision is a process that depends on multiple optical components. For example, in an aquatic visual scene, objects are mainly illuminated from above by light that has been scattered, with a spectrum and intensity affected by attenuation and depth. As light is scattered throughout the aquatic environment, the object is also illuminated by horizontal and upwelling light. Thus, the visual-stimulus reaching the observer's eye is mediated through side welling irradiance that depends on several factors (Fig. 1.1). All of this inevitably causes great variation across aquatic habitats and the heterogeneous nature of the aquatic light environment is reflected in the several adaptations fish eyes exhibit to "see" in such environments. Indeed, several of these adaptations arose as a way to enhance light detection. For example, fish exhibit a variety of optical filters in ocular media (cornea, vitreous and lens) to fine tune the light reaching the retina [12–18]. Another adaptation is the patterning and organization of the retinal-mosaic, which is believed to enhance light detection. This can be achieved by regionalized expression of visual pigments in specific areas of the retina in order to match the wavelengths reaching that visual field, or, by increasing photoreceptor density in the central retina in order to improve visual acuity [19–23], (Fig. 1.2).

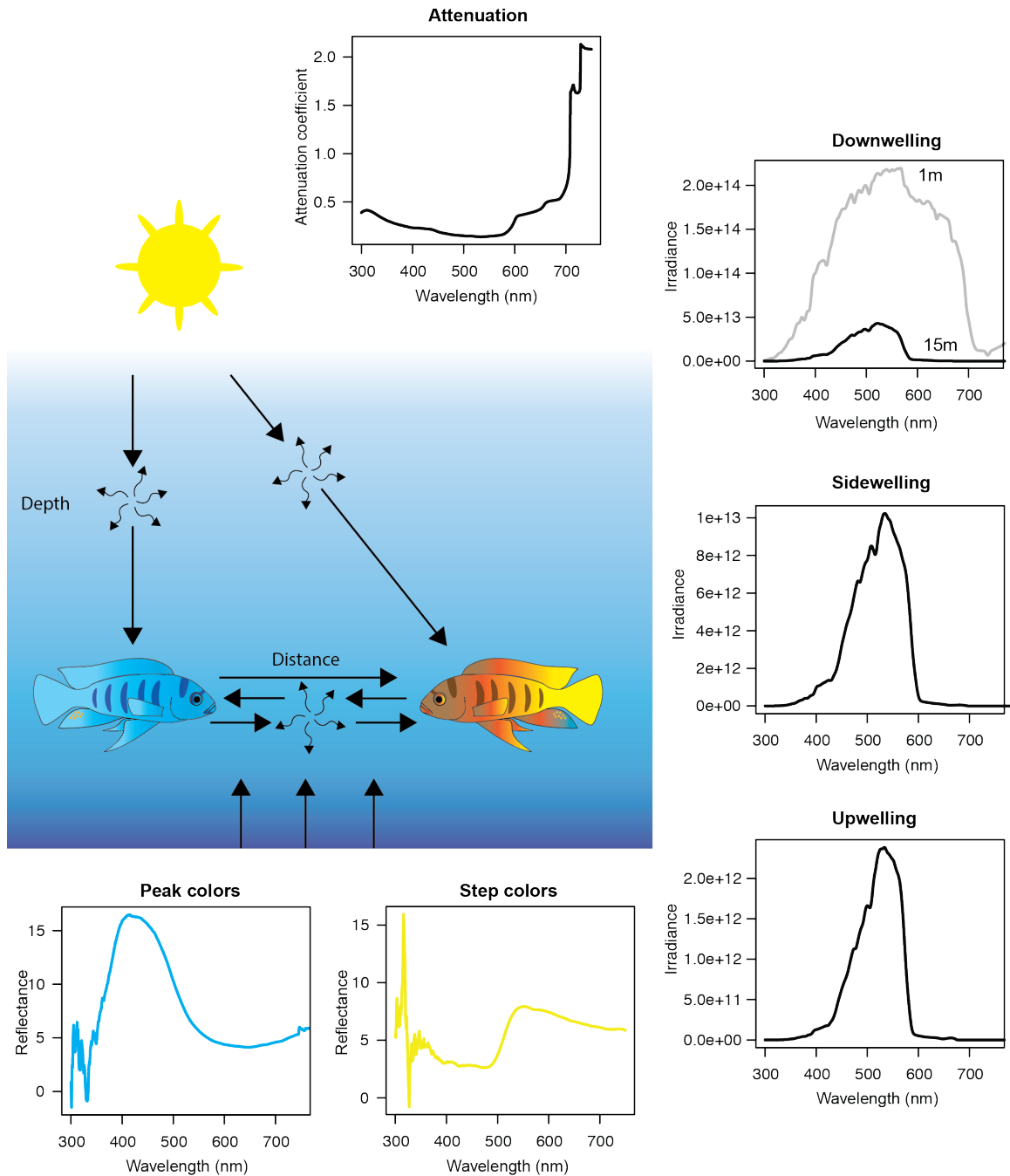


Figure 1.1. Visual scene of a fish. The object (i.e. a fish) is illuminated directly from above (down-welling) where the amount of light reaching the object depends on attenuation, depth, and scattering. Since there are multiple scattering events (curved arrows), the object is also illuminated from horizontal light (side-welling) and from below (up-welling) as light reflects from the bottom too. The visual-stimulus reaching the observer's eye is a combination of light scattered in the water and light reflected from the object (e.g. fish colors (yellow, blue)).

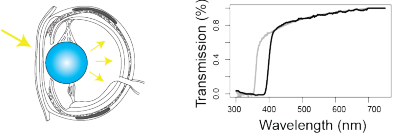
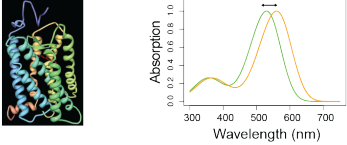
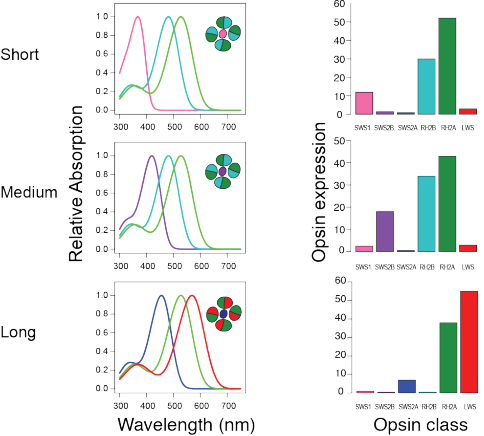
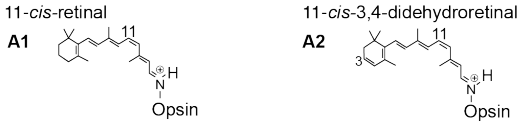
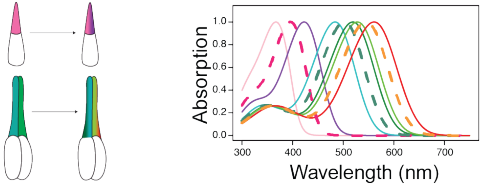
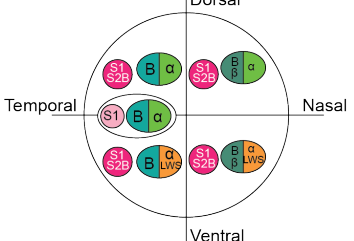
<p>A. Ocular media: Lenses, cornea, and vitreous humour modulate light transmission. Ocular media can filter specific wavelengths and hence, the light that reaches the retina. For example, fishes can have UV-transmissive (gray) and UV-blocking lenses (black)</p>	
<p>B. Opsin sequence tuning: Opsin sequence amino acid variation can have an effect on spectral tuning, particularly if amino acid replacements occur in binding pocket sites where the chromophore lies, and whether the replaced amino acids vary in polarity. To the right, representation of spectral tuning shift due to opsin sequence; to the left, opsin putative structure.</p>	
<p>C. Opsin gene expression: large differences in spectral sensitivities can occur because of differences in opsin gene expression. For example, cichlid species express different sets of opsins from the seven cone opsin genes they possess in their genomes. In addition, the three common combinations (short, medium & long) of expressed opsins may create variability in the colors these fish perceive. To the right, opsin expression of the three palettes; to the left, peak absorbance product of opsin expression.</p>	
<p>D. Chromophore tuning: Fish can switch from chromophore A1 to A2. Switching chromophores can create large shifts spectral sensitivity where visual pigments based on A2-chromophores are long wavelength shifted.</p>	
<p>E. Opsin coexpression: Opsin coexpression can have different effects on color vision because two opsins in the same photoreceptor would shift its peak absorbance (Dashed lines denote the peak absorbance product of coexpression showing the spectral shift from a pure opsin expression: solid lines)</p>	
<p>F. Retinal variation of spectral sensitivity: There can be differences of spectral sensitivity in the retina because there is regional retinal variation of opsin expression and coexpression. In addition, there are different opsin coexpression combinations in different regions of the retina. All of this can have an effect on color vision as some colors could be more or less contrasting from different regions in the retina. Each symbol denotes a different opsin and whenever they are in the same oval/circle it denotes coexpression. Note the different expressed opsins in different parts of the retina</p>	

Figure 1.2. Spectral tuning mechanisms and adaptations that modulate light reaching the fish retina. Information from [12,14,20,24–27].

Second, due to their phylogenetic history, species richness, diverse ecologies, and diverse spectral sensitivities, teleosts offer an excellent system for studying the evolution of color vision. Spectral sensitivities have been documented for hundreds of fish species [18,26,28–31] and the genetic mechanisms producing such variation have been extensively studied for several years. Furthermore, much is known about the dynamic evolution of the different opsin classes in teleosts [6,7,32–36] and the different spectral tuning mechanisms fish employ to shift their spectral sensitivities (Fig. 1.2). Finally, the dimensionality and adaptive significance of color vision in teleosts has been studied through decision-making behavioral experiments for more than a century, from von Frisch studying colored-light detection in minnows [37], to Cheney et al., analyzing color thresholds through Ishihara tests in the Picasso triggerfish [38]. Behavioral experiments mediated through visual tasks are very important as they can demonstrate whether fish have chromatic discrimination. Since physiology, psychology and molecular biology shape color vision, behavioral experiments are a powerful tool for scientists because they can test different hypotheses based on these disciplines.

Altogether, color vision research has produced a tractable genotype to phenotype map, and it is an expanding field where integrative approaches analyzing proximate and ultimate causations are necessary to understand the different mechanisms underlying color vision and its relationship with animal coloration.

1.4 Goals of research

Despite the vast research on color vision evolution, several diverse fish-lineages are vastly underrepresented. Increasing the knowledge of such groups is important as it can shed light on evolutionary patterns of the different traits influencing color vision. Taking advantage of the extensive research about the genetic basis of color vision in African cichlids, my goal is to identify the key mechanisms underlying color vision in non-model teleosts. In order to understand the proximate and ultimate causation of color vision in tropical freshwater fish, I have studied several components that shape their color vision evolution. My first set of studies focus on the genetic mechanisms underlying variation in fish visual sensitivities. In Chapter 2, I examine the visual system of three Amazonian cichlids through genome and transcriptome analyses. The dynamic evolution of their opsin genes and the ecological adaptations of their visual system are also discussed. In Chapter 3, I analyze the visual system plasticity of an invasive Neotropical cichlid species, the peacock-bass (*Cichla monoculus*). Through differential gene expression analysis and electrophysiological experiments, I demonstrate how this species adapts to a turbidity gradient in Lake Gatun, in the Panama Canal. In chapter 4, I examine the genetic basis for color vision evolution in Neotropical Characiformes. Through molecular and electrophysiological experiments, I disentangle the spectral tuning mechanisms in this group.

Generally, a lot more is known about the molecular components that modulate fish color vision, than the behavioral implications. In the remaining chapters I developed hypotheses based on previous knowledge and tested for chromatic discrimination through behavioral experiments. In Chapter 5, I demonstrate that cichlids possess chromatic discrimination through trials based on visual tasks. In this study I trained fish to discriminate colored stimuli and tested their ability to discriminate the rewarded stimuli from several distracter stimuli while controlling for brightness. In Chapter 6, I perform behavioral experiments and visual modeling in order to find the color thresholds in cichlids. For this I employed the Receptor Noise Limited model, and calibrated several stimuli that increased in chromatic distance from the rewarded stimulus. I performed these experiments in order to find the color thresholds in cichlids. The implications of our findings are discussed in relationship to the cichlid-visual-ecology in Lake Malawi. Lastly, in Chapter 7, I synthesize the main results obtained from this body of work and provide recommendations for future studies.

Chapter 2: The opsin genes of Amazonian cichlids

Previously published under: Daniel Escobar-Camacho, Erica Ramos, Cesar Martins and Karen L Carleton. The Opsin Genes of Amazonian Cichlids. *Molecular Ecology*; 2017, 25, 1343-1356

2.1 Abstract

Vision is a critical sense for organismal survival with visual sensitivities strongly shaped by the environment. Some freshwater fishes with a Gondwanan origin are distributed in both South American rivers including the Amazon and African rivers and lakes. These different habitats likely required adaptations to murky and clear environments. In this study, we compare the molecular basis of Amazonian and African cichlid fishes' visual systems. We used next-generation sequencing of genomes and retinal transcriptomes to examine three Amazonian cichlid species. Genome assemblies revealed six cone opsin classes (SWS1, SWS2B, SWS2A, RH2B, RH2A and LWS) and rod opsin (RH1). However, the functionality of these genes varies across species with different pseudogenes found in different species. Our results support evidence of an RH2A gene duplication event that is shared across both cichlid groups, but which was probably followed by gene conversion. Transcriptome analyses show that Amazonian species mainly express three opsin classes (SWS2A, RH2A and LWS), which likely are a good match to the long-wavelength-oriented light environment of the Amazon basin. Furthermore, analysis of amino acid sequences suggests that the short-wavelength-sensitive genes (SWS2B, SWS2A) may be under selective

pressures to shift their spectral properties to a longer-wavelength visual palette. Our results agree with the 'sensitivity hypothesis' where the light environment causes visual adaptation. Amazonian cichlid visual systems are likely adapting through gene expression, gene loss and possibly spectral tuning of opsin sequences. Such mechanisms may be shared across the Amazonian fish fauna.

2.2 Background

Sensory capabilities play a major role in an individual's fitness because they specify a channel through which information from the environment is transmitted to the organism [1]. Vision plays a role in mediating behaviours like foraging, mating, social interactions with conspecifics and predator avoidance. In vertebrates, visual perception begins when light reaches the retina and is detected by the photoreceptive rods and cones. These photoreceptors contain visual pigments composed of a transmembrane protein, opsin, bound to a light-sensitive chromophore. Visual pigment spectral sensitivities can vary due to the type of chromophore (derived from either vitamin A₁ or A₂), and the chromophore's interaction with opsin amino acid residues facing the retinal binding pocket [6,39]. Therefore, opsins are the main components controlling the spectral response of the first step in the visual transduction cascade. Visual systems in fishes are particularly interesting because of the remarkable diversity of visual pigments and the proximate mechanisms that underlie their evolution. Genetic mechanisms that contribute to visual pigment diversity are sequence evolution,

differential gene expression, gene duplication and gene conversion [32,33,36]. Selective pressures from the environment greatly influence fish spectral sensitivities, providing ultimate causation for visual sensitivity shifts to better match environmental light. Cichlids, a diverse group of percomorph fishes with a Gondwanan distribution, are a prime example of teleost visual pigment diversity. Vision research on cichlid flocks from the great African Lakes has identified the genetic basis of their visual sensitivities resulting from seven spectrally distinct cone opsins and a rod opsin gene [26]. The cone opsins belong to four cone opsin classes including UV-sensitive (SWS1), short-wavelength-sensitive (SWS2A, SWS2B), rod opsin-like (RH2Aa, RH2Ab, RH2B) and long-wavelength-sensitive (LWS) opsins [27]. Cichlids typically express three different opsin combinations termed short (SWS1, RH2A, RH2B), medium (SWS2B, RH2A, RH2B) and long (SW2A, RH2A, LWS) [40]. These combinations are believed to match the available light in a particular environment. For example, the “long” combination would be suited to a long-wavelength-shifted environment like turbid waters [41]. While vision in African cichlids has been studied extensively, little is known about vision in Neotropical cichlid lineages. A previous study analyzed the visual system of the Trinidadian pike, *Crenicichla frenata*, and found that this species has a reduced opsin complement where SWS1 has been lost and RH2B pseudogenized [42]. Furthermore, a rod opsin study in Neotropical cichlids suggested there is divergent selection on this gene across cichlid lineages probably caused by ecologically and/or biogeographic differences [43]. Indeed, Neotropical cichlids live in more highly contrasting light environments than clear

African lakes species. In South America, rivers in the Amazon basin can be classified based on water colour (white, black and clear). This is a product of different physicochemical and geological properties of their catchments, as well as rainfall, soil and vegetation which results in water bodies with different concentrations of particulates and dissolved compounds. White water rivers exhibit high quantities of inorganic suspended particles, black water rivers have high concentrations of dissolved organic matter, and clear water rivers are low in both dissolved organic matter and inorganic suspended particles (Costa et al. 2012; Sawakuchi et al. 2016). Thus, Amazonian rivers display an adverse visual environment for fish due to large amounts of suspended particles and dissolved substances that absorb most of the incoming light creating an extremely long-wavelength-shifted light environment. These light conditions may have an effect on the phenotypic adaptation of Amazonian cichlids. Muntz (1973, 1982) studied visual sensitivities of Amazonian fishes and found that several cichlids had ocular media with yellow pigments. Such pigments filter short wavelengths of the incoming light to the retina, reducing the detected level of background scattered light and serving as visual adaptations to the long-wavelength light environments [17,18]. Vision research in Neotropical cichlids is important because it offers a unique opportunity to analyse the evolution of the visual system in different ecosystems within the same cichlid lineage. In this study, we investigated the opsin complement of three Amazonian cichlids. We examined whole genomes and retinal transcriptomes of *Pterophyllum scalare* (Angelfish), *Symphysodon discus* (Discus) and *Astronotus ocellatus* (Oscar) to (1) examine the genomic

opsin palette, (2) analyse their opsin gene expression and (3) discuss the evolution of these species' visual system under the influence of the Amazon environment. Based on next-generation genomic and RNA sequencing, phylogenetic and opsin sequence analysis suggests dynamic evolution of opsin genes between lineages and a “long”-opsin expression profile that is consistent with potential adaptations to Amazonian rivers.

2.3 Materials and Methods

For whole genome sequencing, fish were caught from the Amazon basin (Table S3, Supporting information). Sampling permits were in accordance with Brazilian laws for environmental protection (wild collection permit, ICMBio 22984-1 e 32556-2), and specimens stocked at INPA (National Amazon Institute of Research, Manaus – AM, Brazil). The geographic coordinates of the collected points were 0°52'02.29"S/62°48'035.61"W for *S. discus* and 3°09'043.00'S/59°54'059.40'W for *P. scalare* and *A. ocellatus*. Fish were euthanized through immersion in a benzocaine (250 mg/L) water bath for 10 min, according to the International Guidelines of Sao Paulo State University approved by the Institutional Animal Care and Use Committee (IACUC) (Protocol no. 34/08 – CEEA/IBB/UNESP). For RNAseq, fish were obtained from the aquarium trade and were around five months old. Fish were euthanized with buffered MS-222 according to the University of Maryland (UM) IACUC-approved protocols (R12-90).

2.3.1 Genome analysis

Muscle tissue from two fish (female and male) was used for DNA extraction [44]. Whole genome sequencing was performed through paired-end library preparation (Truseq DNA Library Preparation Kit) and sequenced on an Illumina HiSeq1500 platform. Obtained reads (150 bp length) were trimmed based on base pair sequencing quality (minimum 90% of read base pairs with Phred quality score greater than 30) and removal of sequencing adaptors using FASTX-Toolkit (http://hannonlab.cshl.edu/fastx_toolkit/index.html) and in-house scripts. The trimmed reads were assembled with Velvet [45] using a k-mer value estimated by KmerGenie [46]. Finally, the assembled contigs were evaluated using the CEGMA pipeline [47] and Assemblathon2 scripts [48].

2.3.2 RNA analysis

To ensure high-quality transcriptome assemblies, one specimen of each species was used for transcriptomes. Fish eyes were enucleated, and retinas including retinal pigment epithelia were dissected out and preserved in RNAlater. RNA was isolated from two whole retinas for each species. Total RNA was extracted with an RNeasy kit (Qiagen), and RNA quality was verified on an Agilent Bioanalyzer. RNAseq libraries were made using the Illumina TruSeq RNA library preparation kit (Illumina Inc, San Diego) by the UM Institute for Bioscience & Biotechnology Research sequencing core, and 100-bp paired-end reads were obtained on an Illumina HiSeq1500 sequencer with samples multiplexed in one lane. The data were quality-checked using FastQC version 0.10.1. Data were trimmed using

Trimmomatic version 0.32 [49] to remove over-represented sequences and to retain sequences with a minimum quality score of 20 and a minimum length of 80 bp. The final assembly was performed using Trinity version r20140413 [50] using only paired sequences with a minimum coverage of two to join contigs.

2.3.3 Opsin sequencing by PCR

We used two additional aquarium trade individuals of each species for genomic DNA sequencing. If transcripts or contigs of a certain opsin were incomplete, primers were designed and the complete opsin sequence was recovered with PCR and Sanger sequencing (Table S4, Supporting information). DNA was extracted with a DNeasy kit (Qiagen), and DNA quality was verified in a spectrometer.

2.3.4 Phylogenetic trees

Putative opsin sequences of the three South American cichlids were identified from genome and transcriptome assembled FASTA files by Tblastx querying with the cichlid opsin genes of *Oreochromis niloticus* [40]. We confirmed that sequences for each species were assigned to a particular opsin class based on phylogenetic relationships of the opsin sequences with those from other teleost lineages obtained from GenBank (*Danio rerio*, *Lucania goodei*, *Oryzias latipes*, *Oreochromis niloticus*, *Metriaclima zebra*, *Neolamprologus brichardi*, *Pundamilia nyererei*) [51]. We used MAFFT [52] to align nucleotide sequences, and GARLI

for building maximum-likelihood trees. We ran 10 searches for the best tree and 2000 bootstrap replicates performed at the GARLI 2.0 [53] web service (molecularevolution.org [54]).

2.3.5 Gene expression

For estimating gene expression of each opsin, reads were mapped back to the assembled transcripts using RSEM as part of the Trinity package [50]. Read counts for each opsin class were extracted from the RSEM output (quantified as fragments per kilobase of transcript per million reads, FPKM). Cone opsin read counts were normalized by dividing the sum of all the cone opsin genes to get the proportion of each expressed opsin. For RH2A duplicates, we used GENEIOUS 8.1 to map reads to the distinct first exons to estimate expression levels.

2.3.6 Spectral sensitivities

To determine potential tuning sites, we aligned South American cichlid opsin sequences of each opsin class with bovine rhodopsin (GenBank. NP_001014890.1) and compared them to known spectral tuning sites [6,55]. We also aligned opsin sequences to *O. niloticus* and *C. frenata* for which λ_{\max} and opsin gene sequences have been characterized [40,42]. The alignments were analysed to identify amino acid substitutions that fell in the putative opsin transmembrane regions and the retinal binding pocket facing the chromophore

(Appendix S1, Appendix A) [56]. Substitutions that involve changes in amino acid polarity could alter interactions and potentially create a shift in peak absorption, tuning the sensitivity of the visual pigment. Substitutions were examined only in functional genes to determine their variability in physicochemical properties.

2.3.7 Pseudogenes divergence times

Because pseudogenes were discovered in our analysis, we wanted to estimate when they emerged. For this, we modified the method from Li et al. 1981 (Fig. S10, Appendix A). This method is based on the assumption that the rate of change in a gene's synonymous positions is faster than for its nonsynonymous positions. However, in a pseudogene, the lack of selective constraint causes the rates of change for both positions to be the same. Hence, the increase in pseudogene nucleotide substitutions can be used to determine how long ago this increased rate began [57]. For both the SWS1 and SWS2B opsins, we aligned the nucleotide sequences of one pseudogene (gene A) and two functional genes (genes B and C). Fig. S10 (Appendix A) shows the plausible evolutionary outline for functional opsins and pseudogenes with *O. niloticus* (C) as the more distant lineage. Insertions and deletions that were not shared between pseudogenes and the functional opsin genes were excluded. Proportions of synonymous and nonsynonymous sites were estimated between taxa using MEGA6 [58]. These were corrected for multiple hits using a Jukes–Cantor model to determine DNA sequence differences, d_{ABi} , d_{ACi} and d_{BCi} for $i = s$ or ns [59]. These were then used to calculate the distance difference (y_i) between pseudogenes and

functional genes (eqn 1a). Rates of synonymous and nonsynonymous substitutions per year, a_s and a_{ns} , were calculated based on the divergence time (T_1) between C and the other sequences (A or B) (eqn 1b). For T_1 , we used the divergence time of *O. niloticus* and Neotropical cichlids (77.2 Mya; timetree.org). From these equations, we calculated the time (T_n) since pseudogenization, Eqn 1c.

$$y_{ns} = d_{ACns} - d_{BCns} \quad y_s = d_{ACs} - d_{BCs} \quad (\text{eqn 1a})$$

$$a_{ns} = d_{BCns}/T_1 \quad a_s = d_{BCs}/T_1 \quad (\text{eqn 1b})$$

$$T_n = (y_{ns}-y_s)/(a_s-a_{ns}) \quad (\text{eqn 1c})$$

2.4 Results

2.4.1 Opsin genomic sequences

Genomes were assembled from three Amazonian cichlids including *P. scalare* (1.088 Gb; scaffold N50 7.559 bp), *S. discus* (0.684 Gb; scaffold N50 2.221 bp) and *A. ocellatus* (1.007 Gb; scaffold N50 7.659 bp) (Escobar-Camacho et al. 2016, Ramos et al. unpublished). Blasting the three genomes identified members of six cone opsin classes (SWS1, SWS2B, SWS2A, RH2B, RH2A and LWS) as well as rod opsin (RH1). SWS1, SWS2B and SWS2A opsin genes contained gaps in some species, while RH2B was incomplete in all three genomes. The missing sequences for the SWS genes were recovered by PCR and sequencing using primers based on adjacent regions of each gap, using primers for other species where the opsin genes were present, or the transcriptomes (NCBI

Accession nos in Table S1, Supporting information). Examination of the complete opsin sequences revealed the presence of at least one pseudogene in all three species. These occurred among different opsin classes (Table 2.1). SWS1 is pseudogenized in *A. ocellatus* exhibiting a 4-bp frame shifting insertion in the second exon (position 450) leading to numerous stop codons as well as a codon insertion in the third exon (position 634) (Fig. S1, Appendix A). SWS2B opsin is a pseudogene in *S. discus* with two deletions and a single-bp insertion in the first exon (positions 59 & 303, respectively) (Fig. S2, Appendix A). The single nucleotide insertion seems to be polymorphic as one specimen had it, while others did not. The SWS1 pseudogene of *A. ocellatus* was only found in the genome, whereas the SWS2B pseudogene in *S. discus* was present in the genome and the transcriptome. RH2B appears to be pseudogenized in *P. scalare*, *S. discus* and *A. ocellatus* for both genome and aquarium trade individuals. Despite significant effort, the complete sequence of RH2B was not fully recovered for most species, perhaps as a result of it being pseudogenized. In *P. scalare*, only half of the coding region of RH2B was recovered with a 14-bp deletion in the last exon (Fig. S3, Appendix A), whereas in *S. discus*, a single-bp insertion (position 163) in the first exon was present that caused numerous stop codons (Fig. S4, Appendix A). RH2B in *A. ocellatus* has a 13-bp insertion and 9-bp deletion in the first exon causing a premature stop codon in the first exon (Fig. S5, Appendix A). Overall, it seems that RH2B is a pseudogene in all three species. Further, these data suggest that RH2B mutations were acquired

separately in each of the three species, although we could be overlooking a shared common pseudogenization event.

Table 2.1. Opsin gene classes across species

Species	Opsins						
	SWS1	SWS2B	SWS2A	RH2B	RH2	LWS	RH1
<i>Pterophylum scalare</i>	✓	✓	✓	Ψ	✓ ^A	✓	✓
<i>Symphysodon discus</i>	✓	Ψ	✓	Ψ	✓	✓	✓
<i>Astronotus ocellatus</i>	Ψ	✓	✓	Ψ	✓	✓	✓

[†]Opsin genes are sorted by increasing spectral sensitivity. Ψ denotes pseudogenes.

2.4.2 Opsin RNA seq

Retina samples run on the Agilent Bioanalyzer had RIN (RNA integrity number) values that varied between 7.70 and 9.60. The RNAseq data obtained by multiplexing these retinal samples provided sufficient data to assemble and quantify opsin transcripts. We obtained 71.0, 64.5 and 70.9 M reads for *P. scalare*, *S. discus* and *A. ocellatus*, respectively, and after trimming used, 45.1, 38.5 and 34 M reads for the assemblies. RNAseq reads were submitted to the SRA database (SUB2057474). Amazonian cichlid RNAseq isolated four cone opsins: SWS2A, SWS2B, RH2A and LWS, as well as rod opsin, RH1. These were all complete transcripts except for SWS2B, which had lower transcript abundance in comparison with the other opsins. The SWS2A, RH2A, LWS and RH1 transcripts were verified with genome sequence and matched nearly exactly. There were a few SNPs as the individuals were different between RNA-seq and genomic sequencing (Table S5, Supporting information).

2.4.3 Phylogenetic trees

Maximum-likelihood trees based on these three Amazonian species as well as from *C. frenata* confirmed the identities of all South American cichlids opsins: SWS1, SWS2B, SWS2A, RH2B, RH2A, LWS and RH1. The cichlid opsin lineages are reciprocally monophyletic between the New World and African lineages, with New World opsins placed as sister groups to the respective Nile *Tilapia* orthologs in all opsin classes. *P. scalare* and *S. discus* were placed together in the SWS1, SWS2B, SWS2A and LWS opsin clades. Opsins of *C. frenata* were also nested within the South American clade (Fig. 2.1).

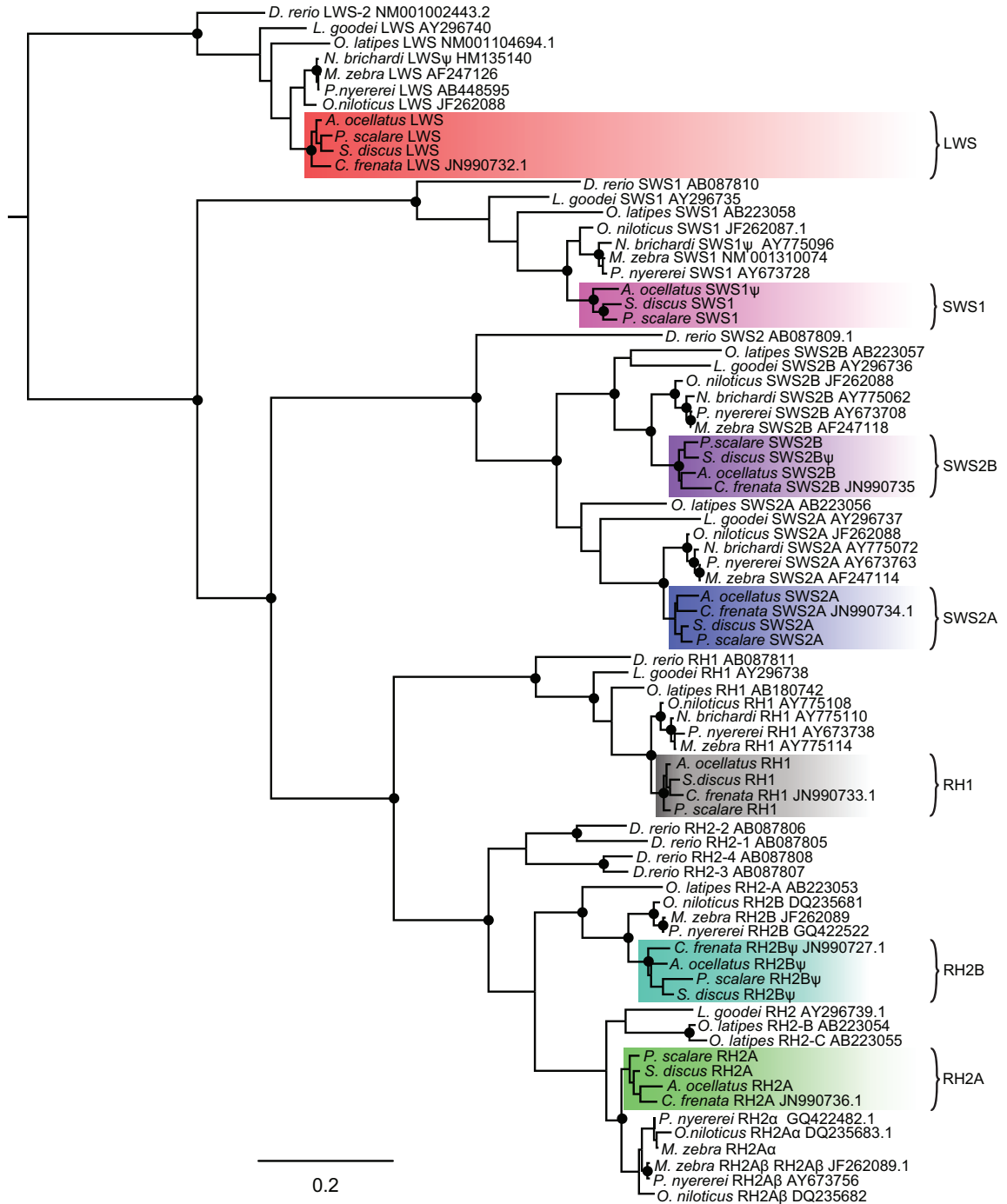


Figure 2.1. Opsin maximum-likelihood phylogenetic tree of Cichlids, *Danio rerio*, *Oryzias latipes* and *Lucania goodei*. Black circles represent bootstrap support over 95%. Colour shades indicate the Neotropical cichlid lineage. Ψ denotes pseudogenes. [Colour figure can be viewed at wileyonlinelibrary.com].

Genome and transcriptome analysis suggested that a gene duplication event generated two copies of RH2A (Fig. S6, Appendix A). Due to the high similarity of the genes, we were only able to obtain full sequences of one expressed RH2A in the RNAseq data. Within the genomes, we noticed that RH2A duplicates in each species were almost identical but had differences located mostly in the 5'UTR (~80 bp) and in the first 150 bp of the coding sequence, indicative of gene conversion. Blasting the exons and performing phylogenetic analysis of only the first exons and 5'UTRs showed that these RH2A copies correspond, although with low support, to the African cichlid duplicates RH2Aa and RH2Ab (Fig. 2.2a). In both copies, coding regions after 150 bp were highly similar to RH2Ab (including the first introns confirmed by PCR, Fig. S7, Appendix A); thus, we believe gene conversion resulted in RH2Aa being replaced in large part by RH2Ab (Fig. 2.2b).

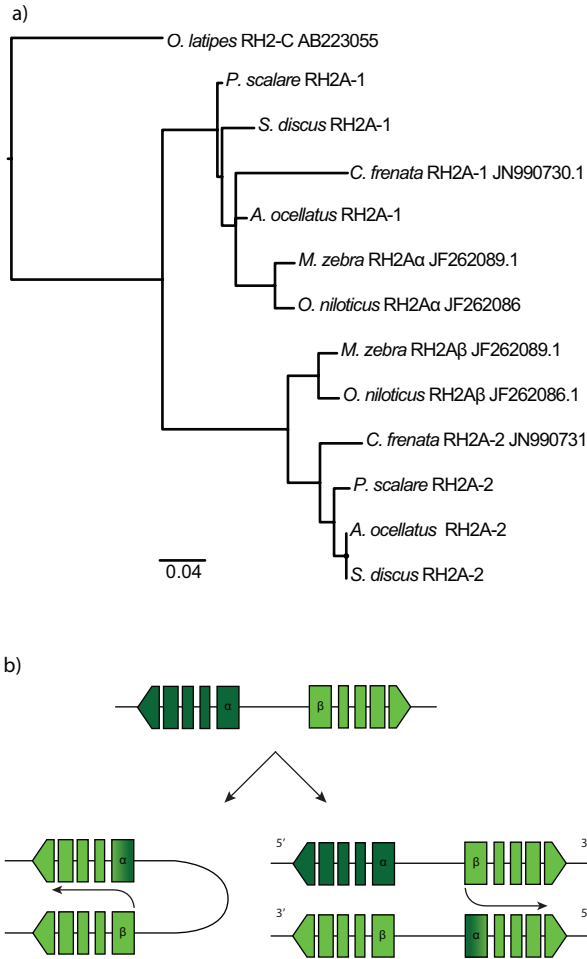


Figure 2.2. RH2A Gene conversion scenario. (a) Phylogeny of upstream UTRs and first exons of the RH2A duplicates. (b) Intrachromosomal and interchromosomal RH2A gene conversion scenario. [Colour figure can be viewed at wileyonlinelibrary.com].

2.4.4 Gene expression

Colour vision in Amazonian cichlids is based mainly on the expression of three cone opsin genes: SWS2A, RH2A and LWS. The three species had similar expression profiles (Fig. 2.3). The most expressed short-wave-length pigment was SWS2A, whereas SWS2B accounted for <5% of expressed cone opsin in *P. scalare*, *S. discus* and *A. ocellatus*. The LWS opsin seems to be much more

expressed accounting for more than 50% of expressed cone opsins. No SWS1 opsin was expressed. In *A. ocellatus*, only traces of RH2B were found. Interestingly, RH2A α is lowly expressed (<1%) in *P. scalare* and *S. discus*, whereas RH2A α and RH2A β are equally expressed in *A. ocellatus*. Pseudogenes were not expressed except for SWS2B Ψ in *S. discus* and RH2B Ψ in *A. ocellatus* accounting for less than 1% of all expressed opsins. RH1 was the most highly expressed visual pigment in the three species (Fig. S8, Appendix A).

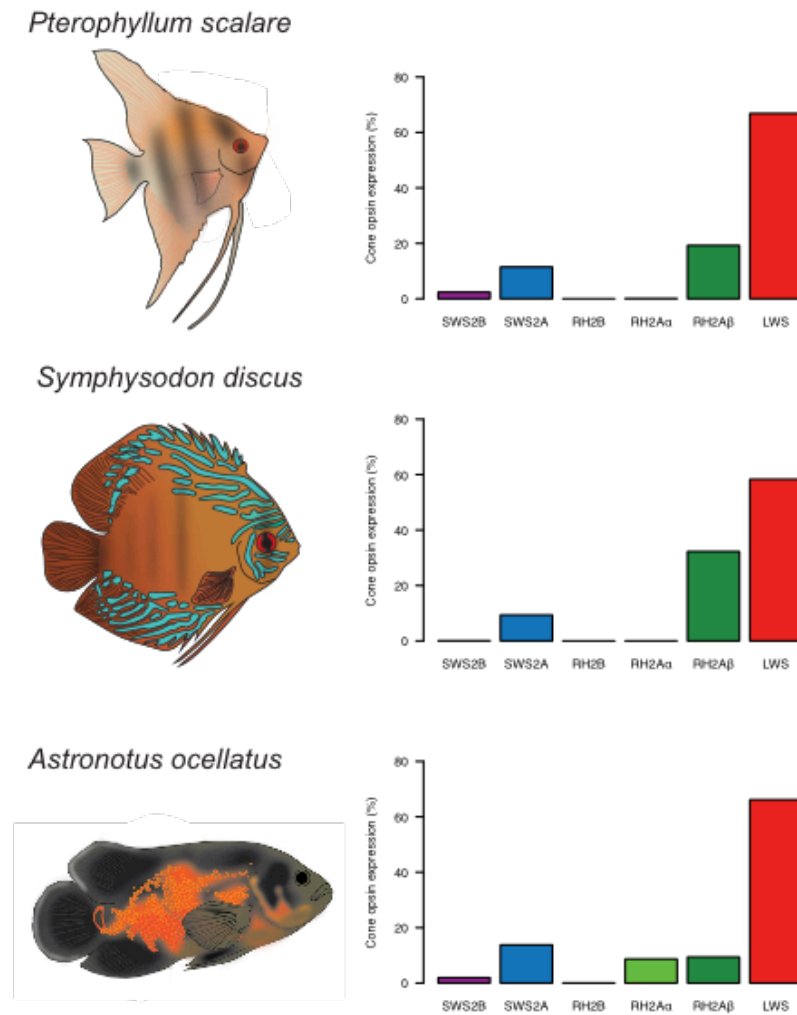


Figure 2.3. Relative cone opsin expression profiles of *P. scalare*, *S. discus* and *A. ocellatus*. Modified from Escobar-Camacho et al, 2017

2.4.5 Spectral tuning

The analysis of Amazonian cichlid opsin sequences revealed evidence of changes that might impact on spectral tuning. There was great variation of amino acid substitutions between the three species in comparison with *O. niloticus* (Fig. 2.4A). The greatest diversity at transmembrane sites was in the SWS2A opsin, with 35 variable transmembrane sites with five of these in the retinal binding pocket (five polarity changes) and three (M44T, M116L, S292A) occurring in known tuning sites (Table 2.2) (Appendix A). SWS1 had the greatest diversity in potentially functional tuning sites with 27 variable transmembrane sites, eleven substitutions in retinal binding pocket sites (seven polarity changes) and one substitution occurring at a known tuning site, A118S. In *S. discus*, the LWS opsin showed a λ_{\max} shifting substitution S164A, previously shown to cause a -7 nm shift [60]. SWS2B in *P. scalare* and *A. ocellatus* also exhibited three amino acid substitutions (F46V, A109G, A269T) in known tuning sites of which the A269T substitution is known to shift λ_{\max} by +6 nm [61]. Variable amino acid sites were also found between the three species and *C. frenata* with SWS2A having the most variable sites (Fig. 2.4B).

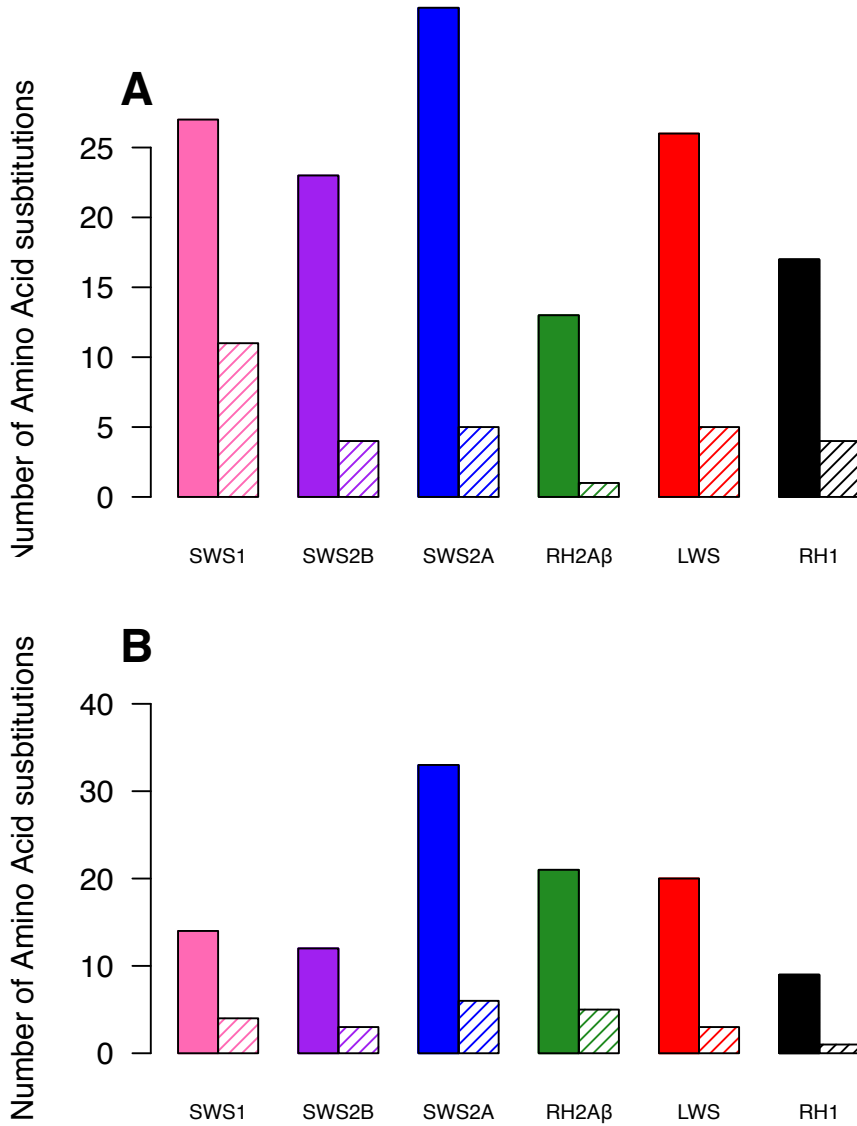


Figure 2.4. Amino acid substitution variation for each opsin class of the three species. Filled bars represent amino acid variation in transmembrane regions of the opsin, and striped bars are amino acid variation in the retinal binding pocket sites. (A) Amino acid substitution variation between *P. scalare*, *S. discus*, *A. ocellatus* and *O. niloticus*. (B) Amino acid substitution variation between *P. scalare*, *S. discus*, *A. ocellatus* and *C. frenata*. SWS1 variation is based only on *P. scalare* and *S. discus*, while SWS2B is based on *P. scalare*, *A. ocellatus* and *C. frenata*. Modified from Escobar-Camacho et al., 2017.

Table 2.2. Summary of South American cichlids variation.

	SWS1	SWS2B	SWS2A	RH2A	LWS	RH1
Total number of nucleotides	1008	1059	1056	1059	1074	1065
Total number of amino acids	335	352	351	352	357	354
Variable nt sites	46	52	67	70	50	38
Indels	0	3	0	0	0	0
<i>Vs. O. niloticus</i>						
Variable transmembrane sites*	27(12)	23(4)	35(12)	13(3)	26(7)	17(4)
Functionally variable retinal binding pocket sites	11(7)	4(2)	5(5)	1(1)	5(3)	4(1)
Number of substitutions at known tuning sites	1(1)	3(1)	3(2)	0(0)	1(1)	2(0)
Synonymous substitution (ds)	0.114	0.129	0.084	0.129	0.083	0.064
Non-synonymous substitution (dn)	0.024	0.024	0.032	0.022	0.017	0.012
dn/ds	0.210	0.186	0.380	0.170	0.204	0.187
Between SA species						
Variable transmembrane sites	14(5)	12(2)	33(12)	21(3)	20(5)	9(1)
Functionally variable retinal binding pocket sites	4(1)	3(2)	6(4)	5(1)	3(1)	1(0)
Number of substitutions at known tuning sites	1(1)	2(2)	2(2)	0(0)	1(1)	1(0)

†Parenthesis indicates number of amino acid substitutions that differ in polarity. Known tuning sites are based on [6,55]. Opsin genes are sorted by increasing spectral sensitivity.

2.4.6 Pseudogene divergence time

The time since opsins became pseudogenes (T_n) was estimated for both the SWS1 (*A. ocellatus*) and SWS2B (*S. discus*) pseudogenes. For SWS1 Ψ in *A. ocellatus*, T_n values varied around -3.8 to 0.07 Mya when compared to functional genes of *P. scalare* and *S. discus*, respectively, while for SWS2B Ψ , *S. discus*, values were between 1.84 and 7.35 Mya compared with *P. scalare* and *A.*

ocellatus (Table 2.3). Based on these values, it seems that SWS2B Ψ appeared in the late Neogene (23– 2.5 Mya), whereas SWS1 Ψ may be very recent (Quaternary, 2.5 Mya to present).

Table 2.3. Distances between sequences (dAC_i , dBC_i), for nonsynonymous and synonymous sites ($l = ns$ or s , as substitutions per site), rates of nonsynonymous and synonymous substitutions (a_i , in substitutions per site per year), and time since pseudogenization (T_n given in My). Ψ denotes pseudogenes.

Pseudogene Sequence A	Sequence B	Sequence C	dAC_{ns}	dAC_s	dBC_{ns}	dBC_s	a_{ns}	a_s	T_n (Mya)
SWS1									
<i>A. ocellatusΨ</i>	<i>P. scalare</i>	<i>O. niloticus</i>	0.042	0.480	0.034	0.452	4.50E-10	5.86E-9	-3.80
<i>A. ocellatusΨ</i>	<i>S. discus</i>	<i>O. niloticus</i>	0.042	0.480	0.037	0.477	4.91E-10	6.18E-9	0.07
SWS2B									
<i>S. discusΨ</i>	<i>A. ocellatus</i>	<i>O. niloticus</i>	0.06	0.35	0.058	0.376	7.53E-10	4.87E-9	7.35
<i>S. discusΨ</i>	<i>P. scalare</i>	<i>O. niloticus</i>	0.06	0.35	0.053	0.348	6.98E-10	4.51E-9	1.84

2.5 Discussion

2.5.1. Opsin gene complement

Through genome and transcriptome sequencing analysis, we have characterized the genetic component of the visual system of three Amazonian cichlids. Genomic and PCR opsin evidence suggests that all three species have seven cone opsin genes and a rod opsin gene. This includes evidence for two separate copies of RH2A each with unique 5'UTRs that could be separately PCR amplified. This supports the idea that the common ancestor of the South American lineages had the same seven cone opsin genes found in the African cichlids, perhaps arising in the Gondwanan ancestor.

Our results show that present-day Amazonian species exhibit a variable complement of functional opsins with different opsin genes inactivated in different lineages. Overall, these species exhibit a less rich palette of functional opsin genes than African cichlids [26]. This is in concordance with previous results on the Trinidadian pike [42], which has RH2B pseudogenized and a possible loss of SWS1. These results confirm that gene inactivation is common among percomorph fishes, thereby creating complex patterns of opsin evolution as adaptation to new spectral environments occurs [35,36].

RH2A opsins appear to have undergone gene conversion where RH2A β converted RH2A α with the recombination location in the middle of the first exon of the coding sequence. This conversion event seems to have happened early in the Neotropical cichlid lineage as it is shared across Amazonian species and *C. frenata* (Fig. 2.2). Gene conversion events can be frequent between adjacent opsin duplicates. This has been shown in primate L and M cone opsin genes where introns exhibit lower nucleotide divergence than exons [62,63]. Furthermore, gene conversion occurring between exons has been found on several teleost lineages [32,36,64,65]. Our results suggest that the RH2A duplication was present early in the cichlid lineage prior to the breakup of Gondwana and the African – South American divergence. Furthermore, RH2 paralogs seem to have been present before the Cichlomorphae–Atherinomorphae split [66] as *O. latipes*' RH2 opsins (RH2-A, RH2-B, RH2-C) are grouped as sister groups in cichlids' RH2B and RH2A clades (Fig. 2.1). This

agrees with previous studies suggesting that opsin gene duplications promote visual pigment diversity in teleosts [33,40,67,68]. Further studies on opsin genes of more divergent cichlids from India and Madagascar are needed to analyze the evolution of RH2 opsins. In the opsin gene trees, Neotropical cichlid opsins were placed as sister taxa to the African cichlid clade as expected. There is general phylogenetic concordance of the taxonomic relationships across the opsin genes. *P. scalare* and *S. discus* are often paired among opsins clades (SWS1, SWS2B, SWS2A, RH2B, LWS), whereas *A. ocellatus* and *C. frenata* are placed as sister taxa (SWS2B, SWS2A, RH2A). This is in agreement with Neotropical cichlid phylogenetic studies where *P. scalare* and *S. discus* shared a more recent common ancestor than *A. ocellatus* [69]. This pattern is not consistent in RH2A and RH1; however, these clades exhibit low support.

2.5.2 Opsin gene expression

In spite of the diversity in genomic opsin complements, all species expressed the same three cone opsins: SWS2A, RH2A and LWS. A reliance on three distinct cone opsins is consistent with previous studies that found a typical cone mosaic arrangement in *A. ocellatus* where one single cone was surrounded by four double (twin) cones [70,71]. The expression profile of *P. scalare*, *S. discus* and *A. ocellatus* is indicative of a long-wavelength-oriented visual system, which is characteristic of cichlids living in murky and riverine habitats [41,72,73]. This agrees with the light environment of Neotropical rivers, particularly in the Amazon, that have very long-wavelength transmission properties. In the Amazon

basin, short and medium wavelengths are scattered/absorbed by coloured dissolved organic matter, suspended inorganic particles and phytoplankton resulting in a red-shifted light environment. Light transmission can vary according to the type of water (white, black and clear waters) and hydrological cycles (receding and rising) [17,74]. Overall, Amazonian rivers exhibit a downwelling irradiance peak (λ_{\max}) beyond 650 nm resulting from high attenuation for blue and green light, and high reflectance for red (Fig. S9, Appendix A) [74–76]. *P. scalare*, *S. discus* and *A. ocellatus* have been documented throughout the Amazon basin inhabiting white, black and clear waters [77–79]. Furthermore, visual studies on Amazonian fishes including *P. scalare* and *A. ocellatus* have shown that they had yellow filters in the lenses and cornea, which would filter out short-wavelength light [17,18]. Because there is little short-wavelength light transmission in Amazonian rivers and yellow pigments in cichlid eyes filter short wavelengths, we suggest that the aquatic environment in the Amazon basin has influenced the visual system adaptation of Neotropical cichlid retinas, inactivating short-wavelength-sensitive opsin genes (SWS1, SWS2B, RH2B) and shifting their opsin expression profile to the long-wavelength palette.

The expression of SWS2A, RH2A and LWS is consistent with previous microspectrophotometry (MSP) studies of wavelength sensitivities in Neotropical cichlids [28,42,80] (Table S2, Supporting information). Based on these studies, we estimate a spectral sensitivity for SWS2A between 450 and 480 nm. Similarly, for RH2A and LWS we suggest values between 530–555 and 560–617 nm

respectively. Finally, rods sensitivity should lie around 500–525 nm. This spectral sensitivity variation may include a significant effect from the type of chromophore (A_1 - A_2) [28]. The effects of changing from A_1 to A_2 chromophore can result in modest 15–30 nm shifts for short- to medium-wavelength pigments, but shifts up to 60 nm in λ_{\max} for long-wavelength pigments [39,73,81]. Similarly, spectral sensitivities of Neotropical cichlids lie within this range suggesting different A_1 - A_2 combinations (Table S2, Fig. S9, Appendix A). There are no records of the peak absorbance of the shortest wavelength-sensitive pigments, SWS1 and SWS2B, yet we would expect sensitivities similar to their African counterparts between 360–378 nm for SWS1 and 415–425 nm for SWS2B [40,82]. However, as Amazonian rivers have little downwelling light below 450 nm, these opsins would not be sensitive to the available light and therefore need not be expressed (Fig. S9, Appendix A) [74].

In cichlids, opsin gene expression can change through development and species can differ in their ontogenetic profiles with shorter-wavelength genes expressed earlier (SWS1, SWS2B, RH2B) followed by longer-wavelength genes (SWS2A, RH2A and LWS) [73]. Specimens used for our transcriptome analyses were aquarium trade juveniles raised in fluorescent light. This could have influenced their opsin expression profile by increasing the expression of longer-wavelength-sensitive opsins. However, fish were at least five months old and also exhibited yellow lenses. As changes in gene expression stabilize by around six months in African cichlids, our results suggest that either these fish were old enough to

obtain the adult expression pattern or that they do not undergo developmental shifts in expression [73,83]. The latter would be consistent with some species having lost the SWS1 and SWS2B opsins that are normally expressed in the larval to juvenile stages.

2.5.3 Opsin sequence variation

Studies in African cichlids have found that the short- and the long-wavelength-sensitive pigments are the most variable with shifts in peak sensitivity of 30 nm in the short-, and 50 nm in the long-wavelength-sensitive opsins [73] (Table S2, Supporting Information). This is concordant with the diversity of total amino acid substitutions in SWS2A and LWS gene sequences found in our results. Opsin sequence analysis showed that the greatest variation in amino acid substitution and polarity changes in the retinal binding pocket sites, was in SWS2A followed by SWS1 and LWS (Fig. 2.4a). These results differ from previous studies that have found the greatest variation in opsins sensitive at both ends of the wavelength spectrum, SWS1 and LWS [41,84,85]. As the Amazon basin exhibits a long-wavelength light environment, the SWS2A gene may be the shortest wavelength gene to be expressed. Changes in SWS2A might be the result of strong selection to enhance sensitivity where functional amino acid substitution would shift the k_{max} of SWS2A to longer wavelengths. In this way, the visual system may still be optimizing the shortest (SWS2A) and longest (LWS) opsins that are relevant to the long-wavelength-shifted environments where these fish are located. Indeed, divergent selective pressures driven by ecological and/or

biogeographic differences have been suggested for Neotropical cichlids' and anchovies' visual pigments [43,86,87]. In addition to amino acid substitutions adapting spectral sensitivities over the long term, shifts in A_1 – A_2 use could also have great impact on λ_{\max} possibly enabling cichlids to adapt to shifts in the light environment over a shorter timescale. Chromophore shifts are known to occur in just a few weeks to provide seasonal adjustments [88]. Indeed, Muntz suggested that Amazonian fishes use mixtures of both chromophores [17,18].

The pseudogenization time of SWS1 Ψ and SWS2B Ψ in *A. ocellatus* and *S. discus* dates back to the late Neogene and the Quaternary. During the Neogene (~7 Mya), the modern Amazon river system, including the present-day configuration of white, clear and black water, had already come into place. Nevertheless, geological shifts, including the Andean uplift (12–4 Mya) on the western lowland and continuous marine incursions until the Pleistocene, played a role in habitat fragmentation and greatly influenced diversification of the Amazon biota [78,89,90]. Furthermore, the glacio-eustatic oscillations in the Quaternary (<2.5 Mya) dynamically altered and reorganized river courses and watersheds resulting in both isolated and expanded fish populations [78]. Consequently, the changing Amazon conditions over the last 7 Mya could have selected for maintenance of expression of some opsins and pseudogenization of others. Although we were not able to date the pseudogenization time for RH2B, it is possible that it might have been inactivated multiple times across lineages. This is supported by the SWS1 inactivation in African cichlids (*Neolamprologus*

brichardi and *N. mondabu* from Lake Tanganyika (O'Quin et al. 2010)) and Neotropical cichlids which arose independently. More species need to be analysed to better understand the pseudogenization process. Yet it is interesting that in spite of opsin genes having been inactivated at different times in different South American lineages, the three species express the same opsin set. This suggests that this expressed gene set arose convergently in Amazonian cichlids (Fig. 2.5).

2.5.4 Ecological adaptation

Our results suggest that these Amazonian cichlids are adapting to their light environment through several different genetic mechanisms. These include changes in opsin gene expression, opsin gene sequence and the accumulation of pseudogenes relative to their African counterparts. This is further supported by yellow filters in their ocular media which filter short wavelengths, reducing the background scattered light common in these long-wavelength-transmitting waters. These traits are shared among other teleost lineages found in the Amazon and may be a signature of adaptation to the Amazon's murky environment. The absence of short-wavelength visual pigments seems to be common among the Amazonian ichthyofauna with a number of species having spectral sensitivities that are red-shifted (Table S2, Supporting information). Gene loss or pseudogenization also occurs in other Amazonian taxa such as the absence of the short-wavelength-sensitive opsin genes in the electric eel (*Electrophorus electricus*) and nonelectric catfish [91]. Furthermore, convergent

opsin inactivation is common in mammals where opsin pseudogenes have arisen independently in response to changes in their behaviour and ecology [92,93]. Additionally, adaptations such as the presence of yellow filters in ocular media have been found in Amazonian fishes besides cichlids, such as the pink-tailed chalceus (Characiformes: *Chalceus macrolepidotus*), the freshwater puffer fish (Tetraodontiformes: *Colomesus asellus*), the freshwater stingray (Myliobatiformes: *Paratrygon motoro*) and several other siluriforms (Fig. 2.5) [17,18,94].

In conclusion, we have described the opsin complement of three Amazonian cichlids using both RNA and genomic sequences. There is evidence for visual pigment evolution in this lineage with both opsin gene pseudogenization and gene conversion taking place. This might be a consequence of the long-wavelength light environment in the Amazon basin. This environment has further influenced cichlid visual system adaptation through adaptation of opsin gene expression, changes in amino acid substitution in spectral tuning sites and yellow filters in ocular media, all traits characteristic of species living in a long-wavelength environment. These traits likely arose convergently in response to environmental selection and seem to be shared among a number of Amazonian fishes. The molecular adaptive traits discussed in this study corroborates the vast body of vertebrate research where it has been shown that as animals occupy different ecological niches, their visual systems adapts through several mechanisms, enabling them to operate in these new spectral environments.

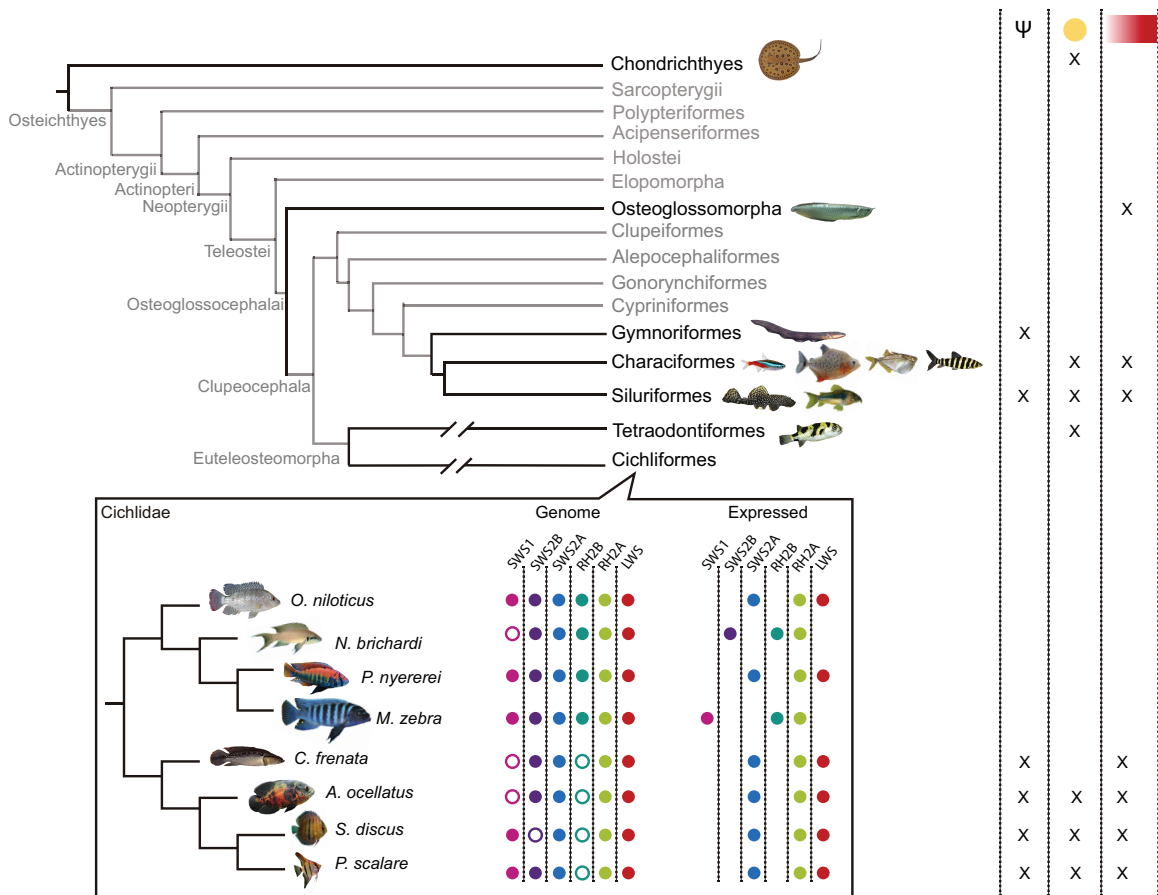


Figure 2.5. Schematic representation of visual system adaptation in a phylogenetic context. Phylogenetic tree topology is based on Betancur-R et al. 2013. Taxonomic groups present in the Amazon where visual systems have been analysed at some level are displayed in black. Based on previous and the present study, “x” denotes the presence of pseudogenes or lost genes (Ψ), yellow pigments in ocular media (yellow circle) or long-wavelength spectral sensitivities, either by opsin expression or MSP, (red rectangle) in a specific group. The cichlid inset denotes the opsin genes in the genome and the ones that are being expressed in the Neotropical and African lineages. Empty circles denote pseudogenes or lost genes. For simplicity, RH2A duplicates were excluded.

2.6 Acknowledgements

We thank the University of Maryland Institute for Bioscience & Biotechnology Research for sequencing the libraries and Ian Misner for helping with the Trinity pipeline. We also thank Carlos Schneider for his collaboration in collecting samples, Jessica Goodheart for advice in phylogenetic trees, and Fabio Cortesi for help with identifying gene duplications through read mapping. We thank three anonymous reviewers for providing helpful suggestions on this manuscript. This work was supported by the National Institute of Health (R01EY024693 to K.L.C.), the Center for Studies of Adaptation to Environmental Changes in the Amazon (INCT ADAPTA, FAPEAM/CNPq 573976/2008-2 to C.M.), Goldhaber Travel Award, International Conference Support Award (ICSSA), Biology Department Travel Award and Summer Research Fellowship through the University of Maryland Graduate School (2015-2016 to D.E-C.). D.E-C. is supported by graduate fellowship of the Secretariat of Higher Education, Science, Technology and Innovation of Ecuador (2014-AR2Q4465).

Chapter 3: Variable vision in variable environments: the visual system of an invasive cichlid (*Cichla monoculus*, Agassiz, 1831) in Lake Gatun, Panama

Previously published under: Daniel Escobar-Camacho, Michele E.R. Pierotti, Victoria Ferenc, Diana M.T. Sharpe, Erica Ramos, Cesar Martins and Karen L Carleton. Variable vision in variable environments: the visual system of an invasive cichlid (*Cichla monoculus*, Agassiz, 1831) in Lake Gatun, Panama. *Journal of Experimental Biology* 2019: doi: 10.1242/jeb.188300

3.1 Abstract

An adaptive visual system is essential for organisms inhabiting new or changing light environments. The Panama Canal exhibits such variable environments owing to its anthropogenic origin and current human activities. Within the Panama Canal, Lake Gatun harbours several exotic fish species including the invasive peacock bass (*Cichla monoculus*, Agassiz, 1831), a predatory Amazonian cichlid. In this research, through spectral measurements and molecular and physiological experiments, we studied the visual system of *C. monoculus* and its adaptive capabilities.

Our results suggest that (1) Lake Gatun is a highly variable environment where light transmission changes throughout the canal-waterway, and that (2) *C. monoculus* has several visual adaptations suited for this red-shifted light environment. *Cichla monoculus* filters short-wavelengths (~400 nm) from the environment through its ocular media and they tunes its visual sensitivities to the available light through opsin gene expression. More importantly, based on shifts in spectral sensitivities of photoreceptors alone, and on transcriptome analysis, *C. monoculus* exhibits extreme intraspecific variation in the use of vitamin A₁/A₂ chromophore in their photoreceptors. Fish living in turbid water had higher proportions of vitamin A₂, shifting sensitivities to longer-wavelengths, than fish living in clear water. Furthermore, we also found variation in retinal transcriptomes, where fish from turbid and clear-waters exhibited differentially

expressed genes that vary greatly in their function. We suggest that this phenotypic plasticity has been key in the invasion success of *C. monocolus*.

3.2 Introduction

The ability of an animal to survive in a changing environment is often determined by its adaptive capabilities. Phenotypic plasticity is a key mechanism by which organisms can respond to short-term environmental changes or fluctuations. Aquatic habitats exhibit substantial spatial and temporal variation in light intensity, spectral composition, angular distribution and degree of polarized light [11], suggesting that the eyes of aquatic organisms might be particularly promising for studies of phenotypic plasticity.

Animals are believed to adapt to their visual environment by matching their photoreceptor sensitivities to the available light. This “sensitivity hypothesis” explains how modulating the visual system spectral sensitivities to a specific wavelength facilitates certain visual tasks [2,95]. Shifts in visual sensitivities can be driven by ecological factors such as water turbidity and foraging targets, or social factors important for communication [41,96,97].

Studying adaptation of retinal visual sensitivities is possible because of a well-defined genotype-to-phenotype map. This map results from our genetic understanding of how visual sensitivities are tuned [35]. Fish visual perception is a product of lens transmission and photoreceptor absorbances across the

wavelength spectrum. The specific spectral sensitivity of a photoreceptor cell is largely determined by the visual pigment(s) it contains, which, in turn, consist of a transmembrane apoprotein, the opsin, bound to the photosensitive chromophore (an aldehyde of vitamin A). Photoreceptor absorbance can be tuned by opsin gene differential expression, chromophore usage (the aldehyde of either vitamin A₁ or A₂), opsin gene sequence variation and regional opsin co-expression in the retina [12,20,25,26,41]. Therefore, several mechanisms can act separately or in concert, giving rise to a diverse palette of visual phenotypes. Unraveling these mechanisms requires techniques such as microspectrophotometry (MSP) of individual photoreceptor cells and molecular experiments in order to characterize opsin gene sequence and expression.

Invasive species (introduced species that have successfully established and spread outside of their native range), are suitable for the study of adaptation because they can exhibit rapid responses to novel biotic and abiotic conditions [98–101]. Hence, invasive species can potentially provide insights into the mechanisms underlying adaptive phenotypic variation. In this study, we examine the Peacock bass (*Cichla monoculus*, Agassiz, 1831), a diurnal predatory cichlid native to the Amazon basin [102]. *Cichla monoculus* was introduced to the Chagres River basin in 1967 for sport fishing, from which it dispersed and subsequently colonized Lake Gatun in the Panama Canal watershed [103]. The introduction of *C. monoculus* has had a dramatically negative effect on the native ichthyofauna. Long-term studies have shown how the introduction of *C.*

monoculus has altered the composition of fish communities in Lake Gatun, decreasing both abundance and biomass of several local species while completely extirpating others [103,104].

Almost half a century after its introduction, *C. monoculus* remains the most common fish in Lake Gatun [104], suggesting it has successfully adapted to the complex environment of the Panama Canal watershed. Lake Gatun was created in 1914 in order to build the Panama Canal by building a dam across the reaches of the Rio Chagres. At least half of the Panama Canal watershed is protected and covered in mature tropical lowland forest; however, there remain several threats to water quality in Lake Gatun [105]. First, deforestation in parts of the catchment has increased surface runoff, increasing the level of sedimentation and turbidity in the Lake [105]. Second, the continuous transit of boats through the canal generates turbulence and wave action that also stir up sediments. Third, operation of the canal requires continual dredging, which has significantly expanded in the past five years as part of the recently completed expansion of the Panama Canal [106]. Together, these factors have resulted in a strong turbidity gradient in Lake Gatun, with increasingly turbid waters as you approach the navigable sections of the water-way. The goal of our study was to analyze the visual system of *C. monoculus* and its adaptability to the variable light environment of Lake Gatun. Through genetic and physiological experiments we evaluated whether the visual system of *C. monoculus* changes across the above-mentioned turbidity gradient.

3.3 Materials and Methods

3.3.1 Study site and sample collection

Our sampling was conducted around Barro Colorado Island (BCI) in Lake Gatun (Fig. 3.1). One side of the island abuts the navigable channel of the Panama Canal and the water is very turbid, whereas the other side of the island lies within the protected Barro Colorado Natural Monument, and the water is very clear (Sharpe, Escobar-Camacho, personal observation). Turbidity affects light intensity but does not necessarily shift spectral wavelengths. However, the different types of suspended particles present in the Panama Canal absorb much of the short-wavelength light causing turbid waters to be long-wavelength shifted. Throughout the article, we will refer to turbid waters as environments with decreased light intensity shifted to longer wavelengths.

Fish were captured from July to August of 2016 using fishing lines with non-live bait. We collected 25 specimens of *Cichla monoculus* Agassiz 1831 from different sites around BCI in Lake Gatun (Table S1A-B). All fish were brought back to the BCI Smithsonian Tropical Research Institute (STRI) station and euthanized using a lethal dose of buffered MS-222 to ensure minimal suffering. Light measurements were taken at several sites (including the ones where fish were captured) at depths down to three meters.

Sampling permits were in accordance with the Panamanian laws of environmental protection (wild collection permits from Ministerio de Ambiente de Panamá, MiAmbiente, permit nos. SE/A-99-16 and SC/A-19-17). Fish were handled following the STRI IACUC protocol (#2014-0901-2017-A3).

3.3.2 Experimental set up

All fish were brought back to the BCI research station, and then used in one of the following ways. First, five individuals (three from clear water, two from turbid water) were killed immediately for RNA sampling. Second, 16 fish (nine from clear water, and seven from turbid water) were used for MSP. In addition, four fish captured in turbid waters were kept in clear outdoor glass tanks at Naos Research Laboratories, STRI (Panama), for 6 months, after which their retinas were analyzed by MSP (Table S1B). This longer-term acclimation experiment was performed because cichlid visual systems have been shown to be plastic [80,107–109]. In this study, we classified our samples as clear, turbid and six-month treated fish.

3.3.3 Spectral measurements

To characterize environmental light, we measured downward light intensity in nine localities around BCI (Fig. 3.1), which were selected *a priori* to cover a suspected turbidity gradient. Downward light intensity was measured in each locality with a 1000 μ m fiber with a fiber-optic spectrometer based on an Ocean Optics USB2000 (Dunedin,FL,USA). We took five replicate measurements at the

subsurface, and at 1,2 and 3 m depth on days of bright sunshine. In addition, we also collected measurements of side-welling irradiance and radiance in two localities (a turbid and a clear site respectively). For irradiance measurements, the fiber was fitted with a cosine corrector (CC-3).

We also characterized the light-transmission of *C. monocolus*' ocular media. Lens and cornea transmission were measured by placing the isolated cichlid lens or cornea on a UV-transparent cover slip, which was illuminated from above by a fiber optic cable attached to a pulsed xenon light source (PX-2, Ocean Optics). Another fiber optic cable was placed directly under the specimen and delivered the signal to the spectrometer. Five replicate measurements were made. The resulting spectral scans were normalized to 100% transmission at 700 nm. Finally, we quantified the T50 values (i.e. the wavelength at which 50% transmission is reached)

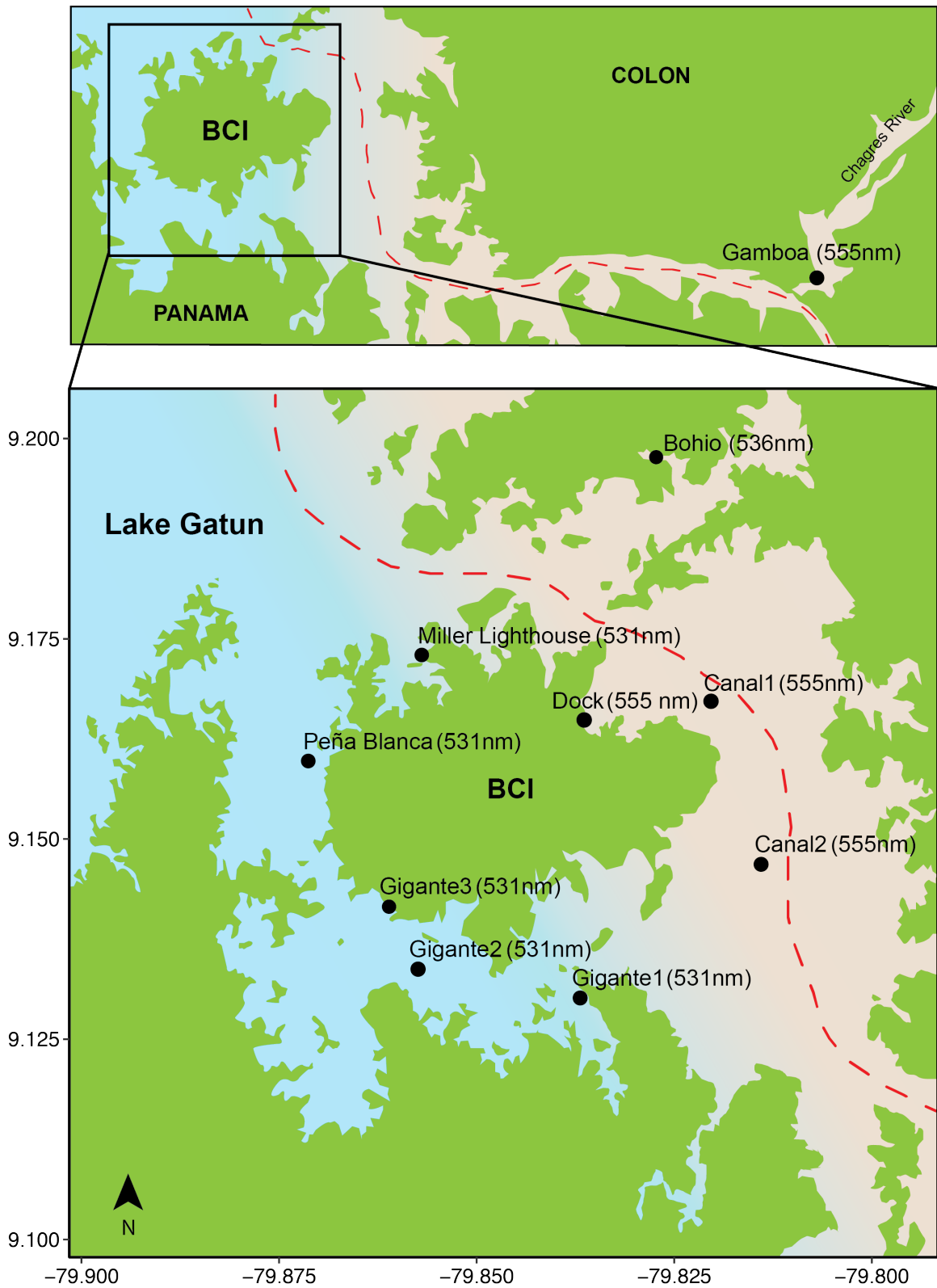


Figure 3.1. Map showing the light sampling localities around Barro Colorado Island (BCI) in Lake Gatun, Panama Canal. Black circles indicate each light sampling locality, and the dashed line indicates the water-way of boats

in the Panama canal. Numbers next to locality names indicate the wavelength of peak intensity (λ_{\max}) for each locality at one meter depth.

3.3.4 Microspectrophotometry (MSP)

In order to identify the peak of maximum sensitivity of *C. monocolus*' photopigments under different light conditions, we performed MSP on wild-caught fish from three different light conditions: clear-water, turbid-water and six-month treated fish.

Each fish was dark-adapted for at least 2 hrs, after which it was killed with an overdose of buffered MS222. Eyes were enucleated under a dissecting scope in dim deep red light. The retina was removed and transferred to a PBS solution containing 6.0% sucrose (Sigma-Aldrich). A small piece of retina was cut out and placed on a glass cover slip in a drop of solution, then delicately macerated with razor blades. The preparation was covered with a second glass cover slip and sealed with high-vacuum silicone grease (Dow Corning).

Spectral absorbance was measured with a computer-controlled single-beam micro-spectrophotometer fitted with quartz optics and a 100W quartz-halogen lamp. Baseline records were taken by averaging a scan from 750nm to 350nm and a second in the opposite direction, through a clear area of the preparation and in proximity to the photoreceptor of interest. A record of the visual cell was then obtained by scanning with the MSP beam through the photoreceptor outer segment. Finally, the cell's absorption spectrum was obtained by subtracting the

baseline record. A custom-designed spectral analysis program (Loew et al. unpublished) was used to determine λ_{\max} from absorbance records using existing templates [110,111]. Individual spectra were smoothed with a nine-point adjacent averaging function and the resulting curves were differentiated to obtain a preliminary maximum value. This was used to normalize curves to zero at the baseline on the long wavelength limb and to one at the maximum value. Whitmore and Bowmaker's (1989) relationship (Eqn 1) was used to recursively fit the observed (normalized) absorption spectra to curves resulting from combinations of different proportions of pure Vitamin A₁ and corresponding pure Vitamin A₂ nomograms [112] (Fig. S1, Appendix B):

Eqn 1
$$\lambda_{\max A1} = (\lambda_{\max A2} - 250)^{0.4} * 52.5$$

Retina preparation for MSP proved to be challenging because of a particularly dense vitreous humor and thick pigment epithelium that required extensive careful manipulation, often causing detachment of the cones' outer segments. For this reason, we could not collect a sufficient number of cone records per individual to allow a satisfactory between-environment comparison. We were, nevertheless, able to characterize cone sensitivities for each spectral class and numerous rod records for analysis. A non-parametric ANOVA on ranks (Kruskal-Wallis test) followed by a pairwise Wilcoxon test were used to compare rod spectral absorbances (λ_{\max}) between fish from different groups.

3.3.4 RNA seq and opsin gene expression analysis

For RNA sequencing (RNA-Seq), fish were euthanized with buffered MS-222. Three individuals from clear-water and two fish from turbid-water were used for RNA-Seq. Fish eyes were enucleated and the retinas were dissected out and preserved in RNAlater. For RNA-Seq, we used both eyes from two of the five fish, resulting in a total of seven samples for transcriptome analysis. Total RNA was extracted with an RNeasy kit (Qiagen), and RNA quality was verified on an Agilent Bioanalyzer. RNA-Seq libraries were prepared using the Illumina TruSeq RNA library preparation kit (Illumina Inc, San Diego, CA, USA) by the University of Maryland Institute for Bioscience & Biotechnology Research sequencing core, obtaining 100-bp paired-end reads with all samples multiplexed in one lane of an Illumina HiSeq1500 sequencer. The data were quality-checked using FastQC version 0.10.1 to remove over-represented sequences and to retain sequences with a minimum quality score of 20 and a minimum length of 80 bp. The seven transcriptomes were combined in order to obtain a single de-novo assembly. This was performed with Trinity version r20140413 [50] using only paired sequences with a minimum coverage of two to join contigs.

For estimating gene expression, reads from each sample were mapped back to the de-novo assembled transcriptome using RSEM, part of the Trinity package [50]. We wanted to examine whether there were differences in gene expression that might alter the visual sensitivities between clear and turbid water fish, including opsins or genes responsible for A_2 chromophore synthesis. In order to

analyze the opsins, read counts from each opsin class were extracted from the RSEM output (quantified as fragments per kilobase of transcript per million reads, FPKM) and then normalized to the β -actin gene. Because the RH2A duplicates are a product of gene duplication followed by gene conversion [113], we mapped back the reads only to the first 140 bp of the the first exon in order to obtain an estimate of expression of each RH2A paralog.

To examine other genes differentially expressed between samples, we performed a differential gene expression analysis using the RSEM output from each sample. This analysis was done with the Bioconductor package DESeq2 implemented in R. We used a one-factor design (levels: clear vs turbid) to analyze all samples. We only considered genes with a sufficient number of mapped reads (FPKM >10) for the analysis.

3.3.5 Opsin sequence analysis

In order to expand our understanding of opsin genes in *C. monoculus*, we analyzed the opsin gene complement in the genome of *Cichla vazzoleri*. For this species, the samples were analyzed under the guidelines of Sao Paulo State University IACUC (Protocol no 34/08-CEEA/IBB/UNESP). See methods in Escobar-Camacho et al. (2017) for genome analysis.

Putative opsin sequences were identified from transcriptome assembled FASTA files of *C. monoculus*. We searched for opsin sequences using Tblastx and

queried with cichlid opsin genes from *Oreochromis niloticus*. If sequences were not found in *C. monoculus*' transcriptome, we looked in the genome of *C. vazzoleri*. Opsin class identity was confirmed based on phylogenetic relationships of the opsin sequences from other teleost lineages obtained from Gen-Bank. We used MAFFT to align nucleotide sequences and PartitionFinder to find the best partitioning scheme and molecular evolution model [114]. Maximum likelihood analyses were conducted using Garli (version 2.0). These included a best tree search with 40 replicates and 2000 bootstrap replicates to evaluate nodal support.

We also aligned *C. monoculus* opsin sequences of each opsin class with bovine rhodopsin, tilapia (*O. niloticus*) and four other Neotropical cichlids (*Astronotus ocellatus*, *Symphysodon discus*, and *Pterophylum scalare* [113], and *Crenicichla frenata* [42]), to identify potential spectral tuning sites. The alignments were analyzed to identify amino acid substitutions that fell in putative transmembrane regions and in the retinal binding pocket facing the chromophore. (See Escobar-Camacho et al 2017). We excluded opsin sequences from *C. vazzoleri* in this analysis because they were almost identical to *C. monoculus* and because sequences such as RH2A opsin were incomplete owing to genome mis-assemblies.

3.4 Results

3.4.1 Light environment in Lake Gatun

We measured downward light intensity from nine localities around BCI (Table S1C). Light diffuse attenuation was greater at sites close to the Panama Canal waterway than in clear water sites away from the canal. For example, light is best transmitted in localities near Gigante (clear) and more strongly attenuated in localities near the canal (turbid) (Fig. 3.2), where light intensity decreases greatly with depth. In general, the dominant wavelengths in Lake Gatun lie between 500 and 600 nm in both turbid and clear sites (Fig. 3.2). Short wavelengths around 400 nm appear to be transmitted only in clear water sites towards the western part of Barro Colorado Island reserve. The island seems to partially shelter these locations from turbid plumes from the main canal waterway.

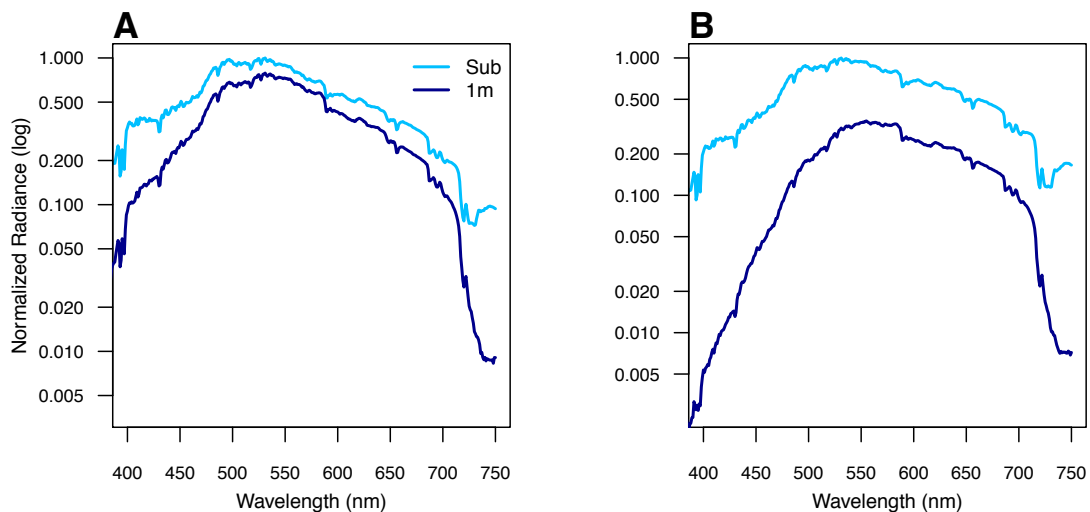


Figure 3.2. Underwater light environment variation around Barro Colorado Island. Downward light intensity at (A) Gigante1 (a clear site) and (B) Canal2 (a turbid site).

3.4.2 Ocular media

The cornea of *C. monoculus* is UV transmissive with a T_{50} cutoff around 378 nm (mean = 377.56 nm, range 368-383 nm, $n=8$). This cut-off differed slightly between 'clear' and 'turbid' water sites (376 and 379.5 nm, respectively, Fig. 3.3A) but the difference was not significant ($t_{5,4} = 0.303$, $df=7$, two-tailed $p = 0.334$). *Cichla monoculus* exhibits UV blocking lenses with transmission yielding a T_{50} cut-off of approximately 409 nm (clear sites individuals: mean = 408.94 nm; s.d. = 1.055, range = 406-410 nm; turbid sites individuals: mean 410.1 nm; s.d. = 2.15, range = 407-414 nm; Fig. 3.3B, Table S1D). There was no difference in lens transmission between individuals caught in turbid vs clear light environments.

During field work, we realized that the temporal region of the cornea was yellow (Fig. 3.3C-D). Transmission measurements showed that this region transmits light differently than other regions of the cornea, with three cut-off peaks at 385, 462, and 486nm (Fig. 3.3C). This reduces the amount of blue light reaching the eye and perhaps acts as a sun shade to reduce scattered light.

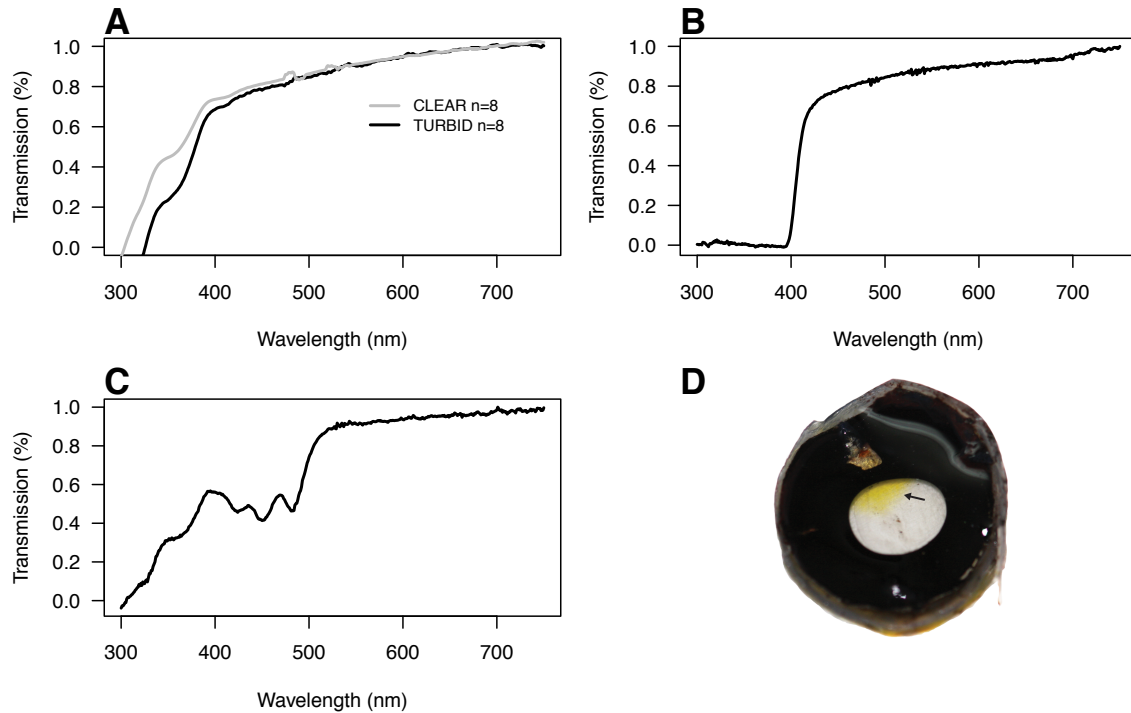


Figure 3.3. Ocular media transmission measurements in *Cichla monoculus*. (A) Cornea transmission spectrum of *C. monoculus* sampled in clear and turbid waters. (B) UV-blocking lens transmission spectrum from *C. monoculus* (n=16). (C) Transmission spectrum of the yellow region (n=4). (D) Dissected corneae of *C. monoculus*. Note the yellow pigmentation in the top region.

3.4.3 Visual sensitivities of *Cichla monoculus*

MSP of rods in *C. monoculus* revealed remarkable variation in peak absorbances (λ_{max}), ranging from 496 to 531 nm (n=271 records) (Table 3.1, Fig. 3.4A, Fig. S2A, Appendix B), suggesting variable mixtures of vitamin A₁ and A₂. Fish from clear water sites had greater variation in rod spectral sensitivities whereas turbid-water and six-month treatment fish exhibited less variation (Fig. 3.4A). Rod spectral sensitivities were significantly different between fish from different locations (Kruskal-Wallis rank sum test, $p < 2.2e-16$; Wilcoxon rank sum test, $p < 2e-16$ and $p < 2e-16$, respectively) (Fig. 3.4C). Because vitamin A₂ shifts visual

sensitivity to longer regions of the spectrum, our results suggest that turbid water fish had higher proportions of vitamin A₂ (Fig. 3.4B). In addition, individuals collected at a turbid water site, and kept in clear water under natural light conditions for six months, exhibited significantly shorter rod peak absorbances (λ_{\max}) than non-treated individuals from the same site, a shift consistent with higher levels of vitamin A₁ (Fig. 3.4A-B).

Table 3.1. Range of cone and rod visual pigment peak sensitivities (λ_{\max}) measured in *C. monocolus* with micro-spectrophotometry. Vitamin A₁ proportion was estimated from the reference 100% A₁ nomograms and the corresponding 100% A₂ nomograms obtained from Whitmore & Bowmaker's (1989) equation (see main text).

Peak sensitivities	Putative opsin					
	SWS2B	SWS2A	RH2A β	RH2A α	LWS	RH1
λ_{\max} (MSP)	419-431	480-491	524-543	530-575	575-605	496-531
Reference $\lambda_{\max A_1}$	420 \pm 5	477 \pm 1	517 \pm 1	528 \pm 2	559 \pm 1	498 \pm 2
Reference $\lambda_{\max A_2}$	430 \pm 6	499 \pm 1	555 \pm 2	571 \pm 3	620 \pm 2	527 \pm 3

We identified five different photoreceptor classes (Table 3.1), which is consistent with the number of opsin genes *C. monocolus* expresses: SWS2B, SWS2A, RH2A β , RH2A α and LWS (see below). Within individuals, their vitamin A₁ content was consistent with the A₁ content of the corresponding rod.

For single-cone photoreceptors, MSP identified two types based on pure vitamin A₁, one sensitive to the violet (λ_{\max} =419-431 nm, N=2), with the other sensitive to the blue/blue-green (λ_{\max} =480-491 nm, N=5). For double-cone photoreceptors we identified three types, a short-green (λ_{\max} =524-543 nm, N=9), a long-green

(λ_{\max} =530-575 nm, N=10), and a yellow-red (λ_{\max} =575-605 nm, N=3) visual pigment (Fig. S2B, Appendix B). The variation in the cones' MSP λ_{\max} is indicative of the presence of A₁/A₂ mixtures.

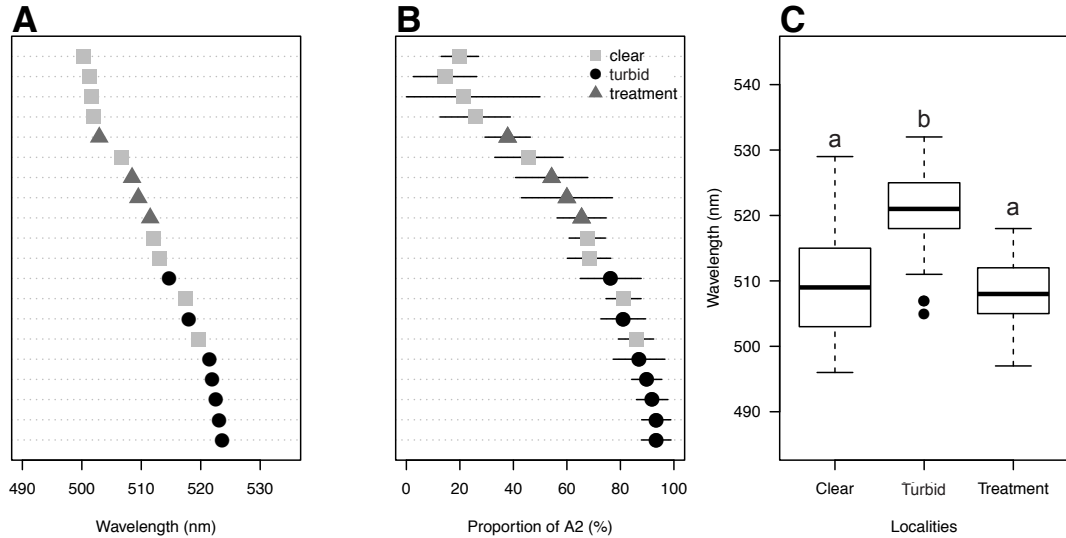


Figure 3.4. Rod spectral sensitivity variation. (A) Maximum absorbance of rods from 20 individuals from sites with different underwater light spectrum. (B) Proportion of vitamin A₁ estimated from rods λ_{\max} in 20 individuals. Error bars denote one standard deviation of all the recordings. Filled squares, circles and triangles denote samples from clear water, turbid water, and the six-months treatment respectively. (C) Boxplots showing the rod spectral sensitivities of samples from different groups.

3.4.4 Opsin gene characterization and sequence analysis

RNA samples showed good quality based on the Agilent Bioanalyzer RIN (RNA integrity number varied between 8 and 9.20). The retinal transcriptomes obtained by multiplexing all samples in one lane provided sufficient data to assemble and quantify opsin transcripts. Total reads per sample varied from 24.09 to 29.33 M, and after trimming from 18.21 to 22.04 M.

We isolated five cone opsins from the retinal transcripts of *C. monoculus* - SWS2B, SWS2A, RH2A β , RH2A α and LWS - as well as a rod opsin, RH1. Most of the opsins were complete except for SWS2B, which had lower transcript abundance than the others. Cichlids are known to have a single SWS2B copy, and we were able to generate a complete SWS2B sequence by assembling individual transcripts into a consensus SWS2B sequence. We further isolated six opsins from the genome assembly of *C. vazzoleri* (SWS1, SWS2B, SWS2A, RH2A β , RH2A α and LWS).

The maximum likelihood tree with other neotropical cichlid species confirmed the opsin classes of *Cichla* spp: SWS1, SWS2B, SWS2A, RH2A, LWS and RH1 (Fig. S3A, Appendix B). The cichlid opsin lineages are reciprocally monophyletic between New World and African lineages, with Neotropical cichlid opsins placed as sister group to the respective African cichlid orthologs in all opsins classes (Fig. S3A, Appendix B). We did not find SWS1 and RH2B opsins in the expressed transcripts for *C. monoculus*, hence we do not know whether those genes are functional or whether they have been lost in the genome. In addition, we did not recover RH2B in *C. vazzoleri*, but we found what seems to be a SWS1 pseudogene in this species, as suggested by the presence of several indels.

Comparisons between *Oreochromis niloticus* and *Cichla monoculus* opsin sequences (Table S1E, Appendix B) revealed evidence of amino acid changes

that might shift visual pigment absorbance. Within the transmembrane region of the opsin molecule, the greatest diversity was observed in the SWS2B opsin class, with 23 variable transmembrane sites, with seven of these occurring in the retinal binding pocket and two (V46F, G109A) at known tuning sites (Table 3.2, Fig. S3B, S1F, Appendix B). Other opsins also showed variable diversity, including LWS, RH1 and SWS2A with 17, 17 and 12 variable transmembrane sites, respectively (Table 3.2). However, when we combine *C. monoculus* sequences with other Neotropical cichlid species, the SWS2A opsin shows the highest variability followed closely by SWS2B (Table 3.3, Fig. S4C, Appendix B).

Table 3.2. Amino acid substitutions between *C. monoculus* and *Oreochromis niloticus*

Location and properties	Opsin gene					
	SWS2B	SWS2A	RH2A β	RH2A α	LWS	RH1
Transmembrane sites	23	12	12	11	17	17
Binding pockets sites	7	3	1	1	3	4
Known tuning site	2	1	0	0	0	2
Polarity change	4	3	3	2	5	5

Table 3.3. Amino acid substitution variation between neotropical cichlids (*Astronotus ocellatus*, *Symphysodon discus*, *Pterophylum scalare* and *Crenicichla frenata*)

Location and properties	Opsin gene				
	SWS2B	SWS2A	RH2A β	LWS	RH1
Transmembrane sites	32	38	28	34	23
Binding pockets sites	7	7	5	7	4
Known tuning site	3	3	0	1	2
Polarity change	7	13	4	9	7
Variable sites	19	34	25	26	14

[†]Because there is no complete sequence of RH2A α opsin, it has been omitted from this comparison.

3.4.5 Gene expression

Color vision in *C. monocolus* is based mainly on the expression of SWS2A, RH2A β , and LWS, 7.6, 8.2 and 82.3%, respectively (Fig. 3.5A,B). The most expressed single-cone pigment was SWS2A while the most expressed double-cone pigment was the LWS opsin. SWS2B and RH2A α accounted for <5% of expressed cone opsins in all samples. RH1 was the most highly expressed visual pigment in all samples (Fig. 3.5C). All samples expressed the same opsins.

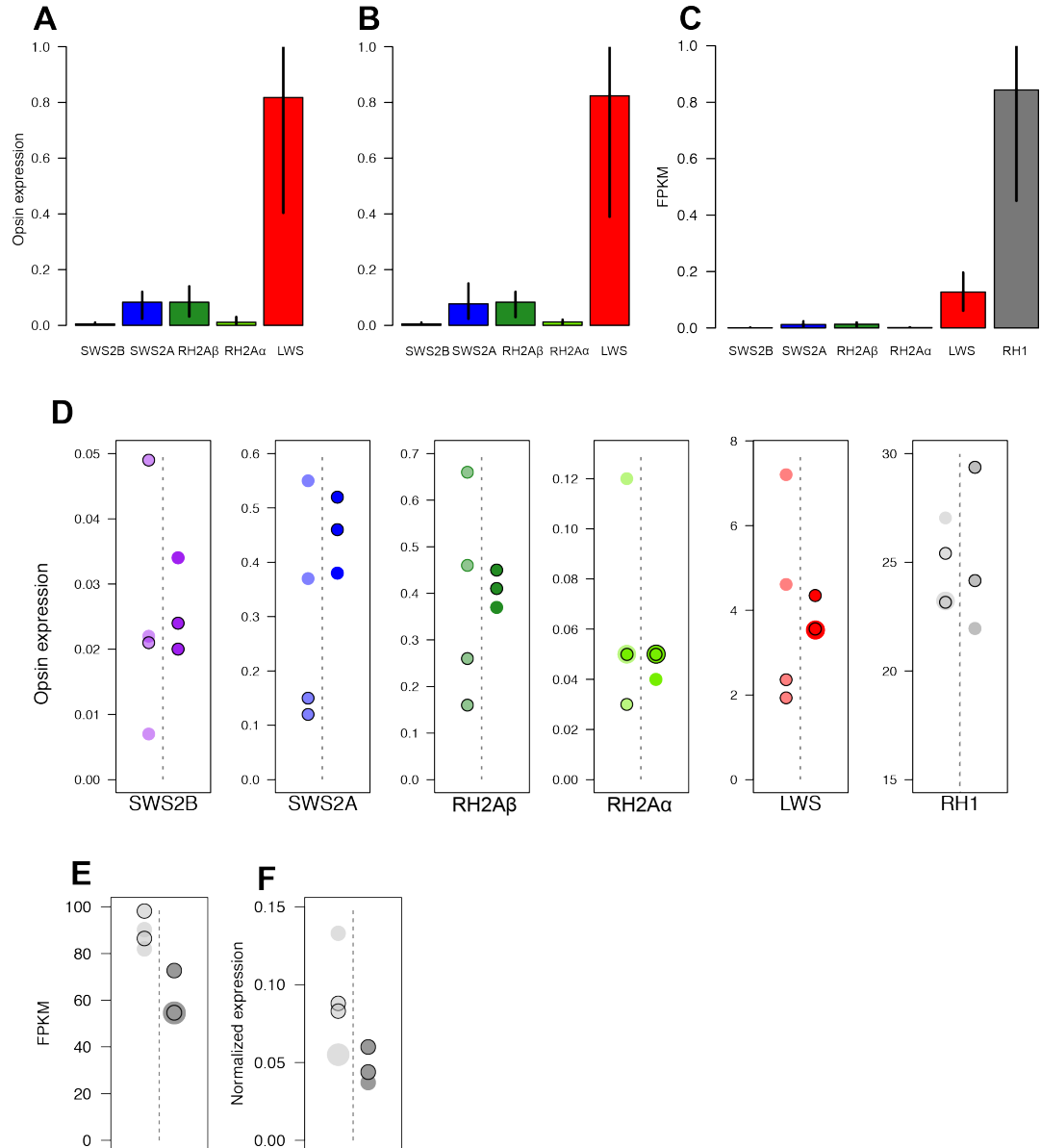


Figure 3.5. Opsin and Cyp27c1 expression. (A) Relative cone opsin expression profile of *C. monocolus* samples normalized to the β -actin gene. (B) Relative cone opsin expression of *C. monocolus* based on FPKM values (fragments per kilobase of transcript per million reads). (C) Normalized opsin expression as total FPKM values. (D) Opsin expression of seven *C. monocolus* samples. Opsin expression values were normalized to the β -actin gene. Each opsin class is specified (colored circles). (E) Gene expression of Cyp27c1 based on FPKM counts and (F) Cyp27c1 expression normalized to β -actin gene (gray circles). Dashed line separates samples from different sites (clear vs turbid). Light circles denote samples from clear waters whereas dark circles denote samples from turbid water sites. Black borders denote duplicates from a single fish and bigger circles are used to reveal overlapping data points.

Opsin expression determined from RNA-Seq data showed considerable variation amongst individuals. This remained true even when gene expression was normalized to a house keeping gene such as β -actin. Considering the individual variation, there was no evidence for differences in opsin gene expression between samples from different light environments (Fig. 3.5D). The substantial differences in visual pigment peak sensitivities highlighted by the MSP analysis suggest variability in chromophore use with the relative A_1/A_2 proportion potentially changing rapidly in response to underwater light conditions. Therefore, we examined the retinal transcripts for expression of *Cyp27c1*, a zebrafish-gene involved in the synthesis of vitamin A_2 from A_1 [115]. However, this gene was not differentially expressed between localities (Fig. 3.5E-F).

We performed a more global analysis of differential gene expression across all genes in the retinal transcriptomes and compared individuals sampled from clear versus turbid sites. A DESeq2 two-factor analysis detected 36 genes as being differentially expressed between clear and turbid water fish, with more genes (31) been upregulated in turbid-water samples and just five being upregulated in clear-water samples (Table S1G, Appendix B).

3.5 Discussion

3.5.1. Visual system adaptation

We have shown that the visual system of *C. monocolus* exhibits remarkable plasticity, which appears to be mediated predominantly by variation in chromophore content. Overall, the visual system of *C. monocolus* adapts to Lake Gatun's environment by four main mechanisms: (1) filtering wavelength scattered light (~400 nm) with ocular filters, (2) tuning visual sensitivities to the available light throughout opsin gene expression, (3) increasing the proportion of vitamin A₂ in its photoreceptors, making sensitivities more red-shifted as necessary, and (4) changing gene expression in the retina as a response to environmental stressors such as turbidity. The plasticity of their visual system has probably enabled fast adaptation to this changing environment because *C. monocolus* is a voracious predator that relies primarily on vision. Indeed, it has been suggested that their hunting strategies are among the traits that make *Cichla* spp successful invaders [116]. Furthermore, *C. monocolus* might benefit from changes in gene expression as these changes provide intraspecific phenotypic variation, facilitating visual function across the diverse light environments found in the lake.

3.5.2 Spectral measurements

Light environment in the Panama canal

Through spectral measurements, we describe for the first time the light environment of Lake Gatun. There is great variability in light transmission throughout Lake Gatun, which is greatly influenced by activities in the canal. There are high concentrations of suspended sediments in Lake Gatun owing to the daily transit of all types of boats, rainwater runoff, and water incursion from the locks. The amount of suspended particles seems to follow the Panama Canal transit path because in our measurements we saw a pattern consistent with this trend (Fig. 3.1-2). Attenuation increases at sites close to the canal water-way including Canal 2 and 3, Miller, Peña Blanca and the BCI Dock, whereas it is lower at sites that remain undisturbed by the canal activity, such as Gigante 1, 2 and 3 (Table S1C, Appendix B). Although our measurements were taken at a specific time of year and so might be subject to temporal variation, these measurements follow a turbidity-gradient pattern that has been characterized by Secchi disc measurements around Lake Gatun (Sharpe et al., unpublished). Overall, our spectral measurements suggest that fish inhabit a wide range of light environments within Lake Gatun. Some of these are strongly impacted by turbidity, which could negatively affect visual perception. Particularly, turbid sites seem to be detrimental for contrast detection owing to the increased light-scattering and light-absorption by suspended particles, which causes light to become very dim as depth increases.

Although Lake Gatun has an artificial origin, our measurements are in agreement with previous studies that have quantified the light environment of fresh-water

neotropical ecosystems such as Lake Managua, (Nicaragua) [117] and rivers from the Amazon [118], which are characterized by being long-wavelength-shifted environments.

Ocular media of *C. monoculus*.

The ocular media transmission from *C. monoculus* follows a similar pattern similar to that of other neotropical and African cichlids [12,117]. Even though the cornea is UV transmissive, all lenses proved to be UV-blocking (Fig. 3.3A-B). The presence of a yellow-pigmented region in the cornea and the UV-blocking nature of the lenses indicates that the visual system of *C. monoculus* specifically filters short wavelengths (<400 nm), reducing the loss of acuity caused by the aberration of violet and blue wavelengths, likely a major source of visual noise in the turbid waters of Lake Gatun, and thus, improving visual resolution. Furthermore, the yellow region in the cornea also filters much of the blue light (<486nm) (Fig. 3.3C); this might be useful for improving contrast by filtering out the “veiling brightness” (diffused blue light) found in the near-surface of the water column [119]. The presence of yellow filters in *C. monoculus* is not surprising given its Amazonian origin and the fact that similar adaptations have been reported for several Amazonian fish (Muntz 1973, 1982; Escobar-Camacho et al, 2017). These filters are suggested to act as an adaptation to long-wavelength shifted environments, thereby contributing to the ability of *C. monoculus* to adapt well to Lake Gatun.

3.5.3 Microspectrophotometry

Photoreceptor spectral sensitivities and vitamin A₁/A₂

The peak rod spectral sensitivities in *C. monoculus* (496-531 nm) are in concordance with those found for other neotropical cichlids (Table S1H, Appendix B). The range in peak absorbance implies extreme variation in A₁/A₂ chromophore combinations, which seem to change according to the light environment the fish live in. Chromophore shifts are plastic and respond to the light environment. Fish sampled from turbid waters exhibited long-wavelength shifted spectral sensitivities with average peak absorbances (λ_{\max}) between 514 and 523 nm when first sampled, whereas six-month treatment fish exhibited shorter wavelength-shifted sensitivities, with λ_{\max} between 500 and 511 nm (Fig. 3.4, Fig. S2A, Appendix B). Furthermore, turbid water and six-month treatment fish had a somewhat narrower set of spectral sensitivities (Fig. 3.4A-C) when compared with individuals collected in clear water. The variation in MSP from clear waters may be explained by fish movement within Lake Gatun. It is possible that fish collected from clear water might have migrated from turbid to clear waters relatively recently before sampling took place, however, this might suggest that fish from turbid waters change their A₁/A₂ ratio at a slower rate when they migrate to clear water sites. Another possibility is that clear water fish MSP variation could be a product of each fish's spectral tuning mechanisms in order to optimize their visual perception owing to their location in the water column. For example, fish living below two meters in clear waters would still need long-

wavelength sensitivities because short-wavelengths are lost below one meter depth.

Cichla monoculus spectral cone classes are similar to those reported for the Midas cichlid [117], but both are different from what has been suggested for neotropical cichlids, as previous studies described only three visual pigments (Table S1H, Appendix B). The cone spectral sensitivities of *C. monoculus* suggest that this species could potentially be tetrachromatic or pentachromatic, as we detected five different classes of photoreceptors (Fig. S2B, Appendix B). Notably, given the absence of an RH2B cone class, the blue cone appears to be particularly long-wavelength-shifted compared with that in the Midas cichlid (477 vs 450 nm). However, long-wavelength-shifted blue cones have been reported for neotropical cichlids, namely in *Crenicichla frenata*, *Pterophyllum* sp, and *Neetroplus nematopus* (Table S1H, Appendix B). Similarly, the short-green (RH2A β) pigment differs from the one reported for the Midas cichlid (518 vs 509 nm) but is similar to the one found for African cichlids *O. niloticus* and *Metriaclima zebra* (518 vs 518/519 nm). These differences between *C. monoculus* and other Neotropical cichlids are the complex result of variation in chromophore usage and the accumulation of amino acid substitutions in several opsin genes.

3.5.4 Transcriptome analysis

Opsin genes from *C. monoculus*

Through transcriptome analysis we have isolated the opsin complement of *C. monoculus*. The opsin complement of this species is similar to that found for other South American cichlids [113]. The absence of RH2B and SWS1 opsins in the transcriptome indicates that the inactivation of these genes has happened repeatedly among Neotropical cichlids [42,113]. This inactivation may occur by suppressing their expression, but may eventually result in pseudogenization. This was confirmed by analysis of the genome of *C. vazzoleri*, which revealed a SWS1 pseudogene and the loss of the RH2B opsin.

When building phylogenetic trees of opsin genes, we observed that the opsins of *C. monoculus* were placed in the neotropical cichlid clade as expected, yet their position in the neotropical cichlid clade varied (Fig. S3A, Appendix B). For the SWS2B opsin class, *Cichla* spp. held the most basal position which is consistent with previous research where Cichlini (*Cichla*) diverges basally before Astronotini (*Astronotus*) and Heroini (*Pterophyllum* and *Symphysodon*) [69]. However, there is phylogenetic discordance between the position of the other *Cichla* opsin classes (SWS1, SWS2A, RH2A, LWS and RH1) and Neotropical cichlid phylogenetic relationships. One possibility is that this disagreement could be the product of the mutational saturation of amino acid sequences. Furthermore, several of the opsin class clades exhibit low support.

Analysis of opsin amino acid sequence variation revealed that SWS2B is the opsin gene with the most substitution variation in *C. monoculus* (Table 3.2, Fig.

S3B, Appendix B). Amino acid changes in the SWS2B sequence could be the result of selection changing the spectral and/or nonspectral aspect of SWS2B function. This gene has been suggested to be under positive selection in the Trinidadian pike (*Crenicichla frenata*) [42]. However, when amino acid variation was analyzed between the opsin-set of five Neotropical cichlids, SWS2A showed the highest variation, similar to previous findings [113] (Table 3.3, Fig. S3C, Appendix B). Both SWS2B and SWS2A in Neotropical cichlids may be under strong selection to optimize visual perception in long-wavelength-shifted environments [42,43,86,87,113]. In addition, it has been shown that opsin amino acid substitutions in Neotropical cichlids improve opsin kinetics. For example, RH1 in *C. monocolus* has a D83N (Table S1E, Appendix B) substitution, which has been suggested to slow down the decay rate of the rhodopsin, which improves visual sensitivity in dim light conditions [121].

Opsin gene and Cyp27c1 expression

Cone opsin expression of *C. monocolus* is dominated by long wavelength-sensitive pigments and, to a lesser extent by SWS2A and RH2A β , a pattern similar to that of other neotropical cichlids [42,113,117]. This opsin expression profile is optimal for red-shifted light environments because the double cone spectral sensitivities match the available light (Fig. S2C, Appendix B). Although *C. monocolus* exhibited individual variation in opsin expression, we did not detect any significant correlation with the underwater light conditions at collection sites (Fig. 3.5D). Thus, we can not conclude whether there is opsin expression plasticity in *C. monocolus*. More studies analyzing changes of opsin expression

in adults and through developmental series are necessary. To date, different cichlid species have been found to exhibit gene expression plasticity at the adult stage or no adult plasticity at all [73,107–109]. Our results could also be masked by sampling effort because we do not have a large set of samples.

Similarly, although we measured large differences in spectral sensitivity between individuals from clear and turbid sites, and successfully experimentally manipulated such sensitivities by treating turbid water individuals in clear water conditions, we did not observe covariation between turbidity and the expression of Cyp27c1. This enzyme has been shown to convert vitamin A₁ into vitamin A₂ in the retinal pigment epithelium of zebrafish where the proportion of A₂ is positively related with its expression [115]. In *C. monoculus*, we found a functional copy of Cyp27c1, however, turbid water fish exhibited low levels of Cyp27c1 expression when compared with clearwater fish samples (Fig. 3.5E-F). This is surprising in light of our rod MSP results, which support more A₂-based visual pigments in turbid water individuals (Fig. 3.4). We hypothesize two possible explanations. First, our samples in particular may not show high levels of Cyp27c1 expression owing to a sampling problem. Notably, the samples used for transcriptomes were not the same samples analyzed for MSP. Second, the conversion of A₁ to A₂ could be controlled by another gene in cichlids. We found other genes highly similar to Cyp27c1 in the transcriptomes. All of these genes belong to the Cytochrome P450 superfamily in teleosts (Fig S4A, Appendix B). Although their expression also varied between samples (Fig S4B, Appendix B), it was very low

and did not show any correlation with habitat lighting. Hence, more experiments are needed to unravel the relationship between Cyp27c1 expression and proportions of A₁-A₂ in the cichlid retina.

Differential gene expression in the *C. monoculus* retina

Considering more global analyses of differential retinal gene expression, our results show that there are differences in gene expression of a number of genes in the *C. monoculus*' retina. DESeq analysis suggests that fish differentially expressed genes between clear- and turbid-water, including genes that vary greatly in function. Genes that were upregulated in clear-water samples are involved in the oxidation of cortisol, preventing apoptosis, neutrophil regulation and intracellular trafficking (see Table S1G, Appendix B). Interestingly, RDH8, a key enzyme in visual pigment regeneration, was found to be upregulated in clear-water samples (Table S1G, Appendix B). This suggests that fish from clear environments may exhibit a faster regeneration rate of visual pigment owing to greater light exposure. Furthermore, individuals from turbid waters exhibited up-regulation of genes involved in transposition, anti-inflammatory processes, and production of collagen. The pattern that seems to emerge is one of elevated stress in fish living in turbid sites in Lake Gatun. Individuals over-expressed genes involved in optimal immune and anti-inflammatory response (ORM1 and ANXA1, respectively); genes involved in neuroblast differentiation (AHNAK), and genes favoring bloodstream circulation (HBB, HBAA, HBAB and PDFGFRL), perhaps in response to low dissolved oxygen conditions. Interestingly, the gene

TCB1, known to be involved in the transposition of transposable elements (TEs), was also found to be upregulated in turbid-water samples, perhaps indicating that turbid-water fish are under risk of developing mutations as a result of TE insertions. While generally detrimental, TEs might contribute to the generation of the standing variation facilitating invasions as suggested for other species [122,123]. Differentially expressed genes may be relevant to the success *C. monocolus* as an invasive species in Lake Gatun. Indeed, it has been suggested that invasive species can have shifted expression of genes that provide physiological advantages in different environments enabling their adaptation and hence, invasion success [124–127].

Invasive species will only be successful if they have mechanisms for rapidly adapting to novel habitats. Here we have documented several mechanisms that enable the visual system of *C. monocolus* to be particularly efficient in the temporally and spatially fluctuating turbidity of Lake Gatun. Its long-wavelength-shifted opsin palette combined with variable chromophore usage pushes its photoreceptor sensitivity to match the prevalent underwater spectrum, optimizing contrast detection in low light intensity and high scatter, even at relatively large distances. Furthermore, exceptionally large individual differences in rod spectral sensitivities correlate with local light conditions and appear to be mainly driven by plasticity in chromophore use rather than cone expression variation. Finally, these mechanisms of spectral tuning are accompanied by differential gene expression in the retina, where several genes are being upregulated and

downregulated, and this varies within the same population. Overall, even though these mechanisms may occur naturally in the Amazon basin, they exhibit intraspecific variation, which is key for phenotypic plasticity and, hence, the invasive potential of *C. monoculus*. Unfortunately, this invasion has been at the expense of other fish as the introduction of *C. monoculus* has likely extirpated several native fish species in the process [104].

3.6 Acknowledgments

We thank the University of Maryland Institute for Bioscience & Biotechnology Research for sequencing the libraries, Matt Conte for helping with the Trinity pipeline and Noor White for help with the phylogenetic trees. We are grateful to Ellis R. Loew for generously providing his MSP machine and analysis software for this project. We thank the Panama Canal Authority (ACP) for granting us access to the canal waters. We also thank all the rangers and staff of the Smithsonian Tropical Research Institute that assisted us during our stay and sampling on Barro Colorado Island. The authors declare that we have no significant competing financial, professional, or personal interests that might have influenced the work described in this manuscript. This work was funded by the National Institute of Health (R01EY024693 to K.L.C) and by the partnership program between the University of Maryland and University of Tübingen for the joint course of animal communication. D.E-C. is supported by a graduate fellowship of the Secretariat of Higher Education, Science, Technology and Innovation of Ecuador (2014-AR2Q4465 to D.E-C.). DNA sequences and

transcriptome libraries are available from GenBank (accession nos: MK562367–MK562373, MK568303–MK568308) and the SRA database (SRR8643940–SRR8643946).

Chapter 4: Visual pigment evolution in Characiformes: insight of dynamic evolution of teleost whole-genome duplication surviving opsins and spectral tuning.

Daniel Escobar-Camacho, Karen L. Carleton, Devika Narain, Michele E.R. Pierotti. (In progress)

4.1 Abstract

One of the aims of evolutionary biology is to understand the origins and adaptations of animal sensory systems, as they provide channels to gather information from the surrounding environment. Among sensory channels vision represents a model to study evolution given the genotype-to-phenotype-map that has been characterized in a number of taxa. Because fish exhibit a remarkable range of visual sensitivities and adaptations to underwater light, this makes them an ideal group to study visual system evolution. In this study, through molecular and electrophysiological experiments, we have characterized the visual system of neotropical Characiformes. Transcriptome and genome analysis revealed three cone opsin classes (SWS2, RH2, LWS) and a rod opsin (RH1). However, their entire opsin gene repertoire is a product of complex evolutionary dynamics characterized by opsin gene loss (SWS1, RH2) and opsin gene duplications (LWS, RH1). The LWS-duplicates are a product of the teleost specific whole-genome duplication and from characin-specific duplication events. Through amino acid substitution, these LWS paralogs have acquired spectral sensitivity to green light. They also exhibit gene conversion, and have variable codons in key tuning sites leading to reversion and parallel evolution. In addition, the SWS2- and RH1-opsin exhibit spectral shifts and changes in gene expression, respectively.

Furthermore, characins possess a diverse set of spectral sensitivities, which is the result of several spectral tuning mechanisms acting in concert. These are

mainly opsin sequence variation, opsin gene loss and duplication, opsin gene expression, and A_1/A_2 chromophore tuning. This study shows how studying speciose, understudied groups, provides a unique opportunity to better understand opsin gene evolution, particularly, opsin gene neofunctionalization.

4.2 Introduction

Vision is an important sensory channel as it allows organisms to obtain information from the environment. In vertebrates, vision starts when light reaches the retina and it is detected by rod (night vision) and cone (diurnal vision) photoreceptors. Photoreceptors are packed with visual pigments which are composed by an apoprotein, the opsin, and a light-sensitive molecule, the chromophore [6,7]. Opsins consist of seven α -helices where the transmembrane regions enclose a ligand-binding pocket with a light sensitive chromophore, 11-cis retinal [7]. There can be multiple cone types containing different visual pigments that absorb light maximally in different parts of the wavelength spectrum.

There are four classes of cone pigments encoded by opsin gene families among vertebrates: a short-wave class (SWS1) sensitive to ultraviolet-violet light (350-400 nm), a second short-wave class (SWS2) sensitive to violet-blue (410-490 nm), a middle-wave class (RH2) sensitive to green (480-535 nm), and a middle-to long-wave class (LWS) sensitive to the green-red spectral region (490-570 nm) [7,128]. All four cone classes are the product of a series of gene duplications

from an ancestral single opsin gene that appeared early in vertebrate evolution (450 MYA) [7,128,129]. Because opsin classes differ in amino acid sequences, this results in a spectral tuning mechanism that is based on nucleotide variation. If a nucleotide substitution leads to the replacement of an amino acid that alters the interaction of the chromophore and the opsin, this will lead to a spectral shift in the maximal absorbance (λ_{\max}) of a visual pigment. Consequently, this is a spectral tuning mechanism in which variation in λ_{\max} between visual pigments is the product of the interaction of different opsin classes and the identical 11-cis retinal. The shift in λ_{\max} caused by a single amino acid substitution varies, from only a few nanometers to very large shifts (e.g. 2 to 75 nm respectively) [6]. In addition, the additive effects of several substitutions can also produce moderately large shifts greater than ~30 nm [6,130,131].

Among vertebrates, fish are ideal for the study of visual pigment evolution. First, because of the physicochemical properties of water, this medium has a profound effect on light transmission. Water absorbs and scatters much of the incoming light, and this inevitably causes great variation across aquatic habitats [11,132], which is reflected in the several adaptations fish visual systems exhibit. Second, due to their phylogenetic history, species richness, diverse ecologies, and diverse spectral sensitivities, teleosts offer an excellent system for studying the evolution of visual pigments. Spectral sensitivities have been documented for several fish species [18,26,28–31] and the dynamic evolution of the different opsin classes have been actively studied [6,7,32–36].

Characiformes, with more than 2000 described species, is an extremely diverse group of freshwater fishes inhabiting a wide range of ecosystems. This order includes at least 23 families with dozens of species being described each year [79,133,134]. Their Gondwanan origin, wide distribution, species richness and colorful patterns, make them an ideal group for studying the evolution of their visual system and its adaptation to the light environment. Research on the visual system in Characiformes have only been reported for the tetra *Astyanax fasciatus* [130,135–138]. Several studies nicely characterized its visual pigments and showed how this species has a duplication in the LWS-opsin in which one copy became sensitive to green light through amino acid substitutions; a remarkable example of convergent evolution with green sensitivity in humans [130]. Recent studies have analyzed the origins of *Astyanax* opsin genes more in depth and have concluded that these duplicates are surviving opsins from the teleost-specific genome duplication (TGD) (300-450 MYA [139–141]).

In this study, we expand the molecular characterization of the visual system in Characiformes. We showcase the complex evolutionary dynamics of their opsin gene repertoire and we examine the diverse set of spectral tuning mechanisms present in this group.

4.3 Materials and methods

4.3.1 Animals

Adult fish specimens were collected using fishing lines, manual seines and cast nets in several locations in Panama and Suriname from May to July of 2017 (Table S1, Appendix C). Sampling permits were in accordance with the Panamanian and Suriname laws of environmental protection (permits from Ministerio de Ambiente de Panamá, MiAmbiente, permit No. SC/A-14-17; and Ministry of Agriculture, fisheries and animal husbandry of Suriname, permit No. 1087). Fish were handled following STRI IACUC protocol (#2017-0501-2020). After sampling all fish were brought back to Naos Research Laboratories at the Smithsonian Research Institute Panama. Three specimens from each species were killed immediately for RNA-Sequencing and a total of 29 species were used for microspectrophotometry (MSP). Fish sampled in Suriname were sacrificed at the laboratories of Anton de Kom University of Suriname. In total we obtained 13 species that belonged to eight different families within Characiformes (Tables S1, Appendix B).

4.3.2 RNA seq

After collection fish were euthanized with buffered MS-222 and their eyes were enucleated and their retinas preserved in RNAlater. Two or three samples per species were used for RNA sequencing. Total RNA was extracted with an RNeasy kit (Qiagen), and RNA quality was verified on an Agilent Bioanalyzer.

RNAseq libraries were prepared using the Illumina TruSeq RNA library preparation kit (Illumina Inc, San Diego) and sequenced to obtain 100-bp paired-end-reads with a total of 36 samples multiplexed in three lanes (12 samples per lane) on an Illumina HiSeq1500 sequencer at the University of Maryland Institute for Bioscience & Biotechnology Research. The quality of the data was checked using FastQC version 0.11.2 to remove overrepresented sequences and to retain sequences with a minimum quality score of 20 and a minimum length of 80 bp. Transcriptomes were combined to obtain 13 de-novo assemblies for each species. This was performed with Trinity version r20140413 [50] using only paired sequences with a minimum coverage of two to join contigs.

4.3.3 Opsin phylogenetics and molecular analysis

Candidate opsin sequences were identified from the assembled transcriptome FASTA files by Tblastx querying with the characid opsin genes of *Astyanax fasciatus* [130,135,136,138]. Because we found opsin duplicates in the transcriptomes we used GENEIOUS 8.1 to map paired-reads for each paralog and correctly assemble each opsin sequence. We confirmed the identities of gene sequences for each species to a particular opsin class based on their phylogenetic relationships with opsins sequences of lamprey (*Geotria australis*) and several teleosts obtained through Genbank [51]. Furthermore, we added to our analysis opsin sequences of the available genomes of the Mexican cavefish, (*Astyanax mexicanus*), and the red-bellied piranha (*Pygocentrus nattereri*). We used MAFFT [52] to align amino acid sequences and ProtTest 3.4.2 [142] to

obtain the evolutionary models for each opsin class (Table S2, Appendix C). We used RAXML for building maximum-likelihood trees. We ran 10 searches for the best tree and 1000 bootstrap replicates performed in RAXML 8.0 on CIPRES [143].

Once we identified characin opsin classes, we searched for amino acid substitutions that could shift the spectral sensitivity of visual pigments. To do this we aligned characin opsin sequences with bovine rhodopsin and with opsins from other teleosts. We looked for substitutions that fell in putative transmembrane regions and in the retinal binding pocket facing the chromophore or in known spectral tuning sites [6,55,56,137].

Finally, since there were opsin duplicates in most analyzed species, we tested whether there was gene conversion because it is a common phenomenon in teleosts [64,65,113,144,145]. For this we used the program GARD (Genetic Algorithm Recombination Detection) [146] on separate alignments of the LWS duplicates to detect the presence or absence of recombination. To corroborate patterns of gene conversion we performed phylogenetic trees based on the fragments between the recombination breakpoints.

4.3.4 Ancestral state reconstruction

Previous research has characterized the molecular basis of spectral tuning in the LWS pigments where five amino acid changes (S164A, H181Y, Y261F, T269A,

A292S) can shift λ_{\max} up to 50 nm [130,137,147]. Because we found variation in the occurrence of three of these amino-acid substitutions (S164A, Y261F, T269A) that are known to short wavelength shift the λ_{\max} of LWS-opsins by 7, 10 and 16 nm respectively [6,60,137,148], we analyzed the evolutionary relationships between the spectral tuning sites in Characiformes. We observed seven combinations of the three sites in our LWS-data set (Table S3, Appendix C). We assigned one of these combinations to each LWS-opsin gene and we performed a discreet trait ancestral state reconstruction analysis.

In addition, we observed that, among the three sites, site S164A was the most variable tuning site. In order to understand the molecular mechanisms leading to this variation, we reconstructed the evolutionary changes leading to both serine or alanine, and identified parallel changes and reversions. For this we characterized the extant codons in each gene and performed ancestral state reconstruction where we incorporated the respective codon to each gene as a trait.

For ancestral state reconstruction analyses we used the ace function in the APE package [149]. The ace function employs a maximum likelihood approach where the reconstructed ancestral states are given as a proportion of the total likelihood for each state for each node.

4.3.5 Opsin gene expression

For estimating gene expression of each opsin, reads were mapped back to the assembled transcriptomes using RSEM as part of the Trinity package [50]. Read counts for each opsin class were extracted from RSEM output (quantified as fragments per kilobase of transcript per million reads, FPKM). In order to avoid non-independent bias of opsin expression owing to variation in the expression of each opsin class, cone opsin read counts were then normalized to those of the β -actin gene. We also normalized for total cone opsin expression and divided each opsin's expression by the sum of all cone opsin counts to get the proportion of each expressed opsin.

4.3.6 Microspectrophotometry

To identify the λ_{\max} of photopigments, we performed MSP on wild-caught fish in different localities of seven characin species. To prevent visual pigments from bleaching, each fish was dark-adapted for at least 2 hrs, after which it was sacrificed with an overdose of buffered MS222. Eyes were enucleated under a dissecting scope in dim deep red light. The retina was removed and transferred to a PBS solution containing 6.0% sucrose (Sigma). A small piece of retina was cut out and placed on a glass cover slip in a drop of solution, then delicately macerated with razor blades. The preparation was covered with a second glass cover slip and sealed with high-vacuum silicone grease (Dow Corning).

Spectral absorbance was measured with a computer-controlled single-beam micro-spectrophotometer fitted with quartz optics and a 100W quartz-halogen

lamp. Baseline records were taken by averaging a scan from 750nm to 350nm and a second in the opposite direction, through a clear area of the preparation and in proximity to the photoreceptor of interest. A record of the visual cell was then obtained by scanning with the MSP beam through the photoreceptor outer segment. Finally, the cell's absorption spectrum was obtained by subtracting the baseline record. A custom-designed spectral analysis program (Loew et al. in prep) was used to determine λ_{\max} from absorbance records using existing templates [110,111]. Individual spectra were smoothed with a nine-point adjacent averaging function and the resulting curves were differentiated to obtain a preliminary maximum value. This was used to normalize curves to zero at the baseline on the long wavelength limb and to one at the maximum value. Whitmore and Bowmaker's (1989) relationship (Eqn 1) was used to recursively fit the observed (normalized) absorption spectra to curves resulting from combinations of different proportions of pure Vitamin A₁ and corresponding pure Vitamin A₂ nomograms [112] (Fig. S1, Appendix C).

$$\lambda_{\max A1} = (\lambda_{\max A2} - 250)^{0.4} * 52.5 \quad \text{Eqn 1}$$

Retina preparation for micro-spectrophotometry proved to be challenging due to a red pigment which envelops characin photoreceptors [16], which required extensive manipulation and often caused the mixing of this pigment in the preparation.

4.3.7 DNA extraction, sequencing and phylogenetic analysis

To analyze the evolutionary relationships of the sampled characins and confirm species identification we sequenced nuclear and mitochondrial genes (16S, Cytb, Myh6, RAG1 and RAG2) from all collected species except *C. spilurus*. DNA was extracted with a DNeasy kit (Qiagen), and DNA quality was verified using a Nanodrop. PCR reactions were performed in a total volume of 50µl using a thermocycler (Eppendorf). Reactions contained 25µl DreamTaq DNA polymerase, 20µl of sterile distilled H₂O, 2µl of each primer (10µM), and 1µl template DNA. Conditions were as follow: 94°C (2 min); 35 cycles of 94°C (30s), °54 (30s), and 72°C (2 min) followed by 72°C (4min). Nested-PCRs were used to amplify the genes RAG1 and RAG2. Amplified products were checked on 1% agarose gel stained with GelRed.

Once individual genes were sequenced for each species all genes were concatenated. We added our species alignments to a data set of 213 sequenced characins for the same markers from Oliveira et al., 2011 [133]. For performing phylogenetic analyses we used Partitionfinder2 [114] to obtain the most appropriate models and partitioning scheme. Finally, we used RAXML for building maximum-likelihood trees with 1000 Bootstrap repetitions [143].

4.4 Results

4.4.1 Opsin gene sequences

Opsin complements

Through phylogenetic analyses we identified fully functional sequences belonging to three cone opsin classes (SWS2, RH2, LWS) as well as a rod opsin (RH1) (Fig. 4.1-2, Fig S1-4, Appendix C). The opsin-gene set within Characiformes seems highly variable because we found variation in the presence/absence of some opsins and several duplications (Fig. 4.3). We did not find sequences belonging to the UV-light sensitive opsin (SWS1), either in the transcriptomes or genomes (Fig. S1, Appendix C). We also did not detect the RH2 opsin in the transcriptomes of *C. spilurus*, *H. microlepis*, *S. rhombeus*, and *R. guatemalensis*, however, we found a non-functional RH2 opsin in the genome of *P. nattereri*.

Examination of the LWS-opsin class revealed the presence of several duplications and these varied between lineages suggesting the following. First, there was an LWS-duplication event, which is the product of the teleost-specific genome duplication (TGD) (300-450 MYA) (Fig. S4, Appendix C). This is supported by the fact that these initial duplicates appear after the divergence of teleosts and the spotted gar, *Lepisosteus oculatus* (Fig. 4.1). These initial LWS paralogs formed two distinct clades in our analyses, which we will call LWS1 and LWS2. LWS2-opsins grouped with Osteoglossiformes, which are known to share this duplication with characins [141], whereas the LWS1-opsins grouped with the

remaining teleost-LWS-opsins. Second, after TGD, LWS1 and LWS2 underwent subsequent rounds of duplications within Characiformes. This varied across families, however, duplicates do not group in differentiated clades (Fig. S2, Appendix C). The characin exclusive LWS2-opsin duplication is shared in most species. LWS2-1 and LWS2-2 differ by the presence of a 6bp deletion in the first 20 bp of the coding sequence (exon I, extracellular region) in LWS2-2, and by a few amino acids although not in spectral tuning sites.

Furthermore, we found TGD-surviving duplicates of another opsin class: the rod-opsin (RH1) (Fig. 4.2). In similar fashion to the LWS duplicates, these RH1 paralogs (which we will refer to as RH1-1 and RH1-2) grouped in different RH1 clades where the TGD-surviving opsins of Characiformes formed a well-supported clade with the known TGD-surviving copies (RH1-2) present in Cypriniformes [150,151] (Fig. 4.2). Within RH1-2 opsin sequences, several species of Characiformes had numerous deletions in the last exon. We also found disparate amino acid variation at transmembrane sites which suggest the non-functionality of these opsin genes, hence, they were excluded from subsequent analyses. Lastly, characin LWS1, RH2, SWS2, and RH1-1-opsins show a paraphyletic pattern in relation to Siluriformes and Gymnotiformes (Fig. S1-3, Appendix C).

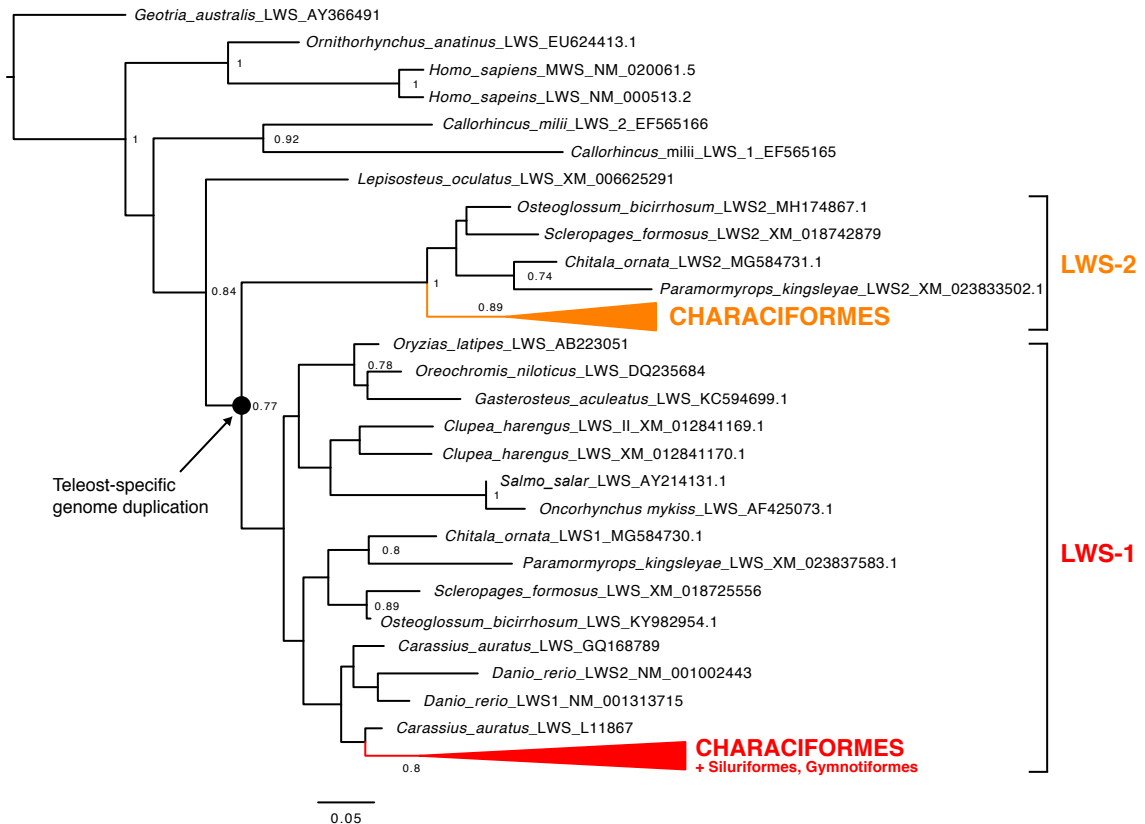


Figure 4.1. LWS-opsin tree of Characiformes. LWS-opsin maximum-likelihood phylogenetic tree based on amino-acid sequences of Characiformes, Osteoglossiformes, Siluriformes, Gymnotiformes, *Geotria australis* (lamprey), *Ornithorhynchus anatinus* (platypus), *Homo sapiens* (humans), *Callorhincus milli* (Elephant shark), *Lepisosteus oculatus* (Spotted gar), *Oryzias latipes* (medaka), *Gasterosteus oculatus* (stickleback), *Clupea harengus* (herring), *Salmo salar* (salmon), *Onchrynchus mykiss* (trout), *Carassius auratus* (goldfish), and *Danio rerio* (zebrafish). Bootstrap support over 75% is shown. This tree confirms that LWS1 and LWS2 arose after the divergence of the spotted gar, probably as a product of TGD. Notice the clustering of characins LWS2-opsins with the osteoglossimorph LWS2-opsins. Characiformes species are compressed color-filled clades (LWS2-orange and LWS1-red).

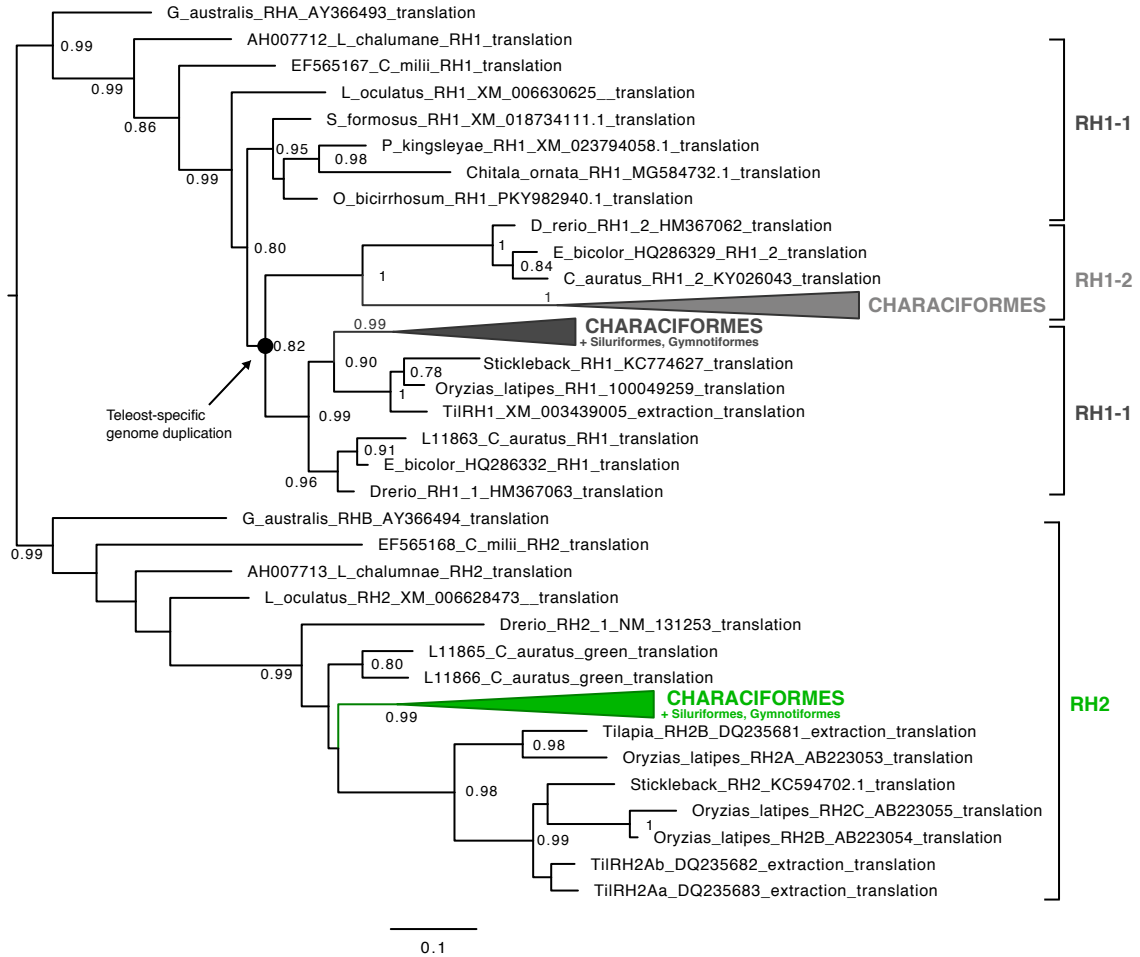


Figure 4.2. RH1-RH2-opsin tree of Characiformes. RH1-RH2-opsin maximum-likelihood phylogenetic tree based on amino-acid sequences of Characiformes, Osteoglossiformes, Siluriformes, Gymnotiformes, Cypriniformes, *Geotria australis* (lamprey), *Latimeria calumnae* (coelacant), *Callorhincus milli* (Elephant shark), *Lepisosteus oculatus* (Spotted gar), *Oryzias latipes* (medaka), and *Gasterosteus oculatus* (stickleback). Bootstrap support over 75% is shown. This tree confirms that RH1-2 arose after the divergence of the spotted gar, probably as a product of TGD. Notice the clustering of characins RH1-2-opsins with the cyprinimorphs surviving RH1-2-opsins. Characiformes species are compressed in color-filled clades (RH1-2-gray, RH1-1, black, and RH2-green).

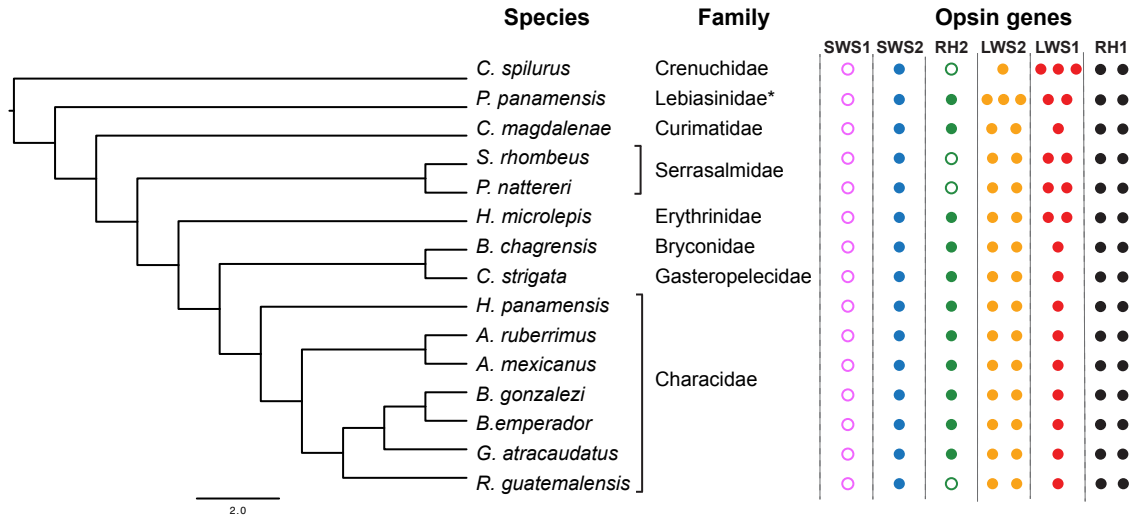


Figure 4.3. Opsin gene complement in Characiformes. To the left, schematic representation of the phylogenetic relationships of characins in this study based on Oliveira et al, 2011, and to the right, the presence or absence as well as the number of opsin genes in each class (Fig. S8, Appendix C). Species names and families are shown for the samples used in this study as well as their opsin complement where each opsin-gene is indicated by a filled circle for each opsin class. Empty circles denote potential gene losses. *Even though *P. panamensis* is considered a member of Lebiasinidae, our results suggest it belongs to Parodontidae.

Gene conversion

Gene conversion analysis with GARD revealed evidence of interspecific gene conversion within LWS1- and LWS2-opsins with two and three breakpoints respectively. In both, LWS1 and LWS2, conversion seems to be prevalent in the first exons (Fig. S5, Table S3, Appendix C). Phylogenetic trees based on fragments between recombination breakpoints exhibit different tree topologies where trees based on exons from three to six, were the ones who recovered most similar phylogenetic relationships between families and ancestral duplications to their known genomic tree topologies [133] (Fig. S5, Appendix C).

Opsin sequence spectral tuning

Our analyses revealed several amino acid substitutions that shift λ_{\max} of visual pigments. The SWS2 opsin exhibited the greatest variation in transmembrane regions, changes in polarity, and variation in binding pocket sites (Fig. 4.4). Several of these substitutions occurred in spectral tuning sites (M44T, A109G, M122I, A269T, A292S) that are known to shift the SWS2- λ_{\max} [6]. We also confirmed the presence of three mutations (S164A, Y261F, T269A) in the LWS2 paralogs that shift λ_{\max} to shorter wavelengths (~30 nm) [6,137]. Although previously reported in *Astyanax fasciatus* [130] and Osteoglossiformes, in our study we found that this trait is prevalent in most characins.

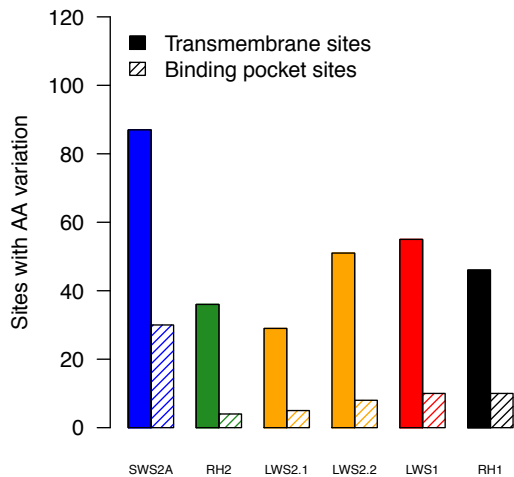


Figure 4.4. Number of sites with amino-acid substitution variation for each opsin class of 15 Characiformes species. Solid bars denote amino acid variation in transmembrane regions whereas striped bars denote variation in binding pocket sites.

Ancestral state reconstruction

By analyzing the evolution of LWS-spectral tuning through ancestral state reconstruction, our results suggest that the ancestral LWS-haplotype of teleosts before TGD was probably red wavelength sensitive (node #2, 73.56% of the scale likelihood) (Fig. 4.5, Table. S5, Appendix C). This suggests that green sensitivity evolved soon after TGD (node #43, 93.7% of the scaled likelihood) (Fig. 4.5, Table. S5, Appendix C).

Furthermore, our analysis examining the molecular basis of spectral tuning of the site S164A, -7 nm shift [6,137], suggests that the LWS2-ancestral haplotype of Characins most probably used the codon GCC (node 43, 99.03% of the scaled likelihood) to encode for Alanine whereas the LWS1-ancestral haplotype used TCT (node 6, 99% of the scaled likelihood) to encode for Serine. However, our analysis suggests there are reversions and parallel evolution occurring at this site. We found reversion in the LWS2-opsins of some earlier divergent lineages within characins (*C. strigata*, *P. nattereri*, *H. microlepis* and *P. panamensis*) because through reverse mutation, the LWS2-opsins changed from codons for Alanine (GCC) back to codons for Serine (TCT or TCC). This occurred in parallel in the characin *P. innesi*. (Fig. S6, Appendix C). Similar to LWS2, there is evidence of parallel evolution in the LWS1-opsins. *H. panamensis* and *C. spilurus* shifted in parallel from serine to alanine utilizing the same codons (TCT to GCT) (Fig. S7, Appendix C). Finally, even though the scope of this study focused on Characiformes, the variability of site 164 is quite impressive as

several teleosts exhibit different codons for either Alanine or Serine (Fig. S6, Appendix C).

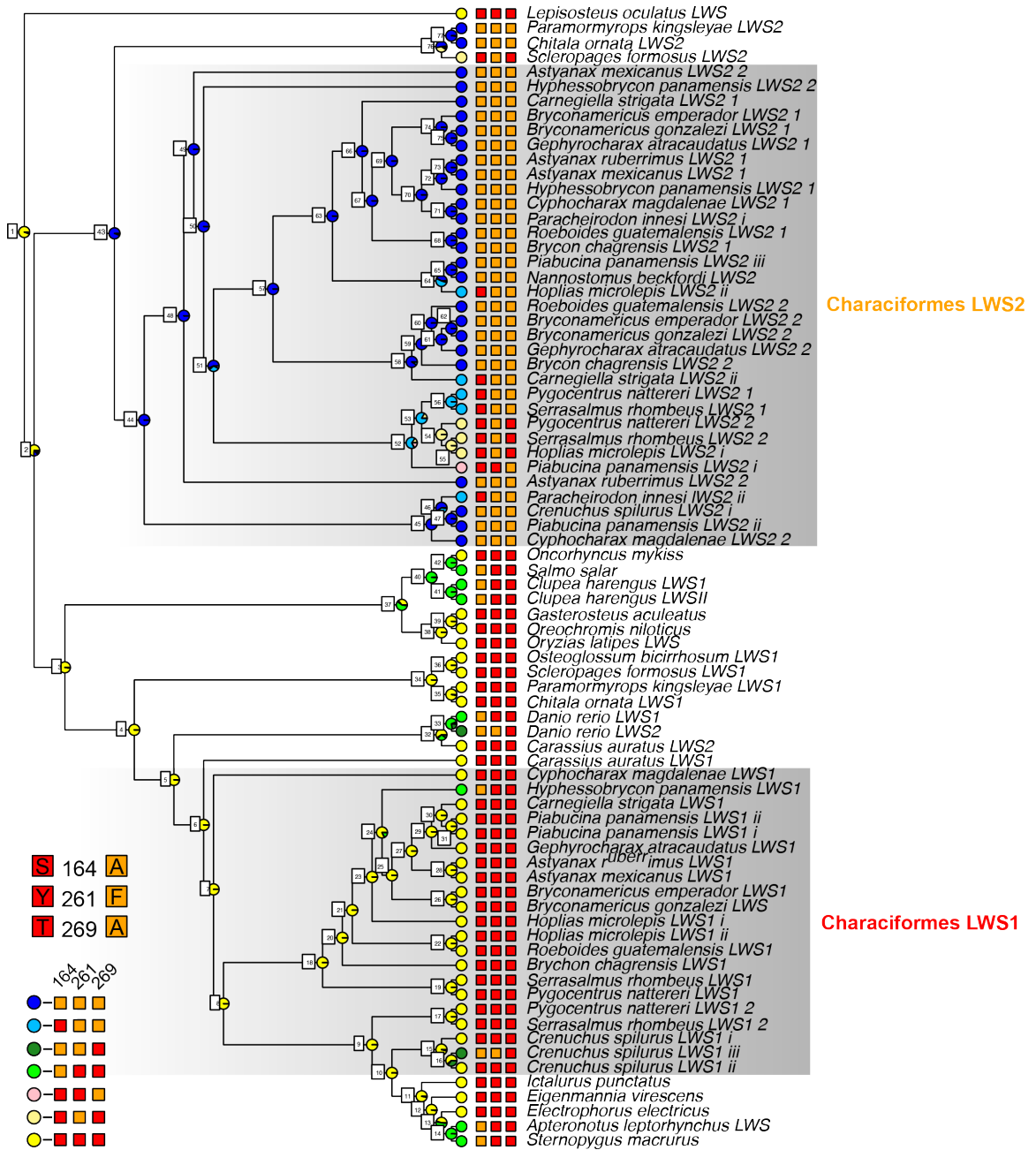


Figure 4.5. Ancestral state reconstruction of the spectral tuning in LWS-opsin-genes. The three known spectral tuning sites (S164A, Y261F, T269A) that are known to convey green sensitivity in Characiformes are shown for each species for each LWS gene. The seven combinations we found of the three

tuning sites in our data set shown, where each combination is represented as a colored circle. Pie charts on the nodes indicate the scaled likelihoods, calculated using the ace function in APE, of each specific combination. Nodes are also labeled consistent with Table S4, Appendix B.

4.4.2 Opsin gene expression

Opsin expression varied between Characiformes ranging from species expressing mainly two opsins, like the sail-fin tetra (*C. spilurus*) or the dogfish (*H. microlepis*), to species expressing up to six (*P. panamensis*). The SWS2-opsin is the only short-wavelength pigment expressed (3 to 15% of total opsin expression), and the LWS duplicates account for the bulk of characin opsin expression (80-95%) (Fig. 4.6). Within LWS expression, there is always at least one copy of the LWS1-paralog being expressed, which is followed by the expression of one or two copies of the LWS2-paralog (Fig. 4.6). There seem to be differences in the expression of the LWS2 paralogs because in some species the LWS2-1 opsin is more expressed than the LWS2-2 opsin (*B. chagrensis*, *A. ruberrimus*, *G. atracaudatus*), and this can be the opposite in other species as well (*H. panamensis*, *B. gonzalezi*, *C. strigata*) (Fig. 4.6).

In addition, RH2 is lowly expressed (<5%) in most samples, except in *B. emperador* (10%), and it was not found at all in the transcriptomes of four species (*C. spilurus*, *H. microlepis*, *S. rhombeus*, and *R. guatemalensis*). Finally, rod-opsin expression is mainly dominated by the former paralog, RH1-1, while RH1-2 is very lowly expressed (<1.1%) in all analyzed species (Fig. S7, Appendix C).

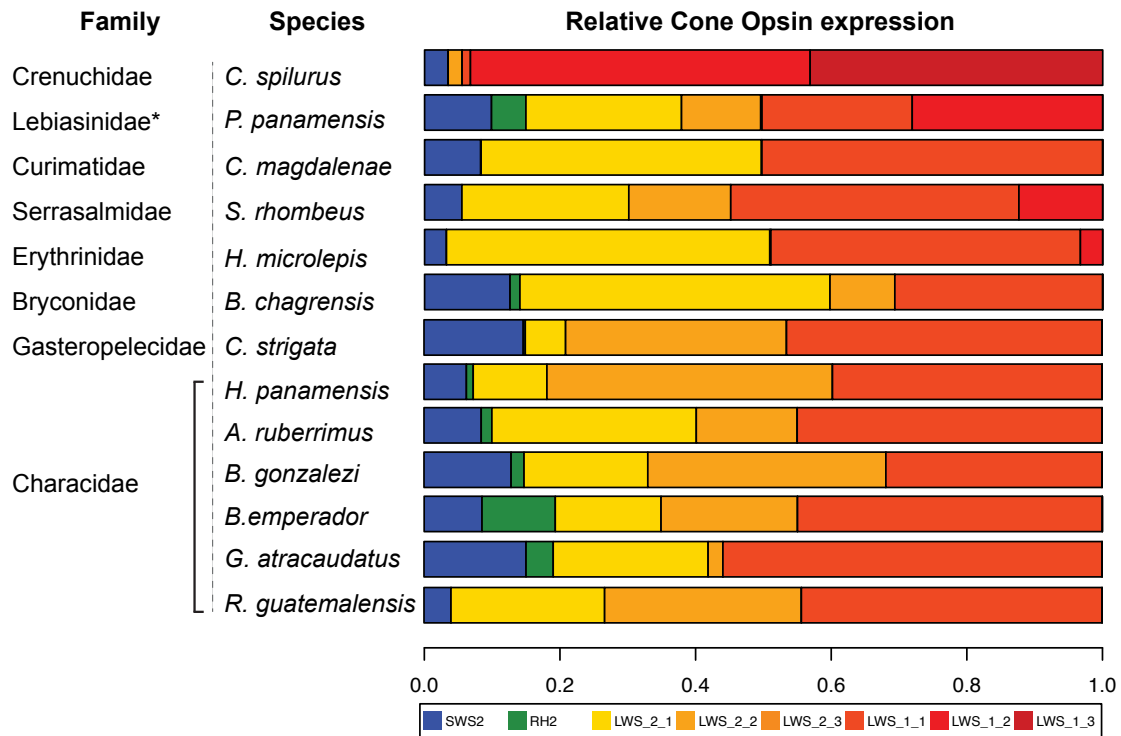


Figure 4.6. Opsin expression in Characiformes. Relative cone opsin expression is shown for each Characiformes species and color-coded for each opsin.

4.4.3 Microspectrophotometry (MSP)

Microspectrophotometry (MSP) of characins revealed a remarkable diversity in photoreceptors λ_{\max} . We identified up to six different cone classes based on spectral sensitivity: for single-cone photoreceptors, MSP identified two photoreceptor types a short wavelenght (SW), sensitive to the blue (λ_{\max} =440-467 nm), and a medium wavelegnth (MWI), sensitive to the blue-green (λ_{\max} =472-496 nm). For double-cone photoreceptors MSP identified four types, a second medium wavelength (MWII), sensitive to the short-green (λ_{\max} =514-545 nm), two medium long (MLWI and MLWII) sensitive to the long-green (λ_{\max} =529-

568 nm), and yellow (545-588 nm), and a long wavelength (LW), sensitive to the red (λ_{\max} =564-614 nm) (Fig. 4.7, Table 4.1). This varied between species where some had a less diverse set of photoreceptors. Within each species, fish also varied in cone λ_{\max} (Fig. 4.7), which is indicative of the presence of A₁/A₂ mixtures. Furthermore, based on our measurements, we were able to estimate the λ_{\max} of each spectral cone with pure A₁ and A₂ (Table 4.2). Based on these estimates, we found that for the majority of medium long cones (MWLI and MWLII), the best fit is a combination of different mixtures of A₁/A₂ and different coexpression ratios of LWS1- and LWS2-opsins.

4.4.4 Genomic sequencing

Our phylogenetic tree based on genomic sequences of characins revealed similar results obtained by previous studies [133], with African and Neotropical Characiformes sharing a monophyletic origin and being sister taxa to Gymnotiformes and Siluriformes (Fig. S8, Appendix C). All of the species used in this study belonged to their expected taxonomic groups except for *Piabucina panamensis* which grouped with Parodontidae instead of Lebiasinidae. Our results confirmed the identity of species used in transcriptomes with a total of five species belonging to Characidae, and one each for Crenuchidae, Parodontidae, Curimatidae, Serrasalminidae, Erythrinidae, Bryconidae and Gasteropelecidae.

Table 4.1. Cone and rod visual pigment peak sensitivities (λ_{\max})

Species	n	Photoreceptor type						
		Rod	SW	MWI	MWII	MLWI	MLWII	LW
Curimatidae								
<i>C. magdalenae</i>	3	517-536	450-455	476-496	535-545	531-554	588	585
Erythrinidae								
<i>H. microlepis</i>	4	510-528	—	489-491	526-543	535-561	564-581	576-614
Bryconidae								
<i>B. chagrensis</i>	4	504-531	446-467	472-485	515-535	532-568	—	564-612
Characidae								
<i>G. atracaudatus</i>	3	504-516	440-459	491	521	530	—	—
<i>B. gonzalezi</i>	6	504-523	449-462	486-495	514-527	530-542	545	576
<i>R. guatemalensis</i>	6	502-423	447-466	481-495	—	530-541	—	—
<i>A. ruberrimus</i>	3	504-519	448-463	472-495	519-522	529-542	—	—

Table 4.2. Cone and rod λ_{\max} based on pure chromophore type

Species	Photoreceptor type							
	Rod	SW	MWI	MWII	MLWI	MLWII	LW	
Curimatidae								
<i>C. magdalenae</i>								
Reference $\lambda_{\max A1}$	504	442	475	514	530	544	560	
Reference $\lambda_{\max A2}$	536	455	496	550	573	595	622	
Erythrinidae								
<i>H. microlepis</i>								
Reference $\lambda_{\max A1}$	503	—	478	514	430	544	560	
Reference $\lambda_{\max A2}$	534	—	500	550	574	596	622	
Bryconidae								
<i>B. chagrensis</i>								
Reference $\lambda_{\max A1}$	504	446	472	514	530	—	560	
Reference $\lambda_{\max A2}$	536	460	492	550	574	—	622	
Characidae								
<i>G. atracaudatus</i>								
Reference $\lambda_{\max A1}$	504	440	480	514	530	—	—	
Reference $\lambda_{\max A2}$	536	453	503	550	574	—	—	
<i>B. gonzalezi</i>								
Reference $\lambda_{\max A1}$	504	449	479	514	530	544	560	
Reference $\lambda_{\max A2}$	536	464	511	550	574	596	622	
<i>R. guatemalensis</i>								
Reference $\lambda_{\max A1}$	502	447	480	—	530	—	—	
Reference $\lambda_{\max A2}$	533	462	503	—	574	—	—	
<i>A. ruberrimus</i>								
Reference $\lambda_{\max A1}$	504	447	472	514	529	—	—	
Reference $\lambda_{\max A2}$	536	462	492	550	572	—	—	

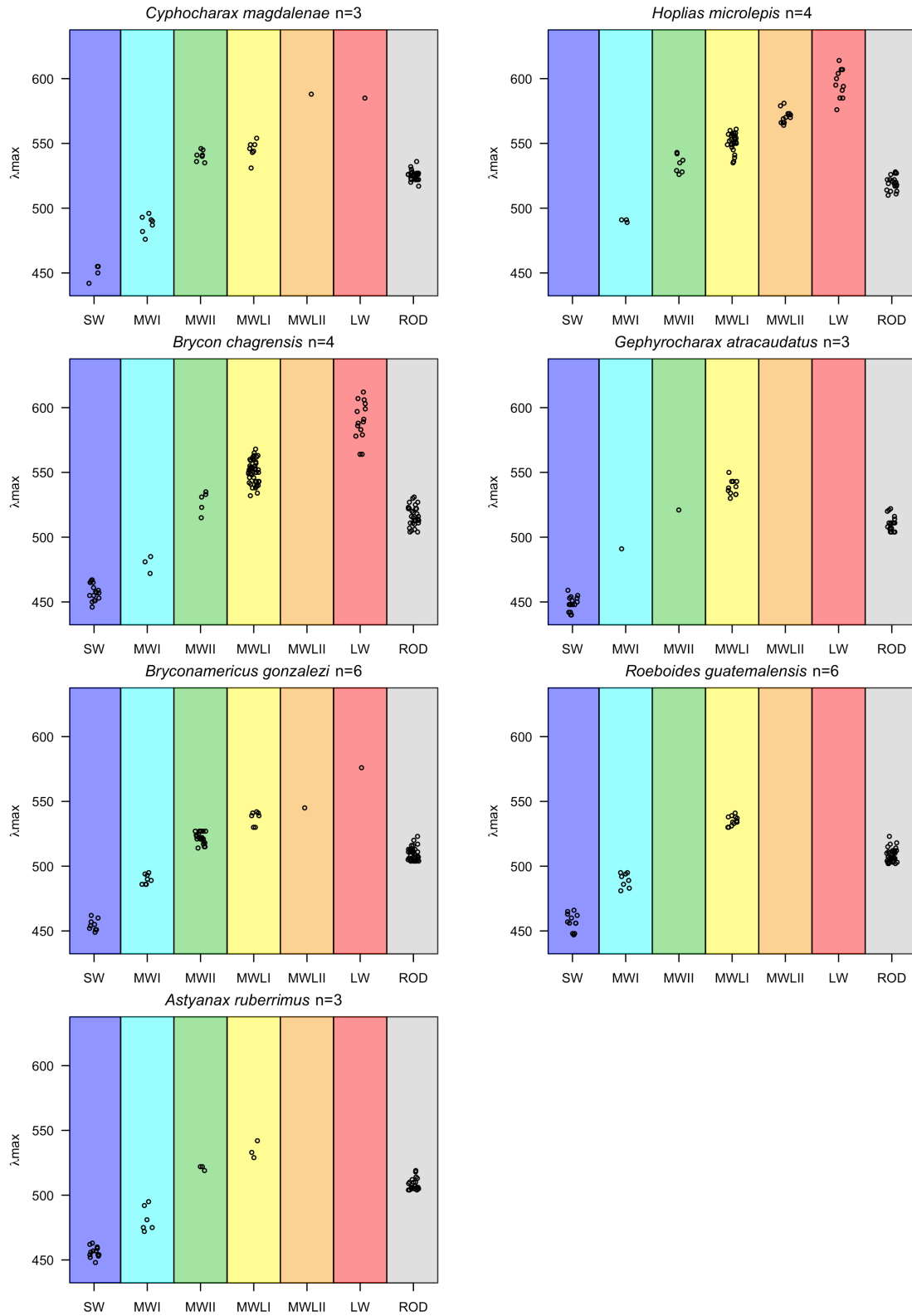


Figure 4.7. Microspectrophotometry of Characiformes. Empty circles represent individual records of maximal absorbance (λ_{\max}) from visual pigments

in wild-caught Panamanian Characiformes. Photoreceptors were classified in different spectral classes indicated by the colored backgrounds. From left to right these spectral classes are short, medium I and II, medium-long I and II, and long, and rods (SW, MWI, MWII, MLWI, MLWII, LW, ROD).

4.5 Discussion

4.5.1 Dynamic opsin evolution in Characiformes

Opsin gene duplication and gene loss

Through transcriptome and genome analysis, we characterized opsin evolution in Neotropical Characiformes. Our results show that the opsin complement varies significantly between species (Fig. 4.3), with species utilizing from four (*R. guatemalensis*), to seven cone opsins (*P. panamensis*). This diverse repertoire includes evidence for at least two separate copies of LWS-opsins (LWS1 and LWS2), each with unique opsin sequences that originated after TGD. This was confirmed because in our trees characin LWS2-opsins clustered with the osteoglossimorph LWS2-opsins which are known surviving copies of TGD [141]. Our results also show how the LWS2 opsin underwent subsequent gene duplications within Characiformes highlighting the susceptibility of opsin genes to duplication. LWS-opsin gene duplications are not uncommon and they have independently occurred in several teleosts [64,67,68,85,141,152]. In addition, we also found another TGD surviving opsin product of a RH1 duplication: RH1-2. We confirmed this as the surviving duplicates clustered with the known RH1-2-opsins of Cypriniformes [150,151] (Fig. 4.2), however their functionality remains unknown. RH1-2 duplicates have also been found in the Japanese eel (*Anguilla*

japonica) [153]. Altogether, Characiformes have maintained TGD duplicates of two opsin classes (LWS and RH1) (Fig. S4, Appendix C) yet these duplicates have not been retained together in other teleosts.

Characin visual pigment repertoires are also characterized by the absence of some opsin classes. The loss of SWS1-opsins seems to have happened early in the evolution of Characiformes because its absence was shared between two phylogenetically distant species (*P. nattereri* and *A. mexicanus*). This was also corroborated by our gene expression and MSP data as we didn't find any SWS1-cones, although see [154]. Additionally, the inactivation of RH2 seems to be variable within characins as it was absent only in some species yet it was fully functional in others and this is supported through MSP and gene expression. Nevertheless, our data suggests a low biological significance of this opsin which could be the product of opsin gene neofunctionalization (See below).

Opsin gene conversion

Furthermore, we found evidence of gene conversion in each LWS opsin (LWS1 and LWS2). GARD analysis showed that the recombination locations are primarily in the first exons, which suggests there might be selective pressures preventing gene conversion to homogenize coding sequences where the “key sites” are located in exons 3, 4 and 5. Gene conversion is further supported by the different tree-topologies, which is more evident in LWS2 because the tree based on fragment #3 suggests LWS2-opsins duplicated in the early ancestor of

Bryconidae, Gasteropelcidae and Characidae. This is a more parsimonious pattern than LWS2 duplications occurring in each family independently, and is also in agreement with our tree based on genomic sequencing (Fig. S7, Appendix C). Overall, our findings are similar to other studies that reported gene conversion acting in different opsin classes where it homogenizes opsin sequences [32,36,113,144,145]. However, it has been suggested gene conversion can increase allelic diversity [155].

4.5.2 Opsin neofunctionalization: evolution of spectral tuning and opsin gene expression

Our MSP data set suggests species have up to six spectrally different cone types (SW, MWI, MWII, MLWI, MLWII, LW), which is consistent with the number of cone opsin genes characins express: SWS2, RH2, LWS2-1, LWS2-2 and LWS1. However, there is variation in visual sensitivities among Characiformes species and this diversity in cones λ_{\max} is the product of different spectral tuning mechanisms acting together. These include opsin sequence tuning, opsin gene expression, opsin gene loss and duplication, opsin coexpression, and chromophore tuning.

Opsin sequence tuning

As discussed above, through opsin gene loss and duplication some characins have lost the RH2-opsin and hence green sensitivity. However, through opsin gene duplication followed by opsin sequence tuning characins have regained

green sensitivity by utilizing another opsin class. Through genetic and electrophysiology experiments we confirm that LWS2-opsins are sensitive to green light and that this is maintained in all analyzed species (Fig. 4.6). This is consistent with early studies that showed that *Astyanax* had green sensitive opsins [130,156] due to mutations in three of the known “five-sites”. In our analysis, the diversity at spectral tuning sites in the LWS-opsins, particularly site 164 (Fig. S6, Appendix C), showed the ability of opsins to acquire new functions through opsin sequence variation. This is important because shifts in λ_{\max} can have profound impacts on fish color vision. As λ_{\max} of a photoreceptor shifts across the wavelength spectrum, chromatic contrast will also vary in the visual color space and this could affect chromatic discrimination.

In addition, although we do not know the exact λ_{\max} of each LWS2-duplicate (LWS2-1 and LWS2-2) in Characiformes, our MSP data identified several MW-cones, which could also be product of the expression the LWS2-1 and LWS2-2 opsins. These paralogs differ in a few amino acids which might cause the shifts we observed between MW-cones. More studies are necessary to correctly characterize the exact spectral absorbance of the LWS2 duplicates and its molecular basis.

Furthermore, given the presence of LWS2-opsins in Osteoglossiformes and Characiformes, LWS2-green sensitivity probably evolved in an early ancestor before the split of Osteoglossomorpha and Clupeocephala (~240 MYA [157]).

This also implies that LWS2-opsins have been maintained for over 300 million years [141] while they have been lost in several teleost lineages. Indeed, there is evidence that most duplicated genes were lost in the first 60 million years after TGD [158]. Green sensitivity might have evolved during the Permian, which is characterized by several fish-extinction events in its early and middle epochs followed by the end-Permian mass extinction around 251 MYA [159]. Therefore, the LWS2-neofunctionalization through opsin sequence tuning may be a result of strong environmental pressure in the Permian.

Opsin expression

Novel opsins can also acquire new functions through gene expression mechanisms [36]. In Characiformes, it seems that the rise of the LWS2-opsins might have changed the regulatory architecture of RH2 expression, leading to downregulation and even to gene loss (Fig. 4.6, S4, Appendix C). Previous studies have found the same pattern between two different opsin classes: whenever a strong shift in λ_{\max} occurs in one opsin, there can be gene loss/downregulation in another one. In flounder and cichlids, the SWS2-opsin has acquired green sensitivity while the functionality of the RH2-opsins has been reduced (Kasagi et al., 2018, Escobar-Camacho et al., 2019). A similar pattern has occurred in Osteoglossiformes where the LWS2-opsin is green sensitive and the RH2-opsin has been lost [141]. Alternatively, the downregulation of the RH2-opsin could also suggest that dichromacy based solely on SWS2 and LWS may be sufficient for visual tasks for some fish. Nevertheless, fish opsin expression

can change due to ontogenetic changes throughout development [73,160,161], or in response to changes in the light environment [108,109,162–164], leading to variation in their visual sensitivities. Therefore, more research analyzing the development and plasticity of characins visual system is necessary.

Furthermore, our results suggest there is differential opsin expression in Characiformes. In Characidae, most species express LWS2-2 more than LWS2-1, whereas this is the opposite in species from other families (Fig. 4.6). Even though our data-set is based on a few individuals and more sampling is needed to quantify differential opsin expression, this suggests there might be a pattern in which opsins are differentially regulated in different species. In addition, we also found significant differential expression between RH1-1 and RH1-2 yet we do not know whether RH1-2 has a specific role in the visual system. More studies are needed to fully characterize its functionality. It has been shown that RH1-2 duplicates can acquire quite complex functions such as regionalized expression in the zebrafish retina [150], or specific ontogenetic expression in the lifecycle of the Japanese eel [153].

Chromophore tuning

Fish visual pigments can be based on different chromophores, 11-cis retinal from vitamin A₁ and 3,4-didehydroretinal from vitamin A₂, and this can create large shifts in photoreceptors λ_{\max} [39]. Thus, the light absorbance of a photoreceptor will depend on the ratio of A₁/A₂ chromophores. In our MSP data-set we found

evidence of intraspecific variation of photoreceptors λ_{\max} . Since we used fish from the same localities for both transcriptomes and MSP, and there were no differences in opsin gene expression between individuals, our results imply that photoreceptor λ_{\max} variation is probably the product of different A_1/A_2 ratios in each specimen. These results are concordant with previous research that also found different A_1/A_2 ratios in cones and rods of *A. fasciatus* [154], and in rods of several other characins [17,31]. Furthermore, due to our low sample size, we did not analyze correlations between light environment and A_1/A_2 ratios, however, A_2 -based visual pigments are characteristic of fish inhabiting long-wavelength-shifted habitats [42,117,165–168]. The presence of A_1/A_2 ratios in characin visual pigments agrees with the light environment of Neotropical rivers which are red-shifted [118,169].

4.5.3 Opsins and characins phylogenetics

Even though our genomic multilocus phylogeny suggested a monophyletic origin of Characiformes, including African and Neotropical lineages (Citharinoidei and Characoidei respectively) (Fig. S8, Appendix C), several of our opsin trees contradict this pattern because characins appear paraphyletic in relation to Siluriformes and Gymnotiformes (Fig. S1-3, Appendix C). These contrasting results are not surprising as the non-monophyly of Characiformes has been reported before [170–172], although, other comprehensive studies have resolved Characiformes as monophyletic [66,157,173]. Studies that find Characiformes paraphyletic often find discrepancies between Citharinoidei and Characoidei,

where the latter often clusters as sister group to Siluriformes [170–172]. Interestingly, we obtained paraphyletic results in our opsin trees because opsin sequences from Gymnotiformes and Siluriformes clustered within the opsin clades of Characiformes, although we did not include opsin sequences of African species. The opsin tree topologies of this study could be the result of substitution saturation over evolutionary time or indeed a signal of paraphyletic origins of Characiformes. Future studies should also analyze opsins of African characins in order to elucidate this pattern.

4.6 Conclusions

Through molecular and electrophysiological experiments we have characterized the visual system of Neotropical Characiformes. Their opsin repertoire is a product of complex evolutionary dynamics characterized by opsin gene loss (SWS1, RH2) and opsin gene duplication (LWS and RH1). These opsin duplicates are a product of a teleost whole genome duplication (TGD) and from characin-specific duplication events that have been maintained for hundreds of millions of years. The LWS duplicates have acquired new functions through amino acid substitution in key sites that shift their maximal absorbance to green light. These duplicates exhibit gene conversion, and utilize variable codons in key tuning sites leading to reversion and parallel evolution. In addition, the SWS2-opsin exhibits great amino acid variation across species that might shift spectral

sensitivities, and the RH1-2-opsin has a different pattern in opsin expression as it is always downregulated in our samples.

The diversity of visual pigments in Characiformes is the product of several spectral tuning mechanisms acting in concert. These are mainly opsin sequence variation, opsin gene loss and duplication, and A_1/A_2 chromophore tuning. Overall, the visual system of Characiformes showcases how opsins acquire new functions and the divergent evolutionary pathway of this group compared to other teleosts. This study shows how studying speciose, understudied groups, provides a unique opportunity to better understand opsin gene evolution.

4.7 Acknowledgements

Special thanks go to Suwei Zhao for training during library preparations. We thank the University of Maryland Institute for Bioscience & Biotechnology Research for sequencing. We also thank Michaela Taylor for help during genomic sequencing and Danielle Adams for help during ancestral reconstruction analysis. We thank Alejandra Rodríguez-Abaunza and Aureliano Valencia for their assistance during sampling. We also thank all of the staff at Bocas del Toro Research Station and at Naos Laboratories, Smithsonian Tropical Research Institute (STRI), Panama, for their help during our field season. We also thank Owen McMillan and Richard Cooke for their valuable insight during our field season. This work was supported by a STRI Short Term Fellowship [ID 102755 to D.E-C], by the National Institute of Health [R01EY024693 to K.L.C] and by a

graduate fellowship of the Secretariat of Higher Education, Science, and Technology and Innovation of Ecuador (SENESCYT; Secretaría de Educación Superior, Ciencia, Tecnología e Innovación) [2014-AR2Q4465 to D.E-C].

Chapter 5: Behavioral color vision in a cichlid fish: *Metriaclima benetos*

Previously published under: Daniel Escobar-Camacho, Justin Marshall and Karen L Carleton. Behavioral color vision in a cichlid fish: *Metriaclima benetos*. *Journal of Experimental Biology*, 2017: jeb.160473.

5.1 Abstract

Color vision is the capacity to discriminate color regardless of brightness. It is essential for many fish species as they rely on color discrimination for numerous ecological tasks. The study of color vision is important because it can unveil the mechanisms that shape coloration patterns, visual system sensitivities and, hence, visual signals. In order to better understand the mechanisms underlying color vision, an integrative approach is necessary. This usually requires combining behavioral, physiological and genetic experiments with quantitative modeling, resulting in a distinctive characterization of the visual system. Here, we provide new data on the color vision of a rock-dwelling cichlid from Lake Malawi: *Metriaclima benetos*. For this study we used a behavioral approach to demonstrate color vision through classical conditioning, complemented with modeling of color vision to estimate color contrast. For our experiments we took into account opsin coexpression and considered whether cichlids exhibit a dichromatic or a trichromatic visual system. Behavioral experiments confirmed color vision in *M. benetos*; most fish were significantly more likely to choose the trained over the distracter stimuli, irrespective of brightness. Our results are supported by visual modeling that suggests that cichlids are trichromats and achieve color vision through color opponency mechanisms, which are a result of three different photoreceptor channels. Our analyses also suggest that opsin coexpression can negatively affect perceived color contrast. This study is particularly relevant for research on the cichlid lineage because cichlid visual capabilities and coloration patterns are implicated in their adaptive radiation.

5.2 Introduction

Animals vary greatly in color pattern, with coloration often playing an important role in speciation. Evolutionary biology aims to understand the selective mechanisms shaping the form and perception of color patterns by conspecifics and heterospecifics. Animals' visual perception of such patterns depends on the detectability of these color signals [174], which can be shaped by the light environment where animals live, the color properties of the signaler and the visual sensitivities of signal receivers [1,2,175]. However, in order to understand how color patterns evolve, we must first study the ultimate mechanisms underlying color vision. Color vision is the ability to discriminate color regardless of brightness. In vertebrates, color vision is achieved through color opponency, by which spectrally opponent channels produce a signal from spectrally distinct cone photoreceptors [128,176,177]. Therefore, color vision requires at least two spectrally distinct types of photoreceptors operating in a similar intensity range [9].

In the retinas of most vertebrates, photoreceptors are classified as rods and cones. Rods function under dim light conditions, whereas cones function in daylight and are responsible for color vision [128,178,179]. In fish, cone photoreceptors are usually arranged in a highly organized manner, the retinal mosaic. Fish exhibit great variation in the number of different cone types that they possess, with some species having only one type of cone with a single visual pigment (monochromatic) and others having four spectrally distinct types

of cones (tetrachromatic) [180–183]. Cone photoreceptors also exhibit morphological differences and can be classified as single or double cones. Double cones are two fused cones that are found in the eyes of most fish species and in several vertebrates [184]. It has been suggested that, in some species, double cones are electrically coupled [185] and that they play a role in luminance detection [186–188]. This is based on the ‘summation hypothesis’, which states that signals of double cones are summed in the retina, conveying a single signal to the brain [182,186]. This is particularly true in birds, in which double cones detect luminance and multiple types of single cones discriminate color [189,190]. However, fish often have only one type of single cone, with single and double cones each contributing to color discrimination [191].

Among teleosts, Cichlidae is one of the largest families, with approximately 2000 species widely distributed across ecosystems from Africa and South Asia to Central and South America [79,192,193]. Cichlids are also diverse in their visual tasks as species forage on different foods, and vary in mating systems and parental care. The colorful body patterns of cichlids can be sexually dimorphic and are likely important for species recognition, mate choice and speciation [194–196]. Thus, visual communication is essential for cichlid behavior. Vision research on cichlid flocks from the African Great Lakes has identified the genetic basis of their visual sensitivities: seven spectrally distinct cone opsins and a rod opsin gene [26]. The cone opsins belong to four cone opsin classes, including UV sensitive (SWS1), short-wavelength sensitive (SWS2A, SWS2B), rhodopsin-

like (RH2A α , RH2A β , RH2B) and long- wavelength sensitive (LWS) [27].

Although much is known regarding the visual system of African cichlids, it is unclear whether cichlids possess chromatic discrimination. Demonstrating color vision requires other approaches, including behavioral methods [197]. Data on photoreceptor spectral sensitivities, behavioral experiments and physiological models combined, provide a unique opportunity to study the neural interactions underlying color vision. Testing for chromatic discrimination in fish is beneficial for vision research because it provides insight about how photoreceptor signals might be processed by the rest of the retina. Visual discrimination experiments in teleosts have elucidated how different photoreceptors are used for chromatic and achromatic tasks [188,191,198–200]. Therefore, quantitative modeling could suggest how photoreceptor signals are combined and compared in discriminating spectrally different stimuli [177].

The aggressive behavior and territoriality of species from the genus *Metriaclima*, makes them an ideal system to test hypotheses through behavioral approaches. *Metriaclima benetos* is a rockdwelling cichlid from Lake Malawi and its color vision has been characterized through microspectrophotometry and opsin gene expression [26,73,201]. *M. benetos* spectral sensitivities are based on a “short” opsin palette expressing three spectrally distinct opsins: SWS1 (379nm), RH2B

(489 nm) and RH2A α (522 nm) [41,201]. However, we still do not know whether there is color opponency in the cichlid retina enabling chromatic discrimination.

In this exploratory research we wanted to know if cichlids are able to discriminate between colors regardless of brightness. This would give us insight into how photoreceptors interact in the retina and its implications in color discrimination. In this study, we took into account how spectrally different photoreceptors are stimulated by different colors, and the role of opsin coexpression and photoreceptor noise in color discriminability.

5.3 Materials and methods

5.3.1 Data measurements

We trained cichlids to recognize the color blue as our main stimulus. Blue is the primary body coloration of male *M. benetos*. Blue has also been used multiple times in color vision experiments [174,183,191,202]. We measured stimuli reflectance, side-dwelling irradiance and lens transmission. Stimuli were made by printing 1.5 cm colored circles on standard paper and then laminating them. In order to create darker and lighter shades of each color, black or white was added using Adobe Illustrator. Stimuli reflectance were measured using a fiber-optic spectrometer based on an Ocean Optics USB2000 (Dunedin, FL, USA), fitted with a 400 μ m fiber, and calibrated with a NIST (National Institute of Standards and Technology) traceable tungsten halogen lamp (LS-1, Ocean Optics). Side-dwelling irradiance was measured inside the tanks under fluorescent lights with a 1000 μ m fiber fitted with a cosine corrector (CC-3). Finally, lens transmission was

measured by placing the isolated cichlid lens on a UV-transparent cover slip, which was illuminated from above by a fiber optic cable attached to a pulsed xenon light source (PX-2, Ocean Optics) and 15 mm above the lens. Another fiber optic cable was placed 5 mm directly under the specimen and delivered the signal to the spectrometer. Transmission was measured by comparing measurements with and without the lens. An XY stage was used to center the lens and maximize the transmission. Three replicate measurements were made of each lens of four fish. The resulting spectral scans were normalized to 100% transmission at 700 nm. Finally we quantified the T50 values (that represent the wavelength at which 50% transmission is reached).

5.3.2 Behavioral approach

We used a similar approach to classic 'grey card' experiments where bees were trained to associate a reward with a specific color, and thereby could be tested for how well they could discriminate the trained color from others [203]. We tested the ability of *M. benetos* individuals to choose blue over distracter stimuli. For this, we trained fish to blue through classical conditioning and subsequently, tested them when offered two or more choices. The same seven fish were used for all tests. Although only males were used, we have never found differences in male and female sensitivities (though see Sabbah et al., 2010).

5.3.3 Fish training

In order to train the fish, a feeding apparatus consisting of a plastic feeder tube (5 mm diameter and 20-30cm long) was attached to a 3 ml syringe filled with a mix of fish flakes and water. The amount of food available to the fish was manually controlled and could be adjusted by varying the pressure applied to the syringe (Fig. S1B, Appendix D). In this way, different amounts of food could be delivered to the fish. The food was delivered at the front of the aquarium. Because we wanted to train fish to touch a specific stimulus (blue) with their mouth (referred as 'taps' [202]), initially fish were fed through the feeder tube alone. Once the fish learned to bite/tap the tube, a colored flat disc was attached to the end of the tube helping the fish learn to tap the color stimuli. The fish were then introduced to a laminated card with the stimuli at the center (the feeder was not inside the tank at this point). As fish learned to associate the color with reward, they started to tap the colored stimuli on the card and consequently were rewarded (Fig. S1C-D, Appendix D).

Fish were trained only for blue and not for light- or darkblue. In order to make sure fish could see all stimuli before choosing, fish were lured towards the posterior section of the tank while the color cards were placed in the front of the tank. The feeder was removed and the fish turned in order to make a choice. The experimenter was able to see which color stimulus fish tapped with a mirror placed above the tank. The fish never saw the experimenter nor other fish during tests. Fish were tested approximately 10 or 20 times to confirm that they could

discriminate colors; when they succeeded 75% of the times, testing started. Seven male fish were trained within a two-month period where some individuals learned faster than others. This seemed to be related to the different levels of confidence that each individual exhibited. Indeed, one of the most difficult steps in the training process was to convince the fish to approach the feeder tube or color card in the presence of the experimenter.

5.3.4 Fish care

Fish were held individually in 26 x 50 cm tanks with a common recirculating system (Fig. S1A, Appendix D) and they were fed daily during training and testing periods. All fish were managed under the guidelines of the University of Maryland IACUC protocol (#R15-54). Fish were tested from November to March in 2015-2016 at the Tropical Aquaculture facility at the University of Maryland.

5.3.5 Experiment 1: Binary choice

The first experiment consisted of a binary choice test where fish chose between two cards with one color circle each, the trained blue stimulus was presented with yellow and gray as distracters. As soon as the fish tapped one of the two cards, the cards were removed, the fish was rewarded, and the trial ended. In order to avoid bias against a specific side of the tank, the same color was not presented on the same side more than two times in a row. Furthermore, if the fish didn't show a response to the stimuli for more than two minutes, the fish was

not rewarded and the trial was not counted. To ensure that fish were not selecting stimuli based on luminance, the trained and distracter stimuli varied in three levels of brightness. In total we tested seven fish to assess whether they had the ability to detect chromatic differences between colored stimuli (blue, yellow and gray).

5.3.6 Experiment 2: multiple-choice gray

To further confirm our results in the first experiment, we used a multiple-choice discrimination test. Cards contained eight color stimuli of which one was blue and the rest were multiple shades of gray. Stimuli were arranged in two horizontal rows with four color-circles each. Five cards were designed with different combinations (Fig. S1E, Appendix D) and were presented to the fish in a random fashion during testing. As in the previous experiment, we added luminance noise to make brightness an unreliable cue for blue, therefore, blue in the cards varied between three levels of brightness. For experiments 2 and 3, each fish was tested five times for each combination card.

5.3.7 Experiment 3: multiple-choice color

Finally, for the third experiment, we wanted to know if fish could discriminate blue from several different wavelengths and if there was a bias against a specific color. Six cards were designed containing different stimuli of which one was blue and the rest were different colors (black, brown, violet, pink, red, yellow and

green) (Fig. S1E-F, Appendix D). Since brightness bias was already tested in the two previous experiments, luminance noise was not introduced in this experiment. As in Experiment 2, the different color card combinations were presented in a random fashion to the fish.

5.3.7 Data analysis

For experiments 1, 2 & 3, a one-tailed binomial test was used to calculate whether the fish could distinguish the trained from distracter stimuli. For this, the number of correct trials was compared to the distribution of taps if a fish were choosing randomly (50% of the time for the Experiment 1 and 12.5% for Experiment 2 & 3). Confidence intervals were calculated assuming a binomial distribution. All binomial tests and visual modeling calculations were done in the statistics package of R software for each fish in each experiment [205].

5.3.8 Differential interference contrast (DIC) images of *M. benetos* cone photoreceptors

One fish was sacrificed with overdose of MS-222, the eyecup was removed and the eye was dissected under a stereoscope. 1x Hyaluronidase/Collagenase was placed into the open eyecup and incubated for ~45 min, adding more if needed. The vitreous humour was removed and the retina gently dissected away from the retinal pigment epithelium (RPE) by flushing with copious cold phosphate buffered saline. As soon as the retina was separated from RPE and the vitreous

humour it was pinned in an agar plate where it was fixed in 4% paraformaldehyde. Photographs were taken with a Leica DM5500 Microscope (Leica Microsystems).

5.3.9 Visual modeling

To quantify how colors stimulate photoreceptors' visual sensitivities, we calculate quantum catches (Q) which represent the number of incident photons that are captured by visual pigments in each photoreceptor [206]. Therefore, estimating quantum catches allows us to examine how spectrally different colors stimulate different cichlid photoreceptors. These calculations include: (1) the spectrum of environmental light, (2) the reflectance spectrum of an object (e.g. stimuli), (3) the lens transmission, and (4) the spectral sensitivities of photoreceptors [177,207].

Quantum catches are based on the seven opsins present in cichlids, and use the MSP spectral sensitivities of *M. benetos*, SWS1, RH2B, RH2A α , and from the closely related species *Metriaclima zebra*, SWS2B, SWS2A, RH2A β and LWS. Genetic analyses show that the opsin sequences of *M. zebra* and *M. benetos* do not differ significantly having identical amino acids in the retinal binding pocket sites [208] Hence, *M. benetos*' visual sensitivities should be, if not equal, highly similar to *M. zebra*. We further consider the possibility of opsin coexpression in single cones and double cones which has been demonstrated in *M. zebra* [20,24,161]. This coexpression varies across the retina and seems to be minimal

within an area centralis (believed to be used in high visual acuity tasks), however, there is significant variation between individuals. Opsin coexpression can have different effects on color vision because two opsins in the same cone would shift its peak absorbance. Therefore, we estimated quantum catches based on pure opsin expression (SWS1, RH2B, RH2A α) and on coexpressed opsins (SWS1/SWS2B, RH2B/RH2A β , RH2A α /LWS) in a single photoreceptor. Since opsins can be differentially coexpressed, we considered four combinations of opsin coexpression that have been found to bound the variation in *M. zebra* (Table S1A, Appendix D) [20,24]. We used different spectral sensitivities based on reported coexpression combinations in order to calculate quantum catches.

Quantum catches were calculated for the short, medium and long (S, M & L respectively) wavelength sensitive cones for each color using Eqn 1, where R_i is the sensitivity (opsin absorbance template) of receptor i , L is the lens transmittance, S is the surface reflectance (color stimuli), I is the illuminant, and K_i is the von Kries factor for receptor i (Table S1, Appendix B).

$$Q_i = K_i \int R_i(\lambda)L(\lambda)S(\lambda)I(\lambda) \quad (1)$$

The opsin absorbance template (R_i) is derived from the quantum catch absorptance coefficient (F_{abs}) which represents the fraction of photons entering a photoreceptor which are actually absorbed [209]. Here k is the absorption coefficient of the photoreceptor at the peak absorption wavelength (the peak absorbance determined by MSP in units of per μm), $A(\lambda)$ is the wavelength

dependent absorbance of the photoreceptor, normalized to a peak of one, and l in the length of the outer segment in μm (Eqn 2).

$$R_i = F_{abs} \propto \int_{300}^{750} (1 - e^{-kA(\lambda)l}) \quad (2)$$

The von Kries factor (Eqn 3) is derived from von Kries' color constancy model in which receptors adapt independently to the background illumination [177,207,210].

$$K_i \propto \frac{1}{\int R_i(\lambda)L(\lambda)I(\lambda)} \quad (3)$$

In order to test if double cones are involved in color vision (color opponency), we modeled quantum catches both separately for each cone member (M and L) and for the combined double cone (DC) with Eqn 4 [191].

$$Q_{DC} = \frac{Q_M + Q_L}{2} \quad (4)$$

Quantum catches also allow us to calculate the contrast between the tested colors to the cichlid eye. For this we use the receptor noise-limited model (RNL) [211]. Briefly, we used quantum catches of each cone class (i) to calculate contrast between pairs of colors, Δf_i [212].

$$\Delta f_i = \ln \left[\frac{Q_i(\text{color 1})}{Q_i(\text{color 2})} \right] \quad (5)$$

Color discrimination is also determined by receptor noise. Relative receptor noise is related to the Weber fraction for a single photoreceptor, v , by: $\omega_i = v_i/\sqrt{n_i}$, and n is the number of receptors of i type [213,214]. Further, we followed Koshitaka et al 2008 in assigning a receptor noise for each cone class (Eqn 6) [215]. In our calculations the long (L) receptor is assumed to have a noise value of 0.1 (see discussion) and the noise value for the short (S) and medium (M) cone classes were calculated using their relative abundance in the retinal mosaic. *M. benetos* has a square mosaic like its close relative *M. zebra* [24] where the S:M:L cones ratio is 1:2:2 (Fig. S1G-H, Appendix D). This gives us a relative noise value of 0.14 for S cones, and 0.1 for M and L cones.

$$\omega_i = 0.1 \sqrt{\frac{n_L}{n_i}} \quad (6)$$

Following Vorobyev and Osorio 1998, we can compute the distance between two colors (ΔS). To further test if cichlids achieve color opponency either through stimulation of each photoreceptor or combining signals from double cones, we computed ΔS for a dichromatic (S, DC; Eqn 7) and a trichromatic (S, M, L; Eqn 8) visual system as follows:

$$\Delta S = \sqrt{\frac{(\Delta f_{DC} - \Delta f_S)^2}{\omega_S^2 + \omega_{DC}^2}} \quad (7)$$

$$\Delta S = \sqrt{\frac{\omega_S^2(\Delta f_L - \Delta f_M)^2 + \omega_M^2(\Delta f_L - \Delta f_S)^2 + \omega_L^2(\Delta f_S - \Delta f_M)^2}{(\omega_S\omega_M)^2 + (\omega_S\omega_L)^2 + (\omega_M\omega_L)^2}} \quad (8)$$

ΔS is the chromatic distance of two colors in the photoreceptor space and its units are “just noticeable differences” (JND). Values <1 JND indicate that the two colors are indistinguishable whereas values above 1 JND indicate that two colors can be distinguished [212]. Because we performed these experiments under fluorescent lights that do not emit short wavelengths (Fig. 5.1) where *M. benetos* is sensitive, and since at lower light intensities photon-shot noise can affect color discrimination [216], we wanted to calculate absolute spectral sensitivity, $R_i(\lambda)$, for each photoreceptor type as:

$$R_i(\lambda) = \nu\tau \left(\frac{\pi}{4}\right)^2 \left(\frac{d}{f}\right)^2 D^2 (1 - e^{-kA(\lambda)l}) \quad (9)$$

where ν is the number of cones per receptive field and τ is the summation time; d/f is the acceptance angle of a cone, d is the diameter of the receptor and f is the lens focal length (2.5 mm, calculated from the lens radius multiplied by Matthiessen’s ratio), and D is the pupil diameter. When $R_i(\lambda)$ is included in Eqn 1, it can give us absolute quantum catches, N . We can then include photon-shot noise into the RNL model in Eqn 3, 5 and 6 by further substituting the noise term from Eqn 10. In this way, we can analyze how spectral sensitivities change with and without the von Kries normalization.

$$\omega_{i,\text{photon}} = \frac{\sqrt{\omega_i^2 N_i^2 + N_i}}{N_i} \quad (10)$$

For these calculations, ν and d were determined from the retinal mosaic (Fig. S1G-H, Appendix D), and D was measured from five fish. l was obtained from [217] and [24]. k and peak wavelengths to estimate $A(\lambda)$ were obtained from [26,201]. To our knowledge τ has not been measured for cichlids so we use 40 ms as estimated for coral reef fish [218].

5.4 Results

5.4.1 Stimuli, illumination, and visual system properties

Color stimuli were designed and their spectral reflectance quantified. Similarly, side-dwelling irradiance was measured in the tanks. Lens transmission yielded a T50 of 370 nm (Fig. 5.1).

5.4.2 Experiment 1: binary choice

For this experiment a total of 3353 tests were performed ($n_{\text{fish}}=7$; $n_{\text{color-pairs}}=18$). This experiment showed that each fish could easily discriminate between blue and yellow and blue and gray. Most fish were more likely to choose the trained (blue) over the distracter stimuli (yellow or gray), irrespective of brightness (Fig. 5.2). On average, fish tapped correctly 99.75% (96-100%) of the trials against yellow and 91% (48-100%) against gray (Fig. 5.2, Movie S1, Appendix D). Two

fish failed to discriminate lightblue and darkgray, and one fish failed in discriminating lightblue and gray. Five fish achieved correct choices significance in all conditions (Table S2A, Appendix D).

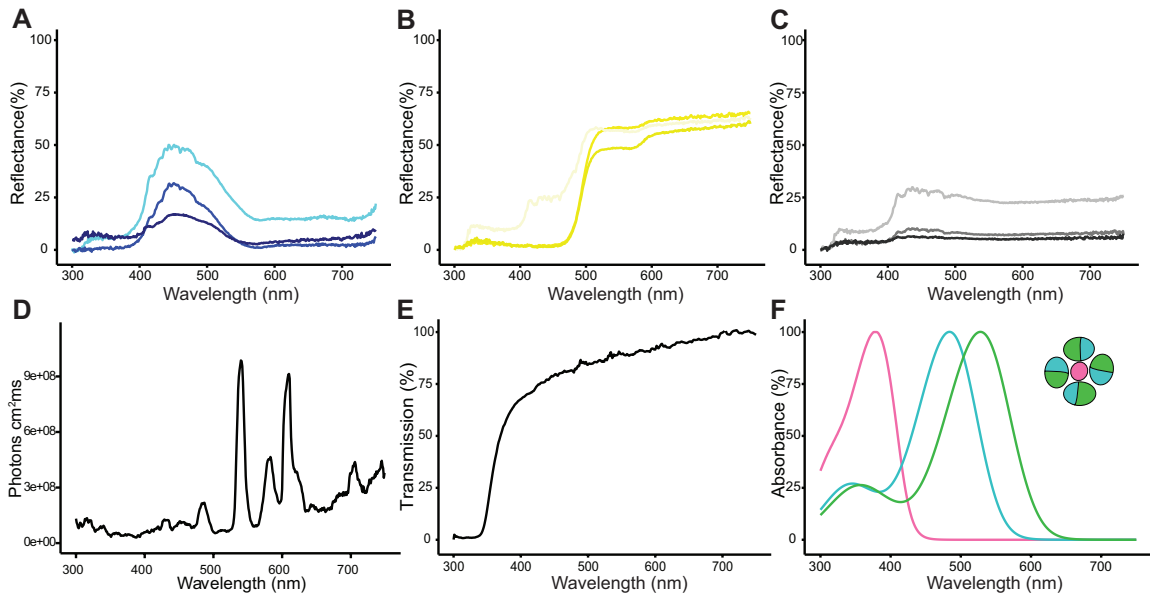


Figure 5.1. Reflectance spectra, side-dwelling irradiance, lens transmission and cone sensitivities. A, B and C indicate reflectance spectra of blue, yellow and gray targets respectively, with stimuli varying in brightness. (D) Illumination in absolute photons. (E) Lens transmission spectra. (F) Color vision plot with spectral sensitivity of the short, medium, and long wavelength pigments. A typical square retinal mosaic is shown in the inset where the short wavelength sensitive opsin (SWS1) is expressed in single cones while medium and long wavelength pigments (RH2B & RH2A respectively) are expressed in alternate double cone members.

5.4.3 Experiment 2 & 3: multiple-choice

The same fish from the binary choice experiment were used in the multiple-choice test. In Experiment 2 (525 tests), fish were more likely to choose blue over the different shades of gray (Fig. 5.3A). Fish tapped correctly blue, lightblue and darkblue, 89% (88-96), 76% (60-96) and 88% (76-96) of the time, respectively,

as compared to the different shades of gray (Movie S1, Appendix D). Similarly, in Experiment 3 (205 tests), all fish were more likely to choose blue over different colors, and fish tapped correctly 74% (70-80) of the time (Fig. 5.3B, Movie S1, Appendix D). All fish achieved significant results in Experiments 2 and 3 (Table S2A, Appendix D). Interestingly, in Experiment 3, we noticed that of the few mistakes fish made (20-30%), i.e. tapping another color instead of blue, most of the mistakes (78%) were with the color purple. Hence, this suggests that these fish have difficulty discriminating blue from purple (Table S2A, Appendix D).

5.4.4 Quantum catches

We estimated quantum catches by two approaches, one considering the spectral absorbance (referred simply as “Quantum catch”) and the second one considering absolute spectral sensitivity (referred as “Absolute quantum catch”). We first considered the simplest case, a dichromatic visual system with pure opsin expression. Here, color pairs like blue-yellow differ in the signals from single cones (SC) and from summed signals of double cones (DC) (Table S2B, Fig. 5.4A, Appendix D). Thus, yellow and blue would be discriminated on the basis of spectral differences between both, SC and DC. By contrast, blue and gray have similar quantum catches for SC and DC respectively (Table S2B, Appendix D; Fig. 5.4A), hence, this could potentially preclude *M. benetos* from discriminating between these colors.

We next considered the trichromatic case, which assumes the three cone types independently contribute to color vision. Quantum catch calculations suggest that the short, medium and long (S, M and L) cones are differentially stimulated for each color target (Fig 5.4C,E, Table S2B, Appendix D). Furthermore, because fluorescent lights do not emit UV light, absolute quantum catch calculations resulted in essentially zero stimulation for single cones (Table S2B, Appendix D). We next considered coexpression for both di- and tri-chromacy. We found that photoreceptors are differentially stimulated as compared with pure opsin expression. In dichromats, signals from SC and DC change for blue-gray comparisons, with blue shifting away from gray but purple is more similar to blue. Yellows also seem to be more different when there is opsin coexpression (Fig. 5.4B,S2, Appendix D). For a trichromatic visual system, differential stimulation from each photoreceptor is maintained (Table S2B, Appendix D, Fig. 5.4D,F) although blue and purple seem to generate similar signals (Fig. 5.4F, S2, Appendix D). Finally, as a consequence of low stimulation of the S photoreceptors, absolute quantum catches suggest color vision under our experimental scenarios primarily relies on stimulation of the two double cone members, the M and L cones (Fig. S3, Appendix D).

5.4.5 Chromatic distances

Color distance (ΔS) analysis, in a dichromatic and trichromatic visual system, provided two main outcomes for colors used in Experiments 1, 2 and 3. First, these analyses suggest that for the cichlid visual system, yellow distracters

exhibit greater ΔS than gray distracters when compared to shades of blue. Second, our results show that opsin coexpression can increase, maintain or decrease ΔS for blue compared to different colors (Fig. 5.5-6, Table S2C-D).

In determining whether cichlids are dichromats or trichromats, we note that for a dichromat, ΔS between blue and gray is below 1 JNDs when there is pure opsin expression (Table S2D, Appendix D). Therefore, in a dichromatic visual system, cichlids would not be able to discriminate blue from gray. While opsin coexpression does increase blue / gray distance, our previous studies suggest that most individuals utilize pure opsins in the area centralis [20]. By contrast, in a trichromatic visual system, blue / gray chromatic distance is greater than 4 JNDs, hence, cichlids could potentially discriminate blue from gray regardless of opsin coexpression (Fig. 5.5). This suggests that cichlids must be trichromatic if they successfully distinguish blue from gray, independent of brightness. Overall, for both types of visual systems, comparisons of pure pigments and opsin coexpression yielded similar or higher ΔS for blues against shades of gray with all four coexpression combinations (Table S2C-D, Appendix D). However, there are some exceptions. In a dichromat, opsin coexpression increase ΔS between lightblue and shade of grays, but it negatively affects ΔS between lightblue and darkgray (Fig. 5.5B).

We find similar results for the broad range of colors used in Experiment 3. Our results suggest there is great variation in ΔS with color stimuli, opsin

coexpression, and visual systems. For example, when compared to blue, ΔS for brown, orange, green, and yellow increases with all coexpression combinations in both dichromats and trichromats (Fig. 5.6) (Table S2C-D, Appendix D). However, ΔS varies for blue versus red and pink, with both increases, and decreases. Overall, most ΔS exceeded 1 JNDs in a pure opsin expression scenario (except for brown in dichromats), and these results were highly similar when ΔS were calculated with or without photon-shot noise (Table S2D, Appendix D).

One important comparison is for blue and purple where ΔS is above 1 for pure pigments but small in all four coexpression combinations, particularly for a dichromatic visual system with JNDs ≤ 0.8 (Fig. 5.6B, Table S2D, Appendix D). Combining these results with those for blue/gray, we find that although coexpression increases blue / gray discrimination, it makes blue / purple discrimination worse. Therefore, coexpression can not compensate for dichromacy in all tested scenarios. This adds further supports that cichlids must be trichromatic to successfully perform all visual tasks.

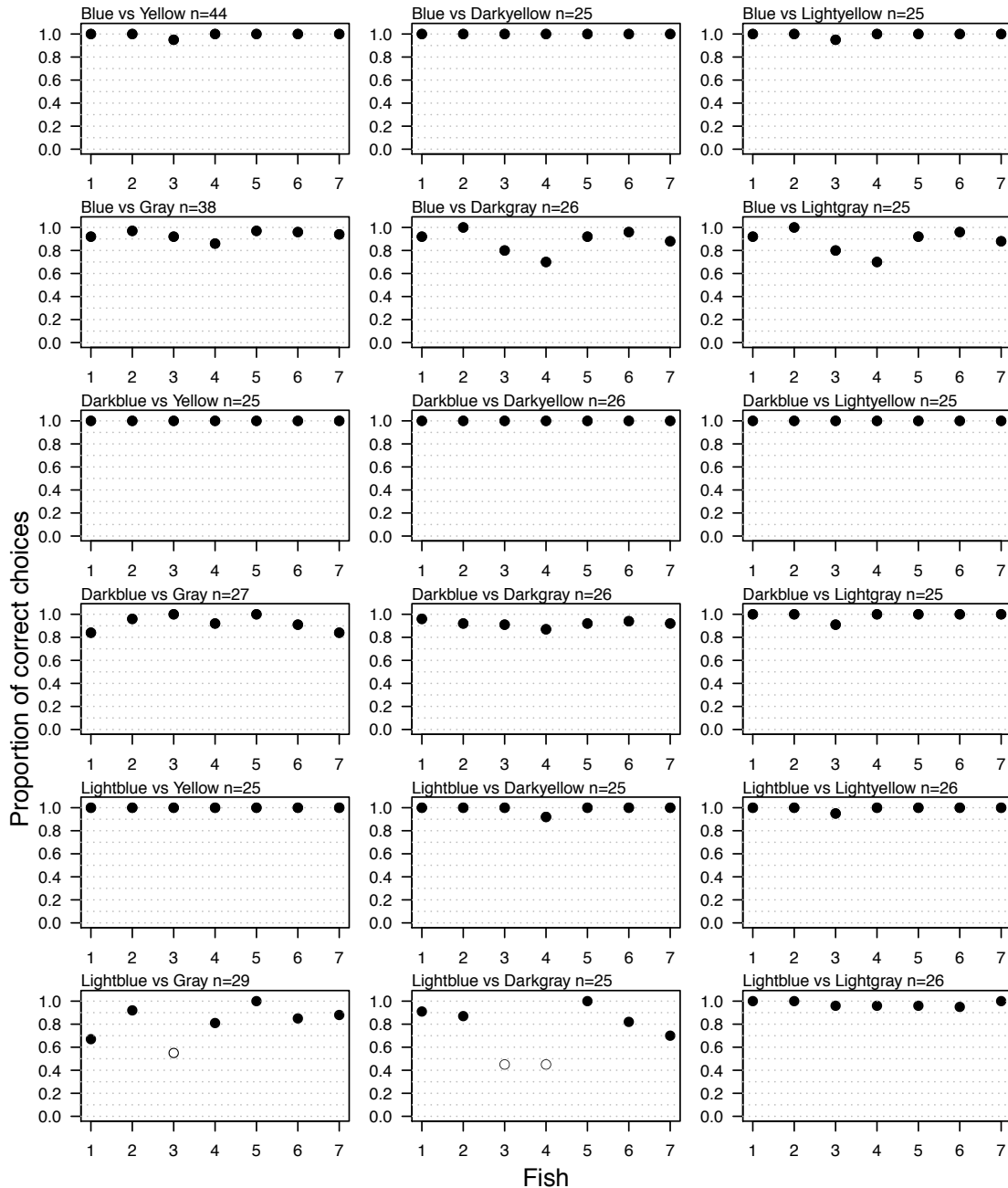


Figure 5.2. Proportion of times the stimuli was chosen correctly in the first binary choice experiment. Each treatment and the number of trials are specified. Numbers at the x axis specify each individual fish whereas the proportion of correct choices are specify on the y axis. Empty symbols denote when the binomial test was not significant ($p^* > 0.05$).

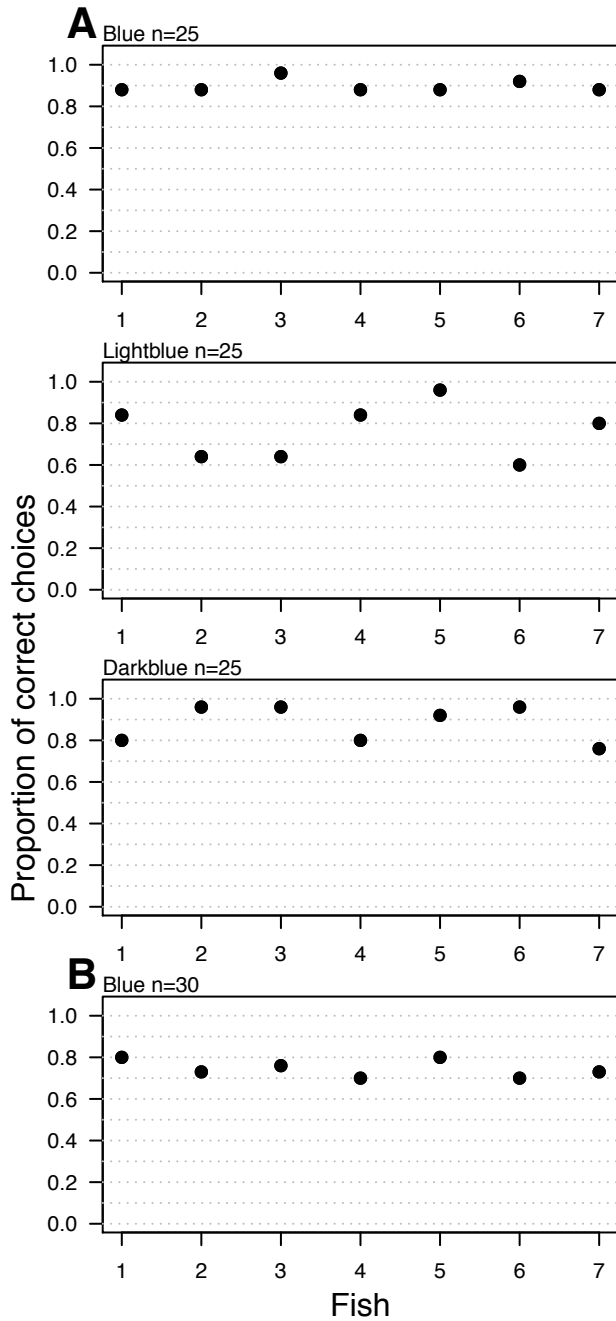


Figure 5.3. Proportion of times the stimuli were chosen correctly for multiple-choice experiments. (A) Experiment 2 for blues versus multiple grays, and (B) Experiment 3 for blue versus multiple colors. The number of trials are specified (n). Numbers on the left specify each individual fish. All binomial tests were significant ($p^* < 0.05$).

5.5 Discussion

The results of this study show that *M. benetos* has color vision. Fishes were able to distinguish blue from other colors regardless of brightness in all the experiments. Our behavioral results also imply that cichlids are trichromats where the three types of photoreceptors (S, M and L) are necessary for color discrimination. This is in agreement with von Kries corrected quantum catches calculations, which suggest that each photoreceptor is differentially stimulated by each color. Thus, we suggest that double cone members (M and L) provide opponent spectral channels used for color vision as modeling where double cones are summed together suggest multiple colors would equally stimulate the photoreceptors. The unique contributions of double cones is further supported by quantum catch calculations without von Kries correction. Under these conditions, there is very low stimulation of the single cones by the lighting in these experiments, such that double cones could mostly mediate color discrimination. Furthermore, our visual modeling suggests that quantum catches and chromatic distance can be affected by opsin coexpression.

5.5.1 Cichlid behavior

Cichlid vision has been extensively studied using a variety of behaviors associated with visual cues. Cichlids are quite adaptable and several species seem amenable to training under lab conditions. Cichlids have shown they are able to recognize facial cues between conspecifics [219], and Lake Malawi

Metriaclima species, have been used for shape discrimination, object categorization and symmetry perception tasks [220–222].

Here we provide some of the first behavioral evidence that the Lake Malawi cichlid, *M. benetos*, possesses color vision. The potential ability for color vision in cichlids has previously been suggested using molecular and microspectrophotometry methods. Those data show that *M. benetos* rely on three visual pigments resulting from expression of three different cone opsin genes. However, the current study is the first behavioral evidence of their chromatic discrimination capabilities. These behavioral experiments confirm that within weeks, *M. benetos* can be trained to perform visual tasks based on color cues alone. These results rely on classical conditioning using color choice [177] as have been used in previous studies on fish color vision [174,183,191,202,223].

5.5.2 Color opponency and opsin coexpression

Our visual modeling assuming a dichromatic visual system (based on double cone summation) predicted that cichlids wouldn't be able to discriminate blue from gray. However, in our behavioral results, all fish successfully distinguished blue from gray regardless of luminance noise. This suggests that cichlids have a trichromatic visual system where color vision is based on the differential stimulation of each photoreceptor (S, M and L).

Based on our visual modeling and behavioral results, we suggest that *M. benetos* achieves color vision probably through color opponency mechanisms. This agrees with the assumption that in DC, spectrally opponent channels exist between each cone members, producing a signal which is the result of differences between spectrally distinct cones [191] (Fig. 5.4C-F). This hypothesis is supported because in our experiments, fish were able to differentiate blue from gray regardless of the similarities of quantum catches of SC and the summed signals of DC (Fig. 5.4A). Therefore, each double cone member is likely generating a different signal causing spectral differences that would be registered by ganglion cells in a trichromat.

In this study, we are assuming that color opponency is the product of two different cone photoreceptor sensitivities that are being compared by ganglion cells. Nevertheless, the retina neural circuit can be highly complex. For example, bipolar and horizontal cells have been shown to already receive feedback from three to four spectral types of cones in cyprinids [224–226]. Morphological and physiological studies analyzing the neural network of the cichlid retina are needed in order to better understand how color opponency takes place.

Color opponency needs at least two different spectral channels whose quantum catches are compared [128]. In cichlids, the presence of multiple cone types to produce these different spectral channels is supported by our previous *in situ* labeling of different opsins to examine the spatial distribution of cone types in the

closely related Malawi cichlid, *M. zebra* [24,161]. In those studies, we found a highly organized retinal mosaic with single and double cones. Both SC and DC contain spectrally different opsins including unique opsins in opposite members of DC. More interestingly, Dalton *et al* (2016) showed that *M. zebra* has an area centralis in the retina close to the optic nerve, with high densities of both photoreceptors and ganglion cells, and minimal opsin coexpression. This suggests that this region in the retina provides high acuity for visual tasks, including color discrimination. We further found that the spatial patterns of opsin coexpression vary between individuals with at least one of six individuals showing coexpression in the area centralis [20].

In our visual modeling opsin coexpression increases ΔS for some colors but decreases ΔS for others (Fig. 5.5-6) (Table S2C-D, Appendix D). Interpretation of the size of JNDs should be done with caution because even though chromatic distance is an indicator of color discriminability, it does not assess perceptual similarity from highly discriminable stimuli (Kelber *et al.* 2003). Large ΔS do not necessarily mean that some colors are more discriminable than others, instead, this suggests that color discrimination is preserved over longer distances because water acts as an attenuating medium making colors more achromatic over larger distances [218]. This effect is irrelevant in our experiment since fish were very close to the stimuli. Even though we have not confirmed opsin coexpression in *M. benetos*, qPCR data suggest that it is likely because of the expression of multiple single cone opsins [12,73]. However, coexpression is less

common in the area centralis, where fish would be viewing objects of interest. We suggest that opsin coexpression might have negatively affected discrimination between specific colors where coexpression decreased ΔS (e.g. blue vs. purple), and this is in concordance with our behavioral evidence. Furthermore, some individuals show more difficulty with discrimination than others, and these may occur in the few individuals with increased coexpression. This would require further genetic testing.

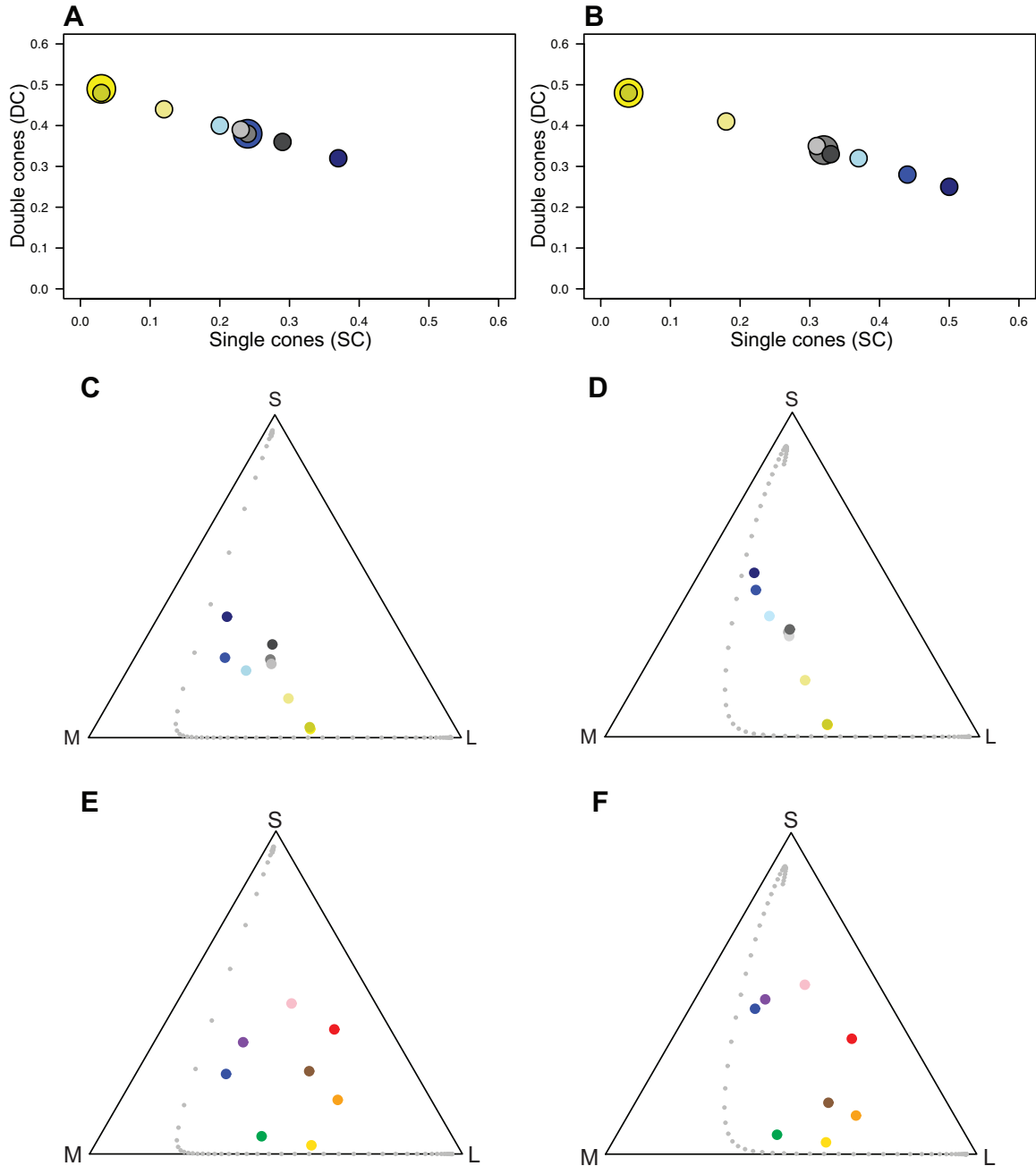


Figure 5.4. Normalized quantum catch of colors in Experiments 1, 2 & 3. In a dichromatic visual system, photoreceptor's stimulations are plotted as signals in single cones (SC, x axis) and as summed signals in double cones (DC, y axis). Quantum catches were normalized using Eqn 1 & 2 for S-, M- and LWS cones. Combined signal-stimulation (summed) of double cones (DC) was calculated with Eqn 4. A, represents quantum catch when there is pure opsin expression whereas B represents opsin coexpression combination 1. Bigger dots are used to reveal overlapping data-points in the SC-DC space. For a trichromatic visual system, photoreceptor stimulations are plotted in chromaticity diagrams with target colors plotted in the color receptor space of *M. benetos* for experiments 1, 2 & 3. Each axis corresponds to the quantum catches of short/UV (S), medium

(M) and long (L) sensitive photoreceptors. Monochromatic loci at 5 nm intervals are represented by gray dots. C & E are based on pure opsin expression visual system (SWS1, RH2B, RH2A α) whereas D & F correspond to opsin coexpression combination 1 (SWS1/SWS2B, RH2A β /RH2B, LWS/RH2A α). Only coexpression combination 1 is displayed since it is the one that has been reported in the area centralis.

5.5.3 Color discrimination and the Weber fraction

In this study, we wanted to take the first step in understanding vision in cichlids and to know if they have true color vision. Further studies are needed to dissect the cichlid visual system as well as its adaptations and limitations, but given our visual modeling and behavioral results, we can infer the physiological characteristics of the cichlid retina. Initially, based on previous fish-vision studies applying the RNL model, we assumed a Weber fraction of 0.05 [20,218,227,228] for the LWS channel. However, in order to better predict cichlids performance, we adjusted this to a higher Weber fraction of 0.1. We did this because even though we are not evaluating color discrimination thresholds, increasing the Weber fraction and hence lowering chromatic distance, would partially explain the mistakes fish made (Fig. 5.2-3). In general, a Weber fraction of 0.05 is accepted for most animals [211] but it is known that predicted thresholds can disagree with experimental data [216,229].

There were a few color combinations where fish were more likely to make mistakes. Fish more often made mistakes with discriminating blue from purple. This might be explained due to their reflectance profile similarities (Fig. S1F, Appendix D). Mistakes of blue vs purple might also be explained by opsin

coexpression. With opsin coexpression combination #2, ΔS is low (<1 JNDs) (Fig. 5.6A, Table S2C, Appendix D) thus, making discrimination 'harder' for the fish. In contrast, mistakes by several of the individuals between lightblue and grays are not explained by either opsin coexpression, similarities in quantum catches or low JNDs. Lightblue and grays exhibit a chromatic distance above 1 JNDs in most coexpression combinations in both, dichromatic and trichromatic visual systems. One possibility is that the receptor noise is greater than 0.1 resulting in lower ΔS . Indeed, if we increase the noise ratio to 0.3, ΔS between lightblue and grays decreases proportionately by a factor of 3 (0.7-1.1 JNDs). Higher levels of noise could be a consequence of the low stimulation of the short sensitive cone (which is UV sensitive in *M. benetos*). This is supported by absolute quantum catches calculations (Table S2B, Appendix D) which remove the von Kries correction and better accounts for the fact that the light environment where fish were tested lacked UV light (Fig. 5.1D), thus, affecting the stimulation of SC (Fig. S3, Appendix D). Hence, the low stimulation of SC and high levels of photoreceptor noise might explain fish mistakes of lightblue and grays.

Overall, only trichromacy would allow fish to successfully choose blue over gray since these colors are only discriminable in a trichromatic visual system (Fig 5.5C). In a dichromat, blue and gray would only be discriminated when there is opsin coexpression (Fig. 5.5D) however we have shown coexpression is uncommon in the area centralis [20]. Further, if cichlids are trichromats, with or

without coexpression, they would be able to discriminate blue and purple (Fig. 5.6A). In contrast, dichromats with coexpression would not be able to choose blue over purple (Fig. 5.6B), which was not the case since all fish significantly chose blue over purple.

These mistakes fit with the RNL model predictions where chromatic discrimination is only plausible under bright illumination and not in low illumination conditions since achromatic mechanisms may become important [211,230,231]. This is because the Weber law suggests that in bright light photoreceptor noise is independent of the signal, whereas in dim light, chromatic discrimination is affected by both internal photoreceptor noise and fluctuations in the number of absorbed photons. Thus, the Weber law is no longer valid [232]. It is remarkable, that even with very little stimulation of SC when photon-shot noise is considered (Table S2B, Appendix D), *M. benetos* succeeded in discriminating color stimuli, reinforcing the assumption that there is color opponency between members of double cones.

Lastly, there might be a behavioral component we are overlooking causing fish to make mistakes. It is noteworthy, that in spite of their mistakes, most fish succeeded in choosing the trained stimuli over the distracter in all tests. Likely, *M. benetos* is achieving color vision using their area centralis, where color discrimination would be best. In addition, in bright environments like Lake

Malawi, there is significantly more ultraviolet light to stimulate SC so that photoreceptor shot noise would be smaller and color discrimination better.

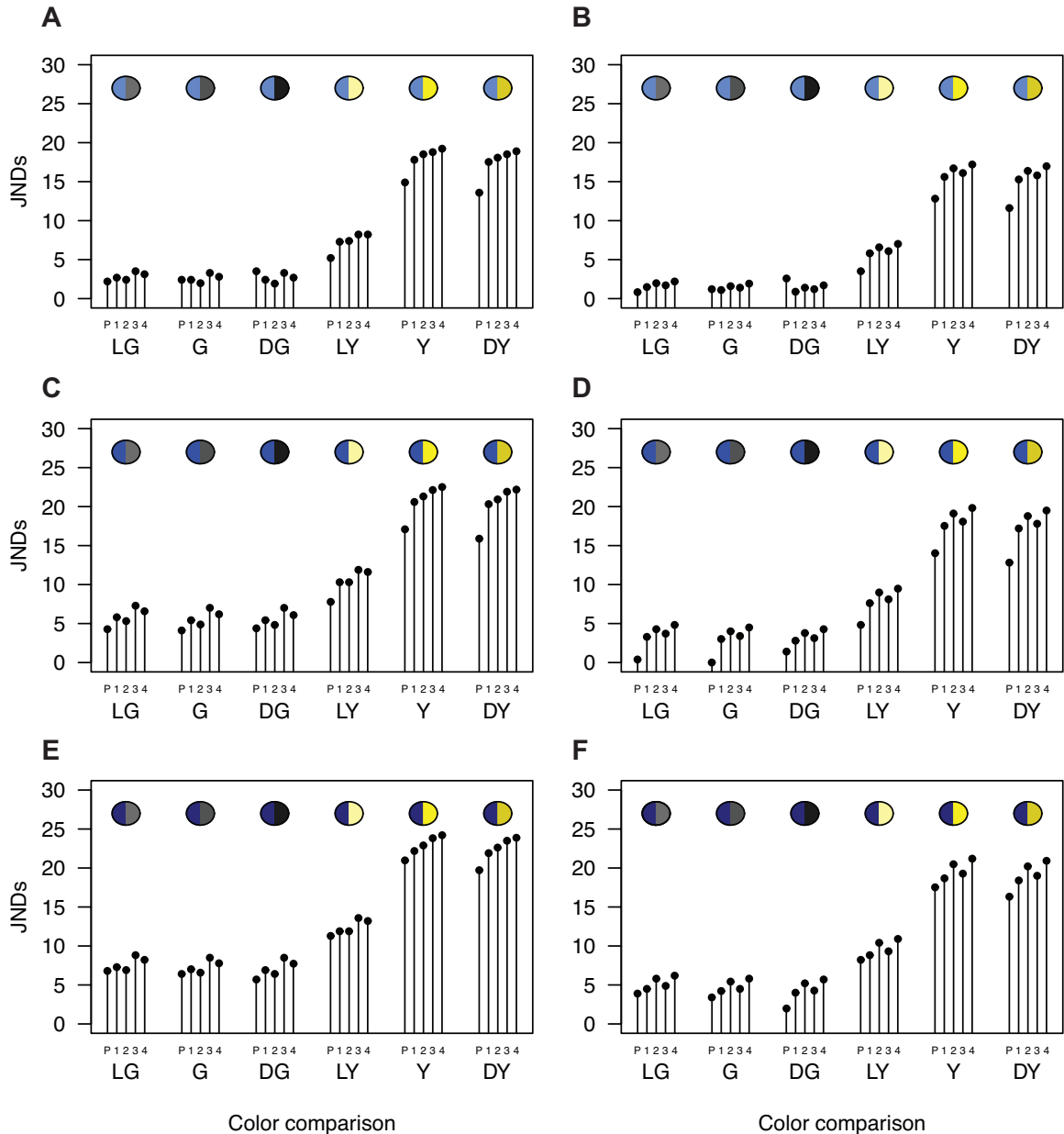
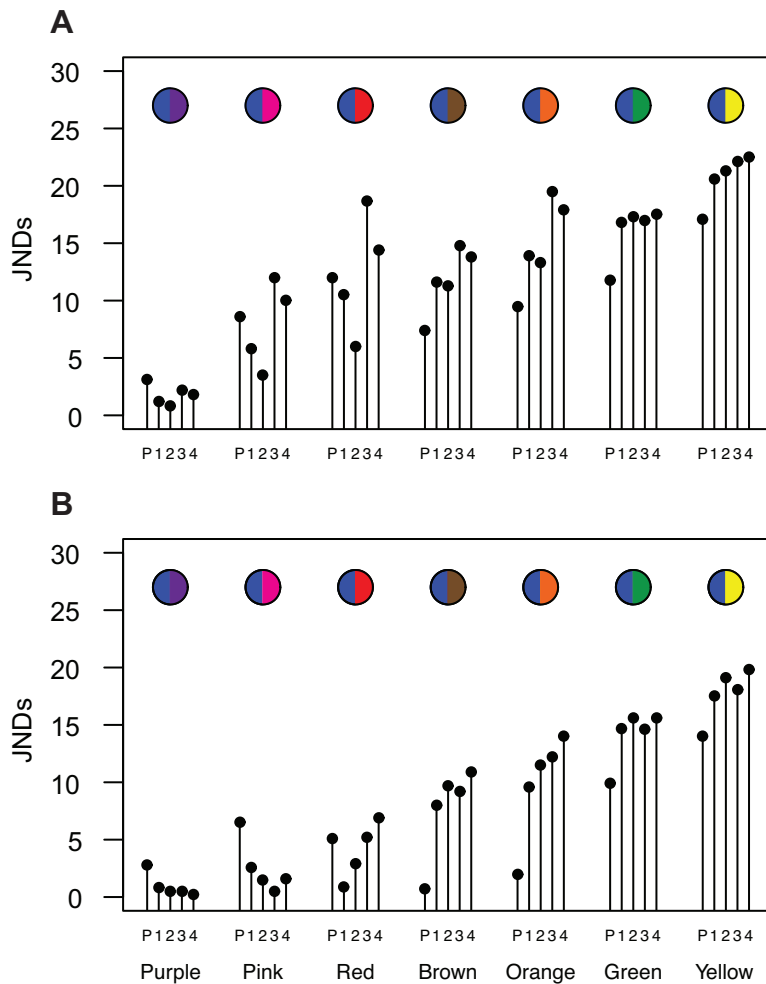


Figure 5.5. Chromatic distances, ΔS (JNDs), of colors in experiments 1 and 2. Chromatic distances between stimuli for experiments 1 and 2 are given for lightblue (A, B), blue (C, D), and darkblue (E, F), against distracter stimuli (G: Gray; LG: Lightgray; DG: Darkgray; Y: Yellow; LY: Lightyellow; DY: Darkyellow). A, C and E are ΔS for a trichromatic whereas B, D and F are for a dichromatic visual system. Pure (P) and coexpression combinations (1-4) are specified for each color pair.



Color comparison

Figure 5.6. Chromatic distances, ΔS (JNDs), of colors in experiment 3. Chromatic distances between blue and colors used in Experiment 3 where A is for a trichromatic and B for a dichromat visual system. Pure (P) and coexpression combinations (1-4) are specified for each color pair.

5.5.4 Color vision and its relationship with cichlid ecology and evolution

Our results are particularly relevant for the study of evolution in the cichlid lineage because the exploitation of color vision allows cichlids to use

communication channels that can be subject to variation. Subsequently, this organismal variation in sensory cues can lead to bursts of signaling evolution, where male secondary sexual characteristics diversify leading to cladogenic events [233,234]. This is likely important for *M. benetos* because its sympatric close relatives, *M. zebra* and *M. sandaracinos*, differ mainly in coloration patterns [235,236].

In the wild, *M. benetos* would benefit from color vision. Similar to many Malawi cichlids, this species relies heavily on visual cues for foraging and mating. *M. benetos* would use color vision to identify conspecifics and to discriminate between dominant and subordinate individuals. This has been suggested because male *M. benetos* are especially UV reflective in the dorsal fin and flanks, which are displayed in mating and social rank signaling [237,238]. Chromatic discrimination would also benefit females since they would be able to choose among conspecifics males. Male coloration pattern is important for African cichlids' assortative mating and this has been studied behaviorally [196,239,240] because visual signals are likely the first step in the multimodal courtship [241].

Color vision would also facilitate foraging tasks for *M. benetos* since rock-dwelling cichlids are notorious omnivores with a broad spectrum of feeding habits and items, ranging from scraping algae to zooplanktivory [242–244]. Color discrimination would enable cichlids to tell apart specific food items from a variety of different objects and backgrounds. Indeed, UV sensitivity improves foraging

efficiency in *M. benetos* [245], however, this discrimination could rely on contrast as well as color vision.

More experiments are needed to further test cichlids' chromatic discrimination capabilities. In this study, fish were trained exclusively for blue but we do not know if cichlids exhibit bias towards specific colors. There is the possibility that *M. benetos*, due to its coloration pattern and their main sensitivity to the "short" range of the wavelength spectrum, succeeded in discriminating blue because of a preexisting preference towards this wavelength. Color bias has been reported in teleosts before. Picasso triggerfish (*Rhinecanthus aculeatus*) seems to avoid yellow and blue, and both the Picasso triggerfish and the lunar wrasse (*Thalassoma lunare*) seem to prefer green and red [174]. Preference towards specific colors in assortative mating could also underlie a sensory bias. This has been reported for stickleback's preference for red [246] and guppies' preference for orange [247]. Because male *M. benetos* exhibit a pale blue nuptial coloration [236], sensory bias studies are needed to test if there is a preexisting preferences for blue.

5.6 Conclusions

In this study, we have showed that cichlids can be trained through classical conditioning in order to perform color discrimination tasks. Cichlids successfully discriminated blue from gray as well as several different color targets. Our visual modeling and behavioral results suggest that cichlids have color vision, probably

through color opponency mechanisms produced by neural interactions of three different photoreceptor spectral channels. Furthermore, we suggest that opsin coexpression can vary in its effects on color perception towards specific wavelengths and hence, color discrimination power. The capability of color discrimination in cichlids can have a big impact in understanding the natural history of this speciose clade because cichlid's visual capabilities and coloration patterns have been associated to their adaptive radiation and evolutionary success.

5.7 Acknowledgements

We thank all the members from the Carleton and Kocher lab for taking care of the fish throughout this project. We also thank Ben Sandkam for helping us in preparing the differential contrast whole mount image of *M. benetos*' retina and Gabriel Arellano and Natalia Umana for guiding us with figures. This work was supported by a Biology Department Travel Award and Summer Research Fellowship through the University of Maryland Graduate School (2015-2016 to D.E-C.). D.E-C is supported by graduate fellowship of the Secretariat of Higher Education, Science, Technology and Innovation of Ecuador (2014-AR2Q4465). This work was also supported by NIH 1R01EY024639. No competing interests declared. This work was supported by the National Institutes of Health [1R01EY024639 to KLC]. This work was also supported by graduate fellowship of the Secretariat of Higher Education, Science, Technology and Innovation of Ecuador (SENESCYT) [2014-AR2Q4465 to D.E-C].

Chapter 6: Behavioral color thresholds in a cichlid fish: *Metriaclima benetos*

In Review under: Daniel Escobar-Camacho, Michael A. Taylor, Karen L. Cheney, Naomi, F. Green, Justin N. Marshall, Karen L. Carleton. Behavioral color thresholds in a cichlid fish: *Metriaclima benetos*. Journal of Experimental Biology. 2019

6.1 Abstract

Color vision is essential for animals as it allows them to detect, recognize and discriminate between colored objects. Studies analyzing color vision usually require an integrative approach, combining behavioral experiments, physiological models and quantitative analyses, which results in a comprehensive characterization of visual systems. Here, we demonstrate, for the first time, the limits of color vision in *Metriaclima benetos*, a rock-dwelling cichlid from Lake Malawi using behavioral experiments and visual modeling. Fish were trained to discriminate between colored stimuli. Color thresholds were then quantified by testing fish chromatic discrimination between the rewarded stimulus and distracter stimuli that varied in chromatic distance. This was done under fluorescent lights alone and with additional violet lights. Our results provide two main outcomes. First, cichlid color thresholds correspond with predictions from the receptor noise limited model but only if we assume a Weber fraction higher than the typical value of 5%. Second, cichlids may exhibit limited color constancy under certain lighting conditions as most individuals failed to discriminate colors when violet light was added. We further used the color thresholds obtained from these experiments to model color discrimination of actual fish-colors and backgrounds under natural lighting for Lake Malawi. Our modeling suggests that for *M. benetos*, blue is most chromatically contrasting against yellows and space-light. This study highlights the importance of lab-based behavioral experiments in understanding color vision in cichlids and in parameterizing the assumptions of the receptor-noise-limited vision model for different species.

6.2 Introduction

Behavioral investigations of color patterns in nature are essential for understanding the evolution of animal coloration patterns. One way to understand the adaptive significance of animal coloration is through color perception. Color vision is the capacity for discriminating color regardless of brightness. It is essential for many living organisms because it facilitates the detection, discrimination and recognition of colored objects. Several behaviors can be mediated by color vision such as predator or prey detection, finding mates, foraging, and other inter- and intraspecific social interactions.

An integrative approach is necessary to comprehensively investigate color vision in animals, which combines physiological models, behavioral experiments, and data on photoreceptor spectral sensitivities. Most animals exhibit multiple spectral cone-types as has been shown through physiological (microspectrophotometry, MSP) [248] and molecular experiments (opsin gene analysis) (Davies et al., 2012; Kelber and Osorio, 2010). However, behavioral experiments are necessary to confirm color vision because photoreceptors can be used for a variety of visual tasks including achromatic (luminance) vision, motion detection, polarized vision, or phototaxis [249]. In addition, theoretical visual models have been developed to predict the visual capabilities of animals in studies of visual ecology. Behaviorally testing for color vision enables us to determine whether assumptions of theoretical visual models are met.

Color thresholds can be estimated using color vision models such as the Receptor Noise Limited (RNL) model (Vorobyev and Osorio 1998). This model, based on physiological principles, has two main assumptions: (1) chromatic contrast is achieved through color opponency where at least two spectrally different photoreceptors are compared to produce a signal, and (2) the limits of color discrimination are set by receptor noise, originating in the proximal visual pathway. The estimation of receptor noise is critical for the correct prediction of color thresholds [250,251]. Noise in the receptor channel is related to the Weber fraction (ω). This is a constant that describes the signal-to-noise ratio that sets discrimination thresholds to the smallest difference in chromatic contrast that can be detected, a just noticeable difference (JND) [189,213,252]. Thus, values below 1 JND are indicative of color pairs that are indistinguishable while values above 1 JND are indicative of color pairs that can be distinguished [212].

Direct measures of receptor noise in single cells can be measured through electrophysiology experiments or estimated based on the relative number of photoreceptor cell types [214]. Noise can also be inferred by adjusting the noise parameter of the model such that an estimated threshold fits the behaviorally determined color discrimination threshold [252]. This is based on the assumption that if noise can be used to estimate the limits of color discrimination, then color-discrimination thresholds can also be used to estimate receptor noise [252].

When viewing colored objects, environmental light may also influence color discrimination. Because the light spectrum hitting an object can change, the capacity of the visual system to perceive colors consistently regardless of changes in illumination spectra is essential for color vision [253]. Without color constancy, color vision would be unreliable because colors would change under different illuminations. Unsurprisingly, a wide range of animals exhibit color constancy [254] including fish [255–257]. One of the ways color constancy is achieved is through photoreceptor adaptation where photoreceptors adapt to stimulus intensity by changing their sensitivity [258,259]. To account for color constancy, color vision models use the von Kries color constancy model where photoreceptors adapt independently to the background illumination [177,210]. One way to quantify color constancy is to perform vision-mediated behavioral experiments under different illuminations.

Fishes are an ideal system to study color vision due to their diverse set of visual pigments and the highly variable light environments they inhabit. Thus, in order to study color vision in fish, behavioral methods are needed to demonstrate color discrimination [197]. These studies often use a classical conditioning approach where fish are trained to a reward stimulus to test for fish visual capabilities [174,183,188,191,202,218,223,260,261]. Characterizing the detection thresholds for chromatic signals is important because it will contribute to an understanding of color vision and the perception of coloration patterns in nature.

Among teleosts, cichlids are a great model for vision-mediated behavioral experiments in laboratory conditions [219–222,260,262]. Cichlids are one of the most diverse vertebrate clades with approximately 2000 species widely distributed across the globe (Friedman et al., 2013; Turner et al., 2001, www.fishbase.org). Like many taxa, cichlids use color vision to detect, identify and discriminate different foods, offspring (if they are mouth-brooders) and sexual mates [194,196,240,241,263] as some can only be distinguished based on nuptial coloration patterns [236]. Species of the genus *Metriaclima* are ideal for chromatic discrimination experiments because their visual system has been characterized through MSP, opsin gene expression [26,73,201] and analysis of retinal anatomy [20,260]. They are also bold as they are highly territorial, which makes them excellent candidates for performing visual tasks.

In a previous study, we showed that cichlids could be trained to discriminate between different colors regardless of brightness [260]. Cichlids successfully discriminated a rewarded blue stimulus from several other colors (grays, yellows, red, green, brown, orange, pink). However, they made errors when discriminating blue from purple [260]. Based on what we know of fish color thresholds [38,218], this led us to take the next step and aim to answer the following questions: (1) What are cichlid color thresholds and how do they compare to those predicted by the RNL model? (2) Does color discrimination change under different illumination? (3) How do these lab-based behavioral results help us understand and interpret cichlid visual tasks in the wild? In this study, we performed a series

of color discrimination experiments and psychometric analyses, and measured color discrimination thresholds between a range of blue and purple stimuli. We also report the potential limitations of color constancy in cichlids and further discuss the color thresholds obtained in this research and their implications for color perception in the wild based on field data from Lake Malawi.

6.3 Methods

6.3.1 Behavioral approach and fish training

We used seven lab-raised individuals of *Metriaclima benetos*, [236], for our experiments. To measure discrimination thresholds, we used a similar approach to the experiments from von Frisch (1914), in which fish are trained to associate a reward with a specific colored stimulus chosen from among a number of distracter stimuli [203]. We trained fish to recognize blue as the rewarded stimulus through classical conditioning, and then tested their capacity to discriminate blue from other colors. We chose blue as our rewarded stimulus because blue is the primary body coloration of male *M. benetos* [236].

To train the fish, a feeding apparatus was created by attaching a feeding tube to a syringe filled with a mix of fish flakes and water (Fig. S1B, Appendix E). Initially, food was delivered in the front of the tank with the feeding apparatus. Once the fish learned to bite/tap the tube in order to obtain food, a flat-laminated, blue-colored circle was attached to the end above the tube using Velcro. This allowed the fish to begin to associate the color stimulus with food. After they learned to

tap the blue stimulus attached to the feeder tube, a laminated card with a blue circle in the center was presented to the fish (Fig. S1C, Appendix E). Initially, the laminated card had the feeding tube attached just above the blue circle with Velcro. Finally, once the fish became comfortable tapping the stimuli in the presence of the tube attached to the laminated card, the fish were then shown a laminated card without the feeding tube. As soon as fish tapped the card independently of food being present in the tank, fish were given several preliminary assays (~30) in a binary choice test (see Experiment 1) to confirm that they could discriminate blue from other colors (green, yellow, and orange). This lasted for approximately two months and when they succeeded 75% of the time, testing started. During testing, in order to make sure fish could see all stimuli before choosing, they were lured towards the back of the tank with the feeding apparatus while the color cards were placed in the front section of the tank. As the feeder was removed the fish then turned to make a choice (as per Escobar-Camacho et al., 2017). Finally, in order to reinforce memory, the rewarded blue stimulus alone was presented to the fish every time before a testing session. Training began in March and was completed by July 2017. Fish had different learning performance, with some learning faster than others, but after approximately 2-4 months all fish were ready for testing. Experiments were run between July 2017 and July 2018.

M. benetos were held in individual tanks of 26 x 50 x 30 cm (Fig. S1A, Appendix E) with continuous water flow from the same recirculating system, and were fed

daily during training and testing periods. Fish were trained and tested in the Tropical Aquaculture facility at the University of Maryland, USA, under the guidelines of the University of Maryland Institutional Animal Care and Use Committee protocol (#R15-54).

6.3.2 Visual modeling

For testing color discrimination thresholds, we analyzed how a series of colors differentially stimulates photoreceptors. This was done by calculating quantum catches (Q), which are the number of photons absorbed by a given photoreceptor. Calculations of quantum catches include (1) the spectral cone-sensitivities of *M. benetos*, (2) reflectance spectrum of an object (e.g. colored circle), (3) the lens transmission, and (4) the spectrum of environmental light (Fig 6.1A-E).

Metriaclima benetos exhibits three visual pigments with a peak absorbance (λ_{\max}) of 379, 489, and 522nm (Fig. 6.1A) [201]. These are classified as short, medium and long (denoted by subscripts S, M and L respectively) wavelength sensitive cones. Quantum catches were calculated for each of these cone types using Eqn 1 [207] where R_i is the sensitivity of receptor i , L is the lens transmission, S is the color reflectance, I is the illuminant and K is the von Kries factor for receptor i

$$Q = K_i \int R_i(\lambda)L(\lambda)S(\lambda)I(\lambda)d\lambda \quad \text{Eqn 1}$$

The opsin absorbance template was based on [264] and the von Kries factor (Eqn 2) is derived from the von Kries' color constancy model in which a receptor adapts independently to the background illumination [177,207,210].

$$K_i \propto \frac{1}{\int R_i(\lambda)L(\lambda)I(\lambda)d\lambda} \quad \text{Eqn 2}$$

In order to obtain the luminance input from double cones we also modeled combined quantum catches of double cones (Eqn 3), which are thought to mediate luminance vision in teleosts [188,191].

$$Q_{DC} = \frac{Q_M + Q_L}{2} \quad \text{Eqn 3}$$

Quantum catches allow us to calculate chromatic contrast between the different colors for which fish were tested. For this we apply the receptor noise limited model (RNL) [211]. Therefore, we used quantum catches of each cone class (i) to calculate contrast between pairs of colors Δf_i [212] (Eqn 4).

$$\Delta f_i = \ln \left[\frac{Q_i(\text{color1})}{Q_i(\text{color2})} \right] \quad \text{Eqn 4}$$

Furthermore, color discrimination is determined by receptor noise. The standard deviation of the noise in a single cone channel (ν) is related to the Weber fraction

(ω) for each photoreceptor type (i) by $\omega = v / \sqrt{n_i}$ where n is the number of receptors of type i . We can assign receptor noise for each cone class (Eqn 5) by first assigning the noise value to the long (L) receptor and then calculating the noise values of the short (S) and medium (M) cone classes based on their relative abundance in the retinal mosaic. For *M. benetos*, the S:M:L ratio is 1:2:2 [260]. Even though estimates of noise can vary among animals [252], in this study we set the standard deviation of noise (v) of the L receptor to 0.05 because it has been used in previous color-vision research studying several organisms [215,230,232], including fish [218]. This gives us a relative noise value of 0.07 for the S cones and 0.05 for M and L cones.

$$\omega_i = 0.05 \sqrt{\frac{n_L}{n_i}} \quad \text{Eqn 5}$$

Photoreceptor noise determines the smallest chromatic contrast (ΔS) that can be detected between two colors (Eqn 6) in units of just noticeable difference (JND). ΔS represents the chromatic distance of two colors in the perceptual color space where values below 1 JND are indicative of colors that can not be discriminated.

$$\Delta S = \sqrt{\frac{\omega_S^2(\Delta f_L - \Delta f_M)^2 + \omega_M^2(\Delta f_L - \Delta f_S)^2 + \omega_L^2(\Delta f_S - \Delta f_M)^2}{(\omega_S \omega_M)^2 + (\omega_S \omega_L)^2 + (\omega_M \omega_L)^2}} \quad \text{Eqn 6}$$

We calculated the chromatic distance of each of the distracter stimuli vs. rewarded blue stimulus. Then, we behaviorally determined the color threshold

when fish chose the rewarded stimulus more than the distracter stimuli (at 65% correct choice, See Data Analysis below). Finally, since ω is inversely related to ΔS we can also experimentally estimate individual receptor noise by fitting behavioral color thresholds between a series of stimuli where ΔS is 1 JND.

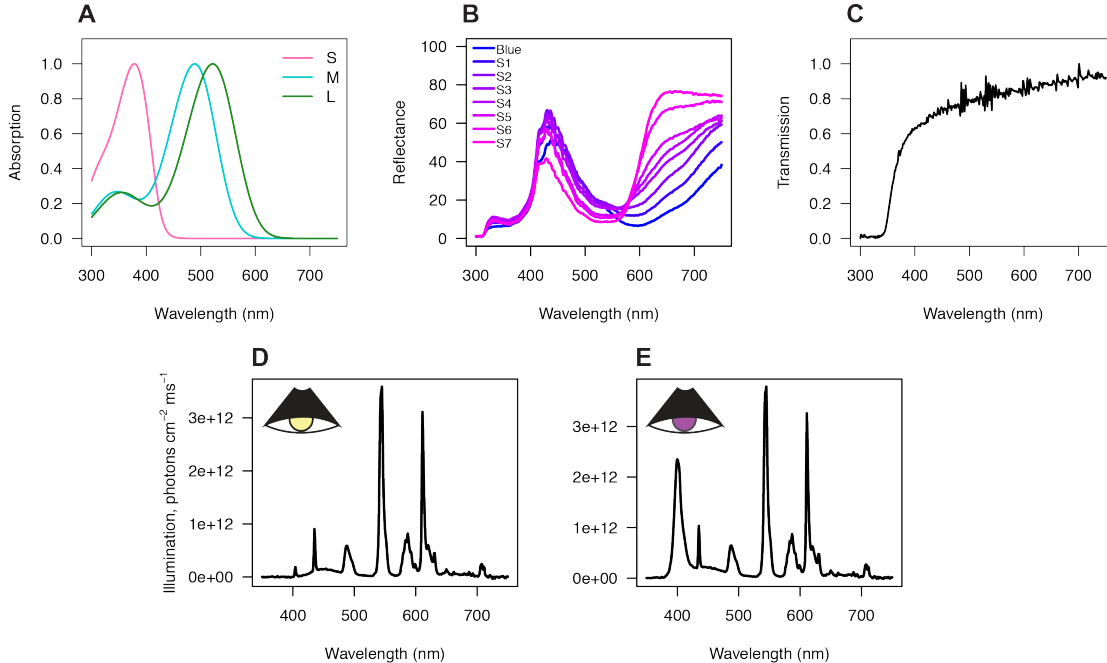


Figure 6.1. Spectral parameters for color thresholds experiments. (A) Spectral sensitivity of the short, medium, and long (S, M, & L) wavelength pigments present in single and double cones of *M. benetos* [201]. (B) Reflectance spectra of blue and distracter stimuli. (C) Normalized *M. benetos* lens transmission spectra (Escobar-Camacho et al., 2017) (Table S1C, Appendix E). (D & E) Aquarium side-welling irradiance of fluorescent (D) and violet lights (E).

6.4.2 Calibration of colored stimuli and quantum catch

To calibrate visual stimuli used in this experiment, we first measured the reflectance of several colors with different RGB values that were printed on multipurpose recycled paper (Eagle Office 30, brightness 92) and were subsequently laminated. We then selected a series of colors that gradually

moved away from blue in color space. Color cards were made then by printing single colored circles (~1.5 cm diameter). Distracter colors were designed so that they would differentially stimulate the short and long-wavelength sensitive cones of *M. benetos* (Fig. 6.1A). To do this, we increased red and decreased blue intensity using Adobe Illustrator. Reflectances of colored stimuli were measured using a fiber-optic attached to a Flame spectrometer (Ocean Optics, Dunedin, FL, USA) fitted with a 400 μm fiber and calibrated with a NIST (National Institute of Standards and Technology) traceable tungsten halogen lamp (LS-1, Ocean Optics) (Table S1A, Appendix E). Side-welling irradiance was measured inside the tanks under fluorescent and fluorescent plus violet-LED light with a 1000 μm fiber fitted with a cosine corrector (CC-3) (Fig. 6.1D-E) (Table S1B, Appendix E). For the rest of this article we will refer to light environments as fluorescent and violet.

Quantum catch calculations suggest that the S, M and L cones are differentially stimulated by blue and purple colors (Fig. 6.2A-B, S2A-D, Appendix E). Distracter stimuli move across the perceptual color space starting with pink and becoming progressively more similar to blue, with S7 being the most different to blue and S1 being the most similar (Fig. 6.2). This successive pattern can be observed in the cichlid perceptual color-space with both fluorescent and violet light (Fig. 6.2A-B). In our modeling we noticed that the location of all stimuli shifts toward the achromatic point in the color space when we include violet light (Fig. 6.2C). Furthermore, ΔS calculations confirmed our quantum catch observations with

stimulus S1 being closest to blue and S7 being the most distant (Fig. S2E-H, Appendix E). Our model shows that the distracter stimuli's distances gradually increased in the color space from the blue reward stimulus (Fig. 6.2).

6.4.3 Experiment 1: Color threshold between blue and purple

This experiment consisted of an array of binary choice tests where fish had to choose between two cards with one color circle on each (Fig. S1C, Movie 1, Appendix E). Fish (n=7) had to choose between the rewarded blue stimulus and a series of purple-violet distracter stimuli. As soon as the fish tapped one of the color cards, both were removed and the fish was rewarded if it chose correctly, and the trial ended. In order to avoid bias for one side of the tank, the same color was not presented on the same side more than two times in a row. If the fish did not respond to the stimuli for two minutes, the fish was not rewarded and the trial was not counted. During testing, white paper was used to block the sides of the tank so that the fish could not see the experimenter or other fish; however, the experimenter could see which color stimulus the fish tapped with a mirror placed above the tank.

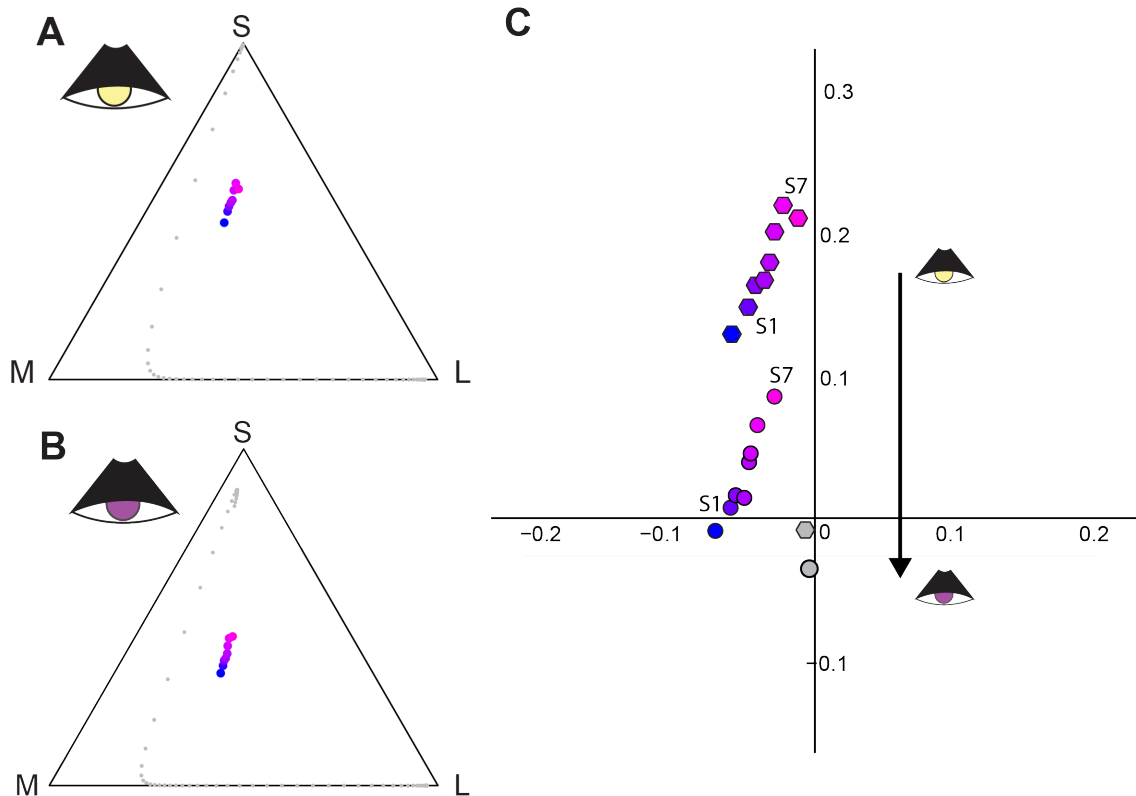


Figure 6.2. Quantum catch of colors from thresholds experiments. Photoreceptor stimulation of each target color in the *M. benetos* color receptor space is plotted in chromaticity diagrams. Each axis corresponds to quantum catches of the short/UV (S), medium (M) and long (L) wavelength-sensitive cones. Monochromatic loci at 5 nm intervals are represented by small gray dots. Color stimuli presented to the fish show their relative positions in the color space under fluorescent (A) and violet light (B). Close-ups of colors in the Maxwell triangle space of stimuli under both fluorescent (hexagons) and violet (circles) light with respect to the white background of the color cards (gray markers) (C).

6.4.4 Experiment 2: Multiple choice with brightness variation

Color stimuli in Experiment 1 were located along a line in SML color space, but were not controlled for brightness. To make sure that fish were discriminating target blue from distracter purples based on chromatic cues alone and not luminance, we added luminance noise to experiment 2. The threshold interval (when fish significantly discriminated blue from purple) in experiment 1 was

between distracter stimuli S3, S4, and S5. We introduced luminance noise by using a multiple-choice test where fish were asked to choose blue from seven distracters on an eight-choice colored card. This color card contained blue, one of the distracter stimuli from the threshold interval (S3, S4, S5), and six other distracter stimuli (Fig. S1E, Movie 1, Appendix E). The six distracter stimuli were all similar in ΔS (within 0.5 JNDs) relative to S3, S4 and S5 but differed in brightness (Fig. S3, Appendix E). The brightness based on the luminance channel was calculated as the average quantum catches from the M and L cones (Fig. S3G-I, Appendix E) [191,260]. Cards in this experiment contained eight colors each and four card arrangements were designed for each of the threshold interval colors. Each of these color card arrangements were presented to the fish six times in a random fashion adding up a total of 24 trials per each distracter stimuli (S3, S4 & S5 respectively) (Fig. S1D, Appendix E) [260].

6.4.5 Experiment 3: Color threshold with different background illumination

This experiment was similar to Experiment 1, but quantified the color threshold under violet light. We performed this experiment to examine if color thresholds changed when stimulation of the short-wavelength (UV) sensitive cone was increased. Therefore, experimental procedures were the same as Experiment 1, but fish were tested under both LED black lights (OPPSK 27W 9LED UV) and fluorescent lights to produce our violet treatment (Movie 1).

6.4.6 Experiment 4: Cichlid visual modeling in Lake Malawi

To consider the implications of cichlid color discrimination, we used the RNL model to calculate color discrimination of the blue of *Metriaclima* species versus a variety of backgrounds and other cichlid colors. Cichlid color reflectances were taken from previous measurements (Dalton et al 2010). Briefly, fish-color reflectance was measured from live specimens where fish were illuminated at a 45 deg to their surface with a pulsed xenon lamp (PX2, Ocean Optics). Reflected spectra were collected with a bifurcated optical fibre (Ocean Optics) where light was collected on the same axis at which the illuminant exited [207]. Additional substrate spectra for grasses, sand and mud were measured using Sub-spec II, a submersible fibre-optic spectrometer based on an Ocean Optics USB2000 (Dunedin, FL, USA), fitted with a 50, 100 or 400 μ m fiber, and calibrated with a tungsten halogen lamp (LS-1, Ocean Optics) (Justin Marshall, unpublished data). These measurements were taken at two locations: the south side of Thumbi West Island near Mitande Point (latitude 14°1'23"S, longitude 34°49'27"E) and the east side of Otter Point (latitude 14°2'17"S, longitude 34°49'22"E). Substrate reflectance spectra were obtained by measuring the substrate reflectance compared with a white Teflon standard placed at the same location. Either downwelling light or a high intensity quartz halogen lamp (Light and Motion, Monterey, CA, USA) were used to illuminate substrates. All reflectance spectra for the new substrates as well as those from previous studies are given Table S1D (Fig. S4, Appendix E).

For our modeling with Lake Malawi data we used the blue of *Metriaclima callainos* (Stauffer and Hert 1992), which has the same blue-hue as *M. benetos* (Stauffer et al 1997) and calculated the ΔS between blue and other fish colors and spectra. Side welling radiances near Otter Island and the Mawlamba Bay on the north side of Thumbi West Island were obtained from Sabbah et al 2011 (Table S1D, Appendix E)

Quantum catches for different cichlid colors and different substrates were calculated using Equation 1 but with the illuminant (I) being the Lake Malawi side-welling irradiance (from Thumbi West Island at a depth of 3 m, Sabbah et al 2011; Dalton et al 2017, Table S1D, Appendix E). For the color blue viewed against the natural space light, we calculated the quantum catch of side welling radiance as one of the targets. In that case, the quantum catch is calculated where $(S * I)$ is the side welling radiance. These quantum catches were then used in Equation 6 to determine the ΔS between blue and several colors.

6.4.7 Data analysis

For experiments 1, 2 and 3, a one-tailed binomial test was used to calculate whether fish discriminated the rewarded from distracter stimuli. The number of correct trials was compared to the distribution of taps if fish would have chosen randomly (50% of the time for Experiment 1 and 3, and 12.5% for Experiment 2). Therefore, the threshold discrimination was established at 65% of correct choices ($n=40$, $p<0.05$ one-tailed binomial test) for Experiments 1 and 3, and at 29% of

correct choices ($n=24$, $p<0.05$, one-tailed binomial test) for Experiment 2. Confidence intervals were calculated assuming a binomial distribution. Finally, we fitted our behavioral results with psychometric curves, where a generalized linear model (GLM) is applied to the data set to fit a logistic regression, to see the relationship between ΔS and proportion of correct choices [216,218]. All binomial tests and visual modeling calculations were done in R using “psyphy” and “modelfree” packages for estimating psychometric functions (www.r-project.org/)

6.5 Results

6.5.1 Experiment 1: Color threshold between blue and purple

For this experiment, a total of 1,960 tests were performed ($n_{\text{fish}}=7$, $n_{\text{color-pairs}}=7$, $n_{\text{trials-per-colorcard}}=40$). In general, all fish exhibited significant discrimination of blue over colors S5, S6 and S7 with proportions of correct choices of 70%, 80% and 90% respectively ($n=40$, $p<0.008$, $p<0.001$, $p<0.001$ respectively) (Fig. 6.3A). There was considerable variation among individuals (Fig. S5B-C, Appendix E), and not all were able to significantly discriminate blue from stimuli S3 and S4 with a wide range of correct choice frequencies (55-72% and 50-70% for S3 and S4 respectively) (Table S1E, Appendix E). All fish failed to discriminate blue from colors S1 and S2 with correct choice frequencies of 55% ($p<0.317$, $n=40$) for both stimuli.

With a standard deviation of noise (v) of 0.05, the stimulus closest to each fish’s behavioral threshold (when fish choice-frequency of blue over distracter stimuli

reached statistical significance) was S4. This behavioral threshold had a ΔS of 3.4 ± 0.52 (Fig. 6.3A).

6.5.2 Experiment 2: Multiple choice with brightness variation

For this experiment, a total of 432 tests were performed using the 8-choice color card ($n_{\text{fish}}=6$, $n_{\text{color-cards-arrangements}}=12$, $n_{\text{trials-per-colorcard}}=6$). Fish were more likely to choose blue vs distracters S4- and S5-like stimuli with correct choice frequencies of 35-40% ($n=24$, $0.006 < p < 0.0001$) but they failed to choose blue over distracter stimuli similar to S3 (correct choice frequencies 24%, $n=24$, $p=0.07$) (Fig. 6.3B) (Table S1F, Appendix E). This confirmed our results from experiment 1, which suggested the color threshold occurs between colors S3 and S4 (Fig. 6.3A).

6.5.3 Experiment 3: Color threshold with different background illumination

For this experiment, a total of 1,680 pairwise tests were performed ($n_{\text{fish}}=6$, $n_{\text{color-pairs}}=7$, $n_{\text{trials-per-colorcard}}=40$). Surprisingly, in this experiment most fish failed to discriminate blue from any distracter stimuli, S1-S7, with correct choice frequencies ranging from 48% to 62% (Fig. 6.3C). We again observed individual variation where some fish significantly discriminated blue from stimuli S3, S4, S6 and S7 yet not with high significance overall (Table S1G, Appendix E). Our results from this experiment show that fish cannot optimally discriminate colors under violet illumination. These results also suggest that either the behavioral

chromatic threshold would occur at greater ΔS as predicted by the psychometric functions or that photoreceptor noise may be greater with this type of violet illumination.

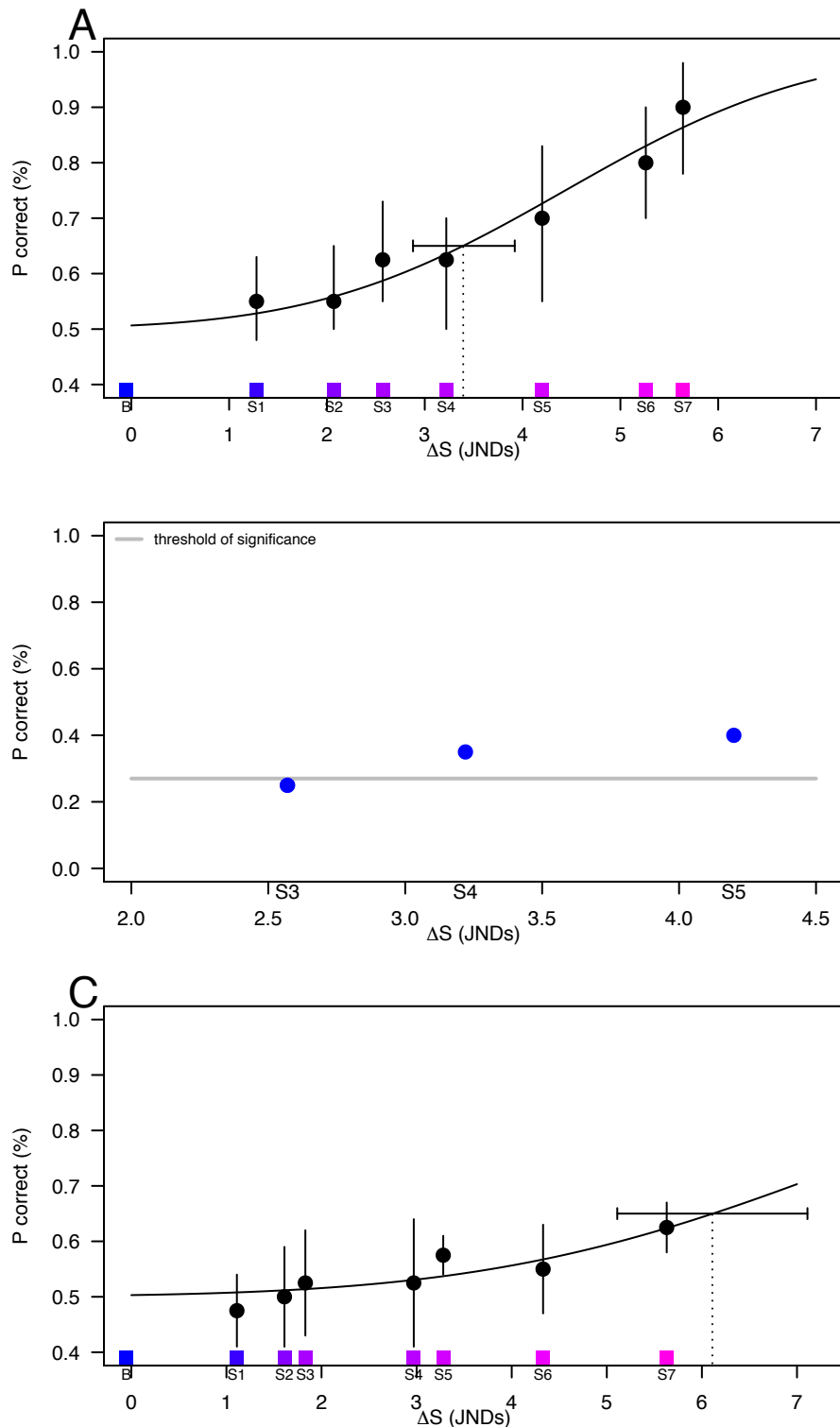


Figure 6.3. Color discrimination in the three experiments. (A) Color thresholds under fluorescent light (Experiment 1) where proportion of correct choices is showed as a function of ΔS (JNDs). ΔS was estimated using a standard deviation of noise (ν) of 0.05. The x-axis represents ΔS between colors. Filled circles denote the fraction of correct choices made by fish for

stimulus S1-S7, and colored inserts represent the respective distracter stimuli appearances. The dotted line denotes where the threshold values is at 65% correct choices. Continuous lines denote the variation (standard deviation) of the correct choices made by fish and at the behavioral threshold. (B) Results of brightness tests (Experiment 2) showing the proportion of correct choices (blue over distracter stimuli) for the different distracter-stimuli groups in the 8-choice test (S3, S4 & S5). (C) Results of color thresholds under violet light (Experiment 3). ΔS was estimated using a standard deviation of noise (ν) of 0.05.

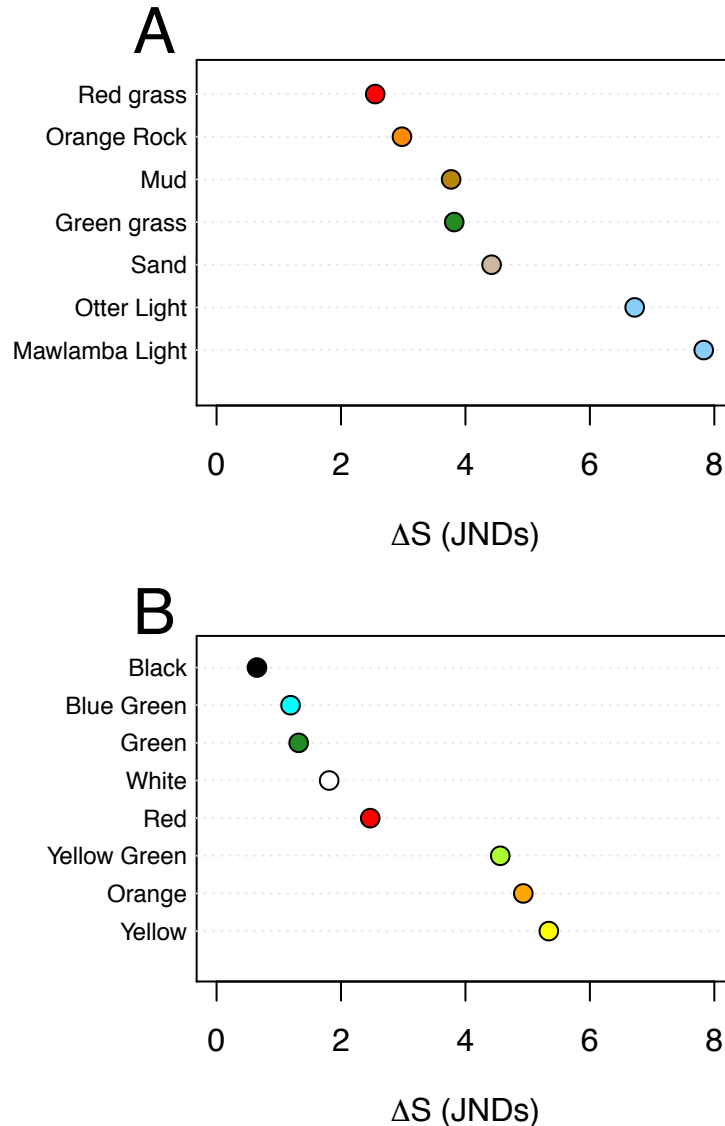


Figure 6.4. Variation of ΔS of cichlid-blue vs. backgrounds and other cichlid-colors. (A) Shows the shift in ΔS between blue and background colors of Lake Malawi. (B) Shows the shift in ΔS between blue and cichlid-colors.

6.5.4 Experiment 4: Cichlid visual modeling in Lake Malawi

Chromatic distance for cichlid-blue versus the different substrates (Fig. 6.4A) and different cichlid colors (Fig. 6.4B) suggest that blue has high chromatic contrast with space-light and long-wavelength colors. There are some cichlid colors where cichlid-blue has low color contrast including black, blue-green, green and white. The cichlid-blue spectra is quite broad and not a very saturated color, making it difficult to distinguish from other broad color hues (Fig. S4, Appendix E). However, it does show high contrast with colors such as yellow, orange and red.

6.6 Discussion

6.6.1 Color thresholds and receptor noise

In this study, we confirmed that *M. benetos* possess color vision because fish were able to discriminate the rewarded from distracter stimuli regardless of brightness. Our results also allowed us to compare the predictions of the RNL model to our behavioral discrimination assays. We used a standard deviation of noise (ν) of 0.05 for the LWS channel, as suggested from previous studies, which coupled with our behavioral results suggest that color thresholds arise when $\Delta S = 3$ which would be equivalent to one JND (Fig. 6.3A). This differs from previous studies that suggest that a ΔS of 1 is enough for color-pairs to become discriminable [212]. However, our results are similar to a previous study that measured color thresholds in triggerfish and found thresholds arise at ΔS greater than 1 [38,218].

Since the RNL model did not fit with our behavioral data using previously parameters, this implies that the cichlid visual system has higher receptor noise levels. The best fit of the behavioral performance of our fish would require increasing the standard deviation noise value (ν) for the LWS channel from 0.05 to 0.16. This would increase the Weber fraction (ω) (0.22 for S and 0.16 for M and L cones) such that the behavioral discrimination threshold would arise at a minimum ΔS of 1, which would correspond to one JND (Fig. S5A, Appendix E) in agreement with the RNL model predictions.

Noise has been shown to vary in animals. For example, in insects direct-noise measurements were found to be around 0.12 [214], and in birds behavioral noise estimates suggest they vary from 0.06 to 0.105 [189,216,252]. In addition, the RNL model predicts the discriminability of colors taking into account several physiological parameters (e.g. visual pigment sensitivity, light transmission, environmental light, etc) [218]. However, the RNL model does not take into account information about retinal-photoreceptor interaction or central color processing, which are currently unknown in cichlids but essential in understanding their color vision. More morphological and physiological experiments analyzing the cichlid retina and their color processing are needed for a better understanding of the relation between photoreceptor noise and color discrimination.

Furthermore, our results are strictly based on laboratory assays in which the light environment is dimmer than the fish's natural habitat, Lake Malawi. Light intensity can have an effect on the performance of the fish and also on our visual modeling because one of the RNL requirements is that experiments must be executed under bright illumination [211]. Bright illumination is ideal in experiments as it suppresses the contribution of the achromatic channel in color discrimination. Although these experiments were well above the photon-shot noise limit [260], there could still be some affect of the light levels being a factor of 10 lower than the natural environment.

Finally, fish in this study were trained for a visual task of discriminating two color elements. However, we cannot exclude the possibility that our results could be the product of cichlids performing artificial tasks in an artificial setting. Conversely, results could be different if cichlids performed other tasks such as species recognition or mate selection in their natural habitat.

6.6.2 Color discrimination under different background illumination

Experiment 3 shows that cichlids exhibit a limited color constancy under these experimental conditions, because fish made more errors when discriminating blue from distracter stimuli under violet light. This contradicts our calculations with the von Kries correction that predicts similar ΔS between blue and distracter stimuli under both light environments (Fig. S2A-D, Appendix E). However, most of our fish were unable to discriminate between blue and purples under violet

light. This decrease in the performance of fish due to changes in the light environment has also been reported in experiments with bees, fish and birds [216,254–256,265–267] and suggests that cichlids have limitations in their color constancy, like other organisms. Additionally, our experiments only tested color discrimination in a specific area of cichlid color space (blues and purples). Previous studies have shown that color constancy correction varies in different areas of an animal's color space [254,255,265] and that it can be “poorer” for colors reflecting shorter wavelengths [265]. The visual system of *M. benetos* is not unlike that of bees in utilizing UV, blue-green and green photoreceptor channels. This suggests that our experiments may have been particularly hard for the fish because the tested colors relied on the long wavelength part of the spectrum.

To understand why the discrimination tasks were harder for fish under violet lighting, we used the RNL model to calculate ΔS between color stimuli and the “white” background of the color cards in our experiments. We noticed that ΔS of all tested stimuli and the white background decreased significantly when illuminated under violet light (Fig. 6.5A). This likely caused color discrimination to become more difficult for the fish because the ΔS of blue and the background under violet light decreases compared to the ΔS of blue and the background under fluorescent light (Fig. 6.5A-B). However, ΔS between the stimuli and background is greater than 1, which suggests stimuli should still be “discriminable”.

The discordance between visual modeling and our behavioral thresholds can again be better explained by assuming a higher noise level. By using a noise level of 0.16 in the LWS channel, ΔS between blue and the background under violet light decreases to ~ 1.6 which is close to threshold (Fig. 6.5B). Greater noise would decrease the chromatic contrast of the rewarded stimuli and the background and it would help explain why our fish couldn't discriminate between two colored stimuli under violet light. As light illumination changed, blue was harder to tell apart from the background and hence, fish made more mistakes (Fig. 6.5C). The overall shift in chromatic distance due to different light environments can also be observed in the cichlid perceptual color space (Fig. 6.2C) where all tested colors are closer to the white background under violet light than when modeled with fluorescent light. This suggests that fish have less chromatic information for chromatic contrast detection. Overall, our results suggest cichlids exhibit only approximate color constancy in Experiment 3 and that color thresholds strongly depend on the chromatic contrast between tested stimuli and the background [254,266].

6.6.3 Individual performance variation

During our experiments we observed individual variation in fish performance, which affected the results of both Experiment 1 and Experiment 3 (Table S1E-G, Fig. S5B-C, Appendix E). Some fish exhibited color thresholds at lower ΔS suggesting "better" color discrimination skills than others. For example, in

Experiment 1 one fish remarkably chose blue over S2 with high frequency despite their small ΔS . Similarly in Experiment 3, one fish was able to discriminate blue from S3 and S4 and three were able to discriminate blue from S7 (Fig. S5C, Table S1G, Appendix E).

This variation in performance among individuals could be the product of different experiences during training and testing and it provides insights into the heterogeneity that is present in Lake Malawi wild populations. This variable capacity in discriminating colors during several behaviors would predict that cichlids exhibit a continuous range in color discrimination thresholds in the wild suggesting that some cichlids would be better at discriminating colors than others and hence, may outperform other fish in several visual-mediated tasks.

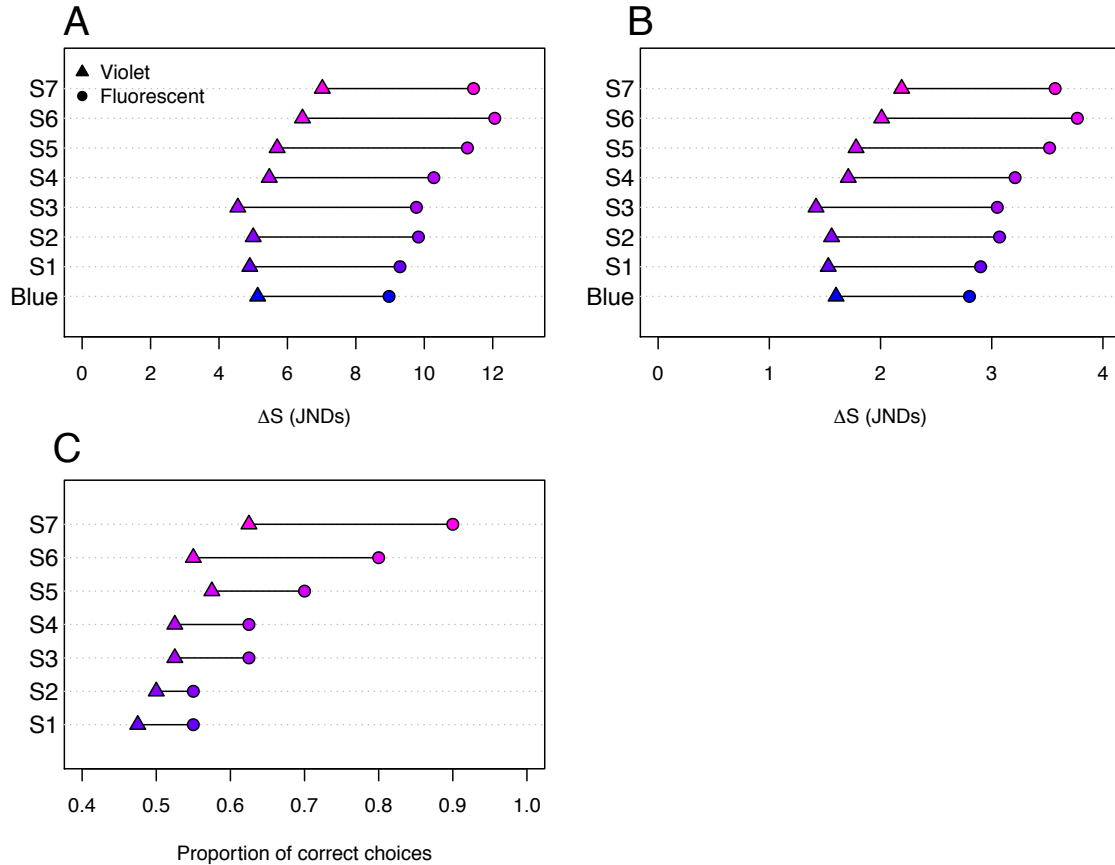


Figure 6.5. Variation under different light illumination of ΔS between colors vs background and correct choice frequency. (A & B) show the shift in ΔS between the color stimuli and the background when illuminated under violet (triangles) and fluorescent light (circles). ΔS was estimated using a Weber fraction of 0.05 (A) and 0.16 (B). (C) Shows the proportion of correct choices (blue over distracter stimuli) when colors were presented in different light environments.

6.6.4 Visual ecology in Malawi

The study of color vision in cichlids is important because cichlids' communicate through colorful visual signals that can be subject to variation and ultimately sexually selected [233,234]. Our results can potentially inform the study of visual ecology of Malawi cichlids to start thinking about their color perception in the wild and their ability to perform different tasks. For example, color discrimination

analyses of blue vs. backgrounds suggest greater ΔS between blue and space-light backgrounds than between blue and orange rock backgrounds (Fig. 6.4A). Furthermore, ΔS are greater between blue and yellow cichlid colors than between blue and greens (Fig. 6.4B). Although large ΔS values are not an indicator of how discriminable color pairs are; they are indicative of how much color discrimination would be preserved over longer distances as water attenuation would gradually make colors more achromatic [227]. Therefore, ΔS is informative about which colors would remain discriminable with increasing distance. Our measurements of noise levels will help inform those estimates.

Behavioral observations in the field are in agreement with the importance of estimating ΔS of some color-background pairs. In Malawi, female *M. benetos* swim above the rocks of male territories with males then swimming up to them to perform their courtship display, trying to lead them back to their territories for mating and spawning (Karen Carleton, personal observation). Hence, the capacity of discriminating between blue and either the rocks or the space-light would be necessary in identifying conspecific males and their visual signals first against the rocks and then in the water column. Furthermore, the large ΔS between blue and yellows would be useful in several behaviors in the rock-dwelling clade including during courtship where females peck male egg-spots and then pick up eggs after spawning, [268] and for discriminating between species that exhibit blue and/or yellow in their nuptial coloration. Blues and yellows are the main nuptial colorations present in Lake Malawi and they have

evolved repeatedly within the lake suggesting that these color signals are favored by sexual selection [269].

6.6.5 Future directions

Although we are starting to learn more about cichlid color vision, several more experiments are needed in order to understand the dimensionality of the cichlid visual color space. In our color threshold experiments we analyzed color discrimination in only one region of the color space (blue and purple). Ongoing research suggests that color thresholds can differ between different directions of the perceptual color space [38]. This would imply that animals' visual systems could be wired to be more sensitive to changes in some colors than in others. This is relevant to cichlids because they exhibit great variation in cichlid visual sensitivities and spectral tuning mechanisms [26,27]. Future experiments should test for color discrimination on a wide range of colored stimuli in different regions of color space.

Additionally, more studies on cichlid color constancy are needed because in this research we only used two different light treatments. Future experiments should consider using light environments that would vary in chromatic-hue because fish have shown to remain "more" color constant under some colors than in others [255]. Color constancy can also be influenced by different backgrounds (e.g. gray and black) [255,256], hence, future experiments should also consider manipulating color card backgrounds during behavior assays. Finally, future color

constancy experiments should consider using light illumination intensities relevant to those in their natural habitat. This would shed light on whether cichlid color constancy depends on light levels. This is relevant to cichlid vision because in Lake Malawi, some cichlids can inhabit from 1 to 20 meters depth where light gets gradually attenuated with increasing depth [270,271].

6.7 Conclusions

In this study, we have shown that cichlids can be trained to perform color threshold discrimination experiments while controlling for brightness and chromatic cues. Cichlids successfully discriminated the rewarded stimuli from a series of distracter stimuli that varied in hue. We further confirmed that cichlids discriminated these colors regardless of brightness by combining luminance noise tests with multiple-choice assays. This study also shows that by using the RNL model we can successfully determine behavioral color thresholds between different colors. However, our results only meet the RNL model assumptions if we increase the Weber fraction, which suggest cichlids have higher receptor noise than previously thought, at least in lab conditions. Furthermore, we show that under some conditions, cichlids have limited color constancy where their ability to discriminate colors decreases under a different light illumination. This likely happened because changing the illuminating light decreased chromatic contrast of the background and the tested colors. Continued research into cichlid color vision is needed as it could help us understand more about the role of vision in cichlid ecology, sexual selection and ultimately cichlid speciation.

6.8 Acknowledgements

We thank all the members from the Carleton and Kocher lab for taking care of the fish throughout this project. This work was supported by the National Institutes of Health [1R01EY024639 to K.L.C.] and by a graduate fellowship of the Secretariat of Higher Education, Science, and Technology and Innovation of Ecuador (SENESCYT; Secretaría de Educación Superior, Ciencia, Tecnología e Innovación) [2014-AR2Q4465 to D.E-C].

Chapter 7: Synthesis

7.1 Introduction

This dissertation provides new insights in the evolution of color vision in freshwater fishes. I have been able to characterize the molecular basis for color vision in Neotropical cichlids and characins, two major groups of teleosts. We discuss aspects of their extant opsin gene complements, which are products of highly dynamic opsin gene evolution; and of their color vision, which is based on the expression of at least three spectrally different visual pigments. In addition, the relationship between their visual system and the light environment these fish inhabit has also been addressed.

In this research we have also examined the adaptive significance of cichlid color vision. Through behavioral assays we show that cichlids do possess color vision and we demonstrate this through chromatic discrimination experiments. This is further complemented with visual modeling where we test different hypotheses about the limits of cichlid color vision. The following main inferences highlight our key findings and suggest future directions for fish color vision research.

7.2 Opsin gene evolution in Neotropical cichlids

Opsin sequencing has revealed that Neotropical cichlids have a reduced visual pigment repertoire because some opsins (i.e. SWS1 and RH2B) have either never been found in the genome [42] or have undergone pseudogenization

[42,113,272] (Fig. 7.1). The opsins that have become non-functional or lost are consistently those which are sensitive to the shorter end of the spectrum from each opsin-class (SWS and RH2). This suggests there is a bias to inactivate opsins sensitive to short wavelengths while maintaining the ones sensitive to longer-wavelengths (e.g. SWS2A, LWS). Additionally, opsin inactivation occurs in parallel in different neotropical lineages because opsins have been pseudogenized independently in some species while remaining functional in others [42,113,117,273]. Interestingly, while opsins become inactivated in Central and South American species, they remain intact in most of the African species. Dozens of African cichlids have been sequenced showing that their entire opsin complement is fully functional [41,274,275] .

Furthermore, sequencing suggests that the SWS2A-opsin seems to be under positive selection as it is the opsin exhibiting most of the diversity in amino acid variation in transmembrane regions, retinal binding pockets, and polarity changes [113]. These findings differ from studies in African cichlids where the SWS1-opsin is the most variable [41]. Although, the SWS1 opsin has not been pseudogenized in all Neotropical species, it is not expressed in the retina [113,117], although see [273], suggesting that SWS1 functionality may not be under selection. Conversely, as SWS2A is the main opsin expressed in single cones, the protein-coding mutations may be occurring in order to fine-tune the spectral sensitivity at this end of the spectrum.

Finally, we found there is gene conversion in the RH2A paralogs of Neotropical cichlids. Gene conversion between opsins occurs often in teleosts [36,64,65,113,144] and in our analysis so far it seems a gene conversion event occurred once between the RH2A paralogs in the early ancestor of Neotropical cichlids.

Our results suggest that opsin evolution in Neotropical cichlids involves processes, such as opsin sequence variation, gene inactivation and gene conversion, and that these processes accompany the adaptation to Neotropical water environments. Because neotropical freshwater ecosystems are characterized for their red-shifted light environment, selection may have favored the expression of longer-wavelength-sensitive over shorter-wavelength-sensitive opsins. A decreased constraint on shorter wavelength opsins could allow for potential gene losses as a result of stochastic genomic events.

7.3 Opsin Expression in Neotropical cichlids

RNA-seq of four Amazonian cichlids (*A. ocellatus*, *S. discus*, *P. scalare*, *C. monoculus*) shows that color vision in Neotropical cichlids is based on a long visual palette (SWS2-RH2A-LWS) [113,272]. This expression profile is typical of fish living in red-shifted environments and our results are similar to opsin-expression studies on Central American cichlids [42,117,273]. The use of the long palette seems to be conserved among the Neotropical cichlid clade whereas the other palettes (short and medium) have not arisen and have remained in

African cichlids (Fig. 7.1). Furthermore, because the riverine ancestor of African cichlids probably also expressed a long palette [274], this suggests the long palette may be the ancestral state of both lineages, Neotropical and African. However, since visual systems adapt to the available light, Neotropical cichlids inhabiting shorter-wavelength light environments should exhibit other palettes. Indeed it has been found that in a few species of Central American cichlids, the SWS2B has increased its expression [273]. More studies are needed to truly sample the visual system diversity among Neotropical cichlids.

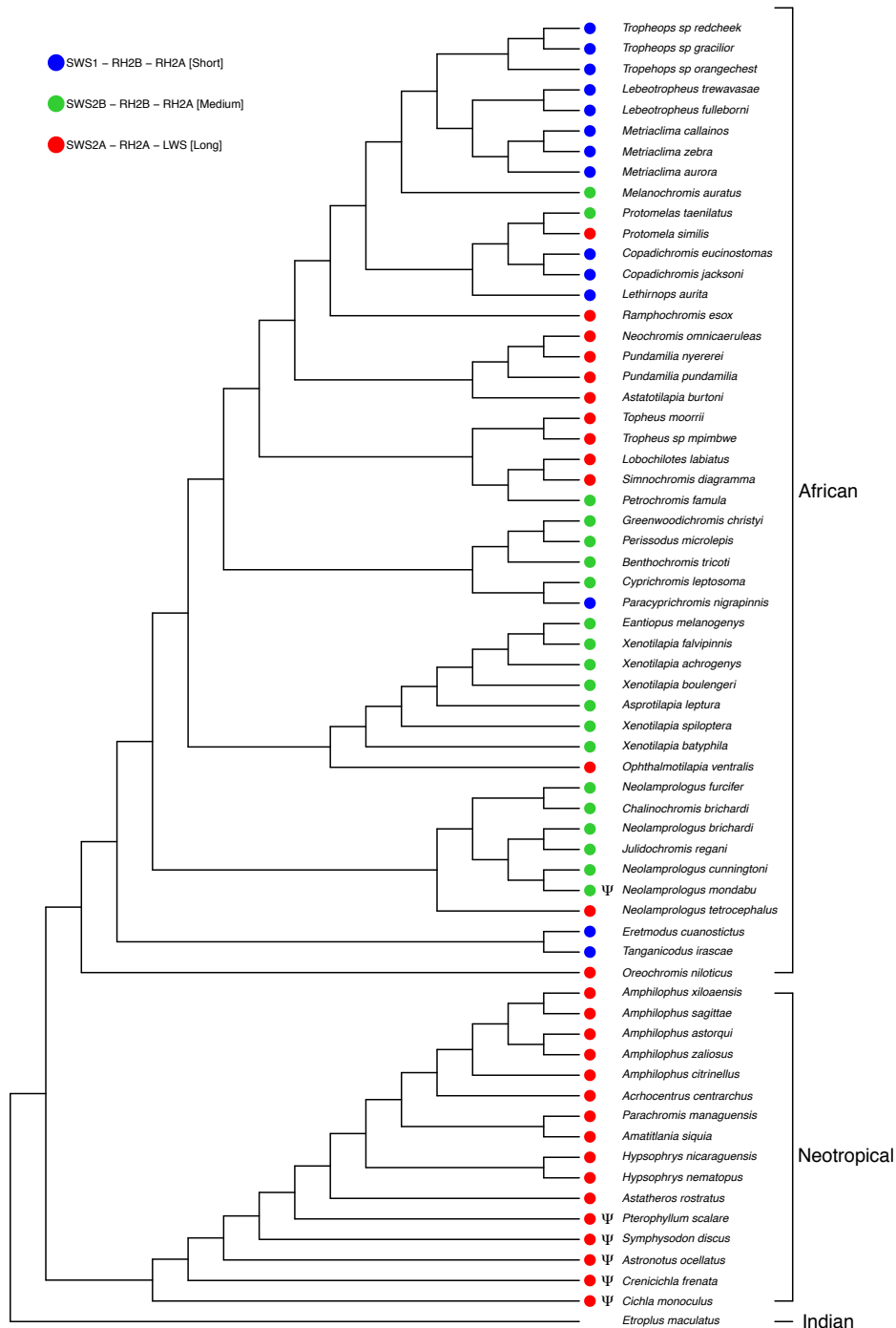


Figure 7.1. Opsin gene expression of Neotropical and African cichlids in a phylogenetic context. Phylogenetic relationships of Neotropical cichlids are based on López-Hernández et al 2010, and of African cichlids based on O’Quin et al 2010. Colored circles indicate the opsin expression palette that the analyzed species use (red-long) SWS2A-RH2A-LWS, (green-medium) SW2B-RH2B-RH2A, (blue-short) SWS21-RH2B-RHA, which is based on opsins that are mainly

expressed [40–42,113,117,273,274]. Notice that Neotropical cichlids do not express the SWS1 opsin at least as adults.

Our opsin expression results are confirmed by MSP studies that show how Neotropical species exhibit long-shifted visual pigments as compared to African cichlids (Fig. 7.2). The spectral sensitivities of the long palette follow the ‘sensitivity hypothesis’ because the λ_{\max} of these visual pigments are the most suitable to the red-shifted light environment of Neotropical rivers (Fig. 7.3). Cichlids express these pigments in order to maximally absorb photons of the available light. Finally, although peak light intensities in water are longer in the wavelength spectrum than the λ_{\max} of fish photoreceptors, these cichlids exhibit some of the longest shifted pigments among fish, which suggests there is a limit in how much sensitivity can be shifted.

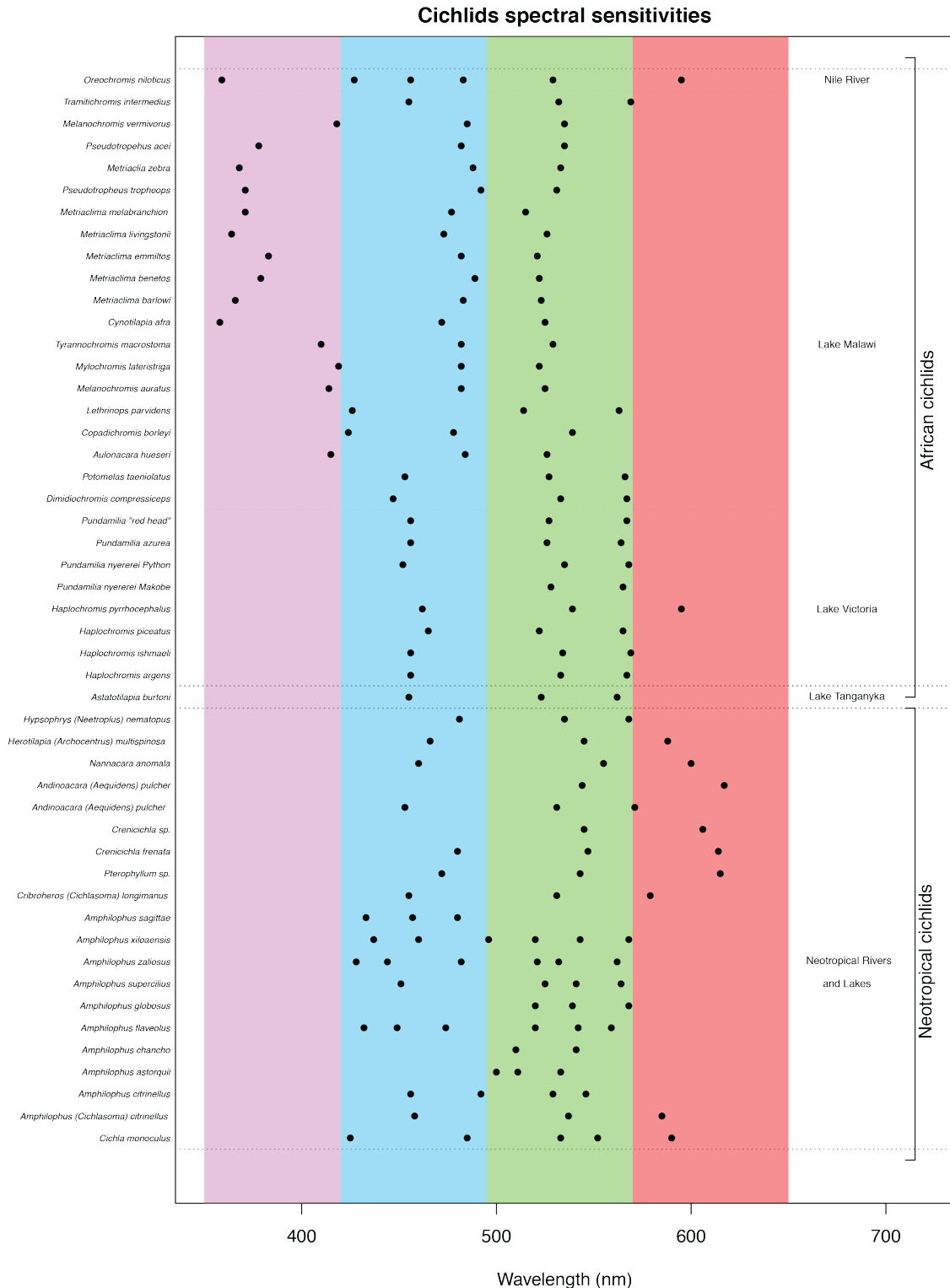


Figure 7.2. Spectral absorbance (λ_{\max}) of visual pigments across Neotropical and African cichlids. Data obtained from [26,28,42,80,117,272,276,277]. Black circles denote the different cones λ_{\max} for each species in the wavelength spectrum. *O. niloticus* MSP is based on protein expression from the seven cone opsin genes in their genome, yet they do not express SWS1 as adults. Notice that UV pigments

are only present in Lake Malawi cichlids, which is the product of the short-palette expression. Cichlids from Lake Tanganyika also express the short palette however there is no MSP data available. Cichlids from Lake Victoria and the Neotropics exhibit a long palette only.

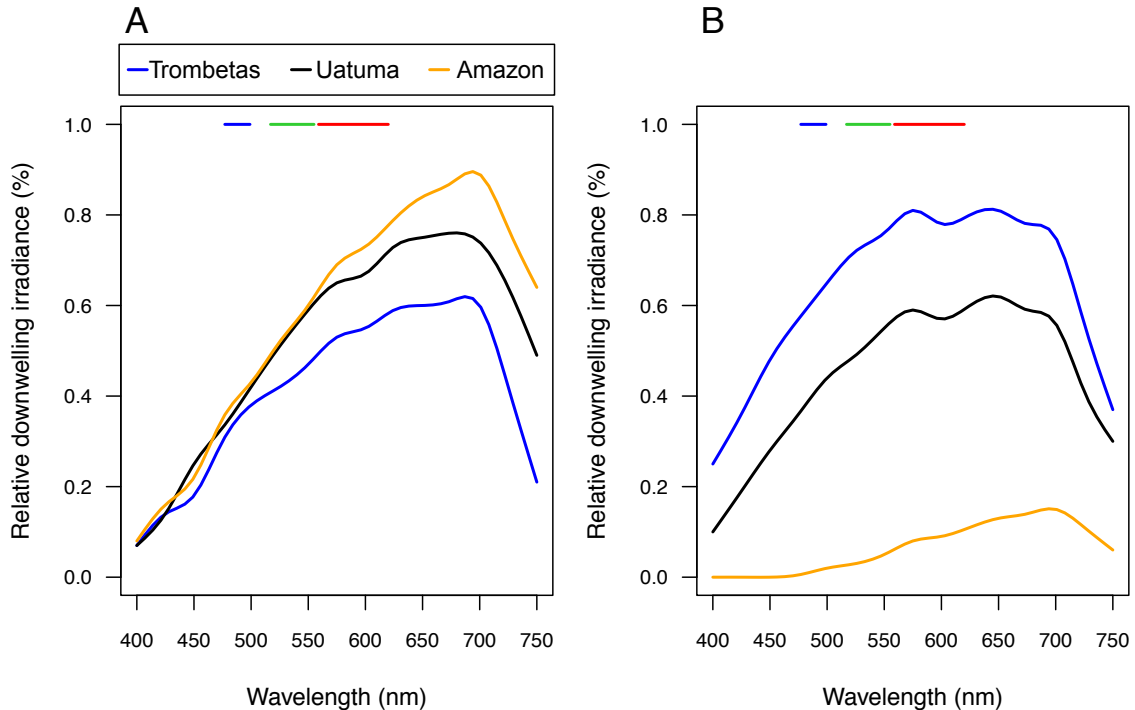


Figure 7.3. Range of the main spectral sensitivities (λ_{\max}) of an Amazonian cichlid, the peacock-bass (*Cichla monoculus*) [272], relative to the downwelling irradiance of incoming light at sub-surface (below 1 m) in Amazonian Rivers. Blue, green and red represent the short (SWS), medium (MWS) and long (LWS) wavelength sensitive pigments respectively (See Chapter 3). Blue, green and red horizontal bars represent the spectral sensitivity range using chromophores A_1 and A_2 . Irradiance lines represent the light environment in Amazonia of white (Amazon, orange), black (Uatumá, black), and clear (Trombetas, blue) water rivers in the receding (A) and rising (B) season. River data replicated from Costa, et al., 2012 [74]. Notice that the cones- λ_{\max} of *C. monoculus* maximizes light absorption of the available wavelengths in Amazonian rivers.

7.4 Visual pigment evolution in Neotropical Characiformes

The Characin opsin gene repertoire is a product of complex evolutionary dynamics characterized by opsin gene loss (SWS1, RH2) and opsin gene duplication (LWS and RH1). These opsin-duplicates are surviving opsin products

of the teleost whole-genome duplication (TGD) and from characins-specific duplication events. Furthermore, characin LWS-duplicates have acquired new functions through amino acid substitution in spectral tuning sites that shift their λ_{\max} increasing green light sensitivity. The LWS-duplicates also exhibit gene conversion, and utilize variable codons in key tuning sites leading to reversion and parallel evolution. In addition, the SWS2- and RH1-opsin exhibit spectral shifts and changes in gene expression respectively. The diverse set of spectral sensitivities found in characins is the result of several spectral tuning mechanisms acting in concert. These are mainly opsin sequence variation, opsin gene loss and duplication, and A₁/A₂ chromophore tuning.

7.5 Fish visual pigment diversity and future directions

By evaluating the opsin gene complement of Neotropical cichlids and characins, we have characterized the different mechanisms that modulate their visual pigment diversity. These are opsin gene duplication, opsin sequence variation, opsin pseudogenization/loss, differential opsin expression, and gene conversion [35,278]. Such mechanisms determine the spectral sensitivities of visual pigments in these groups, which follow the sensitivity hypothesis because their visual systems are long-wavelength shifted (Fig. 7.2-4). Interestingly, Neotropical characins and cichlids reach these spectral sensitivities in parallel but with different main spectral tuning mechanisms. Neotropical cichlids adjust their visual system to the available light by expressing the long palette, a different palette

from their African cousins. In contrast, characins tune their visual pigments through opsin gene duplication and sequence variation.

Furthermore, because red-shifted spectral sensitivities have also been reported in other major groups (Gymnotiformes and Siluriformes) inhabiting Neotropical Rivers (Fig. 7.4), future studies should focus on quantifying the light environment of several neotropical freshwater ecosystems. This would allow us to better examine the relationship between the light environment and visual sensitivities. Since Otophysii (Cypriniformes, Characiformes, Siluriformes, and Gymnotiformes) is the largest freshwater fish radiation [173] and South America harbors the bulk of freshwater fish diversity on Earth [279], future studies should also carry out more extensive sampling across these groups and biogeographic areas. This would allow us to quantitatively examine the different evolutionary patterns that shape visual pigment variation of diverse groups in an unprecedented scale. Finally, by expanding our sampling of fish visual systems, this would increase our knowledge of opsin gene evolution and would shed light on the different adaptive mechanisms that are necessary for seeing in a changing light environment.

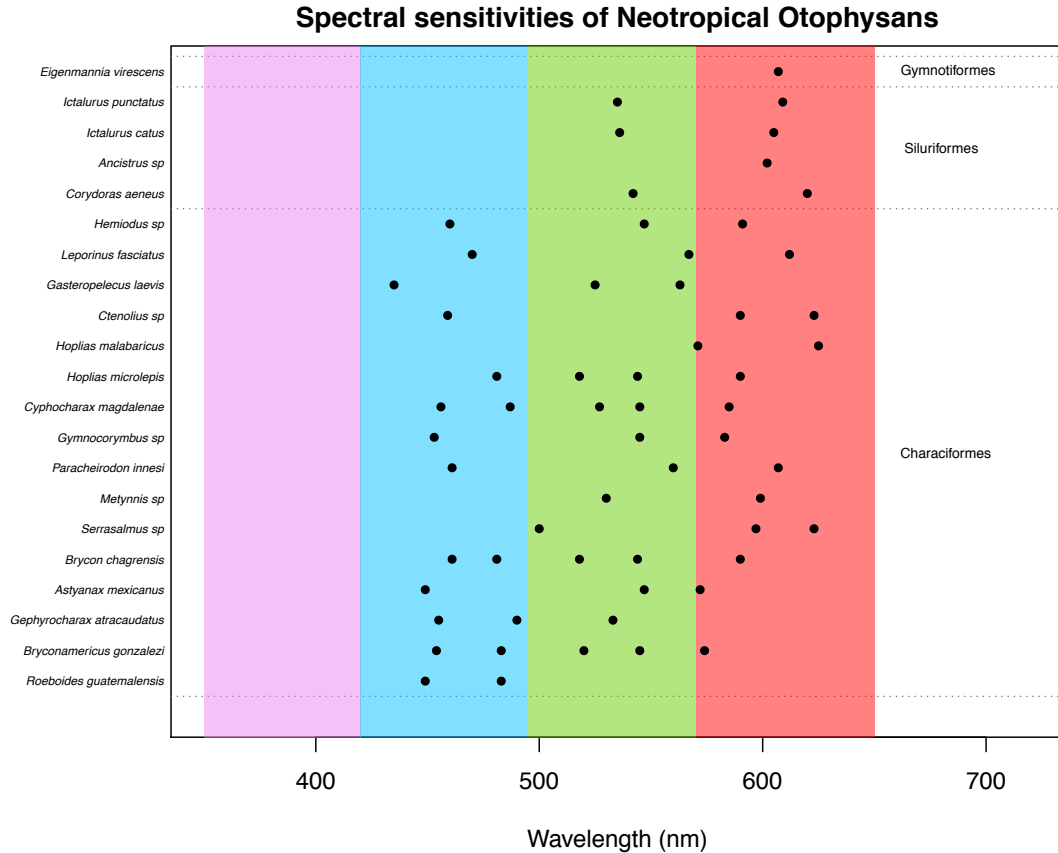


Figure 7.4. Spectral absorbance (λ_{max}) of visual pigments across Neotropical Otophysans. Data obtained from [28,154,165,280] and this study. Black circles denote the different cones λ_{max} for each species in the wavelength spectrum.

7.6 Cichlid behavioral color vision

Through behavioral experiments we have shown that cichlids can be trained using classical conditioning in order to perform color discrimination tasks. Cichlids successfully discriminated a rewarded stimulus from several distracter stimuli that varied in hue and brightness. Our results suggest that cichlid color vision is probably achieved by neural interactions of three different photoreceptor spectral channels. Our experiments also showed that by using the Receptor noise limited (RNL) model we can successfully determine the behavioral color

threshold between different colors, however, this was only possible if we assumed higher receptor noise. Determining the receptor noise is important because we can then make estimates about color vision perception with color data from Lake Malawi. By calculating chromatic distance (ΔS) between blue and other spectral measurements our estimations suggest that for *M. benetos*, there are large ΔS between blue vs. yellow, and between blue vs. spacelight. These results are in agreement with *M. benetos* behavioral ecology because in Lake Malawi females swim above the rocks of male territories with males then swimming up to them to perform their courtship display, trying to lead them back to their territories for mating and spawning [241]. Henceforth, the capacity of discriminating blue vs. spacelight and blue vs. yellow would be necessary in identifying conspecific males and their visual signals. Blues and yellows are the most common nuptial colorations present in Lake Malawi and they have evolved repeatedly within the lake suggesting that these color signals are favored by sexual selection. Altogether, our results demonstrate that cichlids do have color vision and that this capability can have a big impact in understanding the natural history of this speciose clade because coloration patterns have been associated with their adaptive radiation and evolutionary success.

7.7 Cichlid visual palettes and future directions

Until now we have performed behavioral experiments only with *M. benetos*, which is a short palette species. Future studies should focus on reproducing this type of research but on cichlids expressing different visual palettes (Short,

Medium and Long) because this would allow us to examine the visual system dimensionality based on three different sets of visual sensitivities. This would provide invaluable insights about how color vision changes according to different visual systems and its implications in animal behavior.

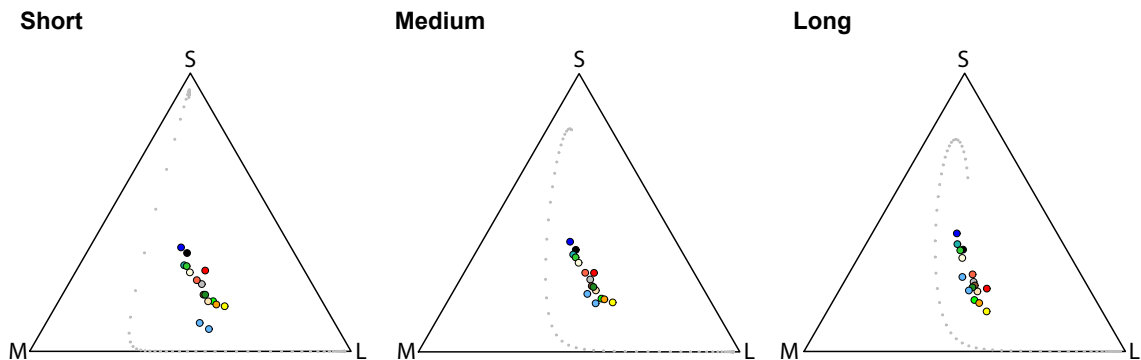


Figure 7.5. Normalized quantum catch of colors from Lake Malawi (Chapter 6) for each visual palette. For a trichromatic visual system, photoreceptor stimulations are plotted in chromaticity diagrams with Malawi colors plotted in the color receptor space of short, medium and long visual palettes. Each axis corresponds to the quantum catches of the short (S), medium (M), and long (L) sensitive photoreceptors. Monochromatic loci at 5 nm intervals are represented by gray dots. These plots are based on pure-opsin expression for each visual palette: short (SWS1, RH2B, RH2A β), medium (SWS2B, RH2B, RH2A β) and long (SWS2A, RH2A β , LWS).

Visual modeling with color data from Lake Malawi shows how colors would be perceived differently for each visual palette. Colors shift in the cichlid visual color-space for each visual palette (Fig. 7.5) due to their different spectral sensitivities. Consequently, ΔS between colors pairs would also be different for each visual palette (Fig. 7.6). For example, using the short palette suggests large ΔS of blue vs. spacelight but when using the long palette ΔS decreases (Fig. 7.6). Conversely, there is high ΔS of blue vs. red when using a long palette yet ΔS

decreases when using the short palette. Therefore, behavioral and visual modeling experiments analyzing ΔS of different color pairs and between visual palettes would allow us to better understand whether cichlids visual palettes are more susceptible to detect specific nuptial coloration patterns, detect objects against the background, or both.

Finally, future studies should also focus on studying the neural circuit of the cichlid retina. This is important because this type of research could elucidate the cone photoreceptor types that ganglion cells are comparing as well as the feedback that bipolar and horizontal cells provide. Morphological and physiological studies are needed in order to better understand how cichlid color opponency takes place.

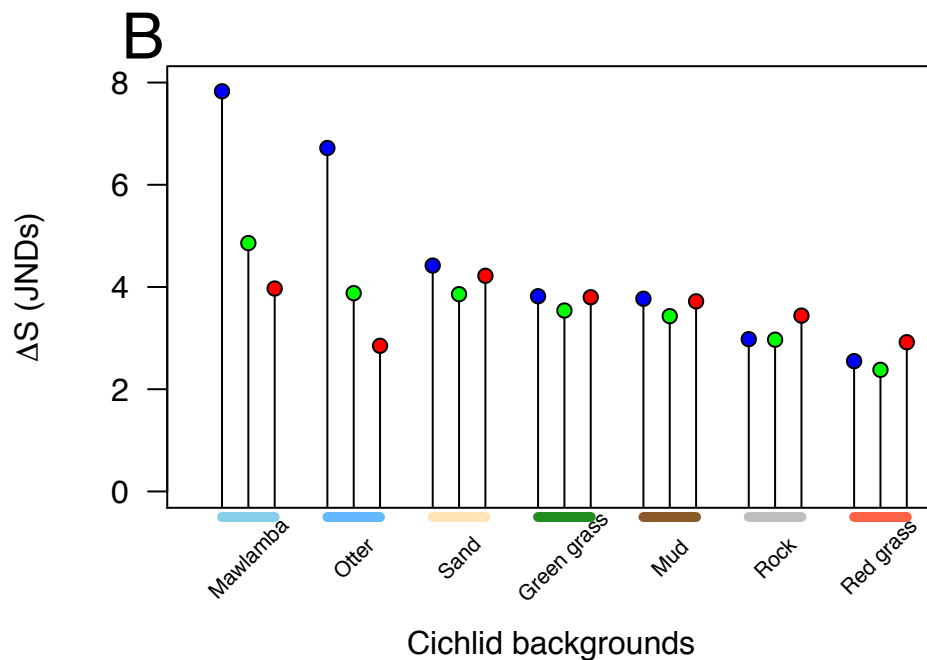
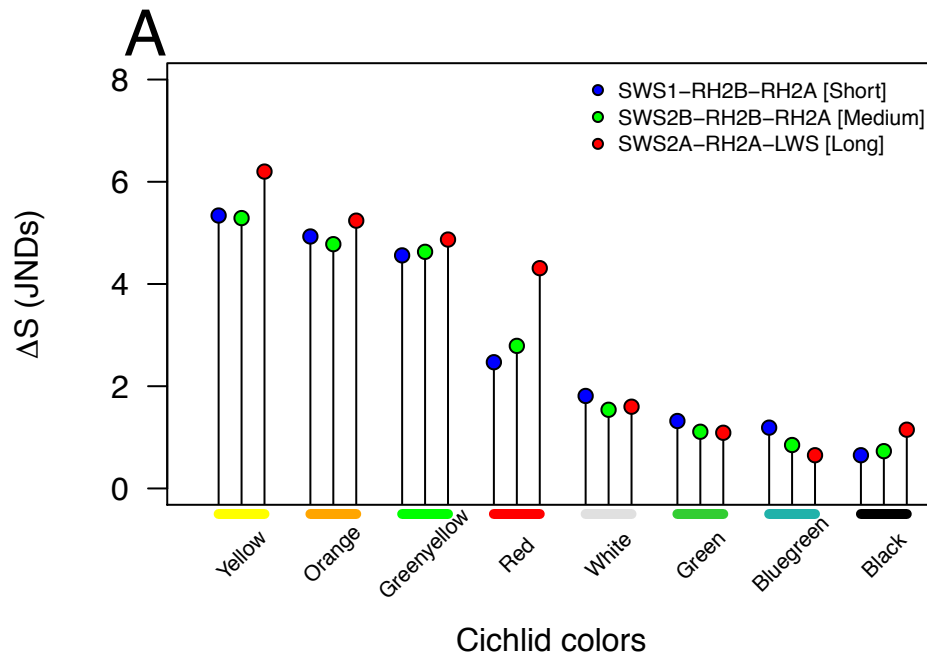


Figure 7.6. Chromatic distances (ΔS) are given of the blue-hue of *M. benetos* vs Lake Malawi colors. (A) ΔS of blue vs. cichlid colors and (B) ΔS of blue vs. Lake Malawi backgrounds. ΔS for each visual palette is specified in colored circles; blue for short, green for medium, and red for long.

Appendix A: Supplementary material Chapter 2

All supplementary files for Chapter 2 are available at
doi: [10.1111/mec.13957](https://doi.org/10.1111/mec.13957)

Appendix B: Supplementary material Chapter 3

All supplementary files for Chapter 3 are available at
doi: [10.1242/jeb.188300](https://doi.org/10.1242/jeb.188300)

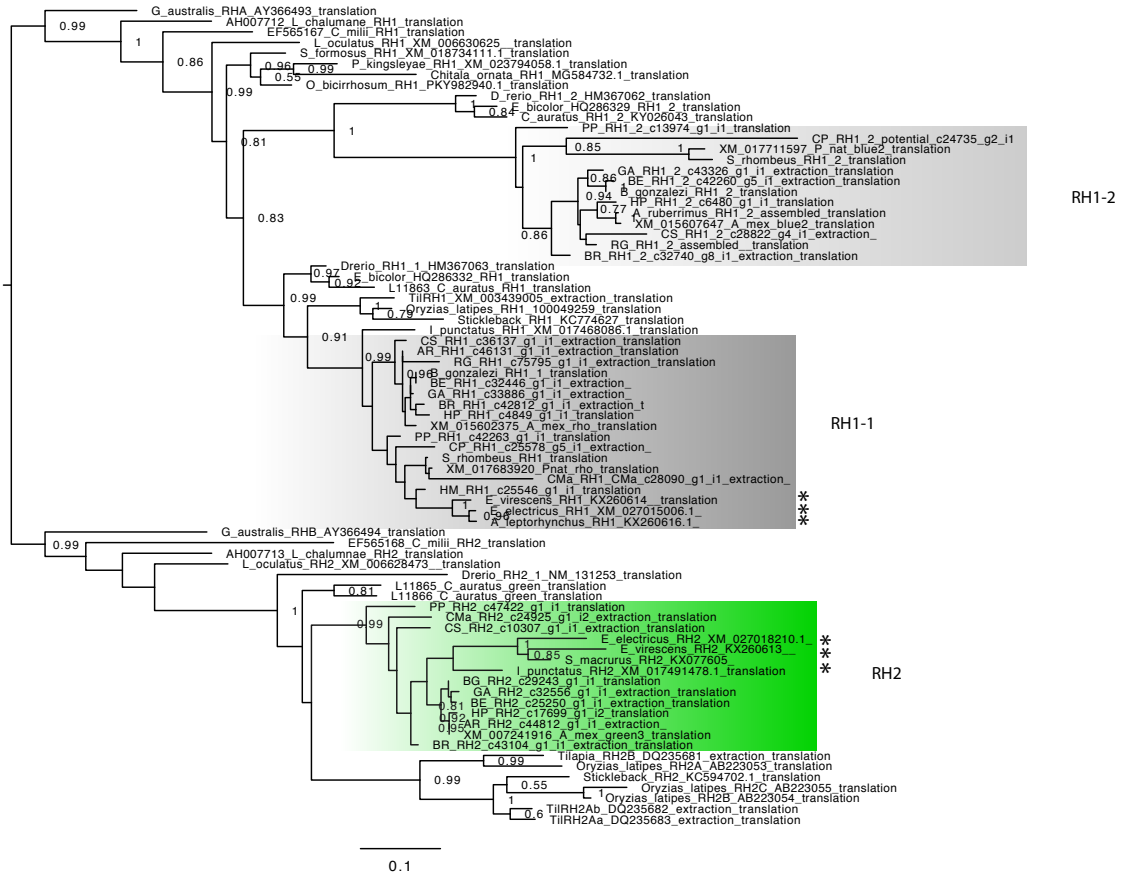


Figure S3. RH1-RH2-opsin tree of Characiformes. RH1-RH2-opsin maximum-likelihood phylogenetic tree based on RH1-RH2-amino-acid sequences of Characiformes, Osteoglossiformes, Siluriformes, Gymnotiformes, Cypriniformes, *Geotria australis* (lamprey), *Latimeria calumnae* (coelacant), *Callorhincus milli* (Elephant shark), *Lepisosteus oculatus* (Spotted gar), *Oryzias latipes* (medaka), *Gasterosteus oculatus* (stickleback). Bootstrap support over 75% is shown. This tree confirms that RH1-2 arose after the divergence of the spotted gar, probably as a product of TGD. Notice the clustering of characins RH1-2-opsins with the cyprinimorphs surviving RH1-2-opsins. Characiformes species clades are shown in different colors (RH1-2-gray, RH1-1, black, and RH2-green). * denotes siluriforms species nested within characins clades.

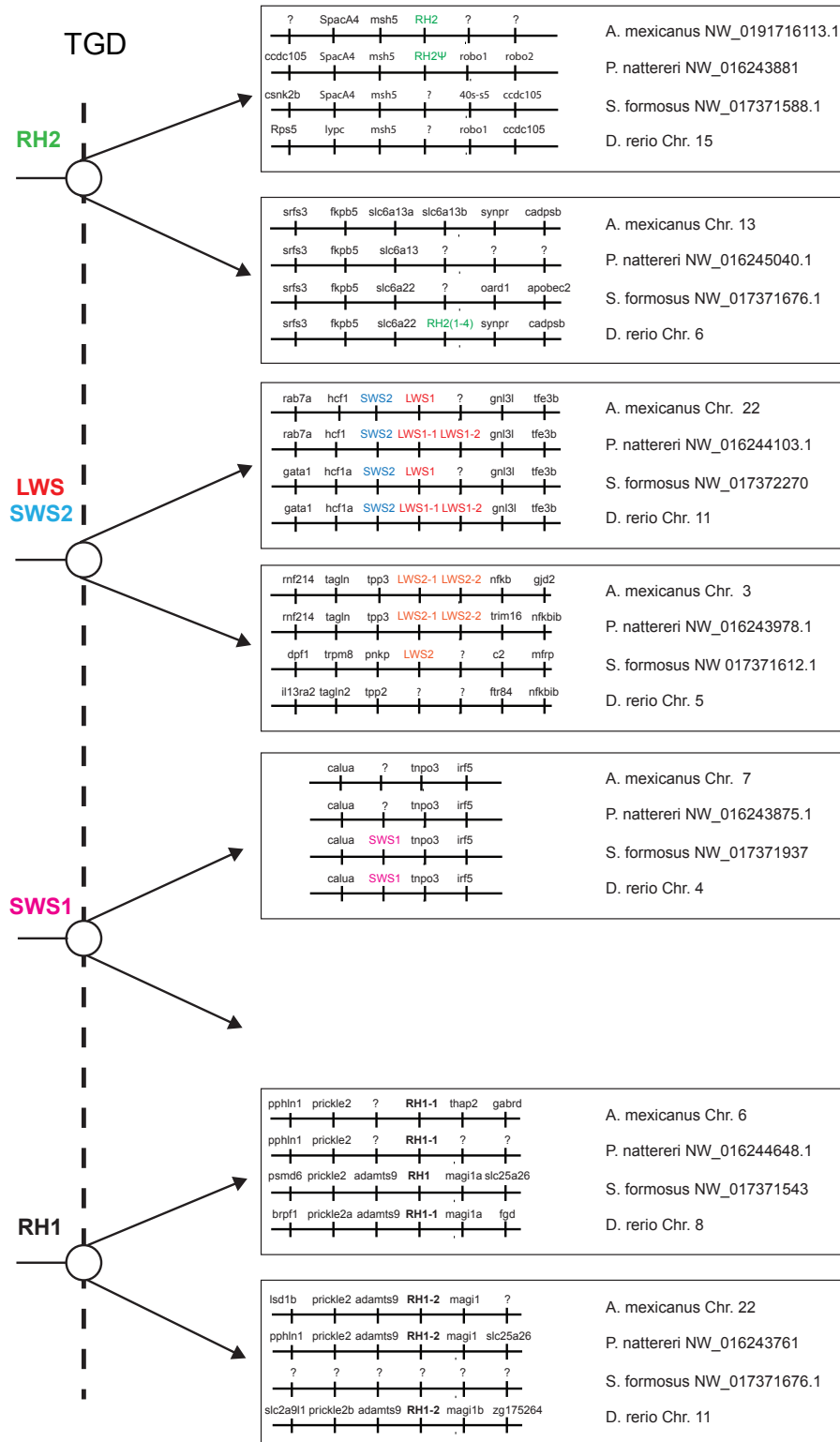


Figure S4. Scenario for opsins duplications produced by TGD based on synteny analysis of putative chromosomal regions surrounding different opsins in *Danio rerio*, *Scleropages formosus*, *Astyanax mexicanus* and *Pygocentrus nattereri*

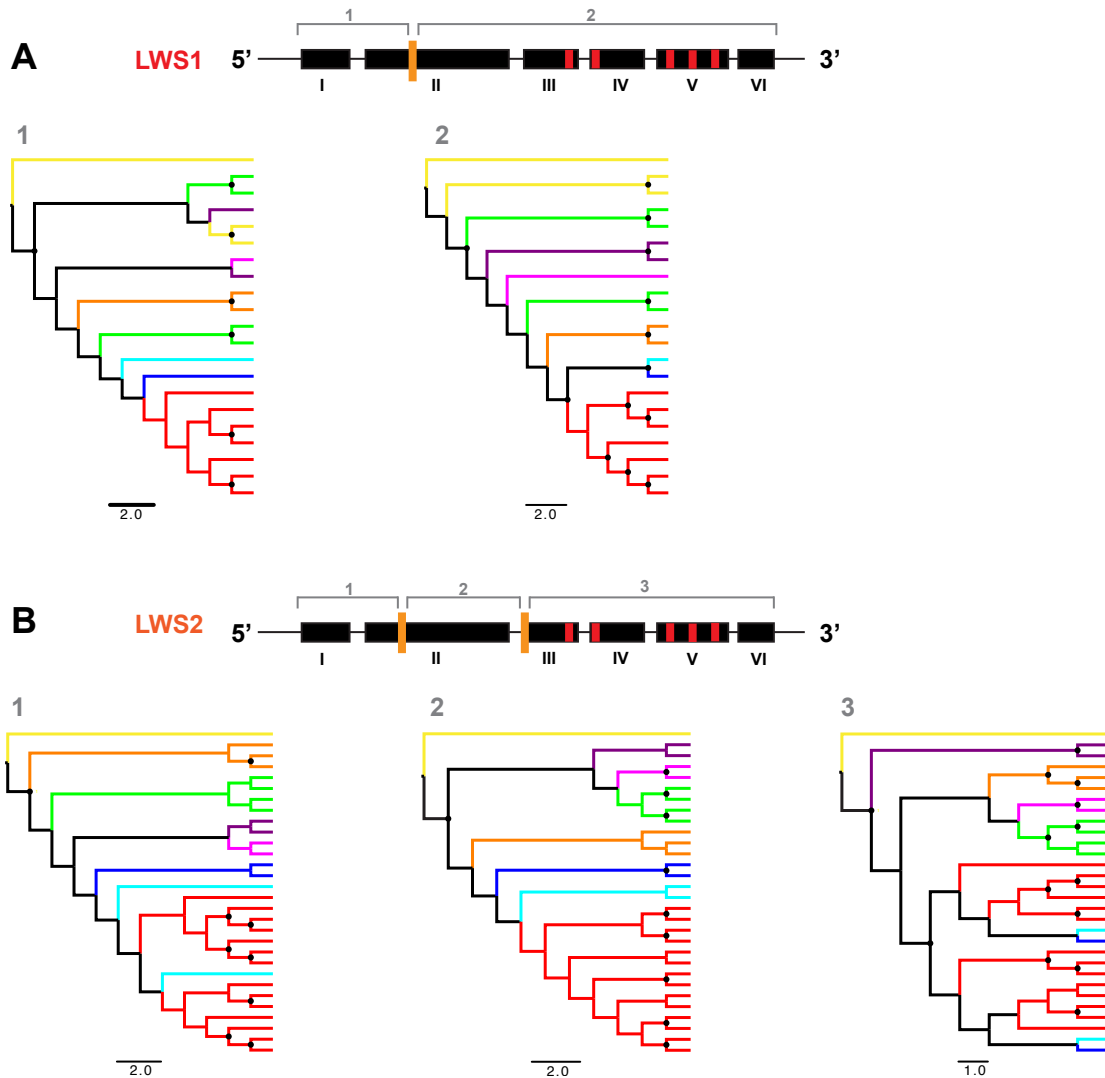


Figure S5. Overview of LWS gene conversion analysis. Schematic representation of exon structure of LWS1 and LWS2 is shown where roman numbers indicate the exon number. Orange vertical bars denote the breakpoints in each LWS opsin and red bars denote the five “key sites” by Yokoyama and Radlwimmer, 2001 [147]. Nucleotide trees based on 15 characin LWS opsins are shown where each family is color coded (Crenuchidae-yellow, Lebiasinidae-orange, Serrasalminidae-green, Erythrinidae-Purple, Curimatidae-violet, Gasteropelecidae-blue, Bryconidae-lightblue, and Characidae-red). Notice how in the tree #3 of the LWS2 it is suggested that Bryconidae, Gasteropelecidae, and Characidae share a LWS2 duplication. For each fragment we used RAXML for building maximum-likelihood trees. We ran 10 searches for the best tree and 1000 bootstrap replicates performed in RAXML 8.0 on CIPRES. A black circle denotes bootstrap support over 75%.

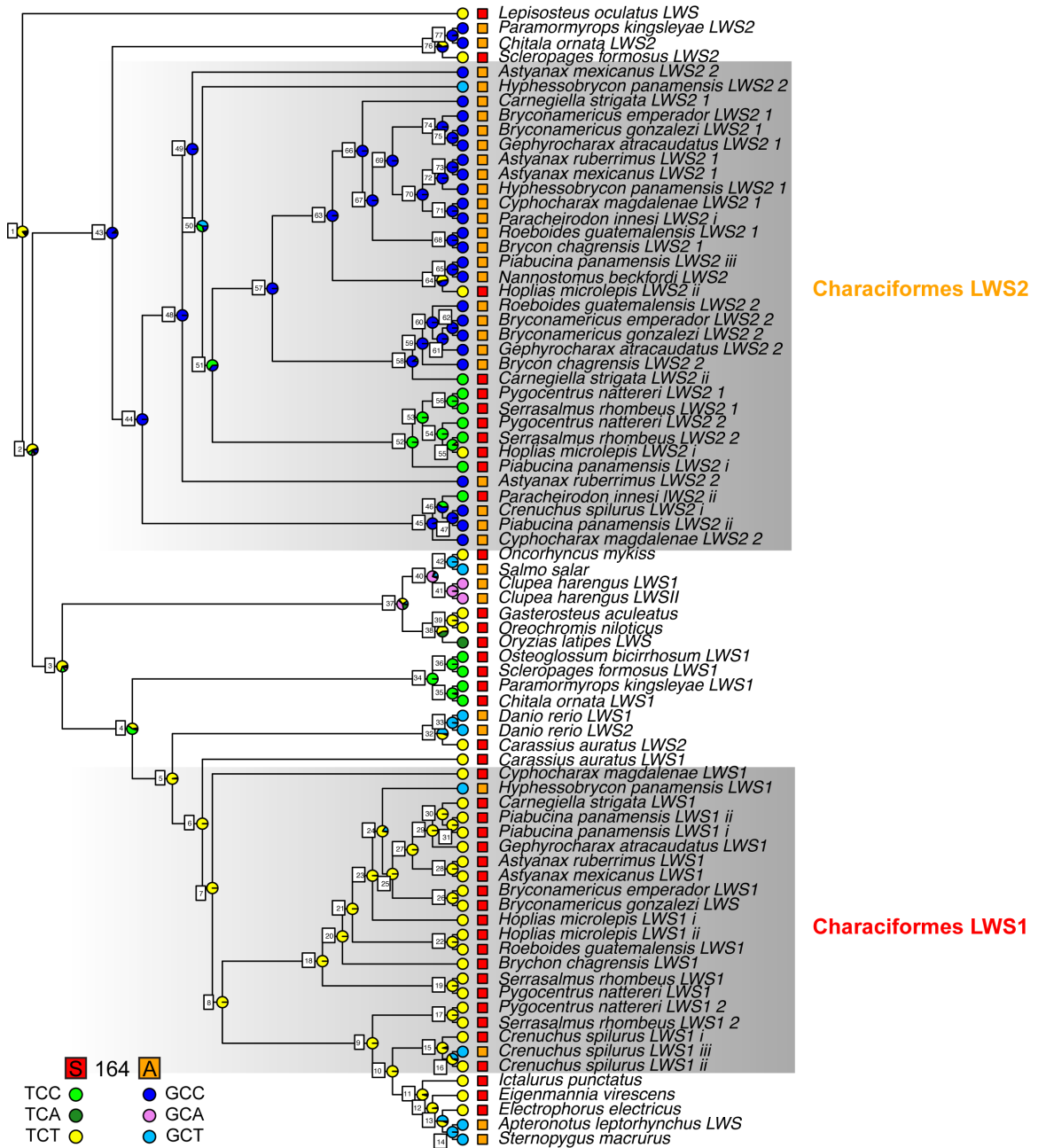


Figure S6. Ancestral state reconstruction results of the spectral tuning site 164. Squares indicate whether the opsin gene sequence has alanine or serine. Codons at site 164 are color coded in colored filled-circles. Pie charts on the nodes indicate the scaled likelihoods, calculated using the ace function in APE, of each specific combination. Nodes are also labeled consistent with Table S4.

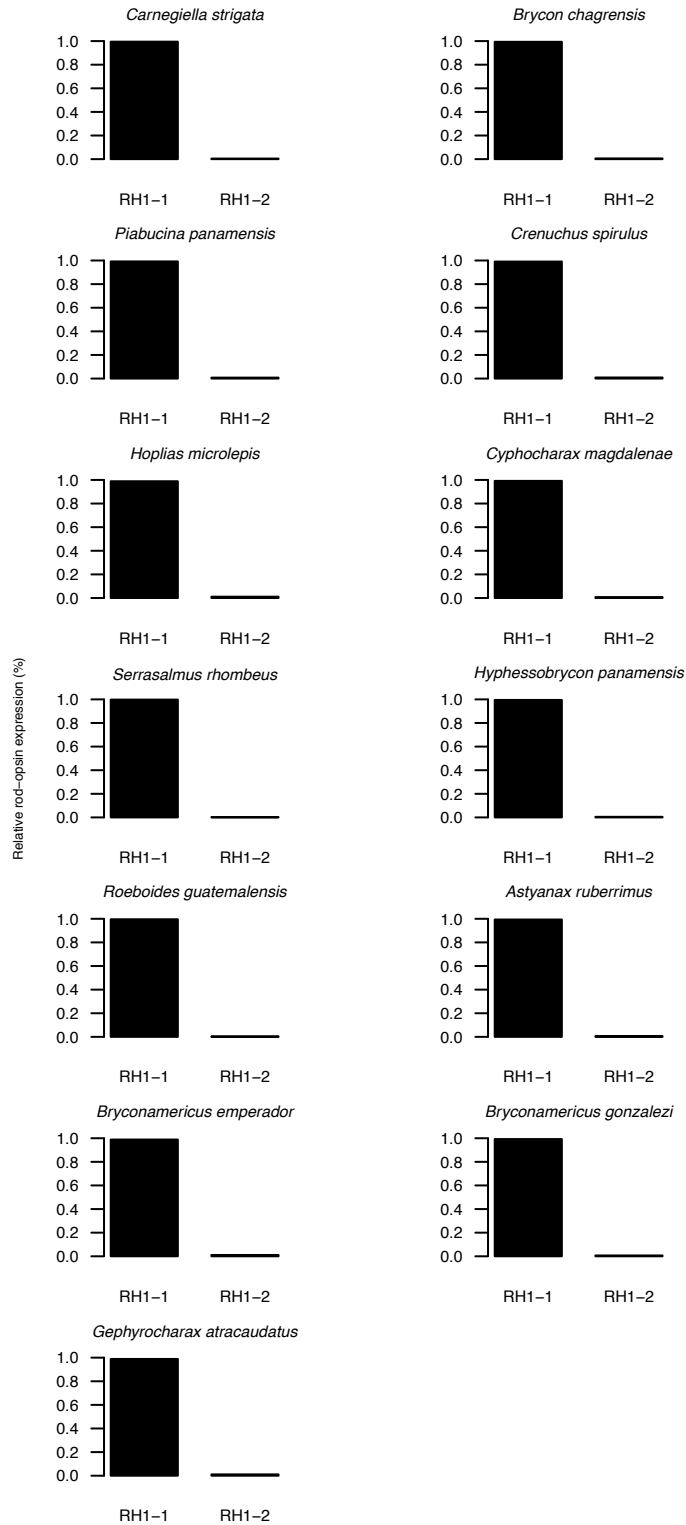


Figure S7. Characiformes rod-opsin expression

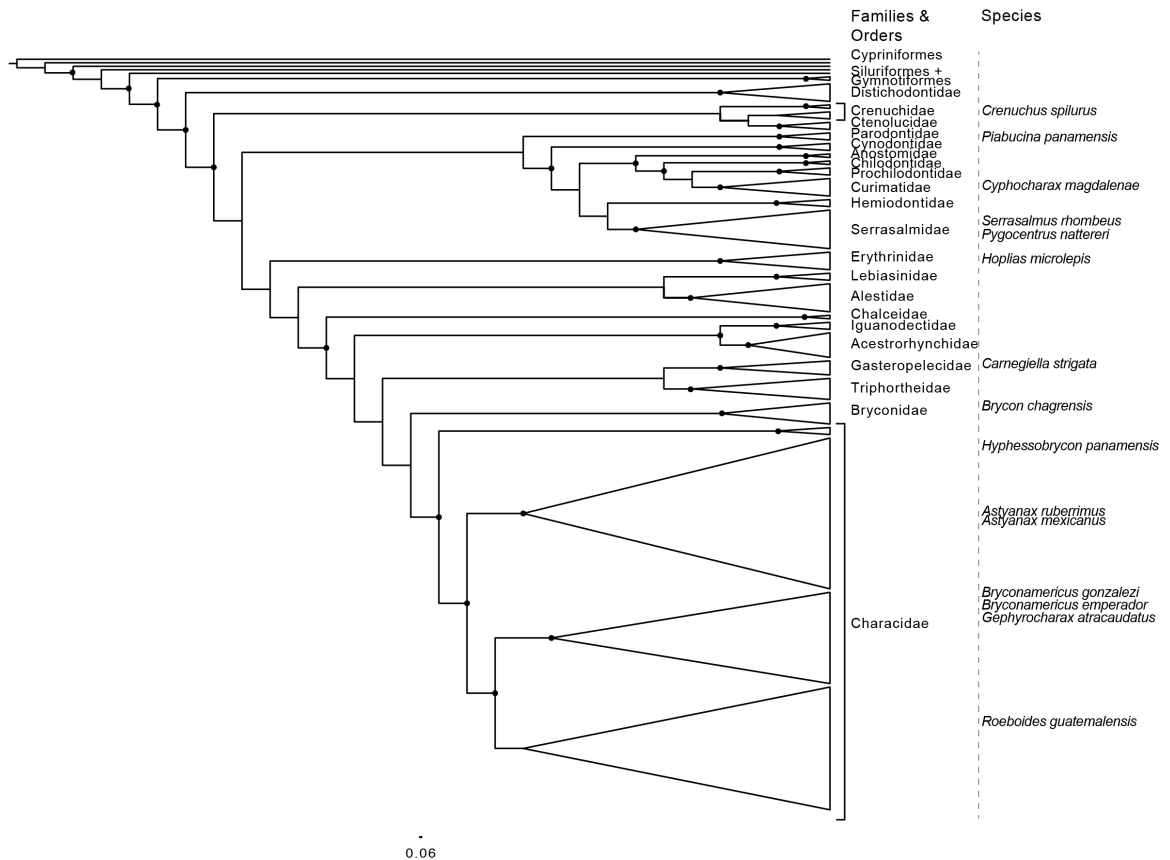


Figure S8. Phylogeny of 228 Characiformes based on genomic sequences. Species sampled in Panama and Suriname are included. Filled circles denote bootstrap support over 75%.

Supplementary Tables

Table S1. Sampling

Species	Family	Locality	Province	Coordinates (Lat/Lon)
<i>Bryconamericus gonzalezi</i>	Characidae	Quebrada Gavilán	Bocas del Toro	9.272083, 82.509444
<i>Roebooides guatemalensis</i>	Characidae	Rio Juan Grande	Colon	9.136361, -79.723576
<i>Piabucina panamensis</i>	Lebiasinidae	Rio Juan Grande	Colon	9.136361, -79.723580
<i>Gephyrocarax atricaudata</i>	Characidae	Rio Juan Grande	Colon	9.136361, -79.723581
<i>Hyphessobrycon panamensis</i>	Characidae	Rio Juan Grande	Colon	9.136361, -79.723587
<i>Bryconamericus emperador</i>	Characidae	Rio Juan Grande	Colon	9.136361, -79.723594
<i>Astyanax ruberrimus</i>	Characidae	Rio Juan Grande	Colon	9.136361, -79.723598
<i>Hoplias microlepis</i>	Erythrinidae	Gamboa Dock	Colon	9.113547, -79.691149
<i>Brycon chagrensis</i>	Bryconidae	Isla de los Monos	Colon	9.119149, -79.779212
<i>Cyphocharax magdalenae</i>	Curimatidae	Los Canelos	Veraguas	8.09508, 80.64141
<i>Carnegiella strigata</i> *	Gasteropelecidae	Coropina creek, Berlijn	Para	5.397194, 55.184306
<i>Serrasalmus rhombeus</i> *	Serrasalminidae	Van-Blommenstein Lake	Brokopondo	4.960222, 54.982444
<i>Crenuchus spilurus</i> *	Crenuchidae	Coropina creek, Berlijn	Para	5.397194, 55.184306

* Denotes samples collected in Suriname where only two transcriptomes per species were performed

Table S2. Evolutionary models

Opsin	Model	Data
SWS	LG+I+G+F	AA
RH2-RH1	LG+G+F	AA
LWS	LG+I+G	AA
Multilocus phylogeny*	GTR+I+G	DNA

* GTR+I+G was used for each partition for every codon position.

Table S3. Combinations of the occurrence of tuning sites

Combination	Tuning sites		
	A164S	F261Y	A269T
1	A	F	A
2	S	Y	T
3	A	Y	A
4	A	Y	T
5	S	F	A
6	S	Y	A
7	A	F	T

Table S4. Recombination points obtained from GARD

LWS1		
Breakpoint 1	Breakpoint 2	
1- 251	252-1074	

LWS2		
Breakpoint 1	Breakpoint 2	Breakpoint 3
1-209	210-404	405-1065

Table S5. Likelihoods of ancestral state reconstruction for LWS2 amino-acid combinations

Nodes	Combinations						
	1(Blue)	2(Yellow)	3(Purple)	4(Pink)	5(Cyan)	6(Green)	7(Magenta)
1	94.155	2.219	0.731	0.671	0.881	0.671	0.671
2	73.564	13.230	2.686	2.259	3.743	2.259	2.259
3	97.450	0.087	0.087	0.087	2.113	0.088	0.087
4	99.700	0.047	0.047	0.047	0.060	0.051	0.047
5	98.735	0.056	0.056	0.056	0.789	0.253	0.056
6	99.746	0.042	0.042	0.042	0.042	0.042	0.042
7	99.809	0.032	0.032	0.032	0.032	0.032	0.032
8	99.950	0.008	0.008	0.008	0.008	0.008	0.008
9	99.746	0.042	0.042	0.042	0.042	0.044	0.042
10	99.489	0.070	0.070	0.070	0.075	0.154	0.070
11	96.510	0.542	0.542	0.542	0.779	0.542	0.542
12	97.775	0.070	0.070	0.070	1.877	0.070	0.070
13	44.620	0.986	0.986	0.986	50.451	0.986	0.986
14	0.060	0.060	0.060	0.060	99.637	0.060	0.060
15	95.896	0.288	0.288	0.288	0.288	2.662	0.288
16	60.843	0.966	0.966	0.966	0.966	34.327	0.966
17	99.927	0.012	0.012	0.012	0.012	0.012	0.012
18	99.999	0.000	0.000	0.000	0.000	0.000	0.000
19	99.945	0.009	0.009	0.009	0.009	0.009	0.009
20	99.938	0.010	0.010	0.010	0.010	0.010	0.010
21	99.953	0.006	0.006	0.006	0.016	0.006	0.006
22	99.631	0.062	0.062	0.062	0.062	0.062	0.062
23	99.316	0.036	0.036	0.036	0.505	0.036	0.036
24	81.896	0.489	0.489	0.489	15.658	0.489	0.489
25	99.994	0.001	0.001	0.001	0.001	0.001	0.001
26	100.000	0.000	0.000	0.000	0.000	0.000	0.000
27	99.917	0.014	0.014	0.014	0.014	0.014	0.014
28	100.000	0.000	0.000	0.000	0.000	0.000	0.000
29	99.992	0.001	0.001	0.001	0.001	0.001	0.001
30	99.778	0.037	0.037	0.037	0.037	0.037	0.037
31	99.754	0.041	0.041	0.041	0.041	0.041	0.041
32	58.954	1.214	1.214	1.214	27.831	8.360	1.214
33	1.541	1.541	1.541	1.541	71.870	20.424	1.541
34	99.459	0.090	0.090	0.090	0.090	0.090	0.090
35	96.753	0.541	0.541	0.541	0.541	0.541	0.541
36	99.944	0.009	0.009	0.009	0.009	0.009	0.009
37	35.894	1.410	1.410	1.410	57.056	1.410	1.410
38	99.898	0.017	0.017	0.017	0.017	0.017	0.017
39	99.052	0.158	0.158	0.158	0.158	0.158	0.158
40	0.285	0.285	0.285	0.285	98.288	0.285	0.285
41	0.272	0.272	0.272	0.272	98.368	0.272	0.272
42	0.003	0.000	0.000	0.000	99.997	0.000	0.000
43	0.438	93.743	4.065	0.439	0.438	0.438	0.438
44	0.002	99.985	0.002	0.007	0.002	0.002	0.002
45	0.062	97.261	0.062	2.428	0.062	0.062	0.062
46	0.673	58.987	0.673	37.647	0.673	0.673	0.673
47	0.073	99.559	0.073	0.073	0.073	0.073	0.073
48	0.000	100.000	0.000	0.000	0.000	0.000	0.000
49	0.000	100.000	0.000	0.000	0.000	0.000	0.000
50	0.018	99.140	0.111	0.567	0.018	0.018	0.128
51	0.538	55.862	5.574	30.435	0.538	0.538	6.515
52	0.872	0.872	13.671	66.775	0.872	0.872	16.065
53	0.216	0.216	16.233	82.689	0.216	0.216	0.216
54	0.000	0.000	100.000	0.000	0.000	0.000	0.000
55	0.022	0.022	99.867	0.022	0.022	0.022	0.022
56	0.006	0.006	0.006	99.963	0.006	0.006	0.006
57	0.010	99.796	0.010	0.155	0.010	0.010	0.010

58	0.196	90.904	0.196	8.117	0.196	0.196	0.196
59	0.004	99.978	0.004	0.004	0.004	0.004	0.004
60	0.000	100.000	0.000	0.000	0.000	0.000	0.000
61	0.002	99.985	0.002	0.002	0.002	0.002	0.002
62	0.000	100.000	0.000	0.000	0.000	0.000	0.000
63	0.038	98.958	0.038	0.852	0.038	0.038	0.038
64	1.588	40.224	1.588	51.834	1.588	1.588	1.588
65	0.035	99.792	0.035	0.035	0.035	0.035	0.035
66	0.007	99.960	0.007	0.007	0.007	0.007	0.007
67	0.004	99.974	0.004	0.004	0.004	0.004	0.004
68	0.023	99.862	0.023	0.023	0.023	0.023	0.023
69	0.005	99.970	0.005	0.005	0.005	0.005	0.005
70	0.007	99.956	0.007	0.007	0.007	0.007	0.007
71	0.042	99.746	0.042	0.042	0.042	0.042	0.042
72	0.005	99.971	0.005	0.005	0.005	0.005	0.005
73	0.000	100.000	0.000	0.000	0.000	0.000	0.000
74	0.007	99.957	0.007	0.007	0.007	0.007	0.007
75	0.000	100.000	0.000	0.000	0.000	0.000	0.000
76	2.276	50.863	37.758	2.276	2.276	2.276	2.276
77	0.317	98.100	0.317	0.317	0.317	0.317	0.317

Table S6. Likelihoods of ancestral state reconstruction for the amino-acid site S164A

Node	Codon					
	1 (GCT)	2 (TCT)	3 (TCC)	4 (GCA)	5 (TCA)	6 (GCC)
1	2.11262	83.90329	4.24989	3.07771	2.38049	4.27600
2	4.73160	54.12430	13.31282	8.60650	5.80710	13.41768
3	2.75465	67.22043	15.94346	8.71049	4.40773	0.96324
4	2.43090	37.06928	55.94196	1.51929	1.51929	1.51929
5	2.61471	96.84637	0.13473	0.13473	0.13473	0.13473
6	0.09339	99.53306	0.09339	0.09339	0.09339	0.09339
7	0.06989	99.65058	0.06988	0.06988	0.06988	0.06988
8	0.01879	99.90644	0.01869	0.01869	0.01869	0.01869
9	0.10197	99.51720	0.09521	0.09521	0.09521	0.09521
10	0.41072	98.84858	0.18517	0.18517	0.18517	0.18517
11	1.68349	93.51384	1.20067	1.20067	1.20067	1.20067
12	2.70069	96.70133	0.14950	0.14950	0.14950	0.14950
13	49.59636	44.56774	1.45898	1.45898	1.45898	1.45898
14	99.33753	0.13249	0.13249	0.13249	0.13249	0.13249
15	3.93150	93.59238	0.61903	0.61903	0.61903	0.61903
16	33.93239	60.39669	1.41773	1.41773	1.41773	1.41773
17	0.02666	99.86670	0.02666	0.02666	0.02666	0.02666
18	0.00036	99.99825	0.00035	0.00035	0.00035	0.00035
19	0.01995	99.90026	0.01995	0.01995	0.01995	0.01995
20	0.02314	99.88669	0.02254	0.02254	0.02254	0.02254
21	0.03592	99.90613	0.01449	0.01449	0.01449	0.01449
22	0.13499	99.32504	0.13499	0.13499	0.13499	0.13499
23	0.75202	98.93517	0.07820	0.07820	0.07820	0.07820
24	15.48279	81.64149	0.71893	0.71893	0.71893	0.71893
25	0.00236	99.98822	0.00236	0.00236	0.00236	0.00236
26	0.00000	100.00000	0.00000	0.00000	0.00000	0.00000
27	0.03032	99.84841	0.03032	0.03032	0.03032	0.03032
28	0.00000	100.00000	0.00000	0.00000	0.00000	0.00000
29	0.00327	99.98367	0.00327	0.00327	0.00327	0.00327
30	0.08158	99.59211	0.08158	0.08158	0.08158	0.08158
31	0.09025	99.54875	0.09025	0.09025	0.09025	0.09025
32	49.10495	45.36182	1.38331	1.38331	1.38331	1.38331
33	98.23178	0.35364	0.35364	0.35364	0.35364	0.35364
34	0.21781	0.21781	98.91097	0.21781	0.21781	0.21781
35	1.18453	1.18453	94.07734	1.18453	1.18453	1.18453
36	0.02060	0.02060	99.89701	0.02060	0.02060	0.02060
37	8.74315	26.73696	3.01433	39.33044	19.16079	3.01433
38	0.94837	57.06267	0.94837	0.94837	39.14385	0.94837
39	0.34851	98.25744	0.34851	0.34851	0.34851	0.34851
40	14.12021	2.71176	2.71147	75.03362	2.71147	2.71147
41	0.59931	0.59931	0.59931	97.00347	0.59931	0.59931
42	99.99688	0.00269	0.00011	0.00011	0.00011	0.00011
43	0.96260	6.11003	0.96385	0.96260	0.96260	90.03833
44	0.00354	0.00354	0.01589	0.00354	0.00354	99.96996
45	0.13825	0.13825	3.67758	0.13825	0.13825	95.76940
46	1.00809	1.00809	38.10212	1.00809	1.00809	57.86553
47	0.16141	0.16141	0.16141	0.16141	0.16141	99.19296
48	0.00000	0.00000	0.00000	0.00000	0.00000	100.00000
49	0.00022	0.00001	0.00019	0.00001	0.00001	99.99957
50	42.17821	0.65379	36.00700	0.64936	0.64936	19.86228
51	0.49497	0.50283	63.35818	0.49497	0.49497	34.65409
52	0.10403	0.10403	99.47985	0.10403	0.10403	0.10403
53	0.00761	0.00761	99.96193	0.00761	0.00761	0.00761
54	0.00000	0.00001	99.99999	0.00000	0.00000	0.00000
55	0.59901	8.19844	89.40554	0.59901	0.59901	0.59901
56	0.01340	0.01340	99.93299	0.01340	0.01340	0.01340

57	0.02205	0.04502	0.11818	0.02205	0.02205	99.77064
58	0.28989	0.28989	8.10116	0.28989	0.28989	90.73929
59	0.00799	0.00799	0.00799	0.00799	0.00799	99.96004
60	0.00000	0.00000	0.00000	0.00000	0.00000	99.99999
61	0.00534	0.00534	0.00534	0.00534	0.00534	99.97328
62	0.00000	0.00000	0.00000	0.00000	0.00000	100.00000
63	0.08302	1.26181	0.08302	0.08302	0.08302	98.40613
64	2.33239	51.22574	2.33239	2.33239	2.33239	39.44468
65	0.07569	0.07569	0.07569	0.07569	0.07569	99.62157
66	0.01460	0.01460	0.01460	0.01460	0.01460	99.92700
67	0.00969	0.00969	0.00969	0.00969	0.00969	99.95157
68	0.05029	0.05029	0.05029	0.05029	0.05029	99.74854
69	0.01089	0.01089	0.01089	0.01089	0.01089	99.94557
70	0.01658	0.01658	0.01658	0.01658	0.01658	99.91712
71	0.09280	0.09280	0.09280	0.09280	0.09280	99.53601
72	0.01062	0.01062	0.01062	0.01062	0.01062	99.94691
73	0.00000	0.00000	0.00000	0.00000	0.00000	100.00000
74	0.01570	0.01570	0.01570	0.01570	0.01570	99.92151
75	0.00000	0.00000	0.00000	0.00000	0.00000	99.99999
76	3.39975	37.67494	3.39975	3.39975	3.39975	48.72606
77	0.69751	0.69751	0.69751	0.69751	0.69751	96.51246

Appendix D: Supplementary material Chapter 5

All supplementary files for Chapter 5 are available at
doi: [10.1242/jeb.160473](https://doi.org/10.1242/jeb.160473)

Appendix E: Supplementary material Chapter 6

Supplementary Figures

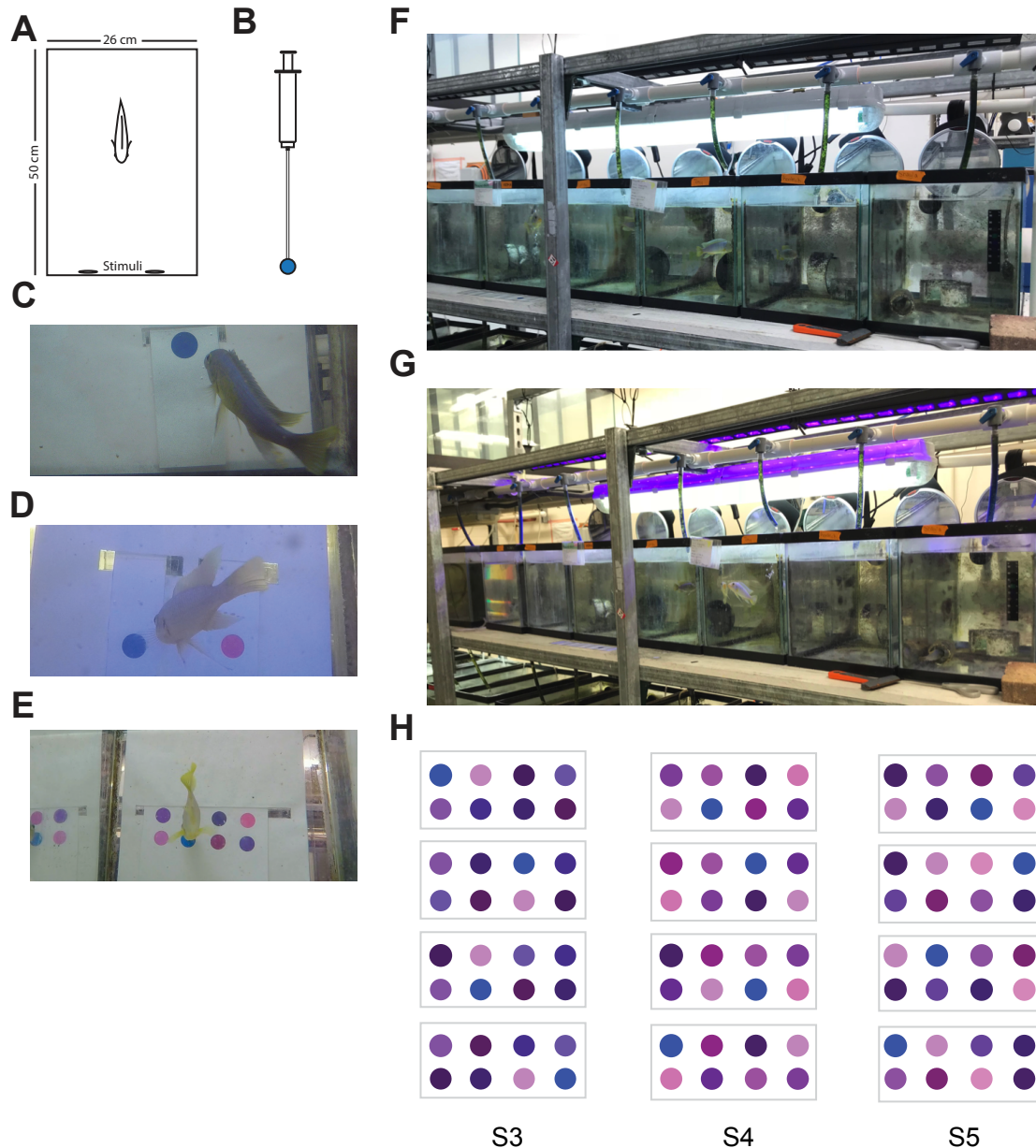


Figure S1. Training and testing set up, modified from Escobar-Camacho et al., 2017. (A) Household tanks. (B) Feeding apparatus for training. (C) Photograph of fish during training displaying a color card with the blue rewarded stimulus. (D) Photograph during a binary (two-alternative) choice test, experiment 1 and 3. (E) Photograph of a fish during testing, experiment 2. (F-G) Lighting set up with fluorescent lights (F) and violet lights (G). (H) Multiple choice color cards used in Experiment 2.

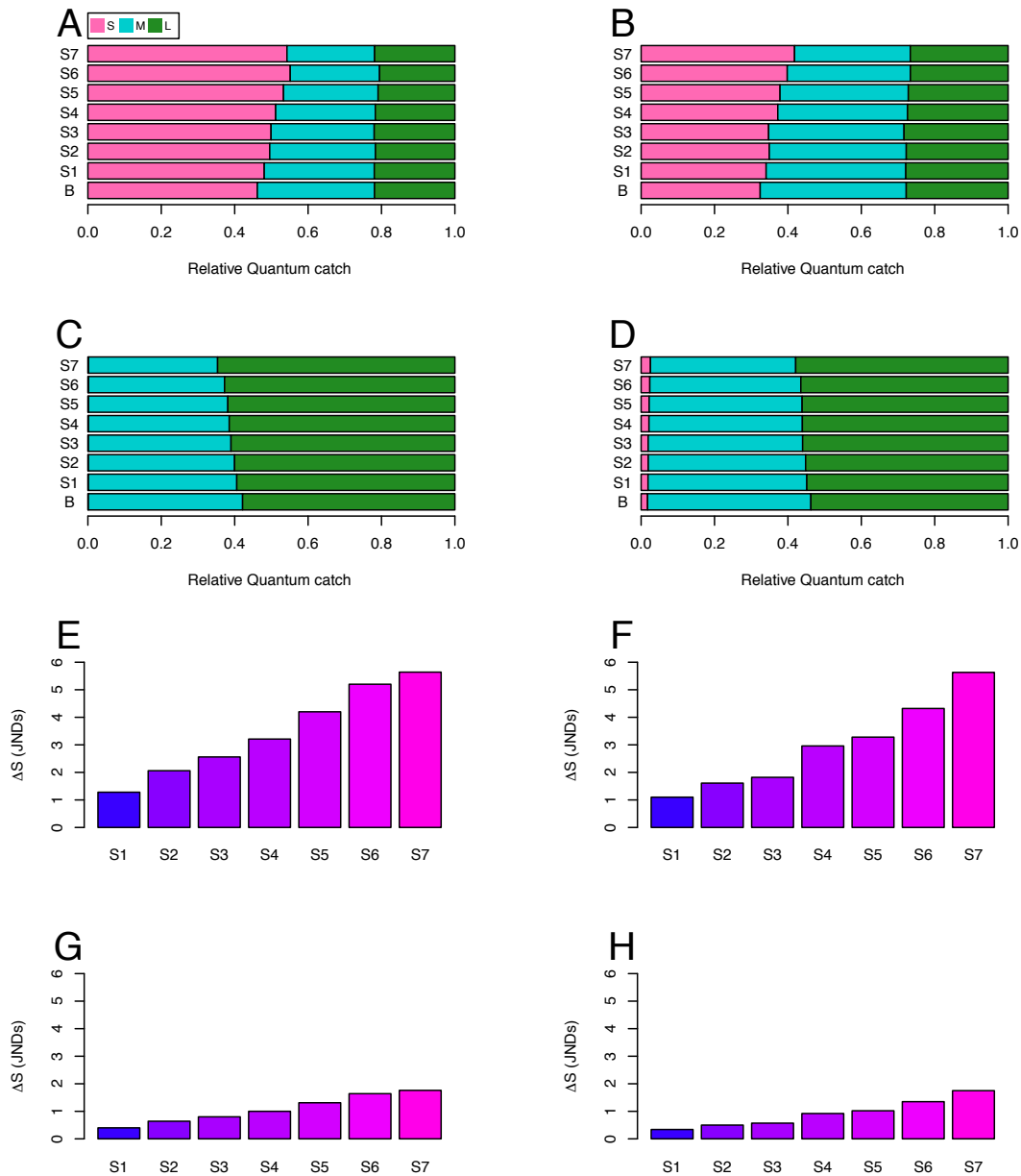


Figure S2. Normalized quantum catches of color stimuli calculated with (A & B) and without (C & D) the von Kries correction. (A & C) were calculated with fluorescent light whereas (B & D) with violet light. (E - H) is ΔS of distracter stimuli calculated with a standard deviation noise value (ν) for the LWS channel of 0.05 (E & F) and 0.16 (G & H). (E & G) were calculated with fluorescent light whereas (F & H) with violet light.

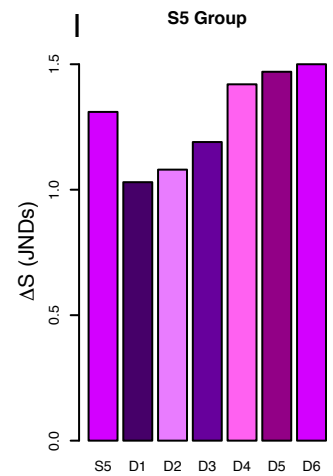
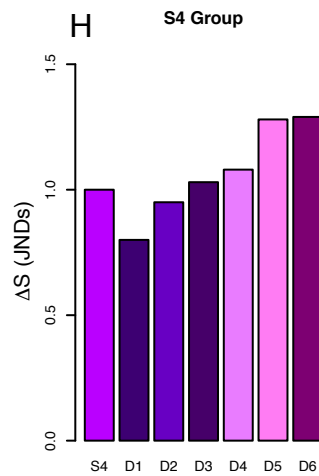
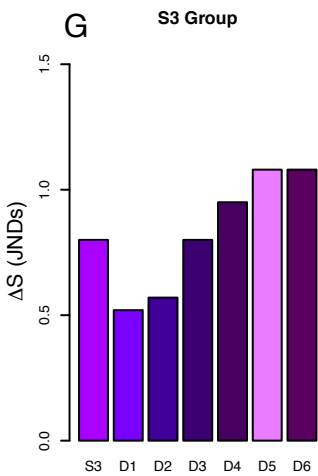
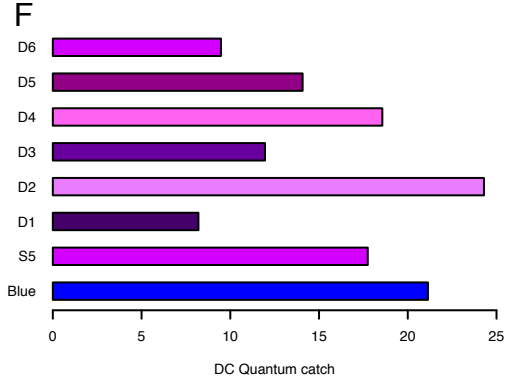
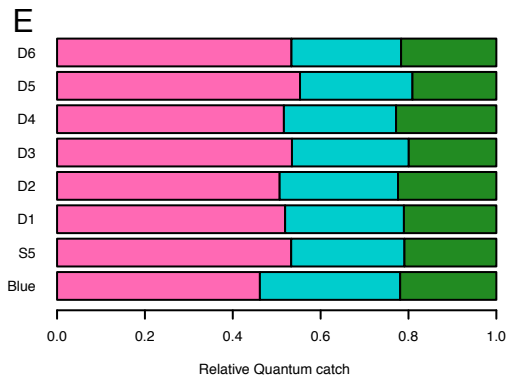
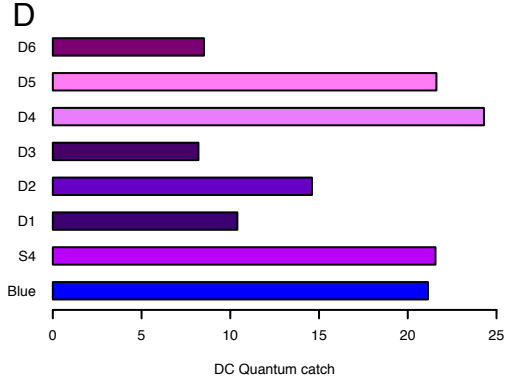
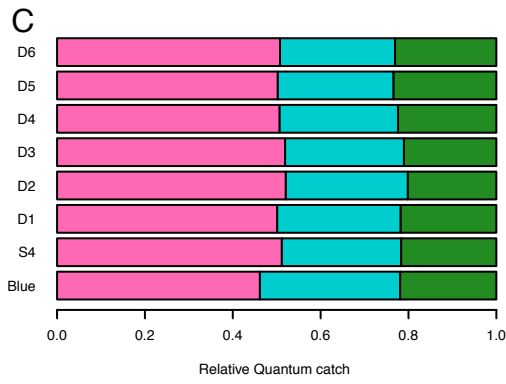
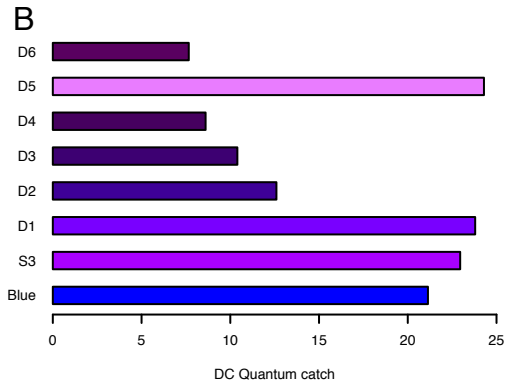
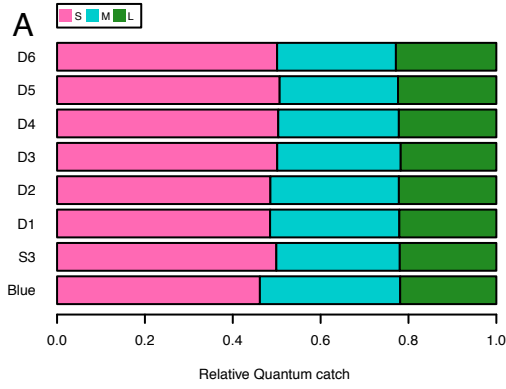


Figure S3. Quantum catches of color stimuli presented in multiple-choice test color cards under fluorescent light in Experiment 2. (A-F) denote quantum catches of blue, the distracter stimuli (from the threshold interval of Experiment 1 S3, S4, and S5) and the respective distracter stimuli from each group (D1-6). (A, C & E) denote normalized quantum catches of each color present in the multiple-choice test color cards (S3, S4 and S5 respectively) with their respective distracter colors (D1-6). Stacked bars show the stimulation for each type of photoreceptor (S, M and L) for each color. (B, D & F) show the relative quantum catch for the Double Cones (DC) luminance channel, for each color as calculated with Equation 3. (G, H & I) show ΔS of distracter stimuli (for each color group S3, S4 and S5 respectively) from rewarded stimuli (blue) using a standard deviation noise value (ν) for the LWS channel of 0.16.

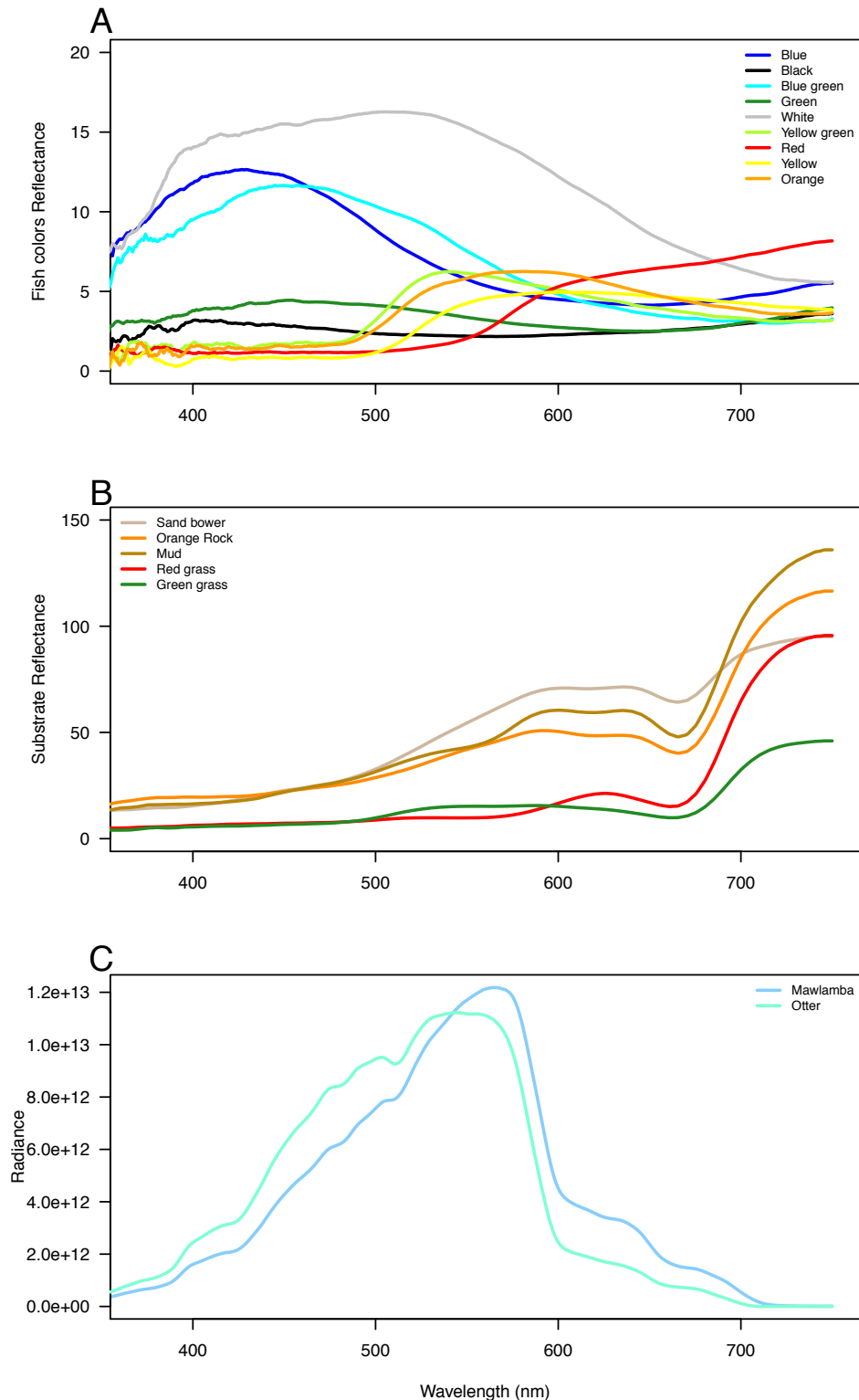


Figure S4. Spectral measurements from Lake Malawi. (A) denotes the reflectance from cichlids' colors (B) denotes reflectance from background substrates and (C) denotes side-welling radiance at 3 meter depth from Mawlamba Bay and Otter Point.

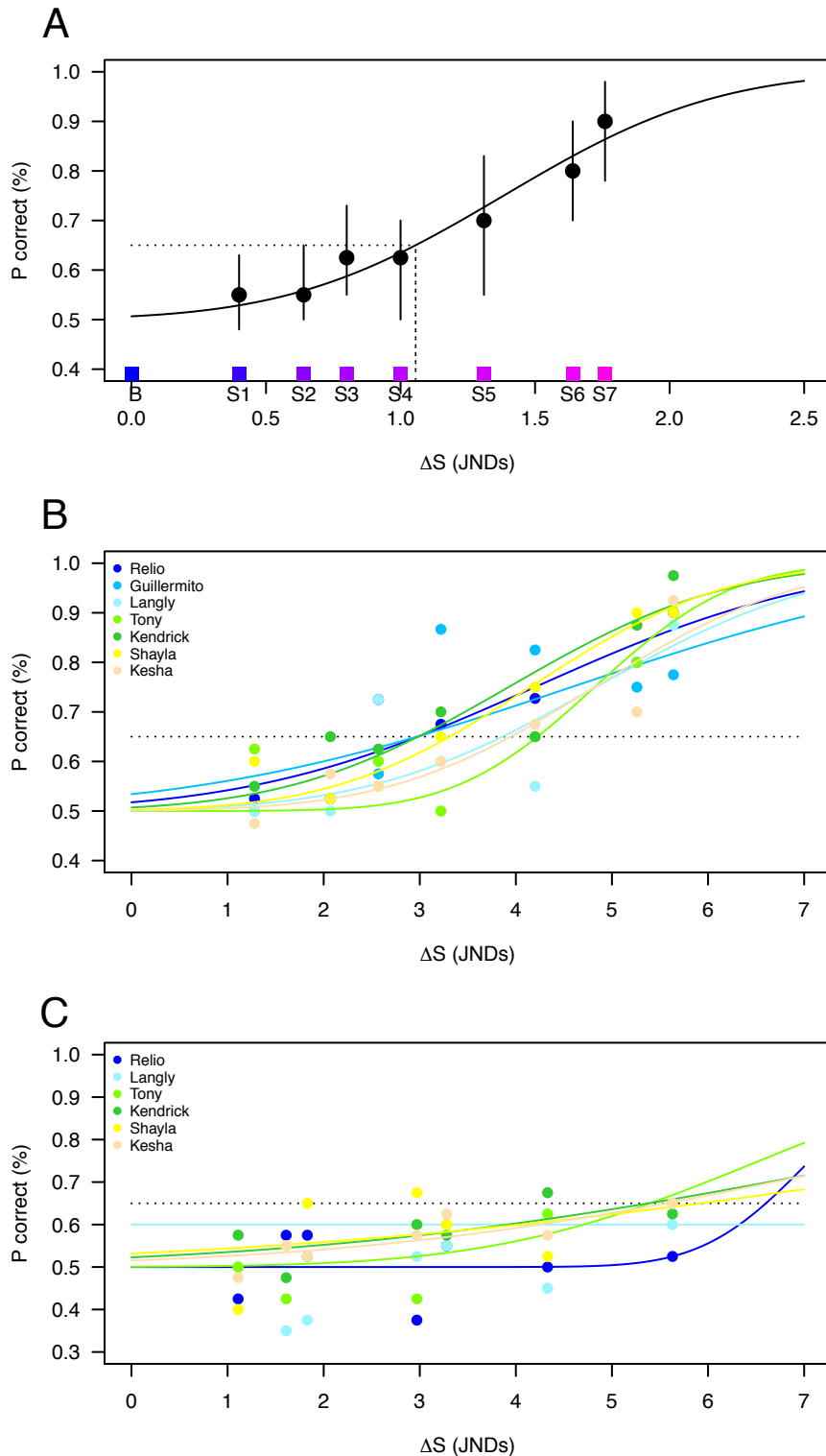


Figure S5. (A) Color thresholds under fluorescent light where proportion of correct choices is showed as a function of ΔS (JNDs). The x-axis represent ΔS in JNDs. Filled circles denote the fraction of correct choices made by fish for stimulus S1-S7, and colored inserts represent the respective distracter stimuli appearances. Chromatic distance was estimated using a standard deviation

noise value (ν) for the LWS channel of 0.16. (B & C) Individual variation of behavioral color thresholds expressed as Proportion of correct choices as a function of ΔS under fluorescent (B) (Experiment 1) and violet light (C) (Experiment 3). The x-axis represents ΔS . Filled colored circles denote the fraction of correct choices made by each fish for stimulus S1-S7. ΔS was estimated using the standard deviation noise value (ν) for the LWS channel of 0.05

Supplementary Tables

Table S1

http://cichlid.umd.edu/cichlidlabs/DEC_thesis/DEC_thesis_supp_data.html

Supplementary File

Movie 1

http://cichlid.umd.edu/cichlidlabs/DEC_thesis/DEC_thesis_supp_data.html

Glossary

1. SWS1 UV sensitive opsin gene
2. SWS2B Short-wavelength sensitive opsin gene
3. SWS2A Short-wavelength sensitive opsin gene
4. RH2B B rhodopsin like gene
5. RH2A α A α rhodopsin like gene
6. RH2A β A β rhodopsin like gene
7. LWS Long wavelength sensitive
8. UV Ultraviolet
9. S Short type photoreceptor
10. M Medium type photoreceptor
11. L Long type photoreceptor
12. Q Quantum catch
13. R The sensitivity (opsin absorbance template) of receptor, is the lens
14. i Receptor type
15. L Lens transmittance
16. S Surface reflectance (color stimuli),
17. I Illuminant,
18. K von Kries factor for receptor i
19. T_{50} Represents the wavelength at which 50% transmission is reached.
20. nm Nanometer
21. MSP Microspectrophotometry
22. F_{abs} Quantum catch absorptance coefficient
23. k Absorption coefficient of the photoreceptor at the peak absorption wavelength
24. $A(\lambda)$ Is the wavelength dependent absorbance of the photoreceptor, normalized to a peak of one
25. l Length of the outer segment in μm

26. SC	Single cones
27. DC	Double cones
28. RNL	Receptor noise-limited model (RNL).
29. Δf	Contrast in a receptor channel.
30. v	Relative receptor noise.
31. ω	Weber fraction.
32. n	Number of receptors of i type.
33. ΔS	Chromatic distance between two colors measured in JNDs
34. JNDs	Just noticeable differences.
35. v	Number of cones per receptive field and
36. τ	Summation time
37. d	Diameter of the receptor
38. f	Lens focal length
39. D	Pupil diameter.
40. N	Absolute quantum catches.

Bibliography

1. Endler JA. Some general comments on the evolution and design of animal communication systems. *Philos Trans R Soc Lond B Biol Sci.* 1993;340: 215–225. doi:10.1098/rstb.1993.0060
2. Lythgoe JN. *The Ecology of Vision.* New York: Oxford University Press; 1979.
3. Caro T, Stoddard MC, Stuart-fox D, Caro T, Wallace R, Poulton E, et al. Animal coloration research : why it matters. *Philos Trans R Soc B Biol Sci.* 2017;372: 20160333.
4. Endler JA, Mappes J. The current and future state of animal coloration research. *Philos Trans R Soc B Biol Sci.* 2017;372: 20160352.
5. Rodieck RW. *The First Steps in Seeing.* 1st editio. Sunderland, Massachusetts: Sinauer Associates, Inc; 1998. doi:10.1001/archopht.117.4.550
6. Yokoyama S. Evolution of dim-light and color vision pigments. *Annu Rev Genomics Hum Genet.* 2008;9: 259–82. doi:10.1146/annurev.genom.9.081307.164228
7. Bowmaker JK. Evolution of vertebrate visual pigments. *Vision Res.* 2008;48: 2022–2041. doi:10.1016/j.visres.2008.03.025
8. Lamb TD, Collin SP, Pugh EN. Evolution of the vertebrate eye: opsins, photoreceptors, retina and eye cup. *Nat Rev Neurosci.* 2007;8: 960–76. doi:10.1038/nrn2283

9. Kelber A. Colour in the eye of the beholder : receptor sensitivities and neural circuits underlying colour opponency and colour perception. *Curr Opin Neurobiol.* Elsevier Ltd; 2016;41: 106–112. doi:10.1016/j.conb.2016.09.007
10. Kemp DJ, Herberstein ME, Fleishman LJ, Endler J a., Bennett ATD, Dyer AG, et al. An Integrative Framework for the Appraisal of Coloration in Nature. *Am Nat.* 2015;185: 000–000. doi:10.1086/681021
11. Warrant EJ, Johnsen S. Vision and the light environment. *Curr Biol.* Elsevier; 2013;23: R990–R994. doi:10.1016/j.cub.2013.10.019
12. Hofmann CM, O’Quin KE, Marshall JN, Carleton KL. The relationship between lens transmission and opsin gene expression in cichlids from Lake Malawi. *Vision Res.* Elsevier Ltd; 2010;50: 357–363. doi:10.1111/j.1365-294X.2010.04621.x
13. Siebeck UE, Collin SP, Ghoddusi M, Marshall JN. Occlusable corneas in toadfishes: light transmission, movement and ultrastruture of pigment during light- and dark-adaptation. *J Exp Biol.* 2003;206: 2177–2190. doi:10.1242/jeb.00401
14. Siebeck UE, Marshall NJ. Ocular media transmission of coral reef fish--can coral reef fish see ultraviolet light? *Vision Res.* 2001;41: 133–149. doi:10.1016/S0042-6989(00)00240-6
15. Douglas RH, Marshall NJ. A review of vertebrate and invertebrate ocular filters. In: Archer SN, Djamgoz MBA, Loew ER, Partridge JC, Vallerga S, editors. *Adaptive mechanisms in the ecology of vision.*

- Dordrecht/Boston/London: Kluwer Academic Publishers; 1999. pp. 95–162.
16. Best ACG, Nicol JAC. Red Pigment Epithelium of Fish Eyes. *J Mar Biol Assoc UK*. 1984;64: 909–917. doi:10.1017/S0025315400047329
 17. Muntz WRA. Visual Adaptations to Different light environments in Amazonian Fishes. *Rev Can Biol Exp*. 1982;41: 35–46.
 18. Muntz WRA. Yellow filters and the absorption of light by the visual pigments of some amazonian fishes. *Vision Res*. 1973;13: 2235–2254. doi:10.1016/0042-6989(73)90225-3
 19. Viets K, Eldred KC, Jr RJJ. Mechanisms of Photoreceptor Patterning in Vertebrates and Invertebrates. *Trends Genet*. Elsevier Ltd; 2016;32: 638–659. doi:10.1016/j.tig.2016.07.004
 20. Dalton BE, de Busserolles F, Marshall NJ, Carleton KL. Retinal specialization through spatially varying cell densities and opsin coexpression in cichlid fish. *J Exp Biol*. 2017; 266–277. doi:10.1242/jeb.149211
 21. Busserolles F De, Cortesi F, Helvik JV, Davies WIL, Templin RM, Sullivan RKP, et al. Pushing the limits of photoreception in twilight conditions : The rod-like cone retina of the deep-sea pearlsides. *Sci Adv*. 2017;3: eaao4709.
 22. Sukeena JM, Galicia CA, Wilson JD, Mcginn TIM, Boughman JW, Robison BD, et al. Characterization and Evolution of the Spotted Gar Retina. *J Exp Zool Part B Mol Dev Evol*. 2016;326: 403–421. doi:10.1002/jez.b.22710
 23. Garza-Gisholt E, Hart S, Collin P. Retinal Morphology and Visual

- Specializations in Three Species of Chimaeras , the Deep-Sea *R . pacifica* and *C . lignaria* , and the Vertical Migrator *C. milii* (Holocephali). *Brain Behav Evol.* 2018;92: 47–62. doi:10.1159/000490655
24. Dalton BE, Loew ER, Cronin TW, Carleton KL. Spectral tuning by opsin coexpression in retinal regions that view different parts of the visual field. *Proc R Soc B.* 2014;281. doi:10.1098/rspb.2014.1980
 25. Carleton K, Kocher T. Cone Opsin Genes of African Cichlid Fishes: Tuning Spectral Sensitivity by Differential Gene Expression. *Mol Biol Evol.* 2001;18: 1540–1550.
 26. Carleton K. Cichlid fish visual systems: mechanisms of spectral tuning. *Integr Zool.* 2009;4: 75–86. doi:10.1111/j.1749-4877.2008.00137.x
 27. Carleton KL, Dalton BE, Escobar-Camacho D, Nandamuri SP. Proximate and ultimate causes of variable visual sensitivities: Insights from cichlid fish radiations. *Genesis.* 2016;54: 299–325. doi:10.1002/dvg.22940
 28. Levine JS, MacNichol EF. Visual Pigments in Teleost Fishes: Effects of Habitat, Microhabitat, and Behavior on Visual System Evolution. *Sens Processes.* 1979;3: 95–131.
 29. Lythgoe JN, Muntz WRA, Partridge JC. The ecology of the visual pigments of snappers (*Lutjanidae*) on the Great Barrier Reef. *J Comp Physiol A.* 1994;174: 461–467.
 30. Bowmaker JK, Govardovskii VI, Sideleva VG, Shukolyukov SA, Zueva L V. Visual Pigments and the Photic Environment: the Cottoid Fish of Lake Baikal. *Vision Res.* 1994;34: 591–605.

31. Schwanzara SA. The Visual Pigments of Freshwater Fishes. *Vision*. 1967;7: 121–148.
32. Rennison DJ, Owens GL, Taylor JS. Opsin gene duplication and divergence in ray-finned fish. *Mol Phylogenet Evol*. Elsevier Inc.; 2012;62: 986–1008. doi:10.1016/j.ympev.2011.11.030
33. Hofmann CM, Carleton KL. Gene duplication and differential gene expression play an important role in the diversification of visual pigments in fish. *Integr Comp Biol*. 2009;49: 630–643. doi:10.1093/icb/icp079
34. Lin JJ, Wang FY, Li WH, Wang TY. The rises and falls of opsin genes in 59 ray-finned fish genomes and their implications for environmental adaptation. *Sci Rep*. Springer US; 2017;7: 1–13. doi:10.1038/s41598-017-15868-7
35. Davies WIL, Collin SP, Hunt DM. Molecular ecology and adaptation of visual photopigments in craniates. *Mol Ecol*. 2012;21: 3121–3158. doi:10.1111/j.1365-294X.2012.05617.x
36. Cortesi F, Musilová Z, Stieb SM, Hart NS, Siebeck UE, Malmstrøm M, et al. Ancestral duplications and highly dynamic opsin gene evolution in percomorph fishes. *Proc Natl Acad Sci*. 2015;112: 1493–1498. doi:10.1073/pnas.1417803112
37. von Frisch K. Über farbige Anpassung bei Fischen. *Zool Jb Physiol*. 1912;32: 209–214.
38. Cheney KL, Green NF, Vibert AP, Vorobyev M, Marshall NJ, Osorio DC, et al. An Ishihara-style test of animal colour vision. *J Exp Biol*. 2019;222:

189787. doi:10.1242/jeb.189787

39. Parry JWL, Bowmaker JK. Visual pigment reconstitution in intact goldfish retina using synthetic retinaldehyde isomers. *Vision Res.* 2000;40: 9–15. doi:10.1016/S0042-6989(00)00101-2
40. Spady TC, Parry JWL, Robinson PR, Hunt DM, Bowmaker JK, Carleton KL. Evolution of the cichlid visual palette through ontogenetic subfunctionalization of the opsin gene arrays. *Mol Biol Evol.* 2006;23: 1538–1547. doi:10.1093/molbev/msl014
41. Hofmann CM, O’Quin KE, Justin Marshall N, Cronin TW, Seehausen O, Carleton KL. The eyes have it: Regulatory and structural changes both underlie cichlid visual pigment diversity. *PLoS Biol.* 2009;7: e1000266. doi:10.1371/journal.pbio.1000266
42. Weadick CJ, Loew ER, Rodd FH, Chang BSW. Visual pigment molecular evolution in the Trinidadian pike cichlid (*Crenicichla frenata*): a less colorful world for neotropical cichlids? *Mol Biol Evol.* 2012;29: 3045–60. doi:10.1093/molbev/mss115
43. Schott RK, Refvik SP, Hauser FE, López-Fernández H, Chang BSW. Divergent positive selection in rhodopsin from lake and riverine cichlid fishes. *Mol Biol Evol.* 2014;31: 1149–1165. doi:10.1093/molbev/msu064
44. Sambrook J, Russel DW. *Molecular Cloning: A Laboratory Manual*. 3rd ed. Cold Spring Harbor: Cold Spring Harbor Laboratory Press; 2001.
45. Zerbino DR, Birney E. Velvet: Algorithms for de novo short read assembly using de Bruijn graphs. *Genome Res.* 2008;18: 821–829.

doi:10.1101/gr.074492.107

46. Chikhi R, Medvedev P. Informed and automated k-mer size selection for genome assembly. *Bioinformatics*. 2014;30: 31–37. doi:10.1093/bioinformatics/btt310
47. Parra G, Bradnam K, Korf I. CEGMA: A pipeline to accurately annotate core genes in eukaryotic genomes. *Bioinformatics*. 2007;23: 1061–1067. doi:10.1093/bioinformatics/btm071
48. Bradnam KR, Fass JN, Alexandrov A, Baranay P, Bechner M, Birol I, et al. Assemblathon 2: evaluating de novo methods of genome assembly in three vertebrate species. *Gigascience*. 2013;2: 10. doi:10.1186/2047-217X-2-10
49. Bolger AM, Lohse M, Usadel B. Trimmomatic: A flexible trimmer for Illumina sequence data. *Bioinformatics*. 2014;30: 2114–2120.
50. Haas BJ, Papanicolaou A, Yassour M, Grabherr M, Blood PD, Bowden J, et al. De novo transcript sequence reconstruction from RNA-seq using the Trinity platform for reference generation and analysis. *Nat Protoc*. 2013;8: 1494–512. doi:10.1038/nprot.2013.084
51. Benson DA, Karsch-Mizrachi I, Lipman DJ, Ostell J, Wheeler DL. GenBank. *Nucleic Acids Res*. 2005;33: 34–38. doi:10.1093/nar/gki063
52. Katoh K, Misawa K, Kuma K, Miyata T. MAFFT: a novel method for rapid multiple sequence alignment based on fast Fourier transform. *Nucleic Acids Res*. 2002;30: 3059–3066. doi:10.1093/nar/gkf436
53. Zwickl DJ. Genetic algorithm approaches for the phylogenetic analysis of

- large biological sequence datasets under the maximum likelihood criterion. PhD dissertation, The University of Texas at Austin. 2006. doi:(<http://www.zo.utexas.edu/faculty/antisense/garli/Garli.html>)
54. Bazinet AL, Zwickl DJ, Cummings MP. A Gateway for Phylogenetic Analysis Powered by Grid Computing Featuring GARLI 2.0. *Syst Biol.* 2014;63: 812–818. doi:10.1093/sysbio/syu031
 55. Hunt DM, Dulai KS, Partridge JC, Cottrill P, Bowmaker JK. The molecular basis for spectral tuning of rod visual pigments in deep-sea fish. *J Exp Biol.* 2001;204: 3333–3344.
 56. Carleton KL, Spady TC, Cote RH. Rod and cone opsin families differ in spectral tuning domains but not signal transducing domains as judged by saturated evolutionary trace analysis. *J Mol Evol.* 2005;61: 75–89. doi:10.1007/s00239-004-0289-z
 57. Li W-H, Gojobori T, Nei M. Pseudogenes as a paradigm of neutral evolution. *Nature.* 1981;292: 237–239.
 58. Tamura K, Stecher G, Peterson D, Filipski A, Kumar S. MEGA6: Molecular evolutionary genetics analysis version 6.0. *Mol Biol Evol.* 2013;30: 2725–2729. doi:10.1093/molbev/mst197
 59. Jukes TH, Cantor CR. Evolution of protein molecules. In: Munro HN, editor. *Mammalian Protein Metabolism, III.* New York: Academic Press Inc; 1969. pp. 21–132. doi:citeulike-article-id:768582
 60. Asenjo AB, Rim J, Oprian DD. Molecular determinants of human red/green color discrimination. *Neuron.* 1994;12: 1131–1138. doi:10.1016/0896-

6273(94)90320-4

61. Yokoyama S, Tada T. The spectral tuning in the short wavelength-sensitive type 2 pigments. *Gene*. 2003;306: 91–98. doi:10.1016/S0378-1119(03)00424-4
62. Zhao Z, Hewett-Emmett D, Li WH. Frequent gene conversion between human red and green opsin genes. *J Mol Evol*. 1998;46: 494–496.
63. Hiwatashi T, Mikami A, Katsumura T, Suryobroto B, Perwitasari-Farajallah D, Malaivijitnond S, et al. Gene conversion and purifying selection shape nucleotide variation in gibbon L/M opsin genes. *BMC Evol Biol*. 2011;11: 312. doi:10.1186/1471-2148-11-312
64. Owens GL, Windsor DJ, Mui J, Taylor JS. A fish eye out of water: Ten visual opsins in the four-eyed fish, *Anableps anableps*. *PLoS One*. 2009;4: 1–7. doi:10.1371/journal.pone.0005970
65. Sandkam BA, Joy JB, Watson CT, Breden F. Genomic Environment Impacts Color Vision Evolution in a Family with Visually Based Sexual Selection. *Genome Biol Evol*. 2017;9: 3100–3107. doi:10.1093/gbe/evx228
66. Betancur-R R, Broughton R, Wiley E, Carpenter K. The tree of life and a new classification of bony fishes. *PLoS Curr Tree Life*. 2013;0732988. doi:10.1371/currents.tol.53ba26640df0ccaee75bb165c8c26288.Abstract
67. Chinen A, Hamaoka T, Yamada Y, Kawamura S. Gene duplication and spectral diversification of cone visual pigments of zebrafish. *Genetics*. 2003;163: 663–75. Available: <http://www.pubmedcentral.nih.gov/articlerender.fcgi?artid=1462461&tool=p>

mcentrez&rendertype=abstract

68. Matsumoto Y, Fukamachi S, Mitani H, Kawamura S. Functional characterization of visual opsin repertoire in Medaka (*Oryzias latipes*). *Gene*. 2006;371: 268–78. doi:10.1016/j.gene.2005.12.005
69. López-Fernández H, Winemiller KO, Honeycutt RL. Multilocus phylogeny and rapid radiations in Neotropical cichlid fishes (Perciformes: Cichlidae: Cichlinae). *Mol Phylogenet Evol*. Elsevier Inc.; 2010;55: 1070–1086. doi:10.1016/j.ympev.2010.02.020
70. Hibbard E. Grid patterns in the retinal organization of the cichlid fish *Astronotus ocellatus*. *Exp Eye Res*. 1971;12: 175–180. doi:10.1016/0014-4835(71)90087-X
71. Braekevelt CR. Anatomy and Embryology in the velvet cichlid (*Astronotus ocellatus*). *Anat Embryol (Berl)*. 1992;186: 363–370.
72. Halstenberg S, Lindgren KM, Samagh SPS, Nadal-Vicens M, Balt S, Fernald RD. Diurnal rhythm of cone opsin expression in the teleost fish *Haplochromis burtoni*. *Vis Neurosci*. 2005;22: 135–141. doi:10.1017/S0952523805222022
73. Carleton KL, Spady TC, Streelman JT, Kidd MR, McFarland WN, Loew ER. Visual sensitivities tuned by heterochronic shifts in opsin gene expression. *BMC Biol*. 2008;6: 22. doi:10.1186/1741-7007-6-22
74. Costa MPF, Novo EMLM, Telmer KH. Spatial and temporal variability of light attenuation in large rivers of the Amazon. *Hydrobiologia*. 2012;702: 171–190. doi:10.1007/s10750-012-1319-2

75. Martinez J, Seyler F, Bourgoïn LM, Guyot JL. Amazon Basin Water Quality Monitoring Using Meris and Modis Data. Proc of the 2004 Envisat & ERS Symposium. 2004. pp. 1–10.
76. Rudorff CM, Novo EMLM, Galvão LS. Spectral mixture analysis for water quality assessment over the Amazon floodplain using Hyperion / EO-1 images. Rev Ambi-Agua. 2006;1: 65–79.
77. Farias IP, Hrbek T. Patterns of diversification in the discus fishes (*Symphysodon* spp. Cichlidae) of the Amazon basin. Mol Phylogenet Evol. Elsevier Inc.; 2008;49: 32–43. doi:10.1016/j.ympev.2008.05.033
78. Albert JS, Reis RE. Historical Biogeography of Neotropical Freshwater Fishes. Berkeley, Los Angeles, London: University of California Press; 2011.
79. Froese R, Pauly D. FishBase. World Wide Web electronic publication [Internet]. 2019. Available: www.fishbase.org, version
80. Kröger RHH, Bowmaker JK, Wagner HJ. Morphological changes in the retina of *Aequidens pulcher* (Cichlidae) after rearing in monochromatic light. Vision Res. 1999;39: 2441–2448. doi:10.1016/S0042-6989(98)00256-9
81. Hárosi FI. An analysis of two spectral properties of vertebral visual pigments. Vision Res. 1994;34: 1359–1367.
82. Parry JW, Carleton KL, Spady T, Carboo A, Hunt DM, Bowmaker JK. Mix and match color vision: tuning spectral sensitivity by differential opsin gene expression in Lake Malawi cichlids. Curr Biol. 2005;15: 1734–9.

doi:10.1016/j.cub.2005.08.010

83. Sabbah S, Hui J, Hauser FE, Nelson W a, Hawryshyn CW. Ontogeny in the visual system of Nile tilapia. *J Exp Biol.* 2012;215: 2684–95. doi:10.1242/jeb.069922
84. Hofmann CM, Marshall NJ, Abdilleh K, Patel Z, Siebeck UE, Carleton KL. Opsin evolution in damselfish: convergence, reversal, and parallel evolution across tuning sites. *J Mol Evol.* 2012;75: 79–91. doi:10.1007/s00239-012-9525-0
85. Phillips GAC, Carleton KL, Marshall NJ. Multiple Genetic Mechanisms Contribute to Visual Sensitivity Variation in the Labridae. *Mol Biol Evol.* 2015;33: 201–215. doi:10.1093/molbev/msv213
86. Nynatten A Van, Bloom D, Chang BSW, Lovejoy NR, Lovejoy NR. Out of the blue: adaptive visual pigment evolution accompanies Amazon invasion. *Biol Lett.* 2015;11: 20150349. doi:10.1098/rsbl.2015.0349
87. Torres-Dowdall J, Henning F, Elmer KR, Meyer A. Ecological and lineage specific factors drive the molecular evolution of rhodopsin in cichlid fishes. *Mol Biol Evol.* 2015;32: 2876–2882.
88. Munz FW, McFarland WN. Evolutionary Adaptations of Fishes to the photic Environment. In: Crescitelli F, editor. *The visual system in vertebrates.* New York: Springer-Verlag; 1977. pp. 193–274.
89. Hubert N, Renno J-F. Historical biogeography of South American freshwater fishes. *J Biogeogr.* 2006;33: 1414–1436. doi:10.1111/j.1365-2699.2006.01518.x

90. Turchetto-Zolet AC, Pinheiro F, Salgueiro F, Palma-Silva C. Phylogeographical patterns shed light on evolutionary process in South America. *Mol Ecol.* 2013;22: 1193–213. doi:10.1111/mec.12164
91. Traeger LL, Volkening JD, Moffett H, Gallant JR, Chen P-H, Novina CD, et al. Unique patterns of transcript and miRNA expression in the South American strong voltage electric eel (*Electrophorus electricus*). *BMC Genomics.* 2015;16: 243. doi:10.1186/s12864-015-1288-8
92. Zhao H, Rossiter SJ, Teeling EC, Li C, Cotton J a, Zhang S. The evolution of color vision in nocturnal mammals. *Proc Natl Acad Sci U S A.* 2009;106: 8980–8985. doi:10.1073/pnas.0813201106
93. Meredith RW, Gatesy J, Emerling CA, York VM, Springer MS. Rod Monochromacy and the Coevolution of Cetacean Retinal Opsins. *PLoS Genet.* 2013;9. doi:10.1371/journal.pgen.1003432
94. Muntz WRA, Church E, Dartnall HJA. Visual Pigment of the Freshwater Stingray, *Paratrygon motoro*. *Nature.* 1973;246:517. doi:10.1038/246517a0
95. Marshall J, Carleton KL, Cronin T. Colour vision in marine organisms. *Curr Opin Neurobiol.* Elsevier Ltd; 2015;34: 86–94. doi:10.1016/j.conb.2015.02.002
96. Ehlman SM, Sandkam BA, Breden F, Sih A. Developmental plasticity in vision and behavior may help guppies overcome increased turbidity. *J Comp Physiol A.* Springer Berlin Heidelberg; 2015;201: 1125–1135. doi:10.1007/s00359-015-1041-4
97. Losey G, Cronin T, Goldsmith T, Hydes D, Marshall N, McFarland W. The

- UV visual world of fishes: a review. *J Fish Biol.* 1999;54: 921–943.
doi:10.1111/j.1095-8649.1999.tb00848.x
98. Prentis PJ, Wilson JRU, Dormontt EE, Richardson DM, Lowe AJ. Adaptive evolution in invasive species. *Trends Plant Sci.* 2008;13: 288–295.
doi:10.1016/j.tplants.2008.03.004
99. Dudeque RZ, Lamy J, Lamarque LJ, Porté AJ. Adaptive evolution and phenotypic plasticity during naturalization and spread of invasive species : implications for tree invasion biology. *Biol Invasions.* 2014;16: 635–644.
doi:10.1007/s10530-013-0607-8
100. Hoffmann AA, Sgro CM. Climate change and evolutionary adaptation. *Nature.* 2011;470: 479–485. doi:10.1038/nature09670
101. Whitney KD, Gabler CA. Rapid evolution in introduced species , ‘invasive traits’ and recipient communities : challenges for predicting invasive potential. *Diversity.* 2008;14: 569–580. doi:10.1111/j.1472-4642.2008.00473.x
102. Kullander SO, Ferreira EJG. A review of the South American cichlid genus *Cichla*, with descriptions of nine new species (Teleostei: Cichlidae). *Ichthyol Explor Freshwaters.* 2006;17: 289–398.
103. Zaret TM, Paine RT. Species introduction in a tropical lake. *Science (80-).* 1973;182: 449–455.
104. Sharpe DMT, De León LF, Gonzalez R, Torchin ME. Tropical fish community does not recover 45 years after predator introduction. *Ecology.* 2016;98: 412–424. doi:10.1002/ecy.1648

105. Ibáñez R, Condit R, Angehr G, Aguilar S, Garcia T, Martfnez R, et al. An ecosystem report on the Panama Canal: monitoring the status of the forest communities and the watershed. *Environ Monit Assess.* 2002;80: 65–95.
106. Wang M. The role of Panama Canal in global shipping. *Marit Bus Rev.* 2017;2: 247–260. doi:10.1108/MABR-07-2017-0014
107. Härer A, Torres-Dowdall J, Meyer A. Rapid adaptation to a novel light environment: The importance of ontogeny and phenotypic plasticity in shaping the visual system of Nicaraguan Midas cichlid fish (*Amphilophus citrinellus* spp.). *Mol Ecol.* 2017;26: 5582–5593. doi:10.1111/mec.14289
108. Nandamuri SP, Yourick MR, Carleton KL. Adult plasticity in African cichlids: Rapid changes in opsin expression in response to environmental light differences. *Mol Ecol.* 2017;26: 6036–6052. doi:10.1111/mec.14357
109. Hofmann CM, O’Quin KE, Smith AR, Carleton KL. Plasticity of opsin gene expression in cichlids from Lake Malawi. *Mol Ecol.* 2010;19: 2064–2074. doi:10.1111/j.1365-294X.2010.04621.x
110. Dartnall HJA. The interpretation of spectral sensitivity curves. *Br Med Bull.* 1953;9: 24–30.
111. Munz FW, Schwanzara SA. A nomogram for retinene₂-based visual pigments. *Vision Res.* 1967;7: 111–120.
112. Whitmore A V., Bowmaker JK. Seasonal variation in cone sensitivity and short-wave absorbing visual pigments in the rudd *Scardinius erythrophthalmus*. *J Comp Physiol A.* 1989;166: 103–115. doi:10.1007/BF00190215

113. Escobar-Camacho D, Ramos E, Martins C, Carleton KL. The opsin genes of amazonian cichlids. *Mol Ecol.* 2017;26: 1343–1356. doi:10.1111/mec.13957
114. Lanfear R, Frandsen PB, Wright AM, Senfeld T, Calcott B. Partitionfinder 2: New methods for selecting partitioned models of evolution for molecular and morphological phylogenetic analyses. *Mol Biol Evol.* 2017;34: 772–773. doi:10.1093/molbev/msw260
115. Enright JM, Toomey MB, Sato S, Kefalov VJ, Guengerich FP, Corbo JC, et al. Cyp27c1 Red-Shifts the Spectral Sensitivity of Photoreceptors by Converting Vitamin A1 into A2. *Curr Biol.* Elsevier Ltd; 2015;25: 3048–3057. doi:10.1016/j.cub.2015.10.018
116. Carvalho DC, Oliveira DAA, Sampaio I, Beheregaray LB. Analysis of propagule pressure and genetic diversity in the invasibility of a freshwater apex predator: the peacock bass (genus *Cichla*). *Neotrop Ichthyol.* 2014;12: 105–116. doi:10.1590/S1679-62252014000100011
117. Torres-Dowdall J, Pierotti MER, Harer, Andreas H, Karagic N, Woltering JM, Henning F, et al. Rapid and Parallel Adaptive Evolution of the Visual System of Neotropical Midas Cichlid Fishes. *Mol Biol Evol.* 2017;34: 2469–2485. doi:10.1093/molbev/msx143
118. Costa M, Telmer K, Novo EMLM. Spatial and temporal variability of light attenuation in the Amazonian waters. *Hydrobiologia.* 2013;702: 171–190.
119. Heinemann PH. Yellow intraocular filters in fishes. *Exp Biol.* 1984;43: 127–147.

120. Escobar-Camacho D, Ramos E, Martins C, Carleton KL. The Opsin genes of Three Amazonian Cichlids. *Mol Ecol.* 2016;26: 301–314. doi:10.5061/dryad.1h272
121. Hauser FE, Ilves KL, Schott RK, Castiglione GM. Accelerated Evolution and Functional Divergence of the Dim Light Visual Pigment Accompanies Cichlid Colonization of Central America. *Mol Biol Evol.* 2017;34: 2650–2664. doi:10.1093/molbev/msx192
122. Stapley J, Santure AW, Dennis SR. Transposable elements as agents of rapid adaptation may explain the genetic paradox of invasive species. *Mol Ecol.* 2015;24: 2241–2252. doi:10.1111/mec.13089
123. Schrader L, Kim JW, Ence D, Zimin A, Klein A, Wyschetzki K, et al. Transposable element islands facilitate adaptation to novel environments in an invasive species. *Nat Commun.* 2014;5: 1–10. doi:10.1038/ncomms6495
124. Ye X, Su Y, Zhao Q, Xia W, Liu S, Wang X. Transcriptomic analyses reveal the adaptive features and biological differences of guts from two invasive whitefly species. *BMC Genomics.* 2014;15: 1–12.
125. Pearce SL, Clarke DF, East PD, Elfekih S, Gordon KHJ, Jermiin LS, et al. Genomic innovations, transcriptional plasticity and gene loss underlying the evolution and divergence of two highly polyphagous and invasive *Helicoverpa* pest species. *BMC Biol.* 2017;15: 1–30. doi:10.1186/s12915-017-0402-6
126. Lockwood BL, Somero GN. Transcriptomic responses to salinity stress in

- invasive and native blue mussels (genus *Mytilus*). *Mol Ecol.* 2011;20: 517–529. doi:10.1111/j.1365-294X.2010.04973.x
127. Zerebecki RA, Sorte CJB. Temperature Tolerance and Stress Proteins as Mechanisms of Invasive Species Success. *PLoS One.* 2011;6: e14806. doi:10.1371/journal.pone.0014806
128. Bowmaker JK, Hunt DM. Evolution of vertebrate visual pigments. *Curr Biol.* 2006;16: pR484–R489. doi:10.1016/j.cub.2006.06.016
129. Bowmaker JK. Evolution of colour vision in vertebrates. *Eye.* 1998;12: 541–547. doi:10.1038/eye.1998.143
130. Yokoyama R, Yokoyama S. Convergent evolution of the red-and green-like visual pigment genes in fish, *Astyanax fasciatus*, and human. *Evolution (N Y).* 1990;87: 9315–9318. doi:10.1073/pnas.87.23.9315
131. Kasagi S, Mizusawa K, Takahashi A. Green-shifting of SWS2A opsin sensitivity and loss of function of RH2-A opsin in flounders , genus *Verasper*. *Ecol Evol.* 2018;8: 1399–1410. doi:10.1002/ece3.3745
132. Loew ER, McFarland WN. The underwater visual environment. In: Douglas RH, Djamgoz MBA, editors. *The Visual System of Fish.* New York, NY: Chapman and Hall; 1990. p. 526.
133. Oliveira C, Avelino GS, Abe KT, Mariguela TC, Benine RC, Ortí G, et al. Phylogenetic relationships within the speciose family Characidae (Teleostei: Ostariophysi: Characiformes) based on multilocus analysis and extensive ingroup sampling. *BMC Evol Biol.* 2011;11: 275. doi:10.1186/1471-2148-11-275

134. Arcila D, Petry P, Ortí G. Phylogenetic relationships of the family Tarumaniidae (Characiformes) based on nuclear and mitochondrial data. *Neotro*. 2018;16: e180016. doi:10.1590/1982-0224-20180016
135. Yokoyama R, Knox BE, Yokoyama S. Rhodopsin from the fish, *Astyanax*: Role of tyrosine 261 in the red shift. *Investig Ophthalmol Vis Sci*. 1995;36: 939–945.
136. Yokoyama R, Yokoyama S. Molecular characterization of a blue visual pigment gene in the fish *Astyanax fasciatus*. *FEBS Lett*. 1993;334: 27–31. doi:10.1016/0014-5793(93)81673-N
137. Yokoyama S, Yang H, Starmer WT. Molecular basis of spectral tuning in the red- and green-sensitive (M/LWS) pigments in vertebrates. *Genetics*. 2008;179: 2037–2043. doi:10.1534/genetics.108.090449
138. Register EA, Yokoyama R, Yokoyama S. Multiple origins of the green-sensitive opsin genes in fish. *J Mol Evol*. 1994;39: 268–273. doi:10.1007/BF00160150
139. Taylor JS, Peer Y Van De, Braasch I, Meyer A. Comparative genomics provides evidence for an ancient genome duplication event in fish. *Philos Trans R Soc B*. 2001; 1661–1679. doi:10.1098/rstb.2001.0975
140. Meyer A, Peer Y Van De. From 2R to 3R: evidence for a fish-specific genome duplication (FSGD). *BioEssays*. 2005; 937–945. doi:10.1002/bies.20293
141. Liu D, Wang F, Lin J, Thompson A, Lu Y, Vo D, et al. The Cone Opsin Repertoire of Osteoglossomorph Fishes: Gene Loss in Mormyrid Electric

- Fish and a Long Wavelength-Sensitive Cone Opsin That Survived 3R. *Mol Biol Evol.* 2018;36: 447–457. doi:10.1093/molbev/msy241
142. Darriba D, Taboada GL, Doallo R, Posada D. ProtTest 3 : fast selection of best-fit models of protein evolution. 2011;27: 1164–1165. doi:10.1093/bioinformatics/btr088
143. Miller MA, Schwartz T, Pickett BE, He S, Klem EB, Scheuermann RH, et al. A RESTful API for Access to Phylogenetic Tools via the CIPRES Science Gateway. *Evol Bioinforma.* 2015; 43–48. doi:10.4137/EBO.S21501.RECEIVED
144. Watson CT, Lubieniecki KP, Loew E, Davidson WS, Breden F. Genomic organization of duplicated short wave- sensitive and long wave-sensitive opsin genes in the green swordtail, *Xiphophorus helleri*. *BMC evolu.* 2010;10: 87.
145. Nakamura Y, Mori K, Saitoh K, Oshima K, Mekuchi M, Sugaya T, et al. Evolutionary changes of multiple visual pigment genes in the complete genome of Pacific bluefin tuna. *Proc Natl Acad Sci.* 2013;110: 11061–11066. doi:10.1073/pnas.1302051110
146. Kosakovsky Pond SL, Posada D, Gravenor MB, Woelk CH, Frost SDW. GARD : a genetic algorithm for recombination detection. *Bioinformatics.* 2006;22: 3096–3098. doi:10.1093/bioinformatics/btl474
147. Yokoyama S, Radlwimmer FB. The Molecular Genetics and Evolution of Red and Green Color Vision in Vertebrates. *Genetics.* 2001;158: 1697–1710.

148. Takahashi Y, Ebrey TG. Molecular basis of spectral tuning in the newt short wavelength sensitive visual pigment. *Biochemistry*. 2003;42: 6025–34. doi:10.1021/bi020629+
149. Paradis E, Schliep K. ape 5 . 0 : an environment for modern phylogenetics and evolutionary analyses in R. *Bioinformatics*. 2018; 1–2. doi:10.1093/bioinformatics/bty633/5055127
150. Morrow JM, Lazic S, Dixon Fox M, Kuo C, Schott RK, de A. Gutierrez E, et al. A second visual rhodopsin gene, *rh1-2* , is expressed in zebrafish photoreceptors and found in other ray-finned fishes. *J Exp Biol*. 2017;220: 294–303. doi:10.1242/jeb.145953
151. Morrow JM, Lazic S, Chang BSW. A novel rhodopsin-like gene expressed in zebrafish retina. *Vis Neurosci*. 2011;28: 325–335. doi:10.1017/S0952523811000010
152. Ward MN, Churcher AM, Dick KJ, Laver CRJ, Owens GL, Polack MD, et al. The molecular basis of color vision in colorful fish : Four Long Wave-Sensitive (LWS) opsins in guppies (*Poecilia reticulata*) are defined by amino acid substitutions at key functional sites. *BMC Evol Biol*. 2008;8: 210. doi:10.1186/1471-2148-8-210
153. Nakamura Y, Yasuike M, Mekuchi M, Iwasaki Y, Ojima N, Fujiwara A, et al. Rhodopsin gene copies in Japanese eel originated in a teleost-specific genome duplication. *Zool Lett. Zoological Letters*; 2017;3: 2–12. doi:10.1186/s40851-017-0079-2
154. Parry JWL, Peirson SN, Wilkens H, Bowmaker JK. Multiple photopigments

- from the Mexican blind cavefish, *Astyanax fasciatus*: a microspectrophotometric study. *Vision Res.* 2003;43: 31–41. doi:10.1016/S0042-6989(02)00404-2
155. Ohta T. Gene Conversion and Evolution of Gene Families: An Overview. *Genes (Basel)*. 2010;1: 349–356. doi:10.3390/genes1030349
156. Yokoyama R, Yokoyama S. Isolation, DNA sequence and evolution of a color visual pigment gene of the blind cave fish, *Astyanax fasciatus*. *Vision Res.* 1990;30: 807–816.
157. Hughes LC, Ortí G, Huang Y, Sun Y, Baldwin CC, Thompson AW. Comprehensive phylogeny of ray-finned fishes (Actinopterygii) based on transcriptomic and genomic data. *Proc Natl Acad Sci.* 2018;115: 6249–6254. doi:10.1073/pnas.1719358115
158. Inoue J, Sato Y, Sinclair R, Tsukamoto K, Nishida M. Rapid genome reshaping by multiple-gene loss after whole-genome duplication in teleost fish suggested by mathematical modeling. *Proc Natl Acad Sci.* 2015;112: 14918–14923. doi:10.1073/pnas.1507669112
159. Romano C, Koot MB, Kogan I, Brayard A, Minikh A V, Brinkmann W, et al. Permian – Triassic Osteichthyes (bony fishes): diversity dynamics and body size evolution. *Biol Rev Camb Philos Soc.* 2016;91: 106–147. doi:10.1111/brv.12161
160. Schweikert LE, Grace MS. Altered environmental light drives retinal change in the Atlantic Tarpon (*Megalops atlanticus*) over timescales relevant to marine environmental disturbance. *BMC Ecol. BioMed Central*;

2018;18: 1–10. doi:10.1186/s12898-018-0157-0

161. Dalton BE, Lu J, Leips J, Cronin TW, Carleton KL. Variable light environments induce plastic spectral tuning by regional opsin coexpression in the African cichlid fish, *Metriaclima zebra*. *Mol Ecol*. 2015;24: 4193–4204. doi:10.1111/mec.13312
162. Luehrmann M, Stieb SM, Carleton KL, Pietzker A, Cheney KL, Marshall NJ. Short-term colour vision plasticity on the reef: changes in opsin expression under varying light conditions differ between ecologically distinct fish species. *J Exp Biol*. 2018;221: jeb175281. doi:10.1242/jeb.175281
163. Sandkam BA, Young CM, Margaret F, Breden W, Bourne GR, Breden F. Color vision varies more among populations than among species of live-bearing fish from South America. *BMC Evol Biol*. *BMC Evolutionary Biology*; 2015;15: 1–11. doi:10.1186/s12862-015-0501-3
164. Rennison DJ, Owens GL, Heckman N, Schluter D, Veen T, Veen T. Rapid adaptive evolution of colour vision in the threespine stickleback radiation. *Proc R Soc Biol*. 2016;283: 1–8. doi:10.1098/rspb.2016.0242
165. Liu D-W, Lu Y, Yan HY, Zakon HH. South American Weakly Electric Fish (Gymnotiformes) Are Long-Wavelength-Sensitive. *Brain Behav Evol*. 2016;88: 204–212. doi:10.1159/000450746
166. Saarinen P, Pahlberg J, Herczeg G, Viljanen M, Karjalainen M, Shikano T, et al. Spectral tuning by selective chromophore uptake in rods and cones of eight populations of nine-spined stickleback (*Pungitius pungitius*). *J Exp*

- Biol. 2012;215: 2760–2773. doi:10.1242/jeb.068122
167. Terai Y, Miyagi R, Aibara M, Mizoiri S, Imai H, Okitsu T, et al. Visual adaptation in Lake Victoria cichlid fishes : depth-related variation of color and scotopic opsins in species from sand / mud bottoms. BMC Evol Biol. BMC Evolutionary Biology; 2017;17: 200. doi:10.1186/s12862-017-1040-x
168. Miyagi R, Terai Y, Aibara M, Sugawara T, Imai H, Tachida H, et al. Correlation between nuptial colors and visual sensitivities tuned by opsins leads to species richness in sympatric Lake Victoria Cichlid Fishes. Mol Biol Evol. 2012;29: 3281–3296. doi:10.1093/molbev/mss139
169. Escobar-camacho D, Pierotti MER, Ferenc V, Sharpe DMT, Ramos E, Martins C, et al. Variable vision in variable environments : the visual system of an invasive cichlid (*Cichla monoculus*) in Lake Gatun , Panama. J Exp Biol. 2019;222: jeb188300. doi:10.1242/jeb.188300
170. Nakatani M, Miya M, Mabuchi K, Saitoh K, Nishida M. Evolutionary history of Otophysi (Teleostei), a major clade of the modern freshwater fishes: Pangaeen origin and Mesozoic radiation. BMC Evol Biol. BioMed Central Ltd; 2011;11: 177. doi:10.1186/1471-2148-11-177
171. Chen WJ, Lavoué S, Mayden RL. Evolutionary Origin And Early Biogeography Of Otophysan Fishes (Ostariophysi: Teleostei). Evolution (N Y). 2013;67: 2218–2239. doi:10.1111/evo.12104
172. Hakrabarty PRC, Aircloth BRCF, Lda FEA, Udt WIBL, Ahan CADMCM. Phylogenomic Systematics of Ostariophysan Fishes : Ultraconserved Elements Support the Surprising Non-Monophyly of Characiformes. Syst

- Biol. 2017;0: 1–15. doi:10.1093/sysbio/syx038
173. Arcila D, Ortí G, Vari R, Armbruster JW, Stiassny MLJ, Ko KD, et al. Genome-wide interrogation advances resolution of recalcitrant groups in the tree of life. *Nat Ecol Evol.* 2017;1: 20. doi:10.1038/s41559-016-0020
174. Cheney KL, Newport C, McClure EC, Marshall NJ. Colour vision and response bias in a coral reef fish. *J Exp Biol.* 2013;216: 2967–73. doi:10.1242/jeb.087932
175. Endler JA. Signals, Signal Conditions, and the Direction of Evolution. *Am Nat.* 1992;139: 125–153.
176. Jacobs GH, Rowe MP. Evolution of vertebrate colour vision. *Clin Exp Optom.* 2004;87: 206–216. doi:10.1111/j.1444-0938.2004.tb05050.x
177. Kelber A, Vorobyev M, Osorio D. Animal colour vision--behavioural tests and physiological concepts. *Biol Rev Camb Philos Soc.* 2003;78: 81–118. doi:10.1017/S1464793102005985
178. Baylor D. How photons start vision. *Proc Natl Acad Sci U S A.* 1996;93: 560–565. doi:10.1073/pnas.93.2.560
179. Yau KW. Phototransduction mechanism in retinal rods and cones. The Friedenwald lecture. *Investig Ophthalmol Vis Sci.* 1994;35: 9–32.
180. Douglas RH, Partridge JC, Marshall NJ. The eyes of deep-sea fish I: Lens pigmentation, tapeta and visual pigments. *Prog Retin Eye Res.* 1998;17: 597–636. doi:10.1016/S1350-9462(98)00002-0
181. Lythgoe JN, Partridge JC. Visual pigments and the acquisition of visual information. *J Exp Biol.* 1989;146: 1–20.

182. Marshall NJ, Jennings K, McFarland WN, Loew ER, Losey GS, Jennings K, et al. Visual Biology of Hawaiian Coral Reef Fishes . III . Environmental Light and an Integrated Approach to the Ecology of Reef Fish Vision
Published by: American Society of Ichthyologists and Herpetologists (ASIH) Stable URL : <http://www.jstor.org/stable/1>. Copeia. 2003;2003: 467–480.
183. Neumeyer C. Tetrachromatic color vision in goldfish: evidence from color mixture experiments. J Comp Physiol A. 1992;171: 639–649. doi:10.1007/BF00194111
184. Ebrey T, Koutalos Y. Vertebrate Photoreceptors. Prog Retin Eye Res. 2001;20: 49–94. doi:10.1007/978-4-431-54880-5
185. Marchiafava PL. Cell Coupling in Double Cones of the Fish Retina. Proc R Soc Biol. 1985;226: 211–215.
186. Marshall NJ, Vorobyev M. The Design of Color Signals and Color Vision in Fishes. In: S.P. C, N.J. M, editors. Sensory Processing in Aquatic Environments. New York, NY: Springer; 2003. pp. 194–222. doi:10.1007/978-0-387-22628-6_10
187. Marshall NJ, Jennings K, McFarland WN, Loew ER, Losey GS. Visual Biology of Hawaiian Coral Reef Fishes. II. Colors of Hawaiian Coral Reef Fish. Copeia. 2003;2003: 455–466. doi:10.1643/01-053
188. Siebeck UE, Wallis GM, Litherland L, Ganeshina O, Vorobyev M. Spectral and spatial selectivity of luminance vision in reef fish. Front Neural Circuits. 2014;8: 1–8. doi:10.3389/fncir.2014.00118

189. Lind O, Chavez J, Kelber A. The contribution of single and double cones to spectral sensitivity in budgerigars during changing light conditions. *J Comp Physiol A Neuroethol Sensory, Neural, Behav Physiol*. 2014;200: 197–207. doi:10.1007/s00359-013-0878-7
190. Maier EJ, Bowmaker JK. Colour vision in the passeriform bird, *Leiothrix lutea*: correlation of visual pigment absorbance and oil droplet transmission with spectral sensitivity. *J Comp Physiol A*. 1993;172: 295–301. doi:10.1007/BF00216611
191. Pignatelli V, Champ C, Marshall J, Vorobyev M. Double cones are used for colour discrimination in the reef fish, *Rhinacanthus aculeatus*. *Biol Lett*. 2010;6: 537–539. doi:10.1098/rsbl.2009.1010
192. Friedman M, Keck BP, Dornburg A, Eytan RI, Martin CH, Hulsey CD, et al. Molecular and fossil evidence place the origin of cichlid fishes long after Gondwanan rifting. *Proc R Soc B Biol Sci*. 2013;280: 20131733. doi:10.1098/rspb.2013.1733
193. Turner GF, Seehausen O, Knight ME, Allender CJ, Robinson RL. How many species of cichlid fishes are there in African lakes? *Mol Ecol*. 2001;10: 793–806.
194. Price AC, Weadick CJ, Shim J, Rodd FH. Pigments, patterns, and fish behavior. *Zebrafish*. 2008;5: 297–307. doi:10.1089/zeb.2008.0551
195. Seehausen O, Terai Y, Magalhaes IS, Carleton KL, Mrosso HD, Miyagi R, et al. Speciation through sensory drive in cichlid fish. 2008. pp. 620–627.
196. Selz OM, Pierotti MER, Maan ME, Schmid C, Seehausen O. Female

- preference for male color is necessary and sufficient for assortative mating in 2 cichlid sister species. *Behav Ecol.* 2014;25: 612–626. doi:10.1093/beheco/aru024
197. Douglas RH, Hawryshyn CW. Behavioural studies of fish vision: an analysis of visual capabilities. *The Visual System of Fish*. London: Chapman and Hall; 1990. pp. 373–418.
 198. Smith AR, Ma K, Soares D, Carleton KL. Relative LWS cone opsin expression determines optomotor thresholds in Malawi cichlid fish. *Genes Brain Behav.* 2012;11: 185–92. doi:10.1111/j.1601-183X.2011.00739.x
 199. Neumeyer C. Evidence for neural interactions between different “cone mechanisms.” *Vision Res.* 1984;24: 1223–1231.
 200. Neumeyer C, Wietsma JJ, Spekreijse H. Separate Processing of “color” and “brightness” in goldfish. *Vision Res.* 1991;31: 537–549.
 201. Jordan R, Kellogs K, Howe D, Juenaes F, Stauffer J, Loew E. Photopigment spectral absorbance of Lake Malawi cichlids. *J Fish Biol.* 2006;68: 1291–1299. doi:10.1111/j.1095-8649.2005.00992.x
 202. Siebeck UE, Wallis GM, Litherland L. Colour vision in coral reef fish. *J Exp Biol.* 2008;211: 354–360. doi:10.1242/jeb.012880
 203. Frisch K von. Der Farbensinn und Formensinn der Biene. *Zool Jahrbücher Abteilung für Allg Zool und Physiol der Tiere*. Fischer,; 1914;35: 1–188. Available: <http://www.biodiversitylibrary.org/item/44193>
 204. Sabbah S, Laria RL, Gray SM, Hawryshyn CW. Functional diversity in the color vision of cichlid fishes. *BMC Biol.* 2010;8: 133. doi:10.1186/1741-

7007-8-133

205. R Core Team. R: A language and environment for statistical computing. [Internet]. Vienna, Austria: R Foundation for Statistical Computing; 2014. Available: <http://www.r-project.org/>
206. Hárosi FI. Visual pigment types and quantum-catch ratios: Implications from three marine teleosts. *Biol Bull.* 1996;190: 203–212. doi:10.2307/1542540
207. Dalton BE, Cronin TW, Marshall NJ, Carleton KL. The fish eye view: are cichlids conspicuous? *J Exp Biol.* 2010;213: 2243–55. doi:10.1242/jeb.037671
208. Smith AR, Carleton KL. Allelic variation in Malawi cichlid opsins: A tale of two genera. *J Mol Evol.* 2010;70: 593–604. doi:10.1007/s00239-010-9355-x
209. Johnsen S. *The optics of life: a biologist's guide to light in nature.* Princetown, New Jersey: Princetwon University Press; 2012.
210. Endler JA, Mielke PW. Comparing entire colour patterns as birds see them. *Biol J Linn Soc.* 2005;86: 405–431. doi:10.1111/j.1095-8312.2005.00540.x
211. Vorobyev M, Osorio D. Receptor noise as a determinant of colour thresholds. *Proc Biol Sci.* 1998;265: 351–8. doi:10.1098/rspb.1998.0302
212. Siddiqi A, Cronin TW, Loew ER, Vorobyev M, Summers K. Interspecific and intraspecific views of color signals in the strawberry poison frog *Dendrobates pumilio*. *J Exp Biol.* 2004;207: 2471–85. doi:10.1242/jeb.01047

213. Vorobyev M, Osorio D, Bennett ATD, Marshall NJ, Cuthill IC. Tetrachromacy, oil droplets and bird plumage colours. *J Comp Physiol - A Sensory, Neural, Behav Physiol.* 1998;183: 621–633. doi:10.1007/s003590050286
214. Vorobyev M, Brandt R, Peitsch D, Laughlin SB, Menzel R. Colour thresholds and receptor noise: Behaviour and physiology compared. *Vision Res.* 2001;41: 639–653. doi:10.1016/S0042-6989(00)00288-1
215. Koshitaka H, Kinoshita M, Vorobyev M, Arikawa K. Tetrachromacy in a butterfly that has eight varieties of spectral receptors. *Proc Biol Sci.* 2008;275: 947–54. doi:10.1098/rspb.2007.1614
216. Olsson P, Lind O, Kelber A. Bird colour vision: behavioural thresholds reveal receptor noise. *J Exp Biol.* 2015;218: 184–193. doi:10.1242/jeb.111187
217. Carleton KL, Hárosi FI, Kocher TD. Visual pigments of African cichlid fishes: evidence for ultraviolet vision from microspectrophotometry and DNA sequences. *Vision Res.* 2000;40: 879–90. Available: <http://www.ncbi.nlm.nih.gov/pubmed/10720660>
218. Champ CM, Vorobyev M, Marshall NJ. Colour thresholds in a coral reef fish. *R Soc Open Sci.* 2016;3: 160399. doi:10.1098/rsos.160399
219. Satoh S, Tanaka H, Kohda M. Facial recognition in a discus fish (Cichlidae): Experimental approach using digital models. *PLoS One.* 2016;11: 1–11. doi:10.1371/journal.pone.0154543
220. Schluessel V, Fricke G, Bleckmann H. Visual discrimination and object

- categorization in the cichlid *Pseudotropheus* sp. *Anim Cogn.* 2012;15: 525–537. doi:10.1007/s10071-012-0480-3
221. Schluessel V, Beil O, Weber T, Bleckmann H. Symmetry perception in bamboo sharks (*Chiloscyllium griseum*) and Malawi cichlids (*Pseudotropheus* sp.). *Anim Cogn.* 2014;17: 1187–1205. doi:10.1007/s10071-014-0751-2
222. Schluessel V, Kortekamp N, Cortes J a. O, Klein A, Bleckmann H. Perception and discrimination of movement and biological motion patterns in fish. *Anim Cogn.* Springer Berlin Heidelberg; 2015;18: 1077–1091. doi:10.1007/s10071-015-0876-y
223. Risner ML, Lemerise E, Vukmanic E V, Moore A. Behavioral spectral sensitivity of the zebrafish (*Danio rerio*). 2006;46: 2625–2635. doi:10.1016/j.visres.2005.12.014
224. De Aguiar MJL, Ventura DF, da Silva Filho M, de Souza JM, Maciel R, Lee BB. Response of carp (*Cyprinus carpio*) horizontal cells to heterochromatic flicker photometry. *Vis Neurosci.* 2006;23: 437–440. doi:10.1017/S0952523806233273
225. Klaassen LJ, de Graaff W, Van Asselt JB, Klooster J, Kamermans M. Specific connectivity between photoreceptors and horizontal cells in the zebrafish retina. *J Neurophysiol.* 2016; jn.00449.2016. doi:10.1152/jn.00449.2016
226. Li YN, Tsujimura T, Kawamura S, Dowling JE. Bipolar cell-photoreceptor connectivity in the zebrafish (*Danio rerio*) retina. *J Comp Neurol.* 2012;520:

3786–3802. doi:10.1002/cne.23168

227. Wilkins L, Marshall NJ, Johnsen S, Osorio D. Modelling fish colour constancy, and the implications for vision and signalling in water. *J Exp Biol.* 2016; jeb.139147-. doi:10.1242/jeb.139147
228. Cheney KL, Skogh C, Hart NS, Marshall NJ. Mimicry, colour forms and spectral sensitivity of the bluestriped fangblenny, *Plagiotremus rhinorhynchos*. *Proc Biol Sci.* 2009;276: 1565–1573. doi:10.1098/rspb.2008.1819
229. Avarguès-Weber A, Giurfa M. Cognitive components of color vision in honey bees: How conditioning variables modulate color learning and discrimination. *J Comp Physiol A Neuroethol Sensory, Neural, Behav Physiol.* 2014;200: 449–461. doi:10.1007/s00359-014-0909-z
230. Vorobyev M. Coloured oil droplets enhance colour discrimination. *Proc R Soc London B Biol Sci.* 2003;270: 1255–1261. doi:10.1098/rspb.2003.2381
231. Kemp DJ, Herberstein ME, Fleishman LJ, Endler JA, Bennett ATD, Dyer AG, et al. An integrative framework for the appraisal of coloration in nature. *Am Nat.* 2015;185: 705–724. doi:10.1086/681021
232. Schaefer HM, Schaefer V, Vorobyev M. Are fruit colors adapted to consumer vision and birds equally efficient in detecting colorful signals? *Am Nat.* 2007;169: S159–S169. doi:10.1086/510097
233. Streelman JT, Danley PD. The stages of vertebrate evolutionary radiation. *Trends Ecol Evol.* 2003;18: 126–131. doi:10.1016/S0169-5347(02)00036-8
234. Kocher TD. Adaptive evolution and explosive speciation: the cichlid fish

- model. *Nat Rev Genet.* 2004;5: 288–298. doi:10.1038/nrg1316
235. Albertson RC, Markert JA, Danley PD, Kocher TD. Phylogeny of a rapidly evolving clade: the cichlid fishes of Lake Malawi, East Africa. *Proc Natl Acad Sci U S A.* 1999;96: 5107–10. doi:DOI 10.1073/pnas.96.9.5107
236. Stauffer JR, Bowers N, Kellogg KA, McKaye KR. A Revision of the Blue-Black *Pseudotropheus zebra* (Teleostei: Cichlidae) Complex from Lake Malaŵi, Africa, with a Description of a New Genus and Ten New Species. *Proc Acad Nat Sci Philadelphia.* 1997;148: 189–230.
237. Jordan R, Kellogg K, Juanes F, Stauffer J. Evaluation of Female Mate Choice Cues in a Group of Lake Malawi Mbuna (Cichlidae). *Copeia.* 2003;2003: 181–186. doi:10.1643/0045-8511(2003)003[0181:EOFMCC]2.0.CO;2
238. Jordan R, Kellogg K, Juanes F, Howe D, Stauffer JJ, Loew E, et al. Ultraviolet reflectivity in three species of Lake Malaw rock-dwelling cichlids. *J Fish Biol.* 2004;65: 876–882. doi:10.1111/j.1095-8649.2004.00483.x
239. Seehausen O, van Alphen JM. The effect of male coloration on female mate choice in closely related Lake Victoria cichlids (*Haplochromis nyererei* complex). *Behav Ecol Sociobiol.* 1998;42: 1–8.
240. Seehausen O, van Alphen JJM, Witte F. Cichlid Fish Diversity Threatened by Eutrophication That Curbs Sexual Selection. *Science.* 1997;277: 1808–1811. doi:10.1126/science.277.5333.1808
241. Escobar-Camacho D, Carleton KL. Sensory modalities in cichlid fish behavior. *Curr Opin Behav Sci.* Elsevier Ltd; 2015;6: 115–124.

doi:10.1016/j.cobeha.2015.11.002

242. Mckaye KR, Marsh A. Food Switching by Two Specialized Algae-Scraping Cichlid Fishes in Lake Malawi, Africa. *Oecologia*. 1983;56: 245–248.
243. Genner MJ, Turner GF, Hawkins SJ. Foraging of rocky habitat cichlid fishes in Lake Malawi : coexistence through niche partitioning ? *Oecologia*. 1999;121: 283–292.
244. Reinthal PN. The feeding habits of a group of herbivorous rock-dwelling cichlid fishes (Cichlidae: Perciformes) from Lake Malawi, Africa. *Environmental Biol Fishes*. 1990;27: 215–233.
245. Jordan R, Howe D, Juanes F, Stauffer J, Loew E. Ultraviolet radiation enhances zooplanktivory rate in ultraviolet sensitive cichlids. *Afr J Ecol*. 2004;42: 228–231.
246. Smith C, Barber I, Wootton RJ, Chittka L. A receiver bias in the origin of three-spined stickleback mate choice. *Proc R Soc London B Biol Sci Biol*. 2004;271: 949–55. doi:10.1098/rspb.2004.2690
247. Rodd FH, Hughes K a, Grether GF, Baril CT. A possible non-sexual origin of mate preference: are male guppies mimicking fruit? *Proc R Soc London B Biol Sci*. 2002;269: 475–481. doi:10.1098/rspb.2001.1891
248. Bowmaker JK. Microspectrophotometry of vertebrate photoreceptors: A brief review. *Vision Res*. 1984;24: 1641–1650.
249. Kelber A, Osorio D. From spectral information to animal colour vision: Experiments and concepts. *Proc R Soc B Biol Sci*. 2010;277: 1617–1625. doi:10.1098/rspb.2009.2118

250. Lind O, Kelber A. Avian colour vision: Effects of variation in receptor sensitivity and noise data on model predictions as compared to behavioural results. *Vision Res.* Elsevier Ltd; 2009;49: 1939–1947. doi:10.1016/j.visres.2009.05.003
251. Bitton PP, Janisse K, Doucet SM. Assessing sexual dichromatism: The importance of proper parameterization in tetrachromatic visual models. *PLoS One.* 2017;12: 1–22. doi:10.1371/journal.pone.0169810
252. Olsson P, Lind O, Kelber A. Chromatic and achromatic vision: Parameter choice and limitations for reliable model predictions. *Behav Ecol.* 2018;29: 273–282. doi:10.1093/beheco/arx133
253. Hurlbert A. Quick guide Colour constancy Primer Quorum sensing. *Curr Biol.* 2007;17: 906–907.
254. Olsson P, Wilby D, Kelber A. Quantitative studies of animal colour constancy : using the chicken as model. *Proc R Soc B Biol Sci.* 2016;283: 1–8. doi:10.1098/rspb.2016.0411
255. Dörr S, Neumeyer C. Color constancy in goldfish: The limits. *J Comp Physiol.* 2000;186: 885–896. doi:10.1007/s003590000141
256. Neumeyer C, Dörr S, Fritsch J, Kardelky C. Colour constancy in goldfish and man: Influence of surround size and lightness. *Perception.* 2002;31: 171–187. doi:10.1068/p05sp
257. Ingle DJ. The Goldfish as a Retinex Animal. *Science.* 1985;227: 651–654.
258. Barbur JL, Spang K. Colour constancy and conscious perception of changes of illuminant. *Neuropsychologia.* 2008;46: 853–863.

doi:10.1016/j.neuropsychologia.2007.11.032

259. Kamermans M, Kraaij DA, Spekrijse H. The cone/horizontal cell network: A possible site for color constancy. *Vis Neurosci.* 1998;15: 787–797. doi:10.1017/S0952523898154172
260. Escobar-Camacho D, Marshall J, Carleton KL. Behavioral color vision in a cichlid fish: *Metriaclima benetos*. *J Exp Biol.* 2017;220: 2887–2899. doi:10.1242/jeb.160473
261. Mitchell L, Cheney KL, Cortesi F, Marshall NJ, Vorobyev M. Triggerfish uses chromaticity and lightness for object segregation. *R Soc Open Sci.* 2017;4: 171440. doi:10.1098/rsos.171440
262. Schluessel V, Hiller J, Krueger M. Discrimination of movement and visual transfer abilities in cichlids (*Pseudotropheus zebra*). *Behav Ecol Sociobiol. Behavioral Ecology and Sociobiology*; 2018;72. doi:10.1007/s00265-018-2476-8
263. Seehausen O. The effect of male coloration on female mate choice in closely related Lake Victoria cichlids (*Haplochromis nyererei* complex). 1998; 1–8.
264. Govardovskii VI, Fyhrquist N, Reuter T, Kuzmin DG, Donner K. In search of the visual pigment template. *Vis Neurosci.* 2000;17: 509–528. doi:10.1017/S0952523800174036
265. Dyer AG, Chittka L. Biological significance of distinguishing between similar colours in spectrally variable illumination: Bumblebees (*Bombus terrestris*) as a case study. *J Comp Physiol A Neuroethol Sensory, Neural,*

- Behav Physiol. 2004;190: 105–114. doi:10.1007/s00359-003-0475-2
266. Lind O. Colour vision and background adaptation in a passerine bird, the zebra finch (*Taeniopygia guttata*). R Soc Open Sci. 2016;3: 160383. doi:10.1098/rsos.160383
267. Dyer AG. Broad spectral sensitivities in the honeybee's photoreceptors limit colour constancy. J Comp Physiol - A Sensory, Neural, Behav Physiol. 1999;185: 445–453. doi:10.1007/s003590050405
268. Hert E. The function of egg-spots in an African mouth-brooding cichlid fish. Anim Behav. 1989;37: 726–732. doi:10.1016/0003-3472(89)90058-4
269. Allender CJ, Seehausen O, Knight ME, Turner GF, Maclean N. Divergent selection during speciation of Lake Malawi cichlid fishes inferred from parallel radiations in nuptial coloration. Proc Natl Acad Sci. 2003;100: 14074–14079. doi:10.1073/pnas.2332665100
270. Smith AR, D'Annunzio L, Smith AE, Sharma A, Hofmann CM, Marshall NJ, et al. Intraspecific cone opsin expression variation in the cichlids of Lake Malawi. Mol Ecol. 2011;20: 299–310. doi:10.1111/j.1365-294X.2010.04935.x
271. Sabbah S, Gray SM, Boss ES, Fraser JM, Zatha R, Hawryshyn CW. The underwater photic environment of Cape Maclear, Lake Malawi: comparison between rock- and sand-bottom habitats and implications for cichlid fish vision. J Exp Biol. 2011;214: 487–500. doi:10.1242/jeb.051284
272. Escobar-camacho D, Pierotti MER, Ferenc V, Sharpe DMT, Ramos E, Martins C, et al. Variable vision in variable environments: the visual system

- of an invasive cichlid (*Cichla monoculus*, Agassiz, 1831) in Lake Gatun, Panama. *J Exp Biol.* 2019; jeb.188300. doi:10.1242/jeb.188300
273. Harer A, Meyer A, Torres-Dowdall J. Convergent phenotypic evolution of the visual system via different molecular routes: How Neotropical cichlid fishes adapt to novel light environments. *Evol Lett.* 2018; 1–14. doi:10.1002/evl3.71
274. O’Quin KE, Hofmann CM, Hofmann H a., Carleton KL. Parallel Evolution of opsin gene expression in African cichlid fishes. *Mol Biol Evol.* 2010;27: 2839–2854. doi:10.1093/molbev/msq171
275. Spady TC, Seehausen O, Loew ER, Jordan RC, Kocher TD, Carleton KL. Adaptive molecular evolution in the opsin genes of rapidly speciating cichlid species. *Mol Biol Evol.* 2005;22: 1412–22. doi:10.1093/molbev/msi137
276. Levine JS, Macnichol EF, Kraft T, Collins BA. Intraretinal distribution of cone pigments in certain teleost fishes. *Science.* 1979;204: 523–526. doi:10.1126/science.432658
277. Ali MA, Hárosi FI, Wagner HJ. Photoreceptors and Visual Pigments in a Cichlid Fish, *Nannacara anomala*. *Sens Processes.* 1978;2: 130–145.
278. Owens GL, Rennison DJ. Evolutionary ecology of opsin gene sequence , expression and repertoire. *Mol Ecol.* 2017;26: 1207–1210. doi:10.1111/mec.14032
279. Reis RE, Albert JS, Dario F Di, Mincarone MM, Petry P, Rocha LA. Fish biodiversity and conservation in South America. *J Fish Biol.* 2016;89: 12–

47. doi:10.1111/jfb.13016

280. Sillman AJ, Ronan SJI, Loew ER. Scanning electron microscopy and microspectrophotometry of the photoreceptors of ictalurid catfishes. *J Comp Physiol.* 1993;173: 801–807.